RESONANCE MEETING
MAY 30 TO JUNE 1, 1999
NATIONAL CENTER FOR PHYSICAL ACOUSTICS
THE UNIVERSITY OF MISSISSIPPI

VOLUME 1. TRANSCRIPTS

Proceedings of a Symposium Sponsored by the
Office of Naval Research

The National Center for Physical Acoustics

The
University of Mississippi

PREFACE

The Resonance Meeting was held May 30 to June 1, 1999 at the National Center for Physical Acoustics (NCPA), University of Mississippi. The purpose of the Resonance Meeting was to cover a broad range of uses of acoustic resonances to determine physical properties of matter. The meeting grew out of prior meetings in 1994 and 1995 that were devoted entirely to Resonant Ultrasound Spectroscopy (RUS). At both the 1997 and 1999 gatherings, the Resonance Meeting included cutting-edge users of RUS and other resonance techniques, as well as researchers and graduate students who wanted to learn about and use these techniques. Universities from the United States and Japan, national laboratories and private research organizations were represented. The Resonance Meetings have proved to stimulate extended discussions outside the scheduled sessions. The organizers are grateful to the participants who made this meeting effective.

At the 1999 Resonance Meeting, Orson L. Anderson, Harold H. Demarest, Jr., and Ichiro Ohno were honored for their contributions to the development of Resonant Ultrasound Spectroscopy and related resonance techniques for determining the elastic properties of solids. These proceedings include a special appendix that presents a short biography on these gentlemen along with a representative publication of their work and photos from the ceremony.

These proceedings of the Resonance Meeting consist of two volumes. Volume 1 contains a verbatim transcript of each presentation and a special appendix. Volume 2 contains accompanying transparencies for each transcript. Anyone interested in obtaining more information on a particular presentation may contact the author(s). Volume 1 contains a complete list of participants and addresses.

TABLE OF CONTENTS

SCHEDULE

SUNDAY, MAY 30 (NOT RECORDED)

MEETING BEGINS | 7:00 p.m. – 9:30 p.m.

    HARGROVE — Welcome and introductory remarks

    PARTICPANTS — Self-introductions

    BASS/FURR — Administrative Announcements

MONDAY, MAY 21 (MORNING AND AFTERNOON SESSIONS RECORDED)

MEETING RESUMES | 9:00 a.m. –12:30 p.m.

    HARGROVE/BASS — Introduction and Administrative Announcements

    ISAAC — *Elasticity of Leucite Through High-Temperature Phase Transitions*

    LEISURE — *Resonant Ultrasound Spectroscopy Studies of Metal-Hydrogen Systems*

    WILLIS — *Industrial Applications of RUS*

    MAYNARD — *Thin Film Characterization Using Resonant Ultrasound Spectroscopy*

    OHNO — *Elasticity of Steel and Silica Glass Spheres Under Gas Pressure by RUS (Poster Presentation)*

    BASS — Announcements

MEETING RESUMES | 2:00 p.m. – 4:00 p.m.

    MIGLIORI — *Phonons, RUS, and Neutron Scattering*

    GUYER — *Nonlinear Mesoscopic Elasticity in Solids*

    MCCALL — *Application of Resonant Ultrasound Spectroscopy to Determine the Elastic Properties of Macroscopic Rock Samples*

    GUYER — *Constant Strain Analysis*

MEETING RESUMES — 9:00 a.m. – 12:30 p.m.

HARGROVE/BASS — Remarks and Administrative Announcements

DARLING — *Global Symmetry, the Phonon Density of States, and RUS*

OGI — *Contactless Mode-Selective Resonance Ultrasound Spectroscopy: Electromagnetic Acoustic Resonance*

LEDBETTER — *Elastic Coefficients and Internal Friction of Silicon Monocrystal Spheres*

KEPPENS — *RUS Studies of Crypto-Clathrates: Perfect Crystals with the Elastic Properties of Glasses*

MARSTON — *Comparison of Radiation and Scattering mechanisms for Objects having Rayleigh Wave Velocities Greater Than or Smaller Than the Speed of Sound in the Surrounding Water*

BASS — Announcements

MEETING RESUMES — 2:00 p.m. – 5:00 p.m.

HEFNER — *Subsonic Rayleigh Wave Resonances on Solid Polymer Spheres in Water and Backscattering Enhancements Associated with Tunneling: Experiments, Models, and the Relative Significance of Material and Radiation Damping*

SINHA — *Remote Ultrasonic Classification of Fluids Using the Acoustic Resonance Characteristics of the Container*

MEHL — *Acoustic Gas Resonators for Measurements of Thermophysical Properties and Thermometry*

DASGUPTA — *Sampled CW Measurements on Single Crystals of $YBa_2Cu_3O_{7-\delta}$ and $Bi_2Sr_2CaCu_2O_8$*

KADUCHAK — *Resonance Acoustic Concentration of Suspended Particles for Optical Discrimination of Aerosols*

HARGROVE/BASS — Adjourn

SPECIAL CEREMONY HONORING ORSON L. ANDERSON, HAROLD H. DEMAREST, JR. AND ICHIRO OHNO — 7:00 pm. – 9:00 pm

LIST OF PARTICIPANTS

Orson L. Anderson, University of California at Los Angeles, Institute of Geophysics and Planetary Physics, 4851 Geology Building, Los Angeles CA 90095-1567, (310) 825-2386, (310) 206-3051 (fax), olanderson@adam.igpp.ucla.edu

Henry E. Bass, National Center for Physical Acoustics, Coliseum Drive, University of Mississippi, University MS 38677, (601) 232-5905, (601) 232-7494 (fax), pabass@olemiss.edu

James Chambers, University of Mississippi, National Center for Physical Acoustics, Coliseum Drive, University MS 38677, (601) 232-5100, (601) 232-7494 (fax), chambers@olemiss.edu

Timothy W. Darling, Los Alamos National Laboratory, MS-K764 P.O. Box 1663, Los Alamos NM 87545, (505) 667-7709, (505) 665-7652 (fax), darling@lanl.gov

Debashis Dasgupta, University of Wisconsin-Milwaulkee, Department of Physics, Milwaukee WI 53201, (414) 229-6438, (414) 229-5589 (fax), deba@csd.uwm.edu

Harry Demarest, Astro Research Inc., 974 NW Circle Blvd, Corvallis OR 97330, (541) 748-1132, (503) 296-2213 (fax), harry@voterlist.com

Libby Furr, University of Mississippi, National Center for Physical Acoustics, University MS 38677, (601) 232-5808, (601) 232-7494 (fax), eacauthe@olemiss.edu

Felipe Gaitan, University of Mississippi, National Center for Physical Acoustics, Coliseum Drive, University MS 38677, (601) 232-5796, (601) 232-7494 (fax), gaitan@olemiss.edu

Robert A. Guyer, Los Alamos National Laboratory, EES-4 Geoengineering, MS D443, Los Alamos NM 87545, (505) 667-6488, (505) 667-8487 (fax), guyer@ kokopelli.lanl.gov

Logan E. Hargrove, Office of Naval Research, ONR 331 Room 503-13, 800 North Quincy Street, Arlington VA 22217-5660 , (703) 696-4221 , (703) 696-6887 (fax), hargrol@onr.navy.mil

Brian Todd Hefner, Washington State University, Department of Physics, Pullman WA 99164-2814, (509) 335-5343, (509) 335-9531 (fax), bhefner@mail.wsu.edu

Craig Hickey, University of Mississippi, National Center for Physical Acoustics, Coliseum Drive, University MS 38677, (601) 232-7222, (601) 232-7494 (fax), chickey@olemiss.edu

Donald G. Isaak, University of California at Los Angeles, Institute of Geophysics and Planetary Physics, 4843 Geology Building, Los Angeles CA 90095-1567, (310) 825-3565, (310) 206-3051 (fax), disaak@adam.igpp.ucla.edu

Gregory Kaduchak, Los Alamos National Laboratory, MST-11: Electronic Materials and Device Research, MS D429, Los Alamos NM 87545, (505) 665-9471, (505) 665-4292 (fax), kaduchak@lanl.gov

Veerle M. Keppens, University of Mississippi, National Center for Physical Acoustics, University MS 38677, (601) 232-5889, (601) 232-7494 (fax), veerle.keppens@fys.kuleuven.ac.be

Hassel Ledbetter, National Institute of Standards and Technology, Materials Science and Engineeing Laboratory, Boulder CO 80303, (303) 497-3443, ledbetter@boulder.nist.gov

Robert G. Leisure, Colorado State University, Department of Physics, Fort Collins CO 80523, (303) 491-5370, (303) 491-7947 (fax), leisure@lamar.colostate.edu

Moises Levy, Monaco Beach Club #807, 4401 Gulf Shore Boulevard North, Naples FL 34103, (941) 403-7265, (941) 403-9564 (fax), Moiseslevy@aol.com

Philip L. Marston, Washington State University, Department of Physics, Pullman WA 99164-2814, (509) 335-5343, (509) 335-9531 (fax), marston@wsu.edu

Julian D. Maynard, Pennsylvania State University, Department of Physics, University Park PA 16802, (814) 865-6353 , (814) 865-3604 (fax), maynard@phys.psu.edu

Katherine R. McCall, University of Nevada, Department of Physics/220, Reno NV 9557-0058, (702) 784-4991/6792, (702) 784-1398 (fax), mccall@physics.unr.edu

Michael McPherson, University of Mississippi, National Center for Physical Acoustics, Coliseum Drive, University MS 38677, (601) 232-7551, (601) 232-7494 (fax), mcph@olemiss.edu

James B. Mehl, Unversity of Delaware, Department of Physics & Astronomy, Newark DE 19716-2570, (302) 831-2676, (302) 831-1637 (fax), jmehl@udel.edu

Albert Migliori, Los Alamos National Laboratory, MS-K764, Los Alamos NM 87545, (505) 667-2515, (505) 665-7652 (fax), migliori@lanl.gov

Romelle Million, Million Reporting, P.O. Box 2419, Alexandria VA 22301, (703) 836-3093

Hirotsugu Ogi, National Institute of Standards and Technology, Materials Science and Engineering Laboratory, Boulder CO 80303, (303) 497-7929, (303) 497-5030 (fax), ogih@boulder.nist.gov

Ichiro Ohno, Okayama University, Department of Earth Sciences, 3-1-1 Tsushima-Naka, Okayama 700 JAPAN, ohno@sci.ehime-u.ac.jp

Richard Raspet, University of Mississippi, Department of Physics & Astronomy, NCPA Room 2018, Coliseum Drive, University MS 38677, (601) 232-5888, (601) 232-7494 (fax), raspet@next1.ncpa.olemiss.edu

Andrea P. Ross, University of Mississippi, Department of Physics & Astronomy, University MS 38677, (601) 232-7928, (601) 232-5045 (fax), apross98@yahoo.com

Wolfgang H. Sachse, Cornell University, Theoretical and Applied Mechanics, Ithaca NY 14853-1503, (607) 255-5065, (607) 255-9179 (fax), sachse@msc.cornell.edu

John A. Scales, Colorado School of Mines, Department of Geophysics, Golden CO 80401, (303) 273-3408, (303)273-3478 (fax), jscales@landau.Mines.EDU

Timothy Simmons, National Center for Physical Acoustics, University of Mississippi, Coliseum Drive, University MS 38677, (601) 232-5843, (601) 232-7494 (fax), tgsimmon@olemiss.edu

Dipen N. Sinha, Los Alamos National Laboratory, MST-11 MS D429, Los Alamos NM 87545, (505) 667-0062, (505) 665-4292 (fax), sinha@lanl.gov

William Slaton, University of Mississippi, Department of Physics & Astronomy, NCPA Room 1113, Coliseum Drive, University MS 38677, (601) 232-5635, (601) 232-7494 (fax), wmslaton@meta3.net

Gordon Smith, University of Mississippi, Department of Physics & Astronomy, NCPA Room 1113, Coliseum Drive, University MS 38677, (601) 232-5635, (601) 232-7494 (fax), slipstk@olemiss.edu

Martin Smith, New England Research Inc., 76 Olcott Drive, White River Junction VT 05001, (802) 296-2401, (802) 296-8333 (fax)

Jin-Hyun So, Pennsylvania State University, Physics Department, 104 Davey Lab, University Park PA 16802-6300, jinso@phys.psu.edu

Carrick Talmadge, University of Mississippi, National Center for Physical Acoustics, Coliseum Drive, University MS 38677, (601) 232-3855, (601) 232-7494 (fax), clt@olemiss.edu

Frank Willis, Dynamic Resonance Systems Inc., 225 Lane 13, Powell WY 82435, (307) 754-5135, (307) 754-5142 (fax), fwillis@ndtest.com

ELASTICITY OF LEUCITE THROUGH HIGH-TEMPERATURE PHASE TRANSITIONS

DONALD ISAAK[1], ANDY SHEN[2], ORSON ANDERSON[1], JOHN CARNES[1]

[1]UNIVERSITY OF CALIFORNIA AT LOS ANGELES

[2]UNIVERSITY OF CAMBRIDGE, UK

ABSTRACT

A mean-field Landau-type model predicts that in some crystals certain elastic moduli experience significant softening in the neighborhood of phase transitions. Experimental verification of the influence of structural phase transitions on elastic moduli are needed to build a complete physical model and to predict the elastic behavior of minerals that undergo structural phase transitions.

At ambient pressure and temperature, leucite ($KAlSi_6O_6$) is tetragonal, but undergoes two structural transitions at about 870 and 900 K to a high-temperature cubic phase. We used resonant ultrasound spectroscopy (RUS) to monitor the resonant modes of leucite ($KAlSi_6O_6$) from room temperature to 1500 K. In the stability field of cubic leucite, the five lowest resonant modes were measured from 900 to 1500 K. These five modes are predominantly shear vibrations, thus constrain the the shear moduli, but not the compressional moduli. We find that C_{44} increases gradually from 19.3(3) GPa to 26.5(7) as temperature increases from 950 K to 1500 K. This behavior in C_{44} demonstrates the influence that phase transitions have on elastic properties at temperatures well removed from the transition temperature.

TRANSCRIPT

DR. ISAAK: My name is Don Isaak and I am from UCLA. The work I will discuss was done at the UCLA lab with Orson Anderson, J.D. Carnes, and Steve Moser. Moser is an undergraduate at Azusa Pacific University.

The abstract focuses on phase transitions in leucite. In my presentation, however, I will show results from our leucite work and from two other major areas of study during the past year.

[Transparency 1]

The first item represents work we have done in the last year on phase transitions at high temperature. The second item refers to information we obtained from rutile data. Specifically, I wish to show inferences we made on the pressure derivatives of elasticity at high temperature based on our high-temperature RUS work and systematics. The third item is included to correct some conclusions I presented in a talk two years ago. Many of you were present at that talk; it is appropriate to update you on the results of our work regarding the pressure derivatives of the shear modulus using the RUS technique.

[Transparency 2]

Let us turn to the leucite work. When I submitted my abstract, I received an e-mail suggesting I misspelled the mineral. I remind you (or inform you) that we studied this white, gray mineral, described on the left side, which is leucite -- not this plastic-like material over here on the right. That material is lucite.

[Transparency 3]

Leucite exists in a tetragonal form at ambient temperature. When heated, it goes through a ferroelastic transition at 918 K and then a small volume-changing transition near 940 K. A tetragonal-to-cubic change in crystal symmetry also occurs at the high temperature transition. We wanted to look at the elastic properties associated with this change in crystal structure.

DR. MIGLIORI: So as you heat this, it goes tetragonal to cubic?

DR. ISAAK: Yes, that is exactly right, the high-temperature phase is cubic, it goes to a higher symmetry form. The elastic constants of that high-temperature cubic phase are unknown and are the subject of our study.

[Transparency 4]

Here is a brief look at the sample description that we used. The density is a little more than 2. The specimen size is between 1 and 2 mm on a side. We used a right-rectangular parallelepiped. The assumed starting C_{ij} for the cubic phase are also shown.

DR. LEDBETTER: How did you get the starting moduli?

DR. ISAAK: I will come back to that in detail shortly, but it would be worth mentioning something now on that. The C_{11} and C_{12} values are actually calculations from Martin Dove at Cambridge, England. This leucite work was a collaboration between the UCLA lab and the Cambridge group: Michael Carpenter; Martin Dove; and Andy Shen. Dove gave us the C_{11} and

2

C_{12} values and suggested a value for the C_{44} modulus that was different from the 20 GPa shown here. I will come back to that point shortly.

[Transparency 5]

These are the five modes we looked at. We could see only these five modes - presumably they are the five lowest modes. We could not make an analysis of the six C_{ij} of the low-temperature tetragonal phase using only five modes.

Furthermore, the low-temperature phase is highly twinned; it is very difficult to make meaningful interpretations in terms of the low-temperature C_{ij}. The modes are very clear below 900 K but, it is not apparent how to interpret them as the C_{ij} of the low-temperature phase.

We wanted to see what happens after the high-temperature transition to the cubic phase.

[Transparency 6]

Here is another diagram of the frequencies as a function of temperature. These thin, solid lines show the calculated frequencies made using C_{44}=20GPa and the C_{11} and C_{12} values provided to by the Cambridge group. The seven lowest modes calculated this way are labeled along the right edge of the plot.

The point of all this is that with a C_{44} value of 20 GPa the calculated modes intersect the measured modes at about the same temperature, 950 K. This answers the question of how, in principle, we arrived at the starting modulus for C_{44}. We just used those values of C_{44} that match the first five calculated modes with the five measured modes.

You can see how sensitive the calculated frequencies are to changes in the C_{44} modulus by changing C_{44} and recalculating the modes. We changed C_{44} by 10%, making it 22 GPa instead of 20 GPa. The ensuing changes in calculated frequencies are shown by the red dashed lines. Thus, we have some idea of the sensitivity of this method of estimating C_{44} at each temperature. By carrying out this analysis of fitting the five lowest calculated frequencies to the measured frequencies at each temperature, we are able to estimate the C_{44} modulus as a function of temperature for cubic leucite.

DR. MIGLIORI: I did not quite get that. You changed C_{44} by 10%, so that is a 5% change -- okay.

DR. SACHSE: But you are using the computed C_{11} and C_{12} and then you are playing around with the C_{44}. I know the computed ones are for the --

DR. ISAAK: Yes, that is what I will now show. As it turns out, those five measured modes are very insensitive to C_{11} and C_{12}. It happens that the modes we were able to see only constrain C_{44} - that is the bottom line - so we have a limited amount of information. At the same time, we can be quite certain that the information we do extract is not obscured by other uncertainties.

[Transparency 7]

This illustrates the point I just made. It shows computed frequencies (thin solid line) using the value of C_{12} given to us originally by Dove and cited earlier in this talk. The frequencies are recalculated (thick dashed line) after changing C_{12} by 10%. There is virtually no change in the computed frequencies. A similar case occurs with C_{11}. So, uncertainty about the values of C_{11} and C_{12} does not obscure our determination of the value of C_{44}.

[Transparency 8]

The story here is that we are able to measure the C_{44} modulus as a function of temperature after this phase transition. This plot shows $C_{44}(T)$ with the uncertainties as determined from the five measured modes discussed earlier. The fact that C_{44} increases over such a wide temperature range is very unusual. It appears that this soft-mode behavior extends over a temperature range of more than 500°C. That is a bit puzzling to me; it does not seem to follow a Landau-type explanation of a transition.

[Transparency 9]

That is almost the end of the story. We wish, however, to make some interpretation in terms of the Landau theory of phase changes. That is the reason the Cambridge group involved us in this study that is still in progress. From our understanding of Landau theory, for the type of transition we are looking at, the C_{44} modulus should not deviate substantially from the normal C_{44} (referred to as C_{44}^o in the diagram) after the transition to the cubic phase.

That, however, is not what our results with leucite show. Again, the C_{44} modulus should be equal to the undisturbed C_{44} modulus. This undisturbed modulus is the C_{44} without the influence from the transition.

Let us conclude this part of the talk with an observation. In geophysical studies, one must consider the effect of phase transitions on mineral elasticity over much broader temperature ranges than is generally appreciated. When modeling properties of the deep Earth, the effects of phase transitions hundreds and hundreds of degrees from the transition must be accounted for.

I compared this to Migliori, et. al (1993) where the C_{44} modulus in that tetragonal-to-cubic transition for strontium titanate was limited to about 15 or 20°C from the phase transition. The C_{11} and C_{12} moduli were affected over a much broader temperature range.

DR. MIGLIORI: In our lanthanum-two copper-four measurements, we got a similar range of variation of the transition that you did; that is, there is a structural phase transition.

DR. ISAAK: I have not reviewed that.

DR. MIGLIORI: We did that around 500 K and it has an amazingly broad range over which the C_{44} increases as you heat it.

DR. ISAAK: As we are seeing here with leucite - interesting.

DR. MIGLIORI: I think basically the entire Landau business does not work on these systems.

DR. ISAAK: I am not that knowledgeable, but my data also seems to say there is a discrepancy.

DR. MIGLIORI: To make the comment precise, if you take the Ginzberg-Landau model for a structural phase transition, you pick anything you want for an order parameter, you have freedom of choice, then you attempt to compute the temperature dependence of that order parameter through the phase transition. That will make very specific predictions about what all the elastic moduli are going to do.

What you have done, really, is simply say the order parameters are linearly or quadratically coupled to the elastic moduli. We found in lanthanum-two copper-four that no functional form of a simple Ginzberg-Landau phase-transition theory would reproduce the behavior of all the elastic moduli, but we had a critical exponent of exactly one for the shear modes. We do not understand it.

DR. ISAAK: Well, I am glad at least what I am saying is similar to that.

DR. LEDBETTER: It seems to me that this condition of the C_{44} as not being equal could be due to factors other than lattice softening. I think there are a lot of examples of this. These ferroelectric materials with phase transitions have normal temperature dependence on both sides. So there is a splitting of the C_{44} term.

DR. ISAAK: Okay, I will just take that as a comment at this point.

What I would like to do now is move on to the second general subject of this talk in which I will show inferences we made about what is called the mixed pressure-temperature derivative of the bulk modulus from high-temperature work on rutile.

[Transparency 10]

Very quickly, rutile is titanium oxide, TiO_2. Here are a couple of spectra of five modes - one is at room temperature, one is at 1500 K.

[Transparency 11]

Very quickly, this is for those who want to see what the high-temperature data look like. Our maximum temperature was 1800 K. The reason the signals are deteriorating at 1800 K is that the polycrystalline alumina buffer rods are losing their integrity. Higher temperatures are possible with single-crystal corundum rods.

[Transparency 12]

We measured the temperature dependences of about 30 modes. Here we show five such modes.

[Transparency 13]

Here is an example of what often happens in high-temperature work. Some modes are not orthogonal to each other, and when they try to cross you get complicated interactions. Modes that coupled like this were not used in our data reduction; we used only modes that were clean all the way through.

[Transparency 14]

One reason we did this experiment was to measure the high-temperature properties of mineral. If you take the previous data that go to about 400 K, they extrapolate to high temperature as shown by the dashed lines. The actual high-temperature data, however, can show significant deviations from the extrapolations.

[Transparency 15]

An interesting result from rutile work is seen in this figure. We looked at systematic relationships between the pressure derivative and the parameter which is the bulk modulus times the cube root of the mean molecular weight divided by the density, which we can measure to high temperature.

Here we see the systematic relationship between these parameters for three isostructural minerals, SiO_2, GeO_2, and TiO_2, at room temperature and show the linear fit by the dashed line.

This relationship is the Law of Corresponding States proposed by Orson Anderson in 1966. There are reasons why SnO_2 deviates from the trend, but we will not have time to discuss that. The Law of Corresponding States suggests that materials with the same structure obey the same type of behavior in their relationship between $K_S(M/\rho)^{1/3}$ and $(\partial K_S/\partial P)_T$.

We make high-temperature placements of TiO_2 on the dashed line by their high-temperature values of $K_S(M/\rho)^{1/3}$. Then we read over to the $(\partial K_S/\partial P)_T$ axis to infer the $(\partial K_S/\partial P)_T$ value at high temperature.

By this process, we obtain the value of the mixed derivative, $\partial[(\partial K_S/\partial P)_T]/\partial T$. For rutile, we find $\partial[(\partial K_S/\partial P)_T]/\partial T$ is $70x10^{-5}$ K^{-1} which seems high when compared with estimates of other materials.

[Transparency 16]

We find, however, further justification for this high value in work I recently did with Frank Stacey. Using thermodynamic arguments, we found that this mixed derivative, i.e., how the pressure derivative changes with temperature, varies with the pressure derivative of the bulk modulus.

Even though we got a high value for $\partial[(\partial K_S/\partial P)_T]/\partial T$, it seems to make sense because the pressure derivative of the bulk modulus is also somewhat large. The ambient value of $(\partial K_S/\partial P)_T$ (written as K_S' on the plot) would be out to the right at around 7, implying a large value of $\partial[(\partial K_S/\partial P)_T]/\partial T$. Most materials have values of $(\partial K_S/\partial P)_T$ around four or five.

My conclusion is that we have estimated the mixed T,P derivative of the bulk modulus for rutile. We obtain what seems to be a high value of about $70x10^{-5}$ K^{-1}, but this value corresponds to what is obtained from the thermodynamic scheme developed recently by Frank Stacy.

We now move on to the third and final section of the presentation. We will relook at work done with the pressure derivative of elasticity of fused silica spheres. This revisits what was reported at the Asilomar meeting a year ago. We present here, however, a different conclusion than what was given at the Asilomar meeting.

[Transparency 17]

We took fused silica spheres and measured certain resonance peaks as a function of pressure. Data on sphere at ambient pressure, 60 bar, and 120 bar for the T_{02} torsional mode are shown here.

[Transparency 18]

This plot shows the data more completely on one pressure run. Going up in pressure is represented by triangles pointing up; going down in pressure is represented by triangles pointing down. The open triangles represent the primary data; the closed triangles represent the data with temperature corrections applied. The temperature-corrected data are very precise and repeatable.

[Transparency 19]

At the Asilomar meeting, I reported how we used argon, nitrogen, and helium as pressurizing gases to determine the effective pressure derivative, $(\partial G/\partial T)_P$, of the shear modulus, G. The idea was to then extrapolate to zero gas mass loading conditions as shown in the plot. The result for zero-mass conditions resulted in the magnitude of $(\partial G/\partial T)_P$ being 3.7 (This actually is negative because fused silica has a negative pressure derivative of elasticity). Earlier ultrasonic plane-wave methods showed that $(\partial G/\partial T)_P$ for fused silica is around 3.4 or 3.5.

This arrow in the plot shows a change of 5%. The difference between our value and the average of the plane-wave was about 8%. Some will recall my suggestion that this 8% difference could be due to effects of bonding between specimen and transducers in the plane-wave experiments.

A couple of people took issue with that suggestion at the Asilomar meeting, and they were correct to do so.

[Transparency 20]

As it turns out, my earlier analysis was incomplete. It ignored this second term on the right-hand side that allows for the effect of sphere radius on resonant modes. As pressure increases the resonant modes will change because of changes in elastic moduli and changes in sphere radius. By ignoring this effect we essentially ignore the second term in the numerator of the expression for dG/dP. This ignored term accounts for about 8% of the whole. So I was wrong.

[Transparency 21]

We now see that the line comes down a little and intersects the axis right between the earlier plane-wave data.

DR. MIGLIORI: So the pulse-echo guys did not blow it?

DR. ISAAK: Well, one guy is a little high and one guy is a little low. (Laughter)

But you are exactly right. The size of that 'X' is basically the standard deviation of a weighted fit to the three data points.

Let us look at one more issue before closing this discussion. We have recently done a more rigorous analysis of the expected effect of gas on the torsional mode. We attempted to remove, using theory, the effect of the viscosity of the gas. This is reasonable since we are looking only at shear torsional modes, not dilatational modes, in this work.

[Transparency 22]

It may not be polite to end a talk with a slide full of math, but please bear with me. When gas viscosity is considered, we obtain a third term in the differential expression for changes in frequencies. We assume the penetration depth of the torsional vibrations into the surrounding gas effectively increases the mass of the specimen and we obtain the third term in the right-hand side of the differential expression. The resulting expression for dG/dP requires another term - the third term in the numerator. We apply this correction to the equations for each of the 3 gases. The added corrective term is opposite in sign from the main term, df/dP, in the denominator. Thus, the magnitude of dG/dP decreases for each gas.

[return to Transparency 21]

When the correction is applied, each effective dG/dP value drops (see diamond shapes) and the values from the three gases line up as shown by the horizontal solid line - a result that is somewhat pleasing.

What is not so pleasing is that the 'answer' for dG/dP found this way is slightly higher (by about 3%) than found by simply extrapolating empirically to zero-mass.

If you want to see the details, I refer you to our JASA publication and have copies here with me. Thank you very much.

DR. DARLING: What is the melting point of leucite? How close did you come on those experiments? I assume it is quite high.

DR. ISAAK: We did not melt it. (Laughter)

DR. DARLING: I think the shear modulus might have diminished a little, had you done that.

DR. ISAAK: Yes. I did that once before with garnet. I pushed it too high. I had the melting temperature in my mind in degrees Kelvin, and I was measuring degrees Celsius. So I misjudged by about 300 degrees the temperature I could go to. I lost my signal and later found the specimen partially melted and fused to the buffer rods. What I mean to say is that I now

always check when going up in temperature. I cannot, however, remember off the top of my head the exact melting point of leucite.

DR. MARSTON: This mass shift effect that you introduced at the very end, did you check your modeling of that by just varying the pressure at a given temperature for one of the denser gases?

DR. ISAAK: Yes, I did that for every experiment. I think the real test of this theory would be that when you make the correction, you make it different for each gas. When all the gases are corrected, do they line up at the same value for dG/dP? Each gas has a different correction because of differences in viscosity and especially density.

DR. MARSTON: The point is you checked the scaling with that form by --

DR. ISAAK: Well, I applied this correction to each of the pressure runs for each of the gases. If that is correct, you would expect this gas dependence to be no gas dependence, or you would get the same answer. I think that is what you are getting at. That is exactly what we got, fairly close to each other.

I also have some ideas as to why the two solid lines on the plot do not converge at the same point.

DR. LEVY: Have you checked that with -- what you have done here seems slightly different. Have you tried the other one?

DR. ISAAK: No, because the other one was radiating energy into the gas. It is basically a different consideration. In the Sorbello paper he was focusing more of his attention on the dilatational energies.

DR. LEVY: No, no, he also did shear at the very end.

DR. ISAAK: I do not know the answer to that. I have some questions about that. That paper is on review and we actually need to discuss some things about that. This assumes a completely different starting point. I am not saying it is contradictory, of course, but it is just a different --

DR. LEDBETTER: I think you said you had only 5 resonance peaks.

DR. ISAAK: That I could see with that leucite, yes.

DR. LEDBETTER: And you spread that to twins. But since this is a natural material, could it also have been due to the voids and cracks? What percentage of theoretical density was it?

10

DR. ISAAK: That I do not know. I did not analyze that specimen that way. I do not want to dodge the question; I just do not know and the reason I do not know is because Andy Shen came to our lab from Cambridge. He brought the specimen and the work is not complete yet. How much is due to the problems due to voids I do not know at this point.

I am trying to recall - we did actually measure the bulk density, we came very close to the actual density. We did a density measurement and are okay with that, but there were problems with twins. The signal to noise was fairly poor. What we are doing now is looking at another specimen. We have not heated it yet but we just made some room temperature runs on it. We see very nice signals.

That previous specimen, we saw 5 signals. They were clear but the signal to noise was not that crisp.

DR. MCCALL: Did you happen to bring a diagram of your experimental setup?

DR. ISAAK: No, and the reason is because at every talk I show those and I did not want to bore people with that. (Laughter)

I will be glad to send you those.

DR. MARSTON: Returning to the torsional mode situation, again, could you say something about how the Q varies with pressure?

DR. ISAAK: Yes, with those torsional modes that we are looking at, the 2 lowest torsional modes, we saw almost no effect with pressure on Q, and that is why we were confident of our analysis.

[return to Transparency 17]

Quickly, this illustrates the situation qualitatively. With applied pressure, the modes they are all the same.

Thanks very much.

Resonant Ultrasound Spectroscopy Studies of Metal-Hydrogen Systems

Robert G. Leisure
Colorado State University

Abstract

Many metals absorb significant amounts of hydrogen. The hydrogen frequently alters the material properties of the host metal with resulting effects that are sometimes beneficial and sometime deleterious, but generally interesting. Resonant Ultrasound Spectroscopy (RUS) has been found useful for the study of these materials. The absorption of hydrogen affects the elastic constants, usually, but not always, causing a softening of the lattice. The diffusive/hopping motion of the hydrogen gives rise to ultrasonic attenuation if the hopping rate in comparable to the ultrasonic frequency. RUS measurements on hydrogen in Laves phase compounds, rare-earth metals, and quasicrystals will be discussed.

Transcript

[Transparency 1]

DR. LEISURE: I would like to tell you about some work we have been doing at Colorado State studying metal-hydrogen systems using the technique of resonant ultrasound. Various people have contributed to this work, both in terms of carrying out the measurements (Foster, Shaklee), supplying us with interesting samples (Kelton, Kim, Skripov) and, in the case of a couple of people in the audience, just generally helping us with resonant ultrasound.

[Transparency 2]

This transparency is a road map of where we are going with the talk today. I will give a little background information on metal-hydrogen systems. I will try to make the connection between hydrogen motion in these materials and ultrasonic attenuation. Then I will discuss measurements on two different metal-hydrogen systems: first I will discuss a Laves-phase material which came from Alexander Scripov in Russia; and second, I will discuss a quasi-crystal and a crystalline approximate which came from Ken Kelton's group at Washington University.

[Transparency 3]

The background: There are really quite a lot of metals that absorb hydrogen and retain their metallic character. Among these are transition metals, rare earths, and actinides. If we include various intermetallic compounds and alloys, there is really a whole host of materials that can take up substantial amounts of hydrogen.

In the typical situation the hydrogen sits on some interstitial site. This transparency illustrates the situation for a face-centered cubic lattice. The black circles indicate interstitial sites and the open circles indicate lattice points. Two types of sites are indicated here, octahedral and tetrahedral. Those are the two common types of sites for hydrogen in metal-hydrogen systems. Metal-hydrogen systems are typically non-stoichiometric. A wide range of hydrogen concentrations is possible. At lower concentrations the site occupancy is random and one has a solid solution. At higher hydrogen concentrations one often finds ordered phases that may be precipitated as hydrides.

The hydrogen usually moves very rapidly because of its light mass. The mobility can be 10 to even 15 orders of magnitude greater than for a heavy interstitial such as carbon. This means that we can see effects due to the interstitial motion in metal-hydrogen systems that, *in principle,* might be present in other systems, but would not normally be seen (they would be too slow). Also, it means that there are going to be more quantum effects because of the light mass.

These materials exhibit a lot of interesting physical effects and they find a lot of practical application. There is a whole community of people who study these materials: physicists, metallurgists, chemists, and electrochemists. People have discussed for many years using hydrogen as a fuel. One problem is how to store the hydrogen? One possibility is to store it in a metal-hydride system. There has been a lot of work on such storage, although I doubt that that is really going to be practical solution in the end except for special applications. If you have a cellular phone, there is a high probability that it has a metal-hydride battery in it. Batteries are probably the biggest commercial application of these materials at the moment.

In the past few years people have found for some of these systems, particularly in the form of films, that you can pump hydrogen in and out and switch these things from a metal to an insulator. The corresponding switch in the optical properties has been described as a switchable mirror. Then there is a long-standing problem of hydrogen embrittlement of metals. Just last

night in talking with Dipen Sinha I learned that there are current problems in that area of which I was not aware.

For all of these useful applications or for the problems, hydrogen has to get into the material and diffuse. It many applications it is necessary to get the hydrogen back out again. Thus the mobility of the hydrogen is a key parameter.

[Transparency 4]

The hydrogen mobility leads into the kind of thing I want to talk about now, the motion of the hydrogen and how to study it. It is typically studied by quite a few different techniques. Three common ones are quasi-elastic neutron scattering, nuclear magnetic resonance, and mechanical spectroscopy.

This transparency indicates typical frequency ranges for these different techniques. I do not mean this to be definitive, but just an illustration. The quasi-elastic neutron scattering typically takes care of the very high-frequency motion. NMR takes care of some mid-point range. Toward the lower frequencies there is mechanical spectroscopy, including, of course, resonant ultrasound spectroscopy.

As we all know, these meetings are important for informal exchanges. At breakfast this morning I was speaking with Tim Darling and he pointed out that there is a whole host of interesting materials effects that lie down in this low-frequency range. The mechanical techniques are very sensitive in this low-frequency range. Some of the other techniques, which are very sensitive and highly touted, do not work so well for very low frequencies.

I think, though, at least for the case of hydrogen in metals, these three techniques are really complementary; it is really nice to have information over a wide frequency scan if you want to make sense of what is going on.

We will focus now on the mechanical aspects, or ultrasonic attenuation. How does the hydrogen motion lead to attenuation? It leads to attenuation because when an ultrasonic stress is applied the hydrogen tends to redistribute itself on the interstitial sites; it will go from high-energy sites to low-energy sites, but that redistribution occurs only if the ultrasound affects the different sites differently.

In other words, the ultrasound has to make some distinction among the sites. For that to occur the site symmetry (defect symmetry) must be lower than the crystal symmetry. The book by Nowick and Berry states this as "the selection rule for anelasticity."

14

[Transparency 5]

This transparency gives a diagram to illustrate how that selection occurs. This diagram is just for illustration, it does not represent any real physical system of which I am aware, but a real physical system gets too complicated to actually draw.

Let's consider some simple cubic material and look at a (100) face. We will consider the interstitial sites indicated and imagine that they are randomly occupied by hydrogen. In the absence of any external influence, obviously, the energies of all those sites are the same. However if we apply some stress (and I have indicated here a uniaxial stress), then it is clear not all the interstitial sites are affected in the same way.

Looking at the bottom part of the transparency we see that some of the sites clearly get "squeezed" when we apply the uniaxial stress and some of the sites do not get "squeezed." The hydrogen will undergo some redistribution on those sites to reach the lower energy sites. Of course, the hydrogen is moving rapidly back and forth at all times and the transitions indicated on the bottom diagram represent some *net* flow from one type of site to the other.

This is only a symmetry argument. We do not know which direction that flow goes, because that would depend on which sites become lower in energy and which become high, and *that* depends on the details of the bonding. However, it is easy to see that the stress breaks the symmetry of these interstitial sites.

The basic idea is we apply a stress and there is an immediate strain. However, during the "relaxation time" the hydrogen adjusts itself to that stress and this adjustment leads to additional strain. As a result, the stress and strain are out of phase. If the stress and strain are out of phase we get ultrasonic attenuation.

[Transparency 6]

The resulting relaxation attenuation is given by a simple Debye-type expression. In the experiments I am going to talk about we measured the Q. Typically we determined the loss, $1/Q$, as a function of temperature. The objective, then, is to determine the relaxation time as a function of temperature and hence infer something about the hydrogen motion.

PARTICIPANT: What is C?

DR. LEISURE: C is actually the elastic constant and delta C is its change. Delta C/C is just the coupling strength.

15

For the case of hydrogen, because of its light mass, there are a variety of effects that can occur. What I have tried to illustrate here is some double-well potential describing hydrogen in two adjacent interstitial sites. The double-well potential, of course, is produced by the surrounding metal atoms. At high enough temperature the hydrogen may go from one site to the next by classical barrier hopping (I). Another possibility is that the hydrogen is excited to some vibrational level in the well and then tunnels through (II) or maybe it just tunnels through from the ground state (III).

This diagram itself is somewhat oversimplified, because there are other effects that can occur as well. There may be some self-trapping, so these two wells are probably not, in fact, of quite equal depth. As a result, some thermal excitation energy may be required to overcome the self-trapping. Because of the light mass, quantum effects are usually very important. It is probably not very common that the purely classical description works. However, even for the quantum effects where there is thermal excitation then tunneling, the equations describing the motion often have some Arrhenius-looking form, although the actual parameters will not be those of classical barrier hopping.

[Transparency 7]

Unlike Don, I do not mind using the same diagram over and over at different meetings. Since we have all of the parents and grandparents of RUS here, I probably should not show such a simple diagram, but here is a schematic of how we do the experiment. I know this is familiar to most people in the audience. We place some parallelepiped corner to corner between the transducers, excite one corner and detect at the other. For our work, the samples are typically 1 – 2 mm on an edge.

[Transparency 8]

This transparency shows a typical frequency scan. We focus attention on a few resonance lines and for those lines we measure the Q as a function of temperature.

[Transparency 9]

The first system I want to discuss is Laves-phase TaV_2. These materials were prepared in Ekaterinberg, Russia, at the Metals Institute there. Many Laves-phase materials absorb hydrogen readily. One reason for the high absorption is that the Laves-phase structure has a high number of interstitial sites. A second reason is that the chemistry is often favorable. Elements such as tantalum and vanadium tend to absorb a lot of hydrogen. The interstitial sites are illustrated at

16

the top part of the transparency. The large number of tetrahedral sites favors hydrogen absorption. The network of the sites is such, apparently, as to favor mobility, because some of these materials show exceptionally high hydrogen mobility.

There has been previous work on C-15 Laves-phase materials by the two complementary techniques I mentioned earlier, quasi-elastic neutron scattering and NMR. For several of those systems the previous work indicates that there are two types of hydrogen motion, labeled, "fast" and "slow."

The interpretation of that motion has been as outlined in the bottom part of the transparency. The diagram gives a two-dimensional representation of the interstitial sites. As we can see from the diagram, the interstitial sites form a series of linked hexagons. The interpretation of the previous work has been that the fast motion corresponds to hydrogen zipping around within one of the hexagons, while the slow motion corresponds to the occasional hop to an adjacent hexagon. The origin of the difference in rates has to do with the distances between interstitial sites. The distance between interstitial sites is less within a hexagon than the distance between adjacent hexagons.

The previous work did not resolve these two types of motions very cleanly. For example, in NMR relaxation data the fast rate just appears as a shoulder on the slower rate. One objective of our work was to see if the effect is observable with ultrasound, i.e. does this motion couple to the ultrasonic strain. A second objective, assuming the effect is observable, was to better resolve these two motions. We expect that we might be able to achieve the second objective because our measurement frequency is much lower than those of the other techniques so that the effects may occur at well-separated temperatures.

[Transparency 10]

This transparency presents ultrasonic attenuation measurements at several frequencies for two different concentrations of hydrogen in TaV_2; we have $TaV_2H_{0.34}$ at the top and $TaV_2H_{0.53}$ at the bottom. There is not very much difference in the results for those two different concentrations, so I will not focus on the concentration dependence.

The measurements extend from about 15 K to about 325 K. Although not shown, measurements in the hydrogen-free material did not give a peak, there was just a flat background. Thus, we attribute these attenuation peaks to the motion of the hydrogen. The peaks behave as expected for thermally activated processes; they shift to higher temperatures

17

with higher frequencies. The solid lines represent fits to the data, and the fit parameters suggest that this is the slow motion that was talked about earlier, not the fast motion.

The conclusion at this point is that there are at least two possibilities why we did not see the fast motion. One reason might be that the fast motion remains much faster than our ultrasonic frequency throughout this entire temperature range in which case we would not see it. The other reason might be that this motion is only weakly coupled to the ultrasound so that the effect is just too small to see.

[Transparency 11]

This transparency shows results of experiments on the deuterated material. The initial experiments, shown on the top part of the viewgraph, extend down to only about 115 K and go up to 325 K. We see similar-looking thermally activated peaks as for the hydrogenated material. The solid lines represent fits to the data, and the fit parameters indicate that these peaks are due to the slow motion. At this point we were about to stop the experiments concluding that we could not see the fast motion. However, we decided to extend the experiments on the deuterated material to lower temperatures. The results are shown on the bottom part of the transparency. Notice that the vertical axis here is quite expanded as compared to the top plot. The green points represent the hydrogen-free material; it is essentially a flat background. The red is the material with hydrogen, which shows the beginning of the high-temperature peak at about 150 K. The deuterated material, represented in blue, shows the high-temperature peak beginning at about 200 K, but in this case the attenuation rises again at low temperatures – below 50 K. We believe that this low-temperature component to the attenuation represents the fast motion for the deuterium. The reason we see this effect for deuterium and not for hydrogen is most likely due to the fact that the deuterium moves more slowly than the hydrogen. This difference would be expected if the motion is due to tunneling. Most likely the hydrogen motion remains fast compared to the ultrasonic frequency throughout the entire temperature range we investigated. We conclude that we have resolved the two types of motion – fast and slow – for the deuterium. We were able to do this because the experiments were done at low frequencies compared to other techniques which meant that everything shifted to lower temperatures. Since the two processes have different temperature dependencies, they split apart.

I am going to skip a discussion of the fitting parameters for the high-temperature peaks for the TaV$_2$ materials and go to the other system we studied, which was a titanium-based quasi-crystal and a crystalline approximate.

[Transparency 12]

These materials were prepared by Ken Kelton's group at Washington University. His group has shown that these materials can absorb substantial amounts of hydrogen, up to a hydrogen-to-metal ratio of 1.6. There has not been much study of hydrogen motion in these materials, because it is relatively new to put hydrogen in them (there has been a preliminary NMR experiment). These materials are interesting for several reasons, including the fact that we can look at hydrogen motion in a nonperiodic potential. We studied two different materials, an icosahedral-phase quasicrystal (*i* phase) and a W-phase crystalline approximant. The W-phase material is a large lattice constant BCC crystal for which it is believed that the local atomic structure is very close to that of the quasicrystal. H enters, apparently, in solid solution in these materials.

[Transparency 13]

This transparency gives ultrasonic loss data for the *i*-phase material. The hydrogen-free material shows a fairly flat background loss. We also did experiments on samples loaded to a hydrogen-to-metal ratio of 0.79. There are fairly large attenuation peaks with the hydrogen, and these peaks shift to higher temperatures with increasing frequency as in a thermally activated process. The solid lines are to guide the eye, they are not a fit to any theoretical model. The general shape of the curve, however, suggests that it will not be possible to fit those data with a single activation energy. Most likely several, or a distribution of, activation energies will be needed.

[Transparency 14]

We also did measurements on the crystalline approximate phase, the *W* phase. The hydrogen-free material shows a relatively flat background loss. The material loaded to a hydrogen to metal ratio of 0.20 gives large ultrasonic loss peaks. In comparing results for the two materials we see that the loss is higher in the *i* phase than in the *W* phase, probably reflecting the higher hydrogen concentration (0.79 as compared to 0.20). The hydrogen motion is faster in the *i* phase (the peaks occur at a lower temperature for a given frequency). Whether this faster

motion is a concentration effect or reflects some basic difference between the i and W phases cannot be determined from the present results.

The work on the quasicrystalline materials is of a preliminary nature. Our work is the first to apply ultrasonic methods to the study of Ti-based quasicrystalline alloys. Only recently has it been possible to load these materials with hydrogen in the bulk form needed for the ultrasonic work. We plan to do experiments where we have the same hydrogen concentration in the i-phase and W-phase materials. In that way we can use hydrogen as a probe of the local structure. If the ultrasonic attenuation results are different for the two materials when the H concentrations are equal, that will imply that the local structure in the two materials is different.

[Transparency 15]

The final transparency summarizes the results. In the $TaV_2D_{0.17}$ system we find evidence for two types of D motion with two different characteristic frequencies. RUS was able to resolve these two components of the motion.

The present work represents the first ultrasonic, or mechanical spectroscopy, study of hydrogen motion in quasicrystals. The results for the i-phase and W-phase materials, loaded to different hydrogen concentrations, are different and suggest future experiments to study this effect.

RUS is a sensitive probe of internal motions in solids. In addition, the RUS experiments occur in a frequency range which is a nice complement to other techniques.

Thank you.

DR. BASS: I will start with the first question. How do you control the amount of hydrogen in these samples and how do you know what it is?

DR. LEISURE: The materials were prepared at Washington University by Ken Kelton's group. They shipped the samples to us. We prepared parallelepipeds and made the RUS measurements on the bare material and then shipped the parallelepipeds back to Washington University to be loaded with hydrogen.

To get the hydrogen to go into these materials they put on a very thin coating of palladium, palladium soaks up hydrogen very readily, and that helps the hydrogen go in. I think they just put the palladium-coated materials in hydrogen gas and raise the temperature.

The hydrogen concentration can be determined quite accurately by measuring the weight gain of the specimen. They are also able to determine how much hydrogen gas is absorbed by monitoring the pressure in a known volume.

In some other hydride materials, where the lattice parameter is well-known as a function of concentration, the concentration can be determined by x-ray measurements of the lattice constant before and after hydrogen absorption.

DR. OGI: How was the activation done?

[Transparency 16]

DR. LEISURE: We determined the activation energy for H and D hopping in TaV$_2$ by fitting the data to an Arrhenius-type expression. In fitting our data, taken at about 1 MHz, we also took into account NMR measurements which were made at around 20 MHz. For H we found it necessary to include two Arrhenius processes to fit results for both types of experiments. The parameters for the two processes are given on this transparency. We "hand-wavingly" attribute these two processes with high activation energy and low activation energy to excitation to some excited state in the well and then tunneling through, and tunneling from the ground state, respectively. For the deuterated material we found that just one single process was sufficient for a description of the data.

Why would the deuterium be different from the hydrogen? If we are right that this second process for H is tunneling through the ground state, then this process might be suppressed for deuterium. Tunneling is highly sensitive to the mass of the tunneling particle and deuterium has twice the mass of hydrogen

DR. MIGLIORI: I just want to make the comment that using transducers very similar to the ones you used we recently saw a Q of 105,000 on *[inaudible]*. It just tells you that when you are measuring Q's around 1000 to 10,000 you are probably pretty accurate. The instrumental losses are really low compared to the material losses.

DR. LEISURE: Right. Usually we are looking at just changes in Q, not absolute value, and we hope that any instrumental part is just a steady background, but certainly low is better than high in that regard, and it is good to know that that is the case.

DR. DARLING: At the 2 frequencies of lines emitted, did you also determine that they had different mode types, so for instance, on the quasi-crystal was there a difference between

longitudinal mode Q's and transverse mode Q's? With a complex crystal structure you may change the energies of the fast and slow modes differently with different types of motions.

DR. LEISURE: We did determine the modes for the lower frequencies. Some of the results I put up were at about 2 MHz and I do not think we determined the modes to that high a frequency, but for the lower frequency ones -- well, for the first 45 to 50 resonances, we identified the modes, but I do not have that information with.

My general picture, which may be incorrect, is that different modes will usually reflect the same motion, but the coupling constant will almost surely be different. In looking at different modes, the peak height of the attenuation peak may be different due to the different modes and different coupling, but I think, unless there is really something strange going on, that the actual shape of the curve should be the same for the different modes, because I think that is just reflecting the same hydrogen motion.

DR. SACHSE: In your experimental setup you had a source and then the transducers and the parallelepiped and receiver. Did you actually record the original waveforms or did you have a commercial system that mapped out what were the amplitudes of the various modes?

DR. LEISURE: We used the DRS system, which records the in-phase and out-of-phase parts of the signal and computes Q. We did something else for the quasicrystals. These are small samples, and when the attenuation gets very high we have problems with some coherent background feeding through. We modeled that coherent background and then fit each individual scan to a Lorentzian line shape plus some coherent background. We determined the Q from such a fit. We did not do that for the TaV_2 material, but the scatter could probably be improved if we went back and did it that way.

Thank you.

INDUSTRIAL APPLICATIONS OF RUS

FRANK WILLIS
DYNAMIC RESONANCE SYSTEMS, INC.

ABSTRACT

Although most attendants of this meeting are concerned with the attribute of RUS that apply to the determination of elastic properties, it should not be forgotten that the major industrial use is part sorting based on mechanical property differences. RUS is rapidly being accepted as an industrial tool for nondestructive testing. Many industrial installations are now in existence, which help define the space for the best applications. The primary uses of the DRS Q9000 is for quick and accurate pass /fail testing. The Q9000 is an effective system to detect defects in ferrous and nonferrous metals, ceramics, and sintered metals. The DRS Q9000 can accurately and economically test parts for cracks, dimensional variations, proper heat treatment and plating thickness. Often a single measurement cycle or scan across a specified frequency range provides sufficient data for multiple tests The Q9000 serves as a stand-alone audit center, providing fast analysis for audit and pre-production verification. By integrating the DRS Q9000 to an assembly or machining center, the Q9000 system can provide 100% in-line testing. Specific examples will be discussed, especially where no other NDT methods were previously successful.

TRANSCRIPT

DR. WILLIS: I am Frank Willis from Dynamic Resonance Systems.

[Transparency 1]

I will start with a little background on the company. It was founded almost two-and-a-half years ago and I have been there for a little over two years myself. We are manufacturing two RUS systems. It is basically identical electronics with small differences in the software. I know a lot of the people here have one of the systems that we call the Modulus 1 for basic research.

We also have another system that we call the Q9000, which we market toward industry. The purpose of that system is as a quality-control aid during manufacturing to separate good parts from parts that contain some sort of defect.

23

I am going to tell you a little bit about some of the types of defects we look for and some of the existing methods -- quality control has been a topic for several years -- and, finally, how we are using RUS to solve some of these problems.

[Transparency 2]

The primary defects that people are trying to look for include things like cracks in a part that has been manufactured. That may be a chip when a part is pulled out of a mould or from just rough handling. Sometimes dimensional variations are considered a defect; if you want parts to fit together properly they have to be the right size.

We have an application in process right at the moment for the actual composition of the material that can be incorrect. There is an application we are working on now for companies manufacturing brake rotors. From time to time, they get the wrong alloy of steel in. It is not really something that is going to lead to a failure of the brake but it is more of an annoyance. If they get the wrong alloy to make the rotor out of, the brakes may squeal or chatter, which is something the end consumer does not like, anyway.

One of the things we have been asked to look at several times now and really have had a tremendous amount of difficulty with is a defect called microcracking, which is a very fine, almost microscopic, networks of cracks in a material.

One of the last things we do is look at the hardness of alloys, for example, to see if the heat treatment has been performed correctly.

[Transparency 3]

These are some of the existing systems that we run into from time to time. The list is not exhaustive by any means but it seems to be the ones that we bid against quite often.

One of the most common ones seems to be eddy current that, as its name suggests, uses eddy currents induced in a metal to look for cracks, primarily. The limitation there is that it obviously works on only materials that conduct electricity.

One of the other things we run into quite often is dipenetrant, where you simply soak a part in a vat of dye (usually a dye that fluoresces under an ultraviolet light), soak the part and, if there are any cracks, the dye will seep into the crack and you wipe it off or rinse it off and then look at it under an ultraviolet light. It is a very simple idea and it works quite well in a lot of cases.

It does have the one problem that eventually you have to get rid of the dye. If you are rinsing the parts off with water you have a weak concentration of dye in the water. If you are

wiping it off with a towel, you have to get rid of the towel or wash the towel. While the dyes are usually fairly nontoxic these days, they still have to be disposed of.

Another technique we run into is called mag particle, which I think is really quite similar to dye penetrant, but it uses the magnetic field to concentrate particles in cracks, and then there is a visual inspection, usually under an ultraviolet light, again, to look for these particles left behind in the crack.

Of course, there are things like x-ray that can be used to look for cracks.

Two of the problems with a lot of these techniques is that they are slow. It may take a minute or so, or even longer, to inspect each individual part. If you are sitting there having a person looking at it, it takes a while.

A related issue to that is it works only as good as the person you have looking at the parts. I imagine the quality can vary a lot from, say, 10 o'clock on a Wednesday morning to 4:30 on a Friday afternoon.

[Transparency 4]

I think resonant ultrasound was first used about five years ago to look at parts by another company and it solved some of the problems of the other methods; it is not perfect by any means itself, but it works in a lot of cases that the others do not.

It works on a lot of different types of materials. We have looked at ceramics, metals, glasses, for example. Really, anything that has a nice acoustic response is a candidate for this technique. Occasionally we get plastic parts that just do not ring at all.

There is really nothing to dispose of. There are no dyes, there are no x-rays floating around that you have to worry about being certified to track. We have even gone to the point of having the system tested for RF exposure and certified that the RF leakage out of the system is within allowed limits.

One of the problems with systems that rely on a visual inspection somewhere along the line is you are going to be able to see defects only on the surface of the parts. The surface may look perfectly fine and you have a gigantic crack right under it that you just do not see, but RUS is sensitive to those types of defects as well.

Finally, it can be completely automated. There are instances where people do what we call a manual pick and place, where a person simply picks up a part and places it on a transducer

assembly, hits a button, records the result, and then repeats that process. It can also be fully automated so that a person does not even need to sit around and watch it.

[Transparency 5]

When we are looking at a part with RUS for nondestructive testing, we have to start with some sample of the manufactured parts. At this point we have to have a set of parts that are free from defects or at least defined to be good and a set of parts that contain the defect.

We have been working on some ways to just look at the good parts without having the bad ones and we have made a little bit of progress in that, but it is not entirely usable yet. We look at the resonance spectra between the good parts and the bad parts and try to find something in the spectra that is common to the good parts but different amongst the bad parts, and then we sort the parts based on that pattern.

It is very important to know that even what we call good parts may very well contain defects. Quite often a crack may be acceptable as long as it is below a certain size, where a chip may be acceptable if its size does not exceed some critical value.

[Transparencies 6-7]

When we are looking at these patterns, right at the moment we have 6 tests that we can apply to the patterns. The first one, and it is relatively common to use it, is just a simple position test. The good parts may have one resonance between 100 and 105 kHz and the bad parts do not have a resonance in that region.

I really do not like using just one of these tests. It is not inconceivable to think of a bad part being defective in a certain method, but it just happens to have a peak in that one region where you are not expecting it. When I do use this test, I usually use a combination of two or three of them to try to avoid that little statistical possibility, which happened to me at a customer site one day.

There was a sheet about half the size of an 8 x 11 piece of paper, a ceramic, and they brought one out and there was about a quarter of it missing. I warned them that it was a pretty simple test and, sure enough, it had a peak right in this window where we did not want one.

Another very useful test in these patterns is what we call a doublet test, which is where you have 2 peaks very close together and if you think about the symmetry of parts, for example, if you have something with a square cross- section, you are going to have 2 resonances at the same frequency, but then you never make anything that is an exact square, so 2 resonances will split

apart by some small amount and you can use that difference to look for other defects that may break the symmetry.

[Transparency 8]

Just to wrap up the final tests that we use, this first one I have listed here, the linked test, is a way of looking for 2 resonances that we just notice have a mathematical relationship between them. We usually look for a linear relation between 2 peaks. I have never really had any need to use any relationship more complicated than that.

It is useful, because we can often use that to correct for small variations in density or small variations in dimensions. We measure one peak and then, based on its position, we can predict where another peak should appear.

The last 3 tests that we have built into the software really are not used very much, oddly enough. Q is a test on the width of a peak of a specific resonance. It is useful sometimes, in particular when you have a relatively large crack in the part. If you have a large crack, you get a large change in Q, and we can use that.

One of the 2 other tests, that I cannot say we have ever really used, is amplitude. I think most people here can imagine the difficulties in trying to measure the amplitude of a particular resonance. It is very dependent on the exact placement of the transducers on the parts.

Our system does measure both components of the response and, in principle, we could use the phase of the resonance to look for defects, but we have never been successful in doing that, either.

[Transparency 9]

I am going to move on to a couple of actual applications now. This first one was a ceramic gas seal, kind of like a ceramic o-ring. It was about a 14-mm-diameter-o-ring, a little over half an inch. One of the things I eventually found out about this part was the tolerances on some of the dimensions were plus or minus 6/1000 of an inch. In industry you often get a curious mixture of metric and English units. They give you diameter in millimeters and tolerance in thousandths of an inch. (Laughter)

Anyway, this was an interesting part, in that I was actually able to see a correlation between the size of the chip missing out of the part and the separation of a doublet. The bigger the chip was, the farther apart these 2 peaks spread. It is something we do not really look for often, but I just happened to notice it in this.

27

The reason I noted the dimensions on here, if you took the diameters in thickness of this part and varied the dimensions by 12,000th of an inch, which was the allowable extreme, it worked out to change in volume of about 9 cubic mm, which really surprised me, that it was that large.

The problem with this part was we could find the big chips but we could not find these little tiny chips that they wanted to find. I started to think about it and eventually realized that a change in volume of 9 cubic mm would be about the same as a 2-mm-diameter chip; that is, if you took the chip as a half sphere.

I calculated that just because of variations from part to part maybe about 2 mm would be the smallest we could find, but then in actually looking at the parts I was able to detect chips down to 1 mm in diameter. One of the obvious ways to reconcile the differences there is a change in diameter is probably a symmetric change, while a chip is probably not symmetric.

[Transparency 10]

Here is a picture of the actual part sitting between some transducers. It has flat faces on this side that form an airtight seal.

[Transparency 11]

These are the sorts of data that I ended up using to set up the test. This is a snapshot of the software that we use. The software is set up to stack the resonances on top of each other, so the top 3 resonances are from these rings that were defined to be good, and the bottom 3 resonances are from these rings that obviously had a chip in them.

As you can see, in the 3 good parts we have a very narrow doublet. In one case the doublet is so narrow you do not even see it (you see just a single peak, which happens from time to time). In the bottom 3 scans for the bad parts you can see the doublet actually became separated by some noticeable amount. We were able to look at the separation of that doublet and make a decision as to whether this part was acceptable or not.

DR. ISAAK: Can you quantify by looking at that separation of the bottom spectra how much it was off?

DR. WILLIS: It was not an exact number by any means, but I did notice that -- it is difficult to measure the size of a chip, there are different depths and they are never circular, they are elongated sometimes. It appeared to me that the more volume that was missing out of the

part, the wider the separation was. I do not have a number for how many millimeters or how many hertz, but it certainly appeared to be that way.

One of the unfortunate things is that we get these parts in and we get data like this and, in this particular case, the company wanted the parts back. They were building an automated system and they wanted to check it to see if it was working properly. In a lot of cases I have a small amount of data archived and I do not have the luxury of going back to reproduce more of them, but I wanted to try to do that a little more quantitatively, because it is one of the few times I have really seen that.

[Transparency 12]

One of the other applications we have under way right at the moment is machined steel bearing race. The problem here is what the company that manufactures them calls grinding burns. The bearing race is a piece of steel that is ground with a grinding wheel. The people who typically do this sort of work, who run the machines, often get paid by the piece, so they try to cut corners and make a few more per hour to get their paycheck up a little bit by the end of the week, and they get the grinding wheel running too fast and it heats the steel and creates a grinding burn.

It is probably, if anything, a hardness variation over a small area on the part, and it is something that is very difficult to detect by any other method. Visually it looks just the same as the rest of the material, you do not even see it, or at least only with great difficulty.

Things like dipenetrant do not seep into it, so you cannot do that, but since it is a hardness variation, which is basically a change in the elastic constants, RUS is a natural candidate to look for these sorts of defects.

In this particular case -- I mentioned earlier that I do not like using one test, often, I just think there is a statistical chance that a bad part will happen to look like a good part in that case -- I actually used 2 resonances that did not seem to be correlated between themselves and I was able to get a much better sort than using either of the resonances individually.

[Transparency 13]

Here is a picture of this part, a steel race sitting on some transducers.

[Transparency 14]

Here are a few of the data that we took on that. Again, the top 3 scans were from supposedly good bearing races that had a resonance at a slightly lower frequency than the ones we were told had grinding burns in them.

Resonant ultrasound for testing parts is relatively new; it has been around for a few years. I did not want to give you the idea that it is an absolutely perfect system yet; we have a lot of problems that we are working through. One of the big ones is simply pattern recognition.

[Transparency 15]

We get the spectra and there is a tremendous amount of data to look through to look for these differences in the patterns. It would be really nice to have an automated software package to look for these patterns and generate the tests, and we are working on something like that, and I have got at least the prototype of a package like that.

One of the problems in writing a pattern-recognition package is the peaks do not line up even amongst the good parts, for example. If you had 2 perfectly good parts, the peaks would line up, hopefully perfectly, but since there are differences in dimensions and composition you get basically the same pattern, but they will shift, so it may look like these 2 peaks are the same peak, when, really, it is these 2, and that is the first problem you have to overcome.

Again, we have differences in dimensions, which may mean that sometimes you see more peaks than you do in other parts. Parts are often big, which means the resonances are very low frequency. To me, a high frequency may be 100 kHz, which probably sounds low to a lot of you, but we are looking to get down into probably the hundredths-of-hertz region. It is difficult enough finding one test, much less trying to find multiple tests.

[Transparency 16]

There is one type of material in particular that seems to give us more trouble than others, and this is a process called a powdered metal part, where you take a metallic powder and mix it with a resin in a mould to make the part and then bake the part in an oven to cure it. For some reason we have a lot of problems with those.

The patterns, even amongst the good parts, just do not line up. Of course, the good parts have to be more consistent than the defects you are looking for. I do not know if it is a composition problem or a dimensional problem; we just really have not figured that out yet.

For all the parts we look at, one of the problems we often run into is that a customer will send us a box of parts and say these are all good, and you take maybe 10 or 20 good parts and

you start looking at the patterns and you will find one of those parts just does not look right, so we go back and start looking at it under the microscope, or we have dye penetrant ourselves that we can look at it with.

Probably, I would say, in one out of three cases, perhaps, we are actually sent parts that have a defect that just got through the process before, so sometimes we do not even get a perfectly good set of good parts to look at.

[Transparency 17]

Some of the things that we are working on right at the moment: We have 2 systems, the Modulus and the Q9000. I am working on systems right now to go to lower frequency. I have a need to go down to at least 500 Hz, and I would like to get down to about 100 Hz some time soon.

We are looking at doing what I call a broad spectrum RUS and, rather than driving a part at one frequency and measuring the response, we will drive it at a lot of frequencies and measure the overall signal onto an FFT to get the spectrum and, of course, pattern-recognition software is in the process of being developed.

[Transparency 18]

Just to finish up here, I think in the future we are going to see tolerances on parts are going to become tighter and tighter, the materials are going to become more consistent -- hopefully, that is the problem with powdered metals (I do not know) -- and even the machines that we use to manufacture parts will be improved.

I think all of these things will make the parts themselves more consistent amongst the good parts, more accurate, and that is going to make RUS easier to use to sort these parts.

Thank you.

DR. MCCALL: For all of the ways that you test parts there must be a rate of bad decision? No matter what you do, there is a certain number of bad parts that get through? When you set up a system for industry, is your rate of bad decisions about the same or better --

DR. WILLIS: About the same as what?

DR. MCCALL: Dipenetrant or whatever other system you might use.

DR. WILLIS: Whenever you ask a manufacturer about these rates that you are talking about, you ask how many of the good parts must I pass and how many of the bad parts must I catch, every one of them will tell you that you have to pass 100% of the good parts and you have

to fail 100% of the bad parts, and I tell them to go away and come back and talk to me when they have realistic numbers.

With this bearing race, I think looking at 30 or 40 parts statistically, the distribution of the frequencies and the standard distributions, I think I predicted we would pass about 99.5% of the good ones and we would fail something over 99% of the bad ones.

The related question to that is if you fail 99% of the bad ones, really, how many bad ones per thousand parts get through, then? In this particular case I think it came down to either 8 or 17 bad parts out of every 10,000 parts manufactured would get through.

Thank you.

Thin Film Characterization Using Resonant Ultrasound Spectroscopy

J. D. Maynard and Jin-Hyun So
The Pennsylvania State University

Abstract

With the development of mesoscopic and nanoscale electronic systems, there is currently great interest in the properties of the thin films which form the environment for the electrons. Diamond-like carbon films have also attracted attention for use as a protective coating against physical damage to delicate electronic components. As with bulk solids, important properties include elastic constants and acoustic attenuation, which may be related to the electron-lattice coupling and other effects. By using resonant ultrasound spectroscopy (RUS) and comparing the normal mode frequencies of a specimen before and after film deposition, the elements of the elastic tensor and attenuation coefficients of the thin film material may be determined. With the ability to perform RUS on samples as small as tens of micrograms, the possibility of examining the properties of thin films is feasible. In order to detect the properties of a thin film using RUS, it is necessary that the substrate supporting the film not dominate the measurement. Numerical estimates show that using substrates with sizes on the order of 500 x 400 x 100 microns enables the study of films as thin as 100 nm.

Ideally, the study of a film should be made by measuring the resonances of the bare substrate, then depositing the film while the sample remains in the RUS apparatus, and then measuring the frequencies shifted by no change other than the film deposition. Unfortunately, most film depositions require geometries or hostile conditions (e.g. heated substrates) which cannot be accommodated with the substrate still mounted in the RUS apparatus. Thus the substrate must be removed for the film deposition, and then replaced. In order to determine changes due to the film alone, it is necessary to demonstrate that simply removing and replacing the bare substrate produces no significant shifts in the measured frequencies.

We have performed numerous tests by measuring substrates before and after several removals. We have found that the frequencies for samples with only moderate quality factors, Q of ~1000, cannot be reproduced with accuracy sufficient for studying thin films; the problem is

not just the width of the resonance peaks, but also the difficulty in fitting the lower level signals with a changing background. However, Q's of ~10,000 are reproducible with more than the factor of ten improvement because of the reduced effect of noise in fitting. We have found that our original choice of substrate, silicon, was unsatisfactory, and has been replaced with strontium titanate.

TRANSCRIPT

DR. MAYNARD: This is some research that was started by a graduate student, Jason White, and we are now getting a lot of help from a postdoc, Jin-Hyun So.

[Transparency 1]

The objective is to study the physical properties that are related to elastic constants and damping. We are doing this for thin films that are deposited on some substrate.

There are some important applications of thin films, of course. There are thin films in magnetic recording media. These can involve more exotic magnetic materials like materials that show colossal magneto-resistance, manganites, and so on.

Also, thin films are used for protective and lubricating coatings, for example, diamond coatings, even quasi-crystalline coatings, and carbon nanotube films (I will say more about carbon nanotubes later).

Also, some important films are superconducting films, in particular, high-temperature superconductors and, also, of course, there are micro- and now nanoelectronic applications.

[Transparency 2]

There are some important scientific issues. For example, the physics is changed by having a thin film, because, for one thing, you have reduced dimensionality. If the thickness of the film is less than some characteristic length, like a coherence length, then the system really does behave as though it were two-dimensional. Of course, in physics the dimension of the system is a very important parameter.

Also, you can have some influence from the substrate. For example, you can have strain or disorder induced into the film because of lattice mismatch with the substrate, and that is very important, and you can have magnetic interaction between atoms or magnetic ions in the film and magnetic atoms or ions in the substrate.

34

You can also study novel properties of unique systems -- here, once again, are the carbon nanotubes (they are a hot topic in physics these days). Also, you can determine properties for practical applications such as elastic constants and hardness of a film, also its effect on friction and damping.

[Transparency 3]

The approach that we use, of course, is resonant ultrasound spectroscopy to measure the elastic constants, all of the elastic constants, for the film and for the damping of the film, and we assume that the properties of the substrate are known. I guess I do not really have to describe how RUS works here.

[Transparency 4]

The measurement for films is a little different from just single samples. What you do is you make a measurement on the substrate and determine its natural frequencies. Then you put a film on the substrate, the same substrate, and then measure changes in the natural frequencies, and from the changes in the natural frequencies you can determine all the elastic constants for the film.

In order for this to work, the film had better occupy some substantial fraction of the size of the sample. Just based on our experience of determining the precision of measuring the natural frequencies, we figure we should be able to measure a film that is only one part in a thousand of the thickness of the substrate. For example, we should be able to measure a 100-nm film on a 100-micron substrate (in other units this is 1000 Å on 1/10-mm substrate).

It is not too hard to get thin substrates, but if you have a film whose elastic properties are anisotropic -- for example, a high-temperature superconductor has certain elastic constants in the planes but quite different properties perpendicular, which would be the thin dimension of the film
-- you want to try to measure these elastic constants over the thickness dimension of the film.

In order to do that you would like to have the lateral dimensions of the substrate to be small as well, and I will just elaborate on that.

[Transparency 5]

Here is the substrate that has lateral dimensions that are only a little bit larger than the thickness, but if you look at the modes, most of the modes are pretty much just plate-like modes. If you went to a mode where you were accelerating the thickness of the film in order to measure

its elastic constants across the thickness of the film, you would have to go to very high frequencies.

If you did that, you would have such a high density of modes from these plate-like modes that it would be almost impossible to pinpoint the right frequency and measure the thickness modes of the film.

[Transparency 6]

What you need to do is to have a sample, like a normal RUS sample, where the dimensions are all comparable. In that case you can excite modes that have all the dimensions involved in the normal modes and in that case you will be accelerating the film across its thickness and you can measure the thickness elastic constants.

[Transparency 7]

Just by a lucky chance we happened to have an apparatus for measuring very small samples. You need to sample where all 3 dimensions are on the order of 100ths of microns.

This looks like just an ordinary RUS apparatus, except that the size of the sample here is just a few hundred microns. Key elements in this apparatus are the transducers. If you have a small sample, then you need small transducers.

[Transparency 8]

For transducers we used piezoelectric film (just a plastic film like Mylar) polyvinylidene fluoride, PVDF (the trade name is Kynar), and you get it commercially in sheets that are only 9 microns thick.

The way we make our transducers is we take a sheet of this PVDF that is a few centimeters on a side and we evaporate gold conducting coating up to a line on one side and then, on the opposite side, we will evaporate the conducting coating up to a line so that they overlap by about half a millimeter. Then we take a razor blade and cut off a strip that is about a half-millimeter wide.

If you look at the edge of this strip with the greatly exaggerated thickness (this is really only 9 microns thick), where the 2 conducting coatings come in they form the leads to the transducer and where the conducting coatings overlap they form a little capacitor with this piezoelectric film in-between. This little half-millimeter square is the active area.

36

The properties of the PVDF are very nice. It has quite high piezoelectric sensitivity, but, also, its Q is very low, which is good for resonant ultrasound applications; you want the sample to resonate and not the transducers.

[Return to Transparency 7]

In this picture these strips here are the strips of the piezoelectric film and the active area where the conducting coatings overlap is shown by this red area here.

To mount the samples -- our samples look like a speck of dust (in fact, we have lost a lot of samples) -- (Laughter)

In fact, we made this special white box that is all clean inside, with sides, and we have to work inside this box, and you have to mount the sample -- we have a fine hypodermic needle that we pull a little vacuum on and then we get the sample sucked down inside this hypodermic needle and this little micro-manipulator positions the sample.

One of the transducers is on a block with a lead screw, so then we just bring up the second transducer until we just catch the sample to hold it between the transducers, just support its weight. The smallest sample we have measured so far is one that weighed 70 microgram -- it got lost. (Laughter)

[Transparency 9]

Here is a picture of one sample. This is actually a very large sample for us. This is a ruler and these are the millimeter lines on a ruler, so one of the dimensions is almost a millimeter but the others are smaller.

[Transparency 10]

Here is a more typical sample. It is not much bigger than the actual millimeter markings on a ruler.

[Transparency 11]

Now we need to address the feasibility of being able to measure thin films. We can measure small samples, 70 mcgm, 100-micron-sized samples, but can you still measure a film on such a sample?

Here I let the elastic constants for the film be c_{ij}', and c_{ij} will be just the elastic constants for the substrate. We wanted to determine with what precision we could measure the elastic constants of just the film. That is given by this expression. It is just proportional to the precision with which you can measure the natural frequencies.

You divide by this factor, which is the rate of change of the frequencies with respect to the elastic constants for the film, and it is normalized this way. This is something you can calculate with a RUS program that is set up to do a layered sample.

How well you can measure the elastic constants of the film depends on the precision with which you can measure the frequency. Usually in RUS, with a good high-Q sample (Q of 100,000), you can measure to a part per million, so this looks as though it ought to be pretty easy.

However, in the process you need to measure the substrate without the film and then measure it with the film. There are some cases -- in fact, probably most cases -- where you cannot actually deposit the film while the sample is in the RUS apparatus, you have to take it out.

For example, for most of these films we are studying, high T_c superconductors and the colossal magneto-resistance materials, the substrate has to be heated up quite high before you can evaporate the film on it, so you have to take the substrate out and deposit the film and then put the substrate back in.

The precision with which you can measure the frequency is determined by how reproducible it is to take the substrate out and, say, just put the same substrate back in and see how well you can get the same frequencies. That was the first part of our research program.

[Transparency 12]

Here is one of our samples. These are the different modes and these are the resonant frequencies the first time the sample was mounted, the second time it was mounted, and so on. We actually mounted the silicon sample nine different times.

Here is the average of all the different mountings and the reproducibility of the frequencies in parts per million. You can see here that it is a couple hundred parts per million reproducibility from taking the sample out and putting it back in, which is actually a fairly involved process.

You might think a few hundred parts per million is pretty good if you were measuring the elastic properties of the silicon, but we need to measure a film that is only 1/1000 the size of the whole sample. In other words, you have to take these numbers in parts per million and multiply by 1000 to get the precision with which you can measure the film.

Then it becomes a few hundred parts per thousand, which is only 20 or 30%, which is not really good enough.

The silicon did not work very well. You notice the thickness of the silicon was 97 microns (it was normally a 100-micron-thick sample).

[Transparency 13]

It turns out that the substrate of choice for high-T_c conductors and the manganite films is actually strontium titanate. So we got one of those samples and put it in and the Q's were much higher than with the silicon. Now we are getting, for mounting and remounting this strontium titanate sample -- and we did 4 different samples, and these are typical data, namely, the best data we ever got (actually, it is typical) -- 10 parts per million.

We have now measured this for each one of the different modes and we can calculate this with our RUS program for films to find out what that precision is.

[Transparency 14]

This is a strontium titanate sample, which in this case was 400-and-some microns thick, and the film on it (which is actually one of these manganite films that is 450 nm thick, so it is about a part in a thousand).

Here are the different modes and their frequencies. We also take the rate of change of the frequencies with respect to the film thickness. You can see that for a film that is a part in a thousand of the sample this number is about 10^{-3}.

These numbers are from that formula. This is the precision with which you can determine C_{11}, given the different modes. This is taking the delta f/f that we measured and dividing by that derivative. What dominates here is the smallest number. We can measure C_{11} with just one mode to a couple of percent.

You are actually going to be taking a least-squares fit of the measured frequencies so, actually, you can determine these to better than these numbers, so just a few percent. In fact, you cannot measure thickness to much better accuracy than a few percent, so it seems as if it is feasible.

Now what I would like to do is to go over the modifications to the algorithm for doing films and I just want to do this kind of quickly, just to show you how easy it is to do any RUS program.

[Transparency 15]

No one has done the theory yet, so I will just review it here. You start off with the definition of strain involving the displacements in the solid in the coordinate directions (this i

and j stand for x, y, and z coordinate directions). There is Hooke's law that relates the stress to the strain with the elastic constants. You take that and you put it in Newton's law, you get a differential equation and, to get a boundary-value problem, you need a boundary condition, which is just the stress-free boundary condition. You can get these 2 equations by minimizing a Lagrangian.

[Transparency 16]

To do that, you use the Rayleigh-Ritz approximation. You take the displacement field and write it as a finite combination of some basis functions. Then the Lagrangian takes this form, just a matrix, and you get a mass matrix (this has the mass density in it and an integral of the basis functions), and a stiffness matrix that has the elastic constants in it.

One of the important things in the RUS code is how you do the indexing. You let one index actually represent, like the p and the i here -- p is which of the basis functions you are talking about and i is the coordinate direction, but you can combine those in some clever way, which I will show in a minute.

When you minimize this Lagrangian, you get just a matrix eigenvalue problem.

[Transparency 17]

One of the new ideas, relatively new ideas, was in the early work by Harry Demarest when computers were not so fast, it was convenient to use an orthogonal set of basis functions so that this E-matrix came out to be diagonal. But Bill Visscher at Los Alamos pointed out that if you use a simpler set of basis functions that are not orthogonal but just linearly independent, then you can do those integrals. You get off-diagonal elements in the mass matrix but the integrals can be done analytically for a number of different shapes, including prisms, spheroids, ellipsoids, shells, bells, eggs, potatoes, sandwiches, and others.

Visscher published this code. In fact, our first programs were written by the graduate students and they just looked like a horrible mess to me, but then I saw Bill Visscher's paper and saw how easy it was to do this stuff and then I realized, gee, I could write a program like this myself, so that is what I did.

In this program we found out that if you scale the basis functions with this a, b, and c, which are half the edge lengths of the sample, you get orders of magnitude better conditioning for the matrix, so that is one modification we did to Visscher's program.

The integrals that you have to do are just between limits of -1 and 1. In any case, you get very simple expressions for the integrals that you have to do, analytic expressions, so you do not have to do any numerical integrals.

There are some important consequences of symmetry. It turns out that if the elastic tensor has orthorhombic or higher symmetry (better symmetry), then the matrix that you have to diagonalize becomes block diagonal. This is a consequence of the parity in these basis functions.

For example, if the power here is odd, then this function is odd for plus and minus x. If you have pairs of these functions, if the overall power is odd, then when you integrate from -1 to 1 you just get 0. Because of that parity symmetry in x, y, and z, it turns out that the matrix is 0 everywhere except for 8 matrices along the diagonal. So instead of having to diagonalize a big matrix, you just have to diagonalize a much smaller matrix 8 times and that gives you an almost 8-fold saving in computer time.

That is the basic RUS algorithm.

[Transparency 18]

If you have a film, I define alpha to be the film thickness divided by half the edge length. The zeta here is the film mass density minus the substrate mass density normalized to the substrate. Then we define an elastic constant tensor as the difference between the elastic constants, the 4 index elastic constants, of the film and the substrate. You will see why we do that in a minute.

If you do that, then the integrals that you have to do, the mass integral, the first term is just like an ordinary RUS sample, but then you have a second term that has the difference in mass and for the stiffness integral you have this expression. Again, this is just like the ordinary RUS sample, but there is another term that has the difference in the elastic constants.

These integrals here are done from -1 to 1 in x and y, but from 1- alpha to 1 in z. Because of this different integral in z for the film, it breaks the symmetry in the z-direction. Instead of having an 8-block diagonal matrix you have only 4 matrices on the diagonal and they are larger than the other matrices, but at least you still have a fourfold increase in computation speed.

The next couple of viewgraphs are going to be pictures of computer code.

[Transparency 19]

41

You are not supposed to see anything in the computer code. I just want to show you these to impress you with how really easy this stuff is. Albert is happy to give you computer code, but I am sure he will agree with me that it is better if you are in control of your own computer code.

This part right here is the only part you have to do yourself; everything else comes out of Numerical Recipes. It uses the Levenberg-Marquart routine to least-squares fit the data. This routine over here is Bill Visscher's routine that is published, the actual source code is published.

[Transparency 20]

Just a couple of things to notice: When we scaled our functions we had to add these lines of code here. When you do the 8-fold block diagonal matrix, that is done in these 3 loops here. The 1 and the 2 for each of these variables are just the odd-and-even parity for the x, y, and z coordinates.

When you change to a film, the only change is that instead of doing this 8-fold loop, you do only a 4-fold loop. This last line here winds up over here and you actually calculate the matrix. You get a matrix that is twice as big but you still get the 4-block diagonal matrices.

[Transparency 21]

The other change is that here is where you actually do the calculation with the index elastic tensor. For our modification of the program we just took this, did a cut and paste and reproduced it down here, changed the c's to d's (this is the difference in the elastic tensor), and then there is function, f, which changes to a g. The only difference there -

[Transparency 22]

Here is Bill Visscher's f function (one line, basically), and here is our one line, and here is the 1-alpha. That is the only change for doing a film. It is probably a total of 10 lines of code difference from Visscher's published program for doing films.

[Transparency 23]

I will just mention one of our applications, as I see time is running out. We are doing manganite materials, and that is working very well, we get nice high Q's for the substrate with the film. We are also having a lot of fun doing mats of carbon nanotubes.

If you remember Buckyballs, if you heat up carbon, when the atoms come back together in a partial vacuum, they form these nice geometric clusters. If you do this with metal ions present, then the metal ion will attach to some site so that the Buckeyball will not close, so you get part of the Buckeyball down here but then you get a cylinder that grows, and even though this is maybe

a few nanometers in size, these cylinders will grow to maybe 100 microns in length. It is undoubtedly the strongest fiber ever made.

There is lots of good physics in the way you can roll up these cylinders, there are different ways the cylinders form. You can have a one-dimensional metal or a semiconductor, depending on how they roll up.

[Transparency 24]

They have interesting mechanical properties (there is an article in Physics Today on that).

[Transparency 25]

People have tried to measure elastic constants for single fibers. This is actually a resonant ultrasound spectroscopy measurement, but this was for a multi-walled fiber.

[Transparency 26]

What we are trying to do is to have these carbon nanotubes deposited on a substrate and then you use RUS to determine the elastic constants for a spaghetti of these carbon nanotubes.

We are finding that there are huge differences in damping. Damping can change from a Q of 17 to a Q of 1000 just depending on what kind of exposure this thing has had to air.

That is it. Thanks.

DR. MEHL: Are those nanotubes in some kind of matrix? What is holding them on the surface?

DR. MAYNARD: They have weak van der Waal's bonding forces to the substrate and to each other. You can actually get those mats that are as thick as a micron, which would be pretty thick for our measurements. You have to bake the samples very carefully and that is what we are doing now. We are trying a slow bake at a temperature that does not melt our PVDF transducers. We are also trying to take the sample out and baking it at 400 C, or something, to give it a good surface treatment.

DR. LEISURE: That was pretty much my question, was how those things are bonded to the surface, and are your results affected by how strongly the film is somehow attached to the surface?

DR. MAYNARD: I cannot answer that until we do a complete bake-out of the system. They were shipped to us through the mail -- they were supposed to come in a vacuum container, but they forgot to do that. With overnight express it gets exposed to air a bit.

DR. ISAAK: The bit about the precision with df/dt, did you play around with maximizing the contrast between the substrate and the expected elastic properties of the film? That would increase your df/dt.

DR. MAYNARD: No, in fact, that was for a real sample, that was for a strontium titanate substrate with a manganite film on it.

DR. ISAAK: Yes, but the contrast between those 2 materials.

DR. MAYNARD: I would have to look at the elastic constants.

DR. ISAAK: I mean, if you had a large df/dt, it would improve the precision. You got at it by getting stuff that gave you really high Q's, so you could find the peaks very accurately, right? That would be another way, I think.

DR. MIGLIORI: What was the Q of the strontium titanate there?

DR. MAYNARD: I think there might have been some peaks that were 10^5. We do not quite understand why the silicon was as bad as it was.

DR. MIGLIORI: Was it glass?

DR. MAYNARD: No, these are single crystals. You have to remember that the Q goes like the surface to volume if you have surface microcracks and losses due to that. As the thing gets smaller and smaller, which our samples do, then the Q goes down, so it is not like a millimeter-size sample.

DR. MIGLIORI: We have had awful problems getting high-Q single-crystal silicon samples because of surface microcracking when you polish them.

DR. LEDBETTER: I think you said you measured oxide superconductor films?

DR. MAYNARD: We are going to. The person who was going to give us those films gave us the manganite films instead.

DR. LEDBETTER: If you had measured them, the question would be how do the measured results compare with the bulk properties. Have you made such a comparison for any materials?

DR. MAYNARD: No.

DR. GILBERT: If you do not get the shapes exactly right, those shapes in the pieces in the sample, how does that enter into your calculation, for example? Suppose your measurements are off, how does that affect what you get out of your calculation for the shifting of the resonances?

DR. MAYNARD: I am sorry?

DR. GILBERT: You are at very high frequencies, I would guess much bigger than some of the modes of the shape, and you showed the shapes twisting around, and that depends on having gross geometry of the pieces correct.

DR. LEVY: Do you mean dimensions?

DR. GILBERT: Dimensions.

DR. HARGROVE: Dimensions or parallel faces?

DR. GILBERT: I mean the gross geometry of the sample, how does that affect what you learn about the elastic constants?

DR. MAYNARD: You are not talking about films now, you are talking about --

DR. GILBERT: Just take the sample, for example.

DR. MAYNARD: A lot of this is in Phil Spoor's thesis. For his samples he did a very careful analysis of how parallel and perpendicular the sides were and he had a program where he could put that information in to see how it shifted the frequencies. This was getting absolute numbers out better than a 10th of a percent.

DR. MIGLIORI: But if you have the dimensions off by a 10th of a percent, you may not get a fit; that is, if your mathematical model does not correspond to the real sample, then you will fail. I think there is a straightforward correspondence between dimensional errors and how badly you do.

DR. GILBERT: I guess I could ask one more question. How is what you get from running these elastic constants affected by the shape of the sample? It should be independent of that, right? The elastic constants are a property of the crystal structure, not --

DR. MAYNARD: Oh, if you know the shape of the sample, you get the answer.

DR. GILBERT: Okay, so, in principle, the shape of the sample somehow does not matter if you do everything right.

DR. MAYNARD: Exactly, yes.

DR. SACHSE: It has to be pointed out that the resonant peaks will shift --

DR. MIGLIORI: In fact, a good way to tell whether you know what you are doing is to polish it and measure again to see if you get the same answers.

DR. MAYNARD: Right.

DR. BASS: Thank you, Jay.

Elasticity of Steel and Silica Glass Spheres under Gas Pressure by RUS

Poster Presentation

I. Ohno[1], M. Abe[1], M. Kimura[1], Y. Hanayama[1], H. Oda[2], and I. Suzuki[2]
[1]Ehime University
[2]Okayama University

This was a poster presentation. The poster pages are included in Volume 2 of these proceedings. An abstract for the presentation follows.

Abstract

Elasticity of minerals under high pressure are of great importance from geophysical view point. In order to develop a new method to measure pressure dependence of elastic constants, resonant ultrasound spectroscopy (RUS) were applied to the condition of gas pressure. We used a three-layered spherical shell assembly of spherical sample-thin gas layer-spherical cavity container, which works to give a well-defined boundary condition in the analysis. The samples measured were spheres of steel and silica glass with diameter of 4-5 mm. Several modes, not only torsional but also spheroidal modes, were observed at least up to 200MPa (2kbar) under helium gas pressure, and pressure shifts of frequencies were obtained definitely in both samples. The data of the slope of pressure shift of frequency yield pressure derivatives of bulk modulus and shear modulus, dK/dP and dG/dP, which are in good agreement with previous data.

PHONONS, RUS, AND NEUTRON SCATTERING

ALBERT MIGLIORI
LOS ALAMOS NATIONAL LABORATORY

Copies of the transparencies used during this presentation were not available at the time of printing. Please contact the author if you would like to obtain copies of the transparencies.

ABSTRACT

Simple but very precise acoustical probes such as RUS can be combined with very sophisticated but less accurate probes such as inelastic neutron scattering and diffuse neutron scattering to provide a powerful picture of the vibrational spectrum of a solid. Such a picture can be used to extract information about fine-scale microstructure, phase transformations and more. We describe here recent work applicable to martensites and Pu.

TRANSCRIPT

DR. MIGLIORI: I am going to talk about recent work at Los Alamos National Laboratory or, as it has become more recently known, the Chinese Takeout Place. (Laughter)

After this Kosovo thing the Chinese have decided to give us back our military secrets. (Laughter)

[Transparency]

I am going to talk about our work on plutonium today. I want to use it primarily as a vehicle to show you how important the measurement of elastic properties is and, of course, the work that we have done has all been done using resonant ultrasound, partly because there is an absolutely stupendous administrative overhead in attempting to make a measurement on plutonium.

At this point we estimate that some of the samples we have measured recently are worth on the order of $2-5 million on the black market just because of the plutonium content. All of these measurements are really the very first ultrasound measurements on plutonium since 1975, when Hassel Ledbetter and Roger Moment published their single-crystal work. I think that was the last one, Hassel, for this.

Plutonium is interesting -- I will show you why in a minute. This has nothing to do with its only known practical application, but it is interesting. We are going to use resonances, because, number one, we will be able to see very small changes in elastic properties with temperature, time, and so on. In fact, I will show you in a second just how good that can be.

Plutonium has a very complicated phase diagram, and because of the very strong dependence of things like interatomic potentials on elastic moduli, studies of elastic properties can eke out some of the details of this complicated phase diagram and make it seem a lot less complicated, and I will touch on that, also -- I am not going to explain anything completely today.

Finally, there are completely thermodynamic quantities, so they are good.

[Transparency]

Okay, plutonium: Plutonium sits right here. For example, these are a bunch of actinidtes. You can see very few of them have more than an fcc and a bcc in a liquid phase, but as you get to this particular electronic configuration the whole thing turns into a complete mess. That provides a wonderful test bed for doing solid-state physics of various sorts.

[Transparency]

These are the phases that plutonium exhibits between room temperature and 640 C, so it is monoclinic, body-centered monoclinic, face-centered orthorhombic, face-centered cubic -- I do not think this is a phase -- and then body-centered cubic. It undergoes a huge number of phase transitions as you warm it up.

[Transparency]

It also has other strange properties. For example, as I begin to warm it up and I look at the length as a function of temperature of a plutonium sample (this is thermal expansion), monoclinic phase, monoclinic, orthorhombic. When it becomes fcc, the volume thermal expansion coefficient goes negative.

Then, as you warm it up, it goes to body-centered cubic and the volume drops 3%, a very large amount. In fact, I am going to concentrate on this region here and try to convince you that it is not really mysterious at all.

[Transparency]

Just to complete the introduction, there are the crystal structures of plutonium, and I think we are going to make some headway in understanding them. Just remember that Willie

Zacharias had figured this thing out in 1961, I think. He had to be a complete mad man to get that crystal structure out of his x-ray data.

[Transparency]

I am going to start by showing you some of the hardware. This is one of the resonant ultrasound cells that is installed in an argon glove box in the plutonium facility at Los Alamos. That is not a piece of plutonium, however.

This is about a half-inch across here, to give you an idea of size. We have used that apparatus so far to make room-temperature measurements, although we have cryogenic and higher-temperature stuff in the works. It takes roughly six months to get any change in your experiment approved for operation in these facilities.

Plutonium turns out, even in the polycrystal alloys we have right now, to be a superb mechanical resonator; the Q's are easily 10^4. Here is a typical mechanical resonance of a plutonium 4% gallium sample. Gallium is often put in plutonium to stabilize the fcc phase at room temperature.

The little arrows here give you an idea of what would change. For example, from here to here is roughly a half-Kelvin change in temperature, so with these kinds of Q's we have extreme precision for following elastic constant shifts. Remember, we can fit this Lorentzian resonance to about 1% of its width, so we can see very small changes.

[Transparency]

I am going to show you data and then talk about what it all means. With nice sharp resonances, here are typical

-- and this, really, by the way, is typical (not like Jay's)

-- errors, measured frequencies, we are looking at RMS errors like this, we get values of elastic constants. Just to get these data is absolutely amazing.

DR. SACHSE: What are fex and fr?

DR. MIGLIORI: That is all explained in this book I wrote, but I will tell you anyway. (Laughter)

These are the measured frequencies and these are a Levenberg-Marquat [phonetic] best fit, adjusting, in this particular case, only two elastic moduli, C_{11} and C_{44}, because it is an isotropic polycrystal. It turns out these alloys are very well prepared and they are very isotropic and very amenable to elastic constant fit.

[Transparency]

Here is how well we do. These are Hassel's and Roger Moment's elastic constant measurements of a 3.3-atomic percent gallium-stabilized fcc plutonium crystal at room temperature, C_{11}, bulk modulus, shear modulus.

Here is our measurement of a polycrystal sample, same composition, so Hassel did pretty well. We also have now, for the first time, different gallium concentrations, and you can see a fairly strong variation in elastic properties with gallium.

For comparison, this is a 1963 measurement of pure plutonium without gallium, and here is our measurement; again, very good correspondence with the pulse echo and the torsional oscillator work.

What is interesting here is that up until recently it has been assumed that when you put gallium in plutonium to stabilize this face-centered cubic phase against monoclinic, the properties are essentially exactly the same as if you did not put it in, and we are starting to see substantial differences in compressional properties with the gallium, which is a little surprising at those concentrations.

DR. ISAAK: You do not have a monotonic change.

DR. MIGLIORI: That is right, it is not a monotonic change, and that is the first surprise for the people funding this work.

[Transparency]

Just to show you the next stage here, this is a thermoelectrically cooled system, because it is very difficult to get cryogen in the secure environments in the plutonium glove box because of both security and safety considerations, so we have a thermoelectric cooler, and here is your resonant ultrasound stage with a sample in it.

This should go -- well, maybe not quite this far, but we should be able to get a reasonable temperature derivative and, therefore, the temperature derivatives of these alloys.

Why do we care about all of this stuff? There are some very strange things about plutonium and we are going to talk about some of them.

[Transparency]

Pure plutonium has a negative in the fcc phase. It has a negative volume thermal-expansion coefficient. As you add gallium it becomes ordinary. The atomic structure guys, who claim they can calculate _ab initio_ the structure of every single element, wind up doing the

following calculation, in which they find that the bcc phase that is observed for plutonium, and the fcc phase that is observed for plutonium are not minima in the free energy, according to their calculations, they are maxima and, therefore, they are maximally unstable, so they have got problems.

[Transparency]

However, all of these guys ignore thermodynamics and entropy when they do these calculations. In plutonium especially -- here are Hassel Ledbetter's data and, of course, you can all read this after lunch and, if you cannot, it is okay, because I am going to tell you what is going on, or at least the important things -- entropy is really important in plutonium.

The reason it is especially important is that the shear wave speeds vary very strongly with direction in the single crystal. In fact, the shear stiffness varies by 7 to 1, which is the highest for any fcc metal. What that does is bring down the entire phonon dispersion curve. This was computed by our co-workers at Los Alamos from the diffuse scattering piece of an elastic scattering spectrum on plutonium that was not great, but these are estimates in which the force constants are computed and then the entire dispersion curve.

[Transparency]

The soft modes are reflected in these little slopes here. What this does is it brings the entire phonon dispersion curve down and it brings it down substantially, so that the following goes on.

[Transparency]

We are trying to understand negative thermal expansion coefficient and the volume collapse as we warm fcc plutonium up to the bcc phase. I can be really dumb and just compute the bulk modulus, or at least compute the change in energy if I compress plutonium when it is fcc. That energy, if I know the volume change, which is about 3%, and I know the bulk modulus, which has been measured by resonant ultrasound, then I can estimate an energy change.

I can also estimate an entropy shift, noting that basically the TS term and the free energy is 3 kT log. All these things are phonon-dominated. Plutonium is really a bunch of mechanical vibrators and every one of them has a certain number of quanta in its simple harmonic oscillator normal mode.

The log of the quantum number, averaged over the entire phonon dispersion curve, is intrinsically the entropy with a few constants on it. So we take kT, the temperature, times

Boltzmann's constant, and some average phonon frequency, this number is sort of the quantum number of the harmonic oscillator and, therefore, the entropy.

Remember, plutonium has a very soft elastic constant in one direction, so this number is extremely large for plutonium, meaning the following: In most metals the bulk modulus is very, very large, like iron, and in plutonium it is very small. In plutonium the average phonon frequencies are very small; therefore, the harmonic oscillator entropies are very large.

Therefore, in plutonium, if I can make tiny changes in the phonon distribution, I can stabilize against almost any energy shift, because I have so much entropy to do it. More precisely, when plutonium goes from fcc to bcc, the bcc phase has a smaller volume, but all bcc materials have even softer shear modes than fcc phases, so they have a lower average phonon frequency and higher entropy. In plutonium that effect is stronger than for almost, I think, any element (I am not sure if it is exactly that) and, therefore, entropy will take you to places that look energetically unfavorable, which is why the electronic structure guys get plutonium as unstable. It is, in fact, entropy-stabilized.

[Transparency]

As you put numbers in, we are looking for this to be true, that is, the change in TS over the change in energy when we go from fcc to bcc, we want that to be true, and it turns out that using unfavorable numbers, that is, the worst that we can find, the energy differences are sort of 2 mV per unit cell in going from fcc to bcc, but that would require only a change of about 1% in the average phonon frequency, a drop of 1% to stabilize.

In plutonium, because of these very soft elastic properties, it is clear that these odd phases with smaller volumes are being stabilized simply because they are more probable via the entropy.

[Transparency]

The thermal expansion is also related to the anisotropies, which are then related to an interesting thing called the Bain route, which goes like this. Here is an fcc crystal.

[Transparency]

I have put on it a body-centered tetragonal set of lines. This is the same crystal structure, but I am drawing here a body-centered tetragonal. Face-centered cubic is the same as body-centered tetragonal, where c (which is this), over b (which is that), is the square to 2. I am just waving my hands now.

52

But look, if I start to squeeze this way, that is, compress the fcc structure, eventually this will equal this and it will become bcc, so I can continuously deform fcc to become bcc. That is called the Bain route and it has the stunningly weird property that goes like this.

As I start to squeeze it -- I am squeezing fcc here -- the initial stress-versus-strain slope is Young's modulus. As I continue to squeeze it, I move it all the way over to bcc. Now, look, I have squeezed something, its crystal structure between my hands is now body-centered cubic and I have free surface boundary conditions here and here, because I am squeezing it on only these faces.

Therefore, by symmetry, this is a symmetry argument, the force goes to zero. That is, as I squeeze it from fcc to bcc, it is stiff, stiff, stiff, and then boom, and there is no longer any force holding it. It is an unstable thermodynamic equilibrium point, but there is no force that is required to hold that there.

This, by the way, is the energy surface for that process, which we have just calculated recently. We have taken very simple, radially symmetric Leonard Jones-like potentials and put together an fcc lattice and squeezed it, and you can see here an fcc and a bcc minimum in the energy surface.

[Transparency]

For parameters that are very similar -- that is, if the potentials that we use for plutonium are taken as the same sort of phenomenological ones we would use for iron, then we find that the bcc phase that we compute has smaller volume and higher energy (just like plutonium). In fact, now, if you think about the thermal expansion process, usually you think of thermal expansion as moving along the fcc line.

This line here that is very faint is the locus of points in which the crystal structure is face-centered cubic. This line is for body-centered cubic. When I put thermal energy into this thing, people usually think it stays here, but, in fact, things do not do that, they run around all over the place and average out to fcc.

[Transparency]

When you do that, you find that this Bain route between fcc and bcc is also a volume-decreasing route and so when you do the averaging you find out that the volume thermal expansion coefficient is negative and it is absolutely a result of this shear anisotropy that is a result of this very soft Bain route in the crystal structure, so you do not need to invoke any

strange electronic structure or anything else to explain this negative thermal expansion coefficient and volume decrease in plutonium.

The whole point here is to touch on the things that you can really do well with elastic constant measurements and how much you can really learn about phase stability in the structure of solids.

Thanks.

DR. ANDERSON: This Bain route, you say it is for iron?

DR. MIGLIORI: Iron has a Bain route between fcc and bcc as well and I believe it takes that route, which you can tell by looking at the crystallograph. You take an x-ray pattern of a single crystal and if it rotates 45 degrees when it goes bcc, then it has taken that Bain route to get from fcc to bcc.

By the way, it is a first-order phase transition, but that route has the minimum atomic displacement, so often it is very easy.

DR. ANDERSON: I have got to learn more about this, that is news to me, and I thought I had worked in iron.

DR. MIGLIORI: Isn't that interesting, the whole symmetry argument? There are other Bain routes, for example, between cubic and rhombohedral.

DR. LEDBETTER: And there are many, many systems beside iron that go fcc to bcc via Bain.

DR. MIGLIORI: Lots and lots. It is a very common way of going and it is entropy-driven, in some sense, because usually the bcc mode has softer elastic constants and, therefore, more phonon entropy, so the system can head in that direction regardless of what the energy or the volume of the bcc phase is.

DR. ANDERSON: What is interesting to me is the fact that --

DR. MIGLIORI: Hassel is the real expert on this, by the way.

DR. ANDERSON: -- four or five years ago there was a belief that there was a bcc phase in iron up at 200 GPa and 4000°, and there was good reason to believe that.

Then the first-principle calculators got busy and said, hey, the Helmholtz energy of bcc will not allow that transition in this domain, so the idea kind of lost its momentum, but now I am wondering if we know anything about that.

DR. MIGLIORI: You know, it would be easy to mistake the thermodynamic free energy for the internal energy, which is what the electronic and band structure people typically do. Those are always zero temperature calculations and they usually say, oh, well --

PARTICIPANT: It has nothing to do with temperature.

DR. MIGLIORI: They are athermal, because they do not include --

DR. ANDERSON: The bcc phase in iron that was disposed of is first on top of fcc.

DR. MIGLIORI: Which is where you would expect it to be, because bcc systems always have -- well, roughly always -- a soft shear modulus in the 110 direction and, therefore, they always have higher entropy than the nearby fcc phase (I mean, you know, "always" within reason, but it is pretty much true).

You can get to a bcc phase that is energetically distinctly unfavorable merely because it is so much more probable because its entropy is so high.

DR. ANDERSON: And you say the reason you can do that is because the entropy has to be large?

DR. MIGLIORI: Yes, and it does not care what the energy is, it can be plus or minus. It does not care what the volume is. If it can head for that spot with lots of entropy, it is going to just drag everything along. Yes, the linear augmented-plane-wave sort of calculation is really a zero temperature -- well, they put in a certain model for the electronic structure. They compute the energy and then they say this is the free energy, having never computed the properties of any of the competing structures.

They put it in fcc, then they compute the energy. They put it in bcc, they compute the energy. If fcc energy is lower than bcc energy, they say fcc is a stable structure. They do not compute the full elastic tensor or the entropy at finite temperature.

DR. ANDERSON: They say it is reasonable to take the entropy [inaudible].

DR. MIGLIORI: Right. I think we have seen that it fails, that the plutonium experts at Los Alamos fail because they do not bother computing the entropy and, in fact, they are probably pretty close to having the right answers if they did.

Thanks

Nonlinear Mesoscopic Elasticity in Solids

R. A. Guyer and P. A. Johnson
Los Alamos National Laboratory

Abstract

A variety of materials reside in the purported elasticity universality class characterized by "nonlinear mesoscopic elasticity". Rocks, the prototypical member of this class, have extreme nonlinearity (NL), hysteresis (H), and discrete memory (DM). The experimental manifestations of NL, H, and DM will be described with Berea sandstone as example. NL, H, and DM lead to unusual behavior in laboratory resonance measurements and in a variety of geophysical contexts. An effort will be made to identify the microscopic features of materials that might be placed in this elasticity universality class.

Transcript

DR. GUYER: This talk was conceived by Paul Johnson -- at least he conceived the title, but then he went on vacation and asked me to give the talk in his stead, so I am going to give you a talk that is at least related to the title.

[Transparency 1]

This is going to be a sort of cultural interlude, because I am going to be telling you about nonlinearity in the elastic properties of materials and I am going to be paying attention to materials that are not the ones that you are necessarily used to talking about.

The materials will be something like sand, soil, rocks, and so forth, and I am going to try to suggest that there is a generalization about the elastic properties of these materials that might be helpful in providing some understanding of each of them based on some understanding you may have of the others. I am heading toward attempting to make a generalization but I am going to start by paying attention to rocks, using as a prototype.

Here is the outline. Somewhere along the way I am going to talk about nonlinearity, hysteresis, and something called discrete memory, so you will see NL-H-DM come back again and again, and I will be trying to emphasize the notion that there are certain experimental signatures of the quality that I am looking for in the behavior of these materials.

[Transparency 2]

If I had to discuss quasi-static measurements, I might, if I were in a freshman class, be telling you about the fact that if you pull on a spring that has a spring constant, you discuss the equation of state of the spring by talking about the relationship between the force and the length. Also, in the freshman class, you put the spring into an oscillator and make it oscillate and you discover that it has a frequency related to the same spring constant. This is really the relationship between the quasi-static equation of state of the material and the dynamics of the material.

I am going to be talking about that relationship but not for simple-minded materials like this, but for real pieces of material.

[Transparency 3]

Just to make a step in the direction of real materials, I am going to be talking about, typically, experiments on rocks. The quasi-static equation-of-state measurements are often made on a rock that might be about the size of a Coke can (7" this way and 2-3" that way). You put a pressure on it, you measure the strain, and discuss the behavior of the strain as a function of the stress.

In dynamics, as all of you know, you essentially resonate a piece of material. When you are doing this on a rock, it might be about that big in diameter and, roughly speaking, that long. You tickle at one end and detect at the other end. We are going to talk about what you see when you do this.

[Transparency 4]

Not everybody here knows how things behave then they resonate. Here is a quasi-static equation of state for a relatively nice material, a piece of Pyrex glass. Another material that is very similar to that in the qualitative sense of being a nice material is a piece of that "other" lucite. It has resonance curves that you are very familiar with. The reason that there are several of them, of course, is that the resonance is driven at several amplitudes, really voltage, v_1, v_2 .... Of course, the resonance curves look exactly the same; you do not go around paying attention to the voltage.

You take a Berea sandstone and take it through a force protocol, nobody even bothered to pay attention to the fact that you might have increased the pressure and decreased the pressure (it just runs up and down this curve, upper left). If you do that to a Berea sandstone, it will run up this side and come back down that side.

If you are fancy about the pressure protocol, there will be events in the interior of what is happening here, which we will pay attention to in a minute, which represent the so-called property of discrete memory.

If you take a Berea sandstone through a resonance curve -- and to show the fact that it is quite exotic (this is a logarithmic scale), you simply (it is the resonance of that little piece of material I described to you) -- you are increasing the voltage and the resonance curve looks relatively nice for a while, begins to drift over, and then whatever this is. These are actually modest accelerations compared to the ones up there on the nice piece of material, and the resonance curve is bent over like crazy and has all kinds of other complicated properties.

[Transparency 5]

Just to get you in the mood -- of course, that was a rock and not a mineral, it is a rock, which is to say it is a piece of material that might look something like that.

[Transparency 6]

Or it might look like this.

Or like that one.

The 2 outside pictures are what are called pore casts, in which you have intruded epoxy into the pore space of the rock, then removed the rock, and you are actually seeing a picture of the pore space.

The important qualitative thing to remember is that in these systems it is not the grains of the rock that cause the elasticity, it is the space between the grains where the important elastic properties occur.

[Transparency 7]

So think this way. You might be inclined to think of a rock as a bunch of pieces of material, but skip the pieces of material and think more, in fact, about what is between them. Because for the purposes of the kinds of elastic properties we are talking about here when you squeeze on the rock, the grains are more or less rigid entities and they simply move relative to one another and it is the elastic properties of what is between them that counts. So that is, in some sense, the elastic system.

PARTICIPANT: Is that well established?

DR. GUYER: Not at all. (Laughter)

58

So here is the abstraction, that the grains are here and that there is some elastic entity that works between the grains, and that is what we are mostly going to pay attention to. It is these elastic entities, whatever they happen to be, that are responsible for those relatively unusual elastic properties that you saw in both the quasi-static measurement and in the dynamic measurement.

I always remind my friends that there are at least 10^6 of these bonds per cubic centimeter, so you might think you ought to pay careful attention to the details of how the bonds reside in the system, but it makes no sense. It is perfectly adequate to think of it as a cubic lattice of unusual elastic elements.

What we really would like to do is to understand what those elastic elements are, or at least what properties they must have to describe what has been observed experimentally.

That is the so-called deep background, I guess.

[return to Transparency 4 – lower left]

Here it is now in a little bit more detail, that quasi-static measurement. The pressure is increased. These little curves here, which are not really very neat, occur when you increase the pressure, stop for a moment, decrease the pressure a little bit, then increase it, again. I said I was going to call this discrete memory and I will say that in a minute, but before I get to that. This is not at all linear.

Linearity, of course, is some straight line. This is extremely nonlinear and if you look at the scale of the pressures here, it is extremely nonlinear. That is hysteresis and it has this fancy feature, which I will now call a little bit more attention to.

[Transparency 8]

The kinds of materials I am talking about typically will have hysteresis in their quasi-static properties. They will be very nonlinear and they will have this property. Now let me point more carefully to that discrete memory. It is the fact that the rock sometimes can "remember" what is happening to it from the point of view of pressure.

[Transparency 9]

You might just decide to increase the pressure on the rock. If you do, it will track a trajectory that looks like this. You might decide to increase the pressure to a certain point, reduce it briefly, and come back, you put a little pressure loop in. The strain field will go to the point where you decided to change the pressure, then cut into the interior, return to this point,

and it does not return asymptotically to where it was going. In fact, if you did not know where it had been, you might think it was going to go that way, but it stops at that point and tracks the trajectory it was originally on, so it knew where it wanted to go.

Just to be sure, put a little loop inside a little loop, and it will do that. There will be a small hysteresis loop here, it will return to this point and take off on that trajectory, and you can make this as complex as you like.

That is an interesting quality, and it is one of the qualities that the modeling men ought, in principle, to be trying to deal with. Some of the work I am going to talk about tries to deal with the fact that the elasticity of rocks has this relatively large nonlinearity, hysteretic behavior, and this property of discrete memory. One of the things we do is to try to model that and then talk about the consequences of the modeling.

What I just showed you in the way of properties are, actually, not particularly unusual. A magnet, random-field Ising model, has the same properties, it is just that it is the magnetic field that is driving the magnetization.

If you are familiar with the fluid configurations in the pore space, the chemical potential drives those fluid configurations and chemical potential protocols will produce fluid configurations that have the same discrete memory I was talking about.

If I am going to explain to you why rocks have those properties, I ought to make the explanation relatively generic (I do not want to make it specific, that various sandstones have this or that interior properties, because, in fact, these are generic properties of a whole variety of materials). That is, again, what we have tried to do. One of the things that I will remark on is that the description you make of these materials is not made at the microscopic detailed level but, in fact, is relatively macroscopic.

[Transparency 10]

What is the common element available among the things I have said that are similar to rocks in having these properties? The magnet, of course, has domains. It has pieces of material within itself, which, from a magnetic point of view, have 2 magnetic states.

What is it about fluid configurations and pore spaces? Well, they are relatively complicated but, at least in some simple situations, the pore is full of fluid or it is empty (or has fluid only on its walls, so there are 2 fluid configurations per pore in some sense: full and empty.

60

In the case of rocks, essentially the elastic elements have, roughly speaking, 2 states, and you can model that in a variety of ways, but the thing that is important qualitatively is the notion that many of the elastic elements between the grains somehow go in a hysteretic way as the domains go in a hysteretic way between being up and down and the fluid configurations in the pore space go hysteretically between being filled and empty.

Let me give you what I will call summary one. The properties that a rock has, nonlinearity, hysteresis, and discrete memory -- I actually pointed only to the quasi-static measurements, and I talked about those, and when I described the modeling that has been done of this system, it began with modeling of the quasi-static measurements (this is work I did with Katherine McCall).

We developed a picture of how you think about the elastic elements in a rock from the point of view of quasi-static behavior. I have to give a second talk in about 20 minutes, so I will elaborate a little bit of this in a couple of minutes. It was very important in a lot of work we did to have some nice experimental help from Greg Boitnott.

When you get done and you have understood the quasi-static measurements by making up your little phenomenology, what are you going to do with it and can you do anything with it? One of the things you can do is you can ask, well, how does this object behave dynamically? In that second experiment, where there was a long rod and it had all that crazy behavior, the dynamic response, the phenomenology that describes the quasi-static measurements here leads to certain very definite predictions about dynamic behavior.

Those predictions are here and that is what my second talk was really intended to be about, the experiment that confirms the predictions. The predictions are, essentially, that for relatively small strain fields or small driving forces the resonance will shift, it will shift to lower frequencies, it will shift proportionally to the magnitude of the strain field. This result is not available to you from traditional theory of nonlinear elastic systems.

Furthermore, it actually produces a prediction of not only the qualitative behavior of the frequency shift, but it provides you with a number that you can deduce from the study and compare to quasi-static data like the data of Greg Boitnott.

[Transparency 11]

Let me show you the answer. I am not going to try to explain to you how all that works or anything, but just to show you those data and to say that when one studies -- this complicated curve and there is a lot of action taking place over here -- if you study it, in particular, as it

begins, with the smallest strain fields, the resonance drifts down proportional to the amplitude of the strain in the rock.

You almost cannot see the frequency shift on this scale and that frequency shift is linear in the magnitude of the strain field, so this amounts to the confirmation that the ideas we have about the quasi-static behavior of the rock can be transferred to a discussion of the dynamic behavior.

DR. ISAAK: Is there any idea that that frequency shift could be due to temperature change with the amplitude?

DR. GUYER: No, you know how much that temperature is and you know the thermal expansion and things like that, so no, not at all.

DR. ISAAK: Because you are driving it at a higher amplitude, you are going to be heating up.

DR. GUYER: Yes, no question, it is a big rock. This is a big rock. Yes, we have checked that very carefully.

There is another property that these systems have that is just beginning to dawn upon us. It is also in dynamics. There is a slow dynamics.

[Transparency 12]

Now I am going to go back and show you this picture again (lower right of Transprency 4). I pointed to the lower part of it and I showed you that curve and I said we sort of understand that now. I did not point to the upper part and you might ask, why fuss with this little tiny diddly business down here?

We paid careful attention to the resonance curve at strains up to about 10^{-6}. There is a lot of action out there, above 10^{-6}. Less attention is paid to that, because at about the same time one began to notice these data and pay attention to them, we also found that there is, in this region, what we called initially just slow dynamics. In fact, you can track a resonance curve, come back through it and it is not the same. Track it and come back through a little slower and it is not the same by a different amount. In fact, it is essentially a slow time evolution to the elastic properties of this material, so if you are going to sweep back and forth through a resonance, the answer you get will depend on how fast you sweep, and that tends to occur up in here, so we paid attention to these data for the purpose of talking about confirmation of the relationship between quasi-static and dynamic measurements.

But then, paying a little more attention to the data up at high amplitudes, we found there is the resonance curve having behavior that depends on how fast you sweep through it and there is a phenomenon -- and it is rather complicated, so I am not going to try to describe it in detail -- where you can drive the system at a fixed frequency for 10 or 15 minutes and then turn that frequency off and just test with a very delicate small probe where the resonance is located, and you will find that when it was being driven, the resonance might have been at 3000 Hz. When you turn the drive off, the resonance will snap up by, let's say, by 7 Hz, and then there will be a remaining 1 Hz frequency shift that will be a recovery back to where it might have been logarithmically in time.

When I first was told that this happened, I did not believe it. Remarkably, if you are willing to wait at least a day tracking the location of the resonance, it recovers logarithmically.

This is work done by Jim Tencate at Los Alamos, a lot of tests of this quality, and it seems to be part and parcel of the nonlinear dynamics I was talking about, and of the quasi-statics, so that we have come to think of rock as having three special properties, the nonlinear, hysteretic, and discrete memory properties in quasi-static measurements, a frequency shift proportional to the amplitude of the strain field, and a logarithmic time dependence in the recovery of some aspects of the modulus or, if you like, the elasticity, as a function of time, and these are the signatures.

[Transparency 13]

We wanted to make the generalization that this property is not just the property of a Berea sandstone but of a class of materials, and here is an illustration of one of the experimental evidences of that, 3 different types of material. This is Lavoux limestone. This is damaged concrete, probably (it just means it was in somebody's sidewalk for 10 or 15 years before the sample was picked up), and a synthetic slate.

All of these have a frequency shift of very modest acceleration that is essentially linear in the amplitude of the strain field to the degree that you can make that decision from a curve that looks like this, so the properties observed for rocks actually seem to be possessed by a few other things.

[Transparency 14]

Our notion is to wonder -- the phrase we use is an "elasticity universality class," saying that all these materials, while very different, one from another, have elasticity properties that are

essentially similar, and trying to decide what might belong in that elasticity universality class we can use that notion to help us understand various kinds of materials.

Of course, the candidates are sand, soil, rocks, concrete, ceramics, things like that. Soils, certainly, with relatively low strain fields, actually have the quasi-static behavior, e.g. work of Veucetic.

We ourselves have looked at these frequency shifts. Koen van den Abeele, who actually was here about five or six years ago, has done the work on slate that is described there, so that is the box you put something in if it belongs in the universality class. Fontainebleau sandstone belongs in there, Berea, Lavoux -- that is a slate. Concrete, fresh concrete or damaged concrete, both, seemingly, have some of the properties we are talking about, and so does soil.

We found that not just Berea sandstone had this logarithmic time dependence to its recovery from certain disturbances, but so does Lavoux and Fontainebleau and the 2 types of concrete. This is actually, in some sense, some of the work that we are currently involved in. We are paying great attention to Berea and, at the same time, looking at these other materials.

The reason one does this, of course, is that if you are going to have an understanding of the behavior of these systems that is not specific to their details, then you transfer it to other systems, and so the principle behind trying to suggest that and to explore whether this makes sense is essentially what is illustrated here.

[Transparency 15]

This is the viewgraph that explains why we pay attention to these things. They are -- the phrase I use is are that they are the "blue collar materials of daily life" -- sand, concrete, stuff like that. We all cross bridges, if you live in the Los Angeles basin you sit on a resonant piece of material that is one of these materials, if you look for oil, the phenomenon of sanding, which has to do with things falling in on your drill bit, have to do with the elastic properties of these kinds of materials, so there is a great deal of interest in them and that is one of the reasons we pay attention to them.

Thank you.

DR. LEVY: An off-line question: Is there any absorption in these systems, attenuation coefficients?

DR. GUYER: Yes, in my second talk I will go into detail about measurements of the attenuation coefficients. This was Paul Johnson's talk. I am going to give the second talk after Katherine.

DR. MARSTON: The question I have is an understanding of these connecting springs in one of your earlier models. Is there a good model developed based on Hertzian contact forces?

DR. GUYER: No, a Herzine model simply will not work, it does not have the properties in a quantitative way that are called for. You can make a Hertzian model have the qualitative properties. That is one of the things we are working on. It requires more and more understanding of what is happening experimentally, you get a better idea of how to narrow yourself as to what kinds of models are involved.

We have also tried deliberately to make the description model-independent. The phenomenon is essentially model-independent. It calls for a 2-state character to the elastic bond and that is all, in some sense, that is called for to get most of what I described. You do not have to say what it is quantitatively, only what it is qualitatively.

Thank you.

Application of Resonant Ultrasound Spectroscopy to Determine the Elastic Properties of Macroscopic Rock Samples

K.R. McCall[1], T.J. Ulrich[2], P.A. Johnson[2], T.W. Darling[2], A. Migliori[2]

[1]University of Nevada

[2]Los Alamos National Laboratory

Abstract

Resonant Ultrasound Spectroscopy (RUS) is a method whereby the elastic tensor of a sample is extracted from measured resonance frequencies. Typically, a rectangular parallelepiped sample is placed between two piezoelectric transducers, a source and a detector. The sample is driven at constant voltage as the frequency is swept through multiple resonances. The measured resonance frequencies are the input to an iterative inversion algorithm that finds the best match between the data and a set of resonances generated from a model. RUS has been used successfully to determine the elastic properties of single crystals of minerals found in the earth's mantle (e.g., [Oda et al., 1992]). We are extending the applicability of RUS to macroscopic samples of rock. Rocks are potentially difficult samples on which to apply RUS, because of their high acoustic attenuation (low Q), inhomogeneity, anisotropy, and the difficulty preparing suitable samples. In preliminary measurements, we have analyzed a variety of rock types to determine optimal sample sizes and aspect ratios, the minimum number of resonances necessary for obtaining an accurate inversion, the sensitivity of RUS to anisotropy in rock samples, and the precision of measurements on samples of varying sizes and aspect ratios.

Assuming isotropy, we have found that RUS provides reliable results for relatively high Q materials such as basalt, primarily because a large number of resonance frequencies can be accurately determined. For example, application of RUS to a sample of basalt with an aspect ratio of 4 yields an RMS error of 0.31% in the fit between the predicted and measured resonance frequencies, and the elastic constants c_11 and c_44 change by 0.54% and 0.12% respectively with a chi-squared increase of 2%. Application of RUS to low Q materials such as sedimentary rock is considerably more difficult, and it remains unclear if RUS is viable for such materials. (Oda, H., O. L. Anderson, D. G. Isaak, and I. Suzuki, Measurement of elastic properties of single-crystal CaO up to 1200K, Phys. Chem. Miner., 19, 96, 1992.)

TRANSCRIPT

DR. MCCALL: I brought my samples with me so that everybody could see them. Please pass them around.

[Transparency 1]

We chose the alliterative title: "RUS and ROCKS."

The work has had a lot of contributors, but most of it was done by TJ Ulrich, who is the graduate student who, of course, does everything I tell him to do in hopes that he will graduate.

[Transparency 2]

I am going to start out by telling you a little bit about the history of my involvement in this project. I was trained as a condensed matter theorist; now I am sort of doing experiments. Sometimes I wonder how I got here.

Then I will tell you about the experimental system we are using, some of the numerical modeling that we use to explore important issues that come up for the samples that I am passing around, a few of our experimental results, and where we want to go.

The history of the project was given to you in the last talk.

[Transparency 3]

I went to Los Alamos in 1992. One of the groups in the division I joined as a postdoc had an enormous bar of Berea sandstone, 6 cm in diameter and 2 m long. It was just beautiful; I loved it. Of all the places that I applied to or interviewed at, Los Alamos was my top choice as a place to work, because people at Los Alamos were doing experiments on this rock.

At the time they were just starting to look at the nonlinear elastic properties of rocks. As you heard in the last talk, we find that if we measure stress versus strain, as shown in the figure, we see nonlinearity, hysteresis, and discrete memory. The inset shows the load versus time. As Robert showed you, this curve was not taken by just going straight up in stress, it was taken by coming up part way, stopping, turning around, going back, going up a little farther, going around, and so forth. If we do a resonance measurement --- the figure shows just a single peak of the frequency versus acceleration --- we see this nice bending here, indicating a nonlinear response.

We started thinking about theoretical models, and I assume that Robert will tell you more about that in the next talk. The idea is that the modulus is nonlinear. The modulus relating stress to strain in this equation here does strange things as a function of strain. We can do an analytic

67

calculation by assuming we have a base-line modulus, with a perturbation that is proportional to strain, and perhaps a second perturbation that is proportional to strain squared, etc. To account for hysteresis we might add something that looks like this, where α is a measure of the strength of the hysteresis, and the multiplicative factor is dependent on the absolute magnitude of the strain, and the sign of the strain.

With these kinds of ideas in mind, we go back to the measurements and try to make predictions. What is β? What is δ? What is α? Can we extract those numbers?

[Transparency 4]

That is where RUS came in. The hypothesis is that while we can start by trying to measure β, δ, and α, the results will be misleading, unless we have a really good handle on the base-line K_0. What is the linear modulus of the material that we are studying? If you pick up some of the samples of rock coming around, you should be able to see that a number for one piece of basalt is not necessarily the number that is appropriate for a piece of basalt from someplace else. So, when we measure the nonlinear properties of rock samples, we also need to measure something that other people will understand characterizes the sample, the linear modulus.

The rock mechanics way of measuring moduli is to measure stress versus strain by pushing very hard on a piece of rock until it breaks, or reaches failure. If we do not look too closely at the stress-strain curve, we can easily draw a straight line fitting the low strain data (the rule of thumb is that you go to somewhere between 70 and 90% of failure), and claim that that the slope is the modulus. There is a problem with this, as far as I am concerned. First of all, the measurement is made at very high amplitude, and we are talking about something that is nonlinear at low amplitudes. I would rather have a low amplitude measurement. The second problem is that we can never look at the same sample again. It is gone; it is dead.

The moduli can also be derived from time-of-flight measurements. There are people making very nice, beautiful time-of-flight measurements. They take a lot of time, though, and the problem with inhomogeneous samples is that the result could very well depend on which path the acoustic wave traverses, that is, where we place the transducers.

I want something that is more of a bulk measurement, an average measurement, of modulus. So we are trying RUS.

[Transparency 5]

68

We have an experimental system that is on loan to us. It includes both the control hardware and the analysis software. We spend a lot of time playing with the analysis software, and I am very happy to say that no, we did not write the analysis software, we just play with it. The transducers are similar, perhaps identical, to the ones you saw this morning at the demo. We have two arms holding the transducers, and the transducers hold the rock sample. Nothing fancy.

There are several issues that we want to consider when we are looking at rocks. Rocks are kind of messy looking; they are not single crystals. First, because of the assumptions made in the analysis software, we need free boundaries. That is not too hard to get. Second, in the analysis we assume that the sample is homogeneous. Our samples are visually inhomogeneous, quite inhomogeneous. Third, we assume that the samples are perfect parallelepipeds. If you look at one of the samples going around, the dark, fat basalt, you can see that the sides are not parallel.

Then we want other conditions to be met in order to get really good results. First, we want the resonance peaks to be distinct. This is an issue because the Q is so low in our samples. We have very broad peaks and they may overlap each other. Also because the Q is so low, sometimes it is very hard to pick the peaks out of the background; we have to look very, very carefully. Second, we want to be able to use the fewest modes to get the most information. Again this is necessary in large part because of the low Q of our samples. If we want to find two moduli, for instance, we need to have a lot of C_{11} dependence in the first few modes. Otherwise we can't resolve both C_{44} and C_{11}. This is where we got to play with the software that we had around. It has been provided at various times by Tim Darling, DRS and Albert.

[Transparency 6]

Okay, so I said free boundaries. That was easy. Then we must think about the homogeneous sample issue. Well, we are looking for constants that people might use in seismic research. They are looking for a general number; they do not really care about the elastic properties of a quartz grain, but they do want to know what the elastic properties or the velocity of sound is where a seismic wave might propagate.

Making a simple little estimate, we start by saying that any experimentalist knows that the probe we use has to have a wavelength about the size of the thing we are trying measure. Conversely, the wavelength has to be much larger than the size of an inhomogeneity in order to average over it, or not see it. Our estimated one-dimensional resonances have wavelengths of

size 2L/n. If ξ is the size of the inhomogeneity, then the length of the sample has to be greater than 5 times the inhomogeneity. I kept this little tiny sample up here because I am going to show you the results from it. The reason that the results are really bad is that the inhomogeneity is getting really big as compared to the sizes of the sides. $L > 5 \xi$ is one of the limits we are going to use as a general estimate.

[Transparency 7]

The importance of an imperfect parallelepiped is determined by just how anti-parallel the sample is. Fortunately, our samples are really big, so our $\Delta L/L$ could be the same size as a $\Delta L/L$ for a very small sample, even though we can see our sample is not parallel by visual inspection.

This is Robert Guyer's work. He did a first-order perturbation theory analysis of what to expect if we have a nick in our sample (for example, one of the samples going around has a nick in it). He asked, how does the frequency change when you put in an imperfection? He found these results. Suppose we take a nick out of the corner that is 1% of the mass. We find a frequency change in the first 20 resonances of about 0.15%. We guessed that this level of error would not matter too much and, empirically, it does not. The sample that is going around that has the nick in it was measured before it had the nick and measured again after it had the nick. The nick did not make much difference in the results that we got, which was really nice.

Robert obtained similar results when he considered the kinds of distortions we have in our samples. For example, we have parallelepipeds with non-parallel sides. We call those distortions symmetric distortions, in that we can draw an average size and make the sample parallel. Even when the symmetric distortion is about 5% of the mass, to first order in perturbation theory we find a 0% frequency change. This is pretty easy to explain, because first-order perturbation theory averages over symmetries. For asymmetric distortions we start to find some pretty big errors, although they are all about 1.5% or less. I am going to claim that the problems we have with our samples are mostly one and two, that is, the nick at the corner and the symmetric distortions.

[Transparency 8]

We want our resonance peaks to be distinct. This is a Q issue. We have a very low Q, in the hundreds mostly, 150 to 250 for most of the samples that we are looking at, so we need to use sample aspect ratio to separate our resonance peaks.

70

What we did here was run a model over and over again. We calculated the resonance frequencies for various aspect ratios. In the figure, a and b are held at a fixed ratio of 1.2, while the ratio of c to a is increased. The ratio of c to a starts out at 1.4 and is increased up to 8. We are using the standard book-value elastic coefficients for basalt. That is, we looked in a book of rock elastic constants under basalt and used the tabulated C_{11} and C_{44} in the program. Then we calculated the first lots of resonance frequencies.

In the figure, the first 3 frequencies are nicely spread. Then we start seeing triplets and doublets, indicating to us that it is going to be really hard to pick out enough resonance frequencies in a sample that is made almost cubically. Because we already have a peak overlap problem due to our low Q, we look to higher aspect ratios. In the calculations, the volume of the sample was kept fixed as the aspect ratio was changed. The fixed volume keeps the resonant frequencies in the same range over the figure. We decided that an aspect ratio of 4 -- actually, 6 is a really nice place, too – would allow us to pick 10 or more frequencies that are nicely separated. It turns out that cutting our samples at an aspect ratio of 4 was reasonable, so that is what we did. We are going to claim our best results come from samples of aspect ratio 4.

[Transparency 9]

We ran the simulation again to look at the C_{11} dependence of the first 8 modes. Here we have exactly the same situation, b/a is 1.2, while the ratio of c to a is increasing. We are looking at the dependence on C_{11} of each of the first 8 modes. Because we have 8 symmetries in the resonances of the sample, we assume that the next 8 modes have essentially the same dependence on C_{11}.

The first mode dependence on C_{11} is 0 (it is hard to see in the figure) and another mode rapidly decreases to 0. However, you can see that as we increase the aspect ratio, we get a lot more of overall dependence on the C_{11} constant versus the C_{44} constant. At an aspect ratio of 4, where we are going to claim our best samples are, we have 25 to 35% dependence on C_{11}.

[Transparency 10]

Okay, so what do the results look like? Here is a nice picture of a spectrum. This is basalt with an aspect ratio of 4. This measurement was made on one of the samples that is going around. The analyzed data has a percent in the fit of 0.31. The fit and the experimental frequencies start at the far left of the figure. This is our first peak, that is the second one, and so forth. We have a huge gain problem here, and must be very careful as we pick out the peaks.

The columns are the experimentally picked frequencies and the fit frequencies obtained from the analysis routine. We are very happy with these results.

[Transparency 11]

Here are comparisons of different aspect ratio samples. We will look at the top table first, the basalt. The green numbers are book values for the elastic moduli, the values we found in the handbook of rock constants. C_{11} is about 87 GPa and C_{44} is about 32 GPa. The results are ordered by aspect ratio, from 1.5 to 4. TJ found ξ, the measure of inhomogeneity, by looking at each sample and measuring the size of the biggest surface blob. The biggest blob was 0.61 cm on the smallest aspect ratio sample, and the fit C_{11} and C_{44} are given here. None of the fit moduli for these samples is far from the book values. However, the percent error changed by a factor of 3. That is quite a bit, actually. As advertised, we found the smallest error for an aspect ratio of 4. The average Q seems to increase with aspect ratio, as well. We feel these are reasonable results.

The second table shows the Sierra white granite results. Here we are in a little more trouble. We start out with book values for the elastic constants of 43 and 19 GPa. The aspect ratios of the granite samples are approximately the same as for the basalt samples. However, the aspect ratio 3.3 sample is this tiny sample I am holding. The fit to the resonances for this sample has a huge error. We claim that the large error is due to inhomogeneity. The biggest blob on the surface of the sample was half the size of one of the sides of the sample. The inhomogeneity is starting to make an average measurement impossible on this sample. Note that the average measured Q's are all similar for these samples, but the C_{11}'s and C_{44}'s are quite spread. I would say that the best measurement here results in moduli quite a bit different from what the book values. One thing that TJ is quite concerned about is that the Poisson ratio is pretty extreme for these samples.

[Transparency 12]

Remember that we started out wanting to know if we can make baseline linear measurements on samples whose nonlinear properties are of interest. Can we stick a core of sandstone into a RUS apparatus and measure the linear properties of the core before making the nonlinear measurements? Actually, sandstone turns out to be a problem sample type. The Q is so low on sandstones that it is very hard to measure enough resonance frequencies to successfully use RUS.

However, most geophysical samples are cores, or cylinders. Thus, that is the first place we want to go with this work. Now that TJ has done the groundwork with parallelepiped samples, a talented undergraduate, Izabela Santos, is going to work on core samples. First she will play with the calculation, forward modeling to study the aspect ratio dependence and the C_{11} dependence. We wish to find out whether we can actually make those measurements on long cores of sandstone.

TJ wants to look at saturation and temperature control. He will attempt to build an apparatus to allow temperature and saturation control of his samples. Unfortunately, building these kinds of cells is something that I do not know very much about.

Thank you very much.

DR. SACHSE: The stress-strain curve that you showed for your rock was very different from the stress-strain curve shown by the previous author. Yours was what I would call a typical stress-strain curve for a metal, with softening, because you had stress and strain on different axes than he did. I'm referring to your schematic drawing where the curve went up and bent over like this. That is the conventional way it is drawn, but his curves always had load on the horizontal axes.

DR. MCCALL: Right.

[return to Transparency 3]

Like this? Physicists like to put load on the horizontal axis, because that is usually what the experimentalist is controlling.

DR. SACHSE: It depends on which kind of machine you are using.

DR. MCCALL: That is also true. For the measurements that we like to use, stress is the control.

DR. SACHSE: The reason I mention this is that the curve on the right shows acceleration versus frequency. I would think that in one case you might get bending one way and in another case you might get bending in the other direction. You can have softening and hardening effects.

DR. MCCALL: Right. You certainly get hardening if you are just pushing down on a sample. You can think of yourself as pushing the grains closer and closer together, making the material stiffer. When you resonate a sample, it gets softer. You have to remember you have free boundaries, so the sample can expand if it wants to.

DR. ANDERSON: I noticed you list Q values. Presumably they are Q's of the individual modes. How do you measure the Q? What is the definition of Q? Is it the half-width?

DR. MCCALL: Those measurements are the result of the program given to us by Tim Darling, so you can ask him how they were made, but I believe it is half-width at half-maximum, isn't it?

DR. DARLING: I do not think I gave TJ any programs that calculate Q. I did not give him the Lorentzian fitting program.

DR. MIGLIORI: One component of the phase, one component of the response. If they adjust the phase so that it looks like it is in phase with the resonance, there is a symmetric peak. Then the Q is the full-width at half-maximum of the real part.

DR. DARLING: It is coming out of the DRS program.

DR. MCCALL: Yes, and TJ did do the calculation by hand as well. He measured the peak heights and widths and divided.

DR. LEISURE: You mentioned that the scale of the inhomogeneities should be less than the wavelength. That seems like a weak condition. I would have guessed you need a factor of 10 or so.

DR. MCCALL: Yes, it is a very weak condition.

DR. LEISURE: Is that sufficient, just slightly under the wavelength?

DR. MCCALL: It seems to be. Our results are totally empirical. I said the wavelength should be 5 times the size of the inhomogeneity, at least. 10 times would be a nice rule of thumb, because scientists like factors of 10, right? However, we have samples that are very definitely visually inhomogeneous, for which we find very low fitting.

PARTICIPANT: [Question inaudible]

DR. MCCALL: That is about 10. That will do it.

DR. SACHSE: On these plots of acceleration versus frequency, the frequency is the driving frequency, is it not?

DR. MCCALL: Yes.

DR. SACHSE: Have you ever made measurements where you plot the response frequency?

DR. MCCALL: No, what we are doing is measuring the response at the driving frequency with a lock-in amplifier. We drive the sample at one frequency and lock in at that frequency at the detector, so we measure the amplitude at the drive frequency.

DR. SACHSE: I know that if you are studying the nonlinear vibrations of plates and you measure the response of the plate at the horizontal axis, you will find, not a curve that goes like this, but a jump that goes back and forth. The frequency oscillates in a very narrow band, and it is not exactly the center frequency. You get these results only if you are at the top, stop the electronics, and then watch the sample go down the free vibration curve, which is the backbone of this curve.

[Simultaneous discussion]

DR. SMITH: The question is, is the receiver selective?

DR. MCCALL: Yes, the receiver is fixed.

DR. MIGLIORI: -- was under 100 Hz.

DR. MCCALL: I am not sure I understand your question, but can I talk to you afterward?

DR. MIGLIORI: I do not, either. (Laughter)

DR. SACHSE: If you are driving a system at large amplitude, with large excitations, you find that when you go through one of the peaks, you go up the curve like this and then you get a sudden discontinuous jump. The jump is seen only if you are applying the excitation frequency to the horizontal axis. If you take the output sensor, let's say the accelerometer, and you plot its frequency output, you will find that the response frequency jumps back and forth between the boundaries of the width of the excitation frequency peak.

DR. MIGLIORI: Wait a minute. If you drive at a given frequency, and the oscillator is anharmonic and you are doing a steady-state measurement, then the response of the object is highly nonlinear, and you can get only a certain collection of --

DR. SACHSE: You are sweeping the frequency of the excitation. You are sweeping through resonance, and you find out that the curve goes something like this and then goes down.

DR. MIGLIORI: That happens only if you are sweeping so fast --

DR. GUYER: It is almost happening at the top of the figure. It is almost happening, not quite.

DR. SACHSE: I think you will see it.

DR. GUYER: Well, if it were not for the slow dynamics, we would have seen it.

DR. MAYNARD: Has anyone done any measurements of these nonlinear effects as a function of humidity?

DR. MCCALL: Not deliberately, but we have done them accidentally. Humidity makes a huge difference in where the resonance is. Fortunately, most of the experiments are done in Los Alamos and it is pretty dry most of the time, but during monsoon season, July and August, you can watch the resonances shift as the storms move through, and then they come back.

PARTICIPANT: Does the pattern change, does the evolutionary pattern change?

DR. MCCALL: No, I do not think so.

DR. HARGROVE: The Q usually goes down because you get into an evaporation-condensation condition, adding another --

DR. MCCALL: You would have to put a lot of energy into it in order to get that during the experiment, but sure, yes. Anything else?

Constant Strain Analysis

Robert A. Guyer
Los Alamos National Laboratory

Abstract

The state of a linear system is independent of how hard it is driven. Not so, a nonlinear system. As you sweep a nonlinear system through resonance you change the state of the system. If you want to study a system in a particular state it is advantageous to maintain it in that state. The antagonism between conventional experimental practice, sweeping through a resonance, and the desire to maintain the system in a particular state is mitigated by constant strain analysis. The analysis of a sequence of resonance curves on a Berea sandstone will be used to illustrate application of constant strain analysis. The idea of constant strain analysis generalizes to constant field analysis. Resonance data can be treated so that the field (displacement, strain, velocity, ...) responsible for the nonlinear behavior of a system can be identified.

Transcript

DR. GUYER: The work that I am going to talk about is done experimentally by Jim Tencate at Los Alamos, the theoretical work by myself and Eric Smith, who is also at Los Alamos.

[Transparency 1 and return to Transparency 6 from his previous presentation]

Just to remind you, Katherine went over a bit of what I might have said about theory, so I will figure out some way to sort of pass over that. Here is another example -- Fontainebleu. This is just to remind you to think of the fabric of defects in the rock as the important thing that determines its elastic properties.

One of the things we are going to be talking about is the theoretical model that relates the quasi-static measurement of the dynamic measurement just to make it seem like this is making a deep statement. There is a traditional model of elasticity that involves Taylor series expansion of the free energy in terms of the strain field. Nonlinear elasticity would just have -- those are the C_{ijkl} and there would be a whole bunch of other fancy coefficients, high-order terms in the strain field.

There would be other higher order terms in the strain field, all of it, basically, on the other hand, assuming analyticity of the free energy, so you develop notions of cubic nonlinearities and if you are a phonon physicist, you talk about the 3-phonon process and the 4-phonon process.

If you do acoustics, you talk about the coalescence of 2 acoustic waves to produce a third, 3 acoustic waves to produce a fourth, and so on, and these are well-studied phenomena in nonlinear elasticity.

If you try to make a theory at all involving hysteresis, discrete memory, the kind of magnitude and sign of the frequency shift we are going to talk about in resonance, this theory simply does not come anywhere near it. It simply cannot be used. In some sense, it would seem that for the kinds of materials we are talking about, or at least that I am talking about, this is simply not the way to start and it is not the way you would go about describing the materials.

[Transparencies 2-5]

In some sense, the traditional theory, which is this theory of strain fields and Taylor series expansions in strain fields, does not really work well. But we know it is not supposed to look at all these phenomena, extremely large nonlinearities, hysteresis, and discrete memory.

But there is a theoretical model and it is the one that I alluded to and I will now allude to it, again, that does describe the quasi-static measurements and I am going to tell you about the experiment that confirms how that theory also, seemingly, describes the dynamic measurements.

Remember, it was a theory where we paid attention to the elastic elements between the grains; the grains were thought of as essentially rigid. This comes with a very fancy name, it is called "PM space," and the reason for that is that the original description of hysteretic elements, whether they be elastic elements or magnetic domains or happen to be fluid configurations, is due to a man named Preisach, a German scientist from the 1930s, and it was elaborated in an engineering context by a man named Mayergoyz, so we called it PM space, but it is a place in which one tracks the hysteretic elements that are in your system.

In our case we will be talking about hysteretic elastic elements, and it is a space in which you track the way in which the hysteretic elastic elements are responding. If you are doing a quasi-static measurement, it is the response to the pressures or the stress fields you are putting on the system or, if you are doing an AC measurement, it is the response to the AC stress fields that happen to be in the system.

I am not going to say a great deal about that, except to remark that the theoretical model actually has a rather nice feature.

[Transparencies 6-7]

The feature is that it gives you the qualitative description of the quasi-static measurement but it also provides you with the recipe where you can take the quasi-static measurement and actually infer some of the quantitative features of the elastic elements that you are talking about, the hysteretic elastic elements, so there is a forward model where, if you happen to know how the hysteretic elastic elements behave, you can predict that curve and you can predict the details of the discrete memory and the various interior loops and so on, but it also has the property that if you have a suitable set of data of this type you can actually infer what the elastic elements that are in the system are like.

Then what you notice, of course, is that this is a discussion about quasi-static measurements, somebody squeezing with 200 atm up and down. Of course, when a sound wave goes through a piece of material, it squeezes it locally with a pressure that might be a fraction of an atmosphere. A sound wave does nothing more in a material than what the quasi-static pressure, except for issues of time scale.

If you have some understanding of the elastic elements in the material for these big 200-atm variations, you might also be able to give a discussion of basically how an elastic wave propagates through the material. That is what we hope we have done.

[Transparency 8]

Here is the program. We have from Greg Boitnott at New England Research a spectacular set of quasi-static measurements. We are able to analyze those quasi-static measurements and actually say something quantitative about the nature of the hysteretic elastic elements that are in the system.

We are then able to take our understanding of those hysteretic elastic elements and imagine now that there is a sound wave going through the system. This measurement goes over 200 atm and that space where we have an understanding of the way in which the hysteretic elastic elements behave is sort of 200 atm from top to bottom --

DR. SACHSE: On that second plot, what are the axes? I have no idea what you are plotting there.

DR. GUYER: The behavior of the elastic elements in this material, how they behave. You squeeze on the material and the elastic elements might, for example, make a discontinuous change from having one spring constant to another at some point in the pressure protocol that is going from, let's say, 0 to 200 atm. I did not want to allude to this in great detail but just to say that it was possible to do this, so this is supposed to be a picture that says I understand how the elastic elements respond to pressure.

DR. LEVY: What are the coordinates?

DR. GUYER: You do want me to talk about this, don't you?

The elastic elements are hysteretic, they behave something like this. The elastic element is in state one, you squeeze with a pressure, it stays in state one. At a certain pressure, it makes a transition to a different state and it stays in that state, i.e., you continue to increase the pressure, it stays in that state. You decrease the pressure, it stays in that state until a second pressure, when it goes, boop, back to the other state.

The coordinates in this so-called PM space are the pressures, the two pressures, at which the elastic elements respond. It is somewhere between 0 and 200 atm, because that is the range over which the measurement was made.

From an understanding of the elastic elements in the quasi-static measurement we can predict the behavior we expect, for now a very small pressure variation in the material, much more modest than the 200 atm, so we can predict the behavior here.

DR. LEVY: On the vertical coordinate, that is, again, number density, probability?

DR. GUYER: That is a density of elastic elements in a space where you track their response to pressure and the two coordinates are two pressure coordinates and the density is the number of elastic elements that respond in a particular way to a particular pressure. That is the part I was trying to avoid talking about in detail.

You would not normally start out describing elasticity this way, you would write down some Taylor series expansion. Who the hell would write down a density of elastic elements in a space where you track their hysteretic behavior? But if you are going to describe this kind of experiment, you cannot get away without doing that.

Here is what traditional theory predicts. Traditional theory is the Landau-Lifschitz-Taylor series expansion. It says, for example, for the fundamental resonance in a bar you would find a shift in the frequency of the maximum going as the square of the strain field in the bar and in

proportion to something which is the quartic anharmonicity -- it is usually called delta among the people who do this for a living. You would find a nonlinear attenuation, a Q, differing from the Q at a basically arbitrarily small strain field, that goes as the square of the strain field.

For the strain fields we have been talking about, (they go to, at most, on the order of 10^{-6}) the coefficient delta is thought to be of the order of 10^6 and would suggest a frequency shift of one part in 10^6 and a one part in 10^6 change in Q.

What is observed experimentally is that -- well, let's go to the other theory, first, I guess. It predicts is a frequency shift proportional to the magnitude of the strain field; that is, this is this nonanalytic function, a coefficient that is related to the density of elastic elements in that space up there. It is related somehow to that density; again, there is a theoretical model that is rather elaborate that has to be carried out to do this.

A change in Q, also proportional to the magnitude of the strain field, again, a nonanalytic function, with a coefficient not quite the same as C1 but related to it by 4 π/3, so of the same order of magnitude and, furthermore, from an understanding of the density in that space you can actually say that these numbers are of the order of 1000. That is a prediction.

Now, what I am going to talk to you about is an experiment to try to confirm it. The experiment, of course, is just a resonance experiment, but if you are doing nonlinear resonance, you have to do things in a rather -- you do not have to -- you ought to do things in a rather different way.

[Transparency 9]

This experiment was done by Tencate. It is the data you have seen now about 4.5 to 7 times. This experiment was done after the Berea sandstone, that long and that big in diameter, had been in a vacuum chamber for about seven months, and it was done during the 8th month. The experiment is still in the vacuum chamber; it has now been about 18 months. It is in a temperature-controlled environment, so we are trying very much to -- in fact, you have to, you have to worry about humidity, as somebody pointed out.

You have to worry about temperature, a rock is a very good thermometer. The measurement is to look at the resonance as a function of the drive amplitude. If you are used to doing linear resonance, then you do not think about this too hard. If you do nonlinear resonance,

then in some sense you think about it in this way, you fix the voltage of the drive amplitude, let's say 81, and you measure a certain number of frequencies that take you through the resonance.

You change the drive amplitude. You go through the same set of frequencies again, change the drive amplitude, go through the same set of frequencies again, that is, generate this set of curves. What you are actually doing is filling out a matrix; that is, there are n values of the voltage, m values of the frequency, so each experiment is, in some sense, a matrix of response at a set of points that are characterized by the voltage you are driving with and by the frequency.

Because of the known delicacy of this system to things like temperature, or whatever, when we actually do this experiment, we accept an experimental run if we go to this voltage and run through the frequency, go to that next voltage and run through the frequency, go through the whole series of resonance curves up and down, as the voltage goes up to the very highest voltage, come back down, do the resonance up and down and --

[Transparency 10]

-- compare the whole set of resonant frequencies you have been finding the whole way and, if they are not consistent with one another by some sensible measure of their value, we generally do not use the experiment, because there are very slow time evolutionary drifts to these systems that one simply cannot avoid, so there is a great deal of effort put into being sure that there are no systematic events taking place at the same time that we are trying to give a discussion about very precise analysis.

What you actually do is you measure the in-phase and out-of-phase component of the response at every voltage and frequency. You actually measure 2 matrices. I call the in-phase matrix A and the out-of-phase matrix B, and if you want to think about how to think about it, plot the frequencies at which you make the measurements this way and then stack the set of voltages back that way.

Why are we doing this? We are doing this because the nonlinear state of a rock is a function of some internal field in the rock, its strain field, the velocity field, something like that. When you go through a resonance curve you are continually changing the strain field, so you are continually changing the very field you are interested in trying to understand; that is, you sweep a resonance and the strain is very small here, it is very large there, very small there, you change the voltage -- the same thing, again.

If you are going to try to talk about the way in which there are various internal fields in a rock (in anything, in anything that is nonlinear), that cause consequences in the behavior of the rock, you might want to look at it at constant values of the field that causes the consequences. That is, you might want to study these data not by studying resonance curves but, rather, by taking a family of resonance curves and studying them on trajectories that cut through the whole set of resonance curves at constant field so that the rock is in the same state along this trajectory the whole time. It is in a continually varying state along that trajectory.

The things we have done in order to be able to make rather careful quantitative measurements is to analyze data --this was called "constant strain analysis" -- sets, if you like, cutting this matrix like that as opposed to tracking it like that.

[Transparency 11]

This is how you do it. You take a bunch of data, there are all kinds of prefacing related to determining internal phase shifts and so on in the instruments. It is supposed to be a set of resonance curves and you essentially cut them that way and produce -- I am going to show you a contour plot of what a nonlinear resonance looks like, and you study it along contours of constant strain to understand its behavior.

[Transparency 12]

There is one other wrinkle -- well, it is not really a wrinkle, but another little thing we do when we do this study -- we do not fit Lorentzians to resonance curves. The Lorentzians actually drive to zero the edges of a resonance curve.

What you ought to do -- there is the in-phase component, it has got this big denominator, so as soon as you get off by a Q-and-a-half to the left or right, you basically drive the amplitude, so you do not want to fit A to a Lorentzian, or the out-of-phase component to a Lorentzian. You can experimentally get rid of this denominator, because it is just the sum of the squares of the 2 fields you are experimentally measuring.

Of course, again, I said these are matrices. You have a matrix entry A_{ij} at each voltage and frequency, a matrix entry B_{ij} and a corresponding magnitude of U, so just manipulate your data like this. What you are studying is simply -- I used a bunch of dimensionless measures here – omega squared minus one, and you can understand where the resonance is very simply in this thing. If you study that quantity, you are basically simply studying omega divided by Q.

If you have got a nonlinear resonance, it has got a very peculiar shape; you certainly do not want to say the width has anything to do with Q. You learn about Q by studying the way in which the amplitude at resonance evolves or you can, if you like, study this function and Q will be the quantity in the denominator.

[Transparency 13]

Here is a sequence of resonance curves. These were the ones that were studied. They were on Berea sandstone and there were about 121 frequencies -- do not ask me what the voltage was but I will tell you that the strains went from 2×10^{-8} for the lowest curve to basically 6×10^{-7} for the highest curve.

You almost cannot see it here, but if you look extremely carefully, you will see that the resonances here (and it is shifted slightly to that side of this dashed line), so this is the very low-strain region of the nonlinearity, and that is what we are going to study to try to see how that frequency shift moves as a function of strain field.

If you take that same set of data and spread it out and do the constant strain-field cut and look at it as a set of contours, now you can actually notice the resonance very cleanly, notice the change in the resonance, because the contour of constant strain actually -- it is not symmetric, but the important quality is that along this trajectory the system is in the same elastic state.

A normal way of doing resonance cuts it this way and then moves from elastic state to elastic state the whole time you are looking at it. This way you look at it along a constant elastic state and you do the various things I described.

[Transparency 14]

I will show you what the answer is. If you do very careful analysis of the behavior of the resonance at constant strain field along each of these various trajectories, you can say what resonance frequency characterizes the system on a particular one of those trajectories and, as you go from trajectory to trajectory, therefore changing the strain, how does the resonant frequency change with strain?

Similarly, you can measure the out-of-phase component and see how the Q varies as you go from one strain field to the next.

[Transparency 15]

84

This is the result. The Q is the amplitude at resonance. It is not related to the width -- of course, it is related to the width, but since the system does not have a constant strain, you cannot quite decide how to handle that -- so find Q from the amplitude.

The Q dependence is that $1/Q$ starts out at a value of $1/Q_O$ and rises linearly in the amplitude of the strain. The units here are arbitrary units but they are close enough to say this is 10^{-6} in strain. This happens to be a linear plot, so 10^{-7} is actually down in there.

DR. MCCALL: What are the triangles?

DR. GUYER: Up and down. Are you asking why are there triangles versus squares? At the very lowest strains we are down at basically 2×10^{-8} and the noise in the system is great enough that there is crazy behavior down here and then there is not so-bad behavior there, and once the strain gets above about 10^{-7}, things start to straighten out and you have to just imagine there are systematics that make it very difficult to pin things down.

I tried to put some error bars up in here, but I did not put the corresponding error bars there, so you get a sense of -- one is talking about fractions of a tenth of a hertz on top of roughly 3000 Hz when you are talking about these kinds of numbers.

The frequency shift is experimentally directly proportional to the magnitude of the strain field. That is confirming the prediction of the fancy theory and, if you like, "disconfirming" traditional nonlinear elasticity.

[Transparency 16]

The only thing that remains -- not the only thing -- is are the numbers right? It is one thing to get a qualitative answer and the answer is, yes, the numbers are right. As we go to Greg Boitnott's experiment, we do the analysis for that stuff that is on the graph without coordinates but, nonetheless, I will tell you that somehow I can show you how it is quantitatively related and it predicts a numerical value for the coefficients that tell you how big the actual linear change in the frequency, the linear change in the $1/Q$ will be, and this is not fantastic agreement, but the fact that it is the same order of magnitude is gratifying, it is within roughly a factor of two of what is observed experimentally.

We take this to mean that you can take an experiment like this one -- this one goes up to strain fields of 10^{-3} and involves pressures of up to, let's say, 200 atm and learn about the elastic elements that are in the system and it also involves times scales (this is a quasi-static measurement, so the time scales here are minutes to hours, multiples of seconds), you learn about

the elastic elements in the system, then propagate a wave, which tickles the system with strain fields of order of 10^{-7}, so four to five orders of magnitude smaller on time scales that are probably four to five orders of magnitude faster and, nonetheless, find that you have learned something about the elastic elements over there that will also tell you, in a quantitative way, about the way in which the elastic elements in the system respond to dynamic measurements.

Here is the conclusion. I said it in words, but there it is in pictures relating -- here is the quasi-static measurement made out here, relatively high strain, relatively low frequency, quantitatively related to the dynamic measurement, which is done at relatively higher frequency and relatively low strain fields.

DR. MAYNARD: Do you have a reference for that PM space analysis?

DR. GUYER: Yes, Jay, there was one in *Physical Review Letters* about 1995. Also, there was a *Physical Review Letters* about a month ago describing this experiment that I just talked about and it makes reference back to this set of papers that are more or less behind it.

DR. SACHSE: Has anyone repeated that curve, that discrete hysteretic type of curve going up and down and then doing it a second time?

DR. GUYER: Oh, yes. You go up and you come down and you do not go back to where you were. You go up and you do not quite come back, and then you go up and about the third time you come back. This all relates to the fact that you pick up a rock off the ground and it has had a pressure experience in its life; you have no idea what elastic state it is in.

Some of the elastic elements in it are going to break, crack, or do whatever they like, the first time you touch it or squeeze it, but after you have fussed with it just a little bit, it will achieve an elastic state that still has hysteresis, discrete memory, and so on, but is repeatable and reversible, and that is, in fact, the elastic state we have been talking about.

PARTICIPANT: Have you tried to add any pore fluids in there to see if there is an --

DR. GUYER: Of course, as I said, this was done in vacuum and one of the things we are very aware of is that pore fluids have a great deal to do with the way in which -- there is a preliminary measurement from France, from Paul Johnson, in fact, that seems to show that saturation has an influence, a striking influence, on nonlinear behavior.

I come from the school that says that saturation is not -- what we have learned here is that the stress field, or the pressure, is not a good variable for characterizing a rock. If you have any experience with pore fluids and pore spaces, you also know that the saturation is a not a good

variable. You have to study the history -- you say the history of the chemical potential, how has the chemical potential of the pore fluid been evolving, what is the state it is in at the moment, what have you done?

Both of those are hysteretic things, the pore-fluid configurations are hysteretic and so is the elasticity, and it makes it a really difficult system to study.

Thank you.

GLOBAL SYMMETRY, THE PHONON DENSITY OF STATES AND RUS

T.W. DARLING AND A. MIGLIORI
LOS ALAMOS NATIONAL LABORATORY

ABSTRACT

RUS measures (in principle) a complete set of the acoustic phonons near the Brillouin zone center. By comparison with a model of an homogeneous solid of known global symmetry and judicious application of a goodness-of-fit measure, the elastic constants can be deduced.

For many solid state phase transitions the change in the symmetry of the object locally and globally is of prime importance, particularly where the transition leads to disorder at some length scale. We will discuss the application of RUS to determination of symmetry and whether in practice this can provide useful information on systems with fine or meso-scale structure.

Such systems are in some sense "intermediate" between homogeneous single crystals (low symmetry) and an homogeneous, isotropic ("glassy") state (high symmetry). We expect this to be reflected in the behavior of the phonon density-of-states and thus into other physical properties such as the specific heat. We discuss the application of RUS to measuring this behavior directly or to guiding other experimental techniques which have access to different length scales.

These topics will be illustrated by analyses of our RUS data on perovskite and martensite systems.

TRANSCRIPT

DR. DARLING: When I started to write this talk a week ago, based loosely on an abstract submitted 2 months ago, I thought I was going to have a lot to say about the thermodynamics that you can extract from RUS measurements and, in fact, what I came up with was a bunch of reminders of undergraduate physics and a set of object lessons, cautionary object lessons, which are actually kind of relevant to some of the talks we have seen.

[Transparency 1]

The first one was relative size. In Douglas Adams' work, *The Hitchhiker's Guide to the Galaxy*, one of the worst fates imaginable is to be put in the total perspective vortex where your ego is demolished by a view of your own size in relationship to the universe.

[Transparency 2]

Here is the universe of the vibrations of a solid and down here on a microscopic dot is where we work and if we think that we are going to extrapolate something we measure down here into the amount of detail that exists over the whole phonon spectrum, then we have got to be pretty careful about what we do here.

At this end of the universe, this scale, which is accessible by scattering experiments, neutrons, x-rays, various optical techniques, strange variations of Mössbauer measurements, generally tend to cut off at about 10^{11} Hz. Our measurements down here tend to cut off usually below 8 MHz of resonances in a system for a number of reasons.

Up here we have -- generally harmonic approximation is used to calculate these modes and that gets rid of a whole load of experimental useless pieces of things like thermal expansion and temperature dependencies of elastic constants, so the calculations up here are fairly straightforward, but the models used actually rely on the fact that the dissipation processes at high frequencies are limited to, say, electronic components and harmonic parts, whereas down here, of course, we have a whole bunch of other things.

High frequencies: We measure total energies by replacing the solid by a whole bunch of harmonic oscillators.

[Transparency 3]

This gives us amplitudes and frequencies for oscillators. You then put in wave numbers by applying a model that gives you plane waves inside the solid, but you end up throwing away any dissipation processes and all of these useless parts and, quite often, you deal with it in a Debye model where you are modeling a continuum.

[Transparenciey4]

Down at our end of the world we have dissipation processes, and I am not going to talk very much about this, just to say this looks like one of the curves that Bob Leisure measures for relaxation processes, which are all low-frequency items.

We have trouble in general dealing with this because of this frequency variation across a scan and only if you measure the temperature dependence with respect to a single peak do you actually get information that you can really extract sensibly.

[Transparency 5]

And we have this problem. This is a tantalum sample and this is a set of plots of a 20-kHz region that I have taken from about 1 MHz up to 4 MHz and, as we can see down here, the density of states is low enough that we can easily select our peaks, but perhaps by the time we have reached 2.5 MHz we are getting to the point where we can no longer extract peaks out of this thing usefully and as we go farther and farther up we find we get into this limit where the density of states is high enough that the phases and amplitudes are averaging out and we are seeing no signal, not because the electronics is incapable of it but just because the material itself is cutting us off, so the 8 MHz that I showed on the first plot is perhaps an upper limit.

[Transparency 6]

How well do we actually do with densities of states? Here is the first cautionary object lesson. This is a strontium titanate sample, a single crystal, it was cut and we measured the green triangles to show the density of states up to about 8 MHz, perhaps a little farther.

It follows exactly -- by accident here, the scaling factor is actually one -- a curve, dN/df follows a curve of f^2. The object lesson involved here are the red and the black dots, which are the results of fits from the program that most of us used, which was supplied by Bill Visscher and various variants that people work on here. It fails, quite seriously, here, and this is not surprising when you look at it, because we know that in order to make the basis functions for this fit we divide up into 8 different parity-organized states and we have another parameter that describes each mode, which is essentially harmonic numbers, which are k and i in the fitting program.

If we are using basis functions that are only going up to an order of 10 in a polynomial, that is about the number of nodes that we expect to see, so in an harmonic idea of waves inside a solid, we expect to see only up to 10 nodes inside this, so when we get to values of i, that is, harmonics that are greater than 10, we are not going to be fitting this material, we do not have a basis function that is capable of actually following it.

What this means -- and this is the i value here, which is approximately 10 and perhaps some variants of the program (we have 12 order polynomials) -- is the total number of lines you

are going to measure to get there is perhaps somewhere between 50 and 60 lines. This will vary a little bit depending upon the geometry of the sample and the actual relative sizes of the C_{ij}'s, but it means that if you are going to measure more than 50 lines and fit it, you are not really doing yourself any favors at all; all you are doing is introducing errors.

DR. ISAAK: What shape is the specimen?

DR. DARLING: It is a rectangular parallelepiped with an aspect ratio of perhaps 2:1 on its large face and 4:1 -- it is a plate. You will not be able to measure more than the order of the polynomial times 8 lines, because then you will almost certainly have exceeded the capability of the basis functions to describe the vibration of the solid.

[Transparency 7]

Of the thermodynamic things we can measure, specific heat is something that is usually looked at. This, of course, ignores all the electronic components. You can describe it by the density of states, multiply it by the specific heat per oscillator, integrate it over the whole of accessible space to give you -- this is in the harmonic approximation as well.

This function here, which, if you use an Einstein specific heat per oscillator, you can see cuts off the integral as the temperature gets lower (there is actually an invisible yellow line there that goes almost straight across at 20 K).

If we are living in this little space of the density of states here, then the only time that we really have anything useful to say about specific heat accurately is when we are down at temperatures of a few micro-Kelvin, which few of us routinely approach. Otherwise, every single thing that we measure is a Debye solid, and that is all we can extract from the density of states out of the RUS system, so we lose, there is no way we will see any of the detail at higher frequencies.

[Transparency 8]

The same thing largely goes for the dispersion curves that can be measured, once again, by neutron-scattering experiments. These are just examples from the literature for silicon and nickel. The blue line is basically the lower limit of experimental data from scattering experiments. The little red bit here is round about where we live in these curves.

What I have really put these up to show is that this is considered to be pretty good agreement between data and experimental fits for calculating via various lattice dynamic approaches to the dispersion curves. In fact, they are not really very good and, in particular, the

only way that these types of approaches have anything to say about the zone center phonons, which is where we are, is by the theoretical extrapolations coming down to the gamma point at the zone center.

This is kind of interesting. Several years ago a publication came out looking at the properties of gold zinc and, based upon data that fitted about the same as this looks, they calculated elastic constants that were a good 200% wrong and published a statement saying that the gold zinc, because of the elastic constants, the low anisotropy from their measured elastic constants, would never show a martensitic transformation, which is now known to be untrue.

[Transparency 9]

This is the measurement of the frequencies of a single crystal of gold zinc and, in fact, it is well known to have a martensitic transformation.

The errors that are introduced by extrapolating high-frequency measurements back down to where we live can be significant. It is very important, in fact, that we make good measurements of the dispersion curves of the zone center to keep these guys honest, to make sure that their models are not actually erring off into strange places.

This also shows something that Don brought up the other day, which is an enormous temperature dependence -- the transformation actually takes place at about 60 K, but up to room temperature we still have negative elastic constant variations with temperature. One of the things I want to do is to actually extend this to see just how far it goes; it shows no tendency to be turning over even that far away from the transformation, and I will mention a little more about that later.

[Transparency 10]

Every result that we derive from our RUS measurements is only as good as the Debye model and this can matter a lot at intermediate temperatures between sort of helium and nitrogen temperatures, where the actual shape of density-of- states curves and the turnover of dispersion curves can matter.

The Debye model is very popular. It is essentially a single parameter model where we extract a sort of geometric average velocity from our measured transverse and longitudinal wave velocities, which we have extracted from our measurements of c_{ij}.

The thing to note, really, about this is that to do this sensibly we really have to know how many independent branches there are of the phonon spectrum, and it means that we have to be

very sure of the number of elastic constants that we are using to fit our spectrum and that, of course, is the global symmetry of the sample.

[Transparency 11]

Once again, using a sample of strontium titanate -- this is just to show that we actually measured strontium titanate -- I took a set of these room-temperature spectra and, using the program, again, to fit, I produced, with the same input data, I fitted a variety of different symmetries. I know it is cubic but I would like the program to be able to tell me it is cubic.

One of the first things you notice is the RMS number that comes out of the program actually can hide a lot of problems. Because it is a percentage error it normalizes the size of the error with the frequency, so as the frequency goes up, whatever the error is, it starts shrinking as 1 over the frequency, so at very high frequencies its contribution to the error measure is small.

I had a look at the actual chi^2 per degree of freedom, which you expect to be around 1 for a good fit, and I was able, just on the basis of that, to reject isotropic and hexagonal fits. In the second line, the iso-star line, I took only 4 lines, the first 4 lines of this measurement, and ran a fit and I got a wonderful RMS value out of the program, but it is a rubbish fit. It has no relationship to the real elastic constants, so a small number of lines can be a serious problem here.

The 3 hexagonal fits are just the 3 possible orientations of the c axis within these samples, supposing I did not know it, but I can reject all of these 32 lines (I can reject the pieces with isotropic components). The cubic one fits pretty well, it has a good chi^2 degree of freedom, good RMS error, but when you get up to tetragonal and orthogonal, I expect these to fit well. The cubic is a special case of tetragonal and orthogonal and, in fact, I expect the fit to improve slightly when I do use these symmetries because I have more free parameters to fit with.

The interesting thing is that in tetragonal, for some reason in this system, I have 2 -- these 2 (the green and the blue are absolutely invisible on this) -- the 2 and 3 fit from the tetragonal are actually the ones that I expect. They are a little bit better than the cubic fit and they have the same values of the elastic constants and the bulk modulus.

But there is one orientation of this that has an excellent fit but it is wrong, it has provided the wrong elastic constants, so if I were to do this, if I were just to start it off with a tetragonal assumption, I might say, great, I have one orientation that fits really well and gives me some

values, and two orientations that are in the wrong c-axis direction, so I might simply throw away cubic as the symmetry of this material just because I seem to have a consistent tetragonal fit.

I have an orthogonal fit as well, which looks like the wrong tetragonal fit and I need to be able to reject these possibilities when I am making these measurements; otherwise I will end up with the wrong number of elastic constants, the wrong symmetry and all sorts of other wrong things when I try to do physics.

The thing that you really need to look at here is the chi^2 error, the actual function, the chi^2 function, at the minimum. In fact, you need to be able to reject fits on the basis of those things as well, so if you are just reading the RMS error out of the program, you are doing yourself a disservice, because you need to be also rejecting places that have too shallow a fit in any of the elastic constants at the minimum.

That means the numbers that are produced by the program (and these are the numbers that come out of the program), the 2% chi^2 confidence limit, it is not really an error, it is a confidence limit that we have placed in the chi^2 hyper-surface. If these numbers exceed a few percent, 2 or 3%, you need to reject them as well, because the fit is too shallow for you to be certain that there is actually not another minimum in there somewhere farther down the road that has not been reached by the program.

This is the second cautionary tale, that you have to be very careful upon reading just this value of the RMS error, because you can reach false minima that look excellent in terms of that error but unless they also have sharp minima they do need to be rejected.

PARTICIPANT: Could you have sharp minima that were also false?

DR. DARLING: I do not know. I have asked myself that question a lot, as to whether or not you can achieve a sharp minimum that is not the right one. I have never seen it, actually, but that would be a wonderful question to be able to answer. I do not know in general if you can do it in an n dimensional space with a chi_2 hyper-surface and say whether the global minimum has always got to be sharp and that no other minimum will also be sharp.

[Transparency 12]

There is a set of magic numbers that we need to take note of and I call them "magic" because they are largely the result of hand-waving and experience but maybe ignoring them is sometimes useful, too.

We know that the number of lines had better be less than the order of the polynomial times the number of parity states, because, otherwise, you will be trying to fit rubbish lines. I have known people who have said, "Hey, I've measured 120 lines and got this incredible fit," and you know that the top 50 lines just do not have any meaning and that the RMS error, because it is a fractional error, has just hidden the fact that there are huge problems there.

In fact, it may turn out to be much lower if you end up using up -- if you have a very low elastic constant you might use up a whole load of harmonics associated with that type of parity motion before you get to 80 lines. By the time you have reached i = 8 for any of the parity modes, you have started to exceed the program's capability to describe the vibration.

You need to use a sufficient number of lines. We arbitrarily suggest that the number of elastic constants times 5 is a good number of lines to be using, at least, because fewer lines will also give you false fits. The reason the 4 lines gave me a wonderful fit with strontium titanate is that the first 3 depended on only one elastic constant, as Don showed us earlier, so 4 lines I can easily fit with 2 parameters to an isotropic fit, because 3 of the lines depend on only one elastic constant, and that is a very common thing with RUS samples.

When you are looking at the errors coming out of the program, we arbitrarily say that if we do not get better than 0.5%, then we do not really have a fit. We would really like it to be much better than that, in fact, better than 0.2%, but the criterion is that you also, if you are going to determine the symmetry of the sample, really have to know how many elastic constants belong to it, you need to make sure that the confidence limit that we have applied does not exceed, let's say, 2 or perhaps 3%.

When you, in fact, increase the number of free parameters and you get an improvement in the RMS error between, say, cubic and tetragonal, numbers of less than, say, 20%, it may not actually have any meaning for it at all just because of the improvement of the number of free parameters.

[Transparency 13]

We are making a Debye model. If we want to calculate free energies, entropies, any of these things that we are extracting numbers from based on Debye temperatures, then we have to understand that we are operating in a Debye model that has, up until the zone edge, an f^2 dependence of the density of states and a linear dependence of the dispersion of the phonons all the way to the zone edge.

If anything depends at intermediate temperatures on the fine structure, that is, cutoffs of the various longitudinal and transverse modes, then we are going to run into problems. We are only as good as the Debye model.

However, measurements, in general, are so good that we definitely need to do them in order to keep the models honest that are measured from high-frequency things. The symmetry is really very important and we determine only the global symmetry and there are various scaling things (a bunch of slides I did not show you that say that we actually miss a whole bunch of interesting regions), where micro-structure and grain structures start to make the wave vector a poor quantum number.

We can see sometimes things to do with micro-structures by looking at the way the symmetry is changed, so, for instance, a polycrystal will look isotropic as opposed to being the symmetry of each single crystal, and you can perhaps extract some things. One of the things I did not talk about very much, the temperature dependence of C_{ij}, which has a connection to the average oscillator amplitude of each of these normal modes, may eventually play back onto a lot of these things. There may be some things you can extract from temperature dependences and we do do temperature dependences very well in RUS, particularly the anomalous varieties of it, such as Don showed and such as gold zinc shows, to be able to correlate that with such things as anomalous thermal expansions and to extract that from our measurements would be, I think, a useful thing and, I think, a profitable way to look.

Thanks.

DR. ANDERSON: I always approach this problem as saying if I am going to measure a single crystal, I have got a good single crystal, so I am going to do x-rays and find out what this crystal is. Then I will know what the symmetry is and then I will put that into the inverse calculation. I never dreamed that you would do it the other way.

DR. DARLING: There is a problem there in that quite a lot of x-ray determinations will not show you small distortions or small deviations if you look at your average Laue back-reflection pattern. The difference between a slightly tetragonal distorted material and a cubic one is very small and you would likely say this is cubic.

We are somewhat more sensitive in measuring the vibrations. We could actually see if there was a small tetragonal distortion and that is kind of important and, also, if we go through a phase transformation, you do not generally get the chance to be watching with x-rays, not many

people have the equipment to do that, but we get to see if the symmetry has changed going through a phase transformation, and we could determine the symmetry, in principle, after having gone through a phase transformation.

DR. ANDERSON: What you are saying is that we have the power through RUS determination to confer the symmetry that you thought you had from an x-ray and you might be surprised.

DR. DARLING: Absolutely. You might be surprised.

DR. MIGLIORI: Take an x-ray of a pattern of a quasi-crystal and that tells you what to do.

DR. DARLING: So you will see a fivefold pattern out of a quasi-crystal but, elastically, it is extraordinarily isotropic.

DR. ISAAK: I think you have highlighted it. It is still pretty dicey to say you can determine the symmetry. You showed those slides and just from my own experience, I have done that, too, where I have taken like rutile, which is tetragonal, I tried an orthorhombic fit (I was just checking some things) and I came into similar problems like that. I was really surprised.

When you give it extra degrees of freedom, you take those liberties and go off somewhere -

DR. DARLING: You need to be extraordinarily careful to do that and sometimes you do not know exactly what the symmetry is. There are some people at the lab who, for reasons of their own, like to splat little rods of aluminum into a brick wall so that it plastically squashes, and I had a look at some of these pieces and I am pretty sure that there is at one unique axis, which is the one perpendicular to the direction that splashed this piece of aluminum, but it turns out that the cross-section you get is elliptical as well, which suggests that the perpendicular axes can be special.

It was very interesting to them to know exactly what the symmetry elastically was to our best measurements of that material, whether, in fact, it was orthorhombic, as the shape suggested -- we, in fact, found that the difference between tetragonal and orthorhombic, elastically, there was very small.

DR. ANDERSON: If you put in a certain symmetry the machine will find, your program will find a minimum for you and you will say "aha."

DR. DARLING: Absolutely, you need to be watching, and that is why the question of whether a false minimum can actually also be sharp, can actually fit all of these criteria that I put

down, is a very interesting one, but I do not know the answer to it and I have not seen a false minimum that is sharp, but it would be very interesting to know whether you can be led truly astray. We know that the solution is not unique in principle.

DR. DEMAREST: When you are calculating the low-temperature specific heat, you can probably get even better results if you do not use the RUS calculation but, rather, these periodic boundary conditions.

DR. DARLING: That is certainly true. One of the problems with RUS is that the free boundary conditions mix up the modes. In periodic boundary conditions you manage to keep everything essentially as plane waves that fit inside the particular solution. With free boundary conditions, as everybody knows, your modes are never pure anything. The picture of the squashed cubes that is so popularly shown just tells you there are no plane waves living in the RUS spectrum until you get to high-enough frequencies. That is certainly a complication for calculations of specific heats.

If you needed to, you could, in fact, use that spectrum to get detailed real specific heats out of the real modes at the low-frequency end of the spectrum.

DR. LEDBETTER: Your results imply that you can take one crystal and measure the RUS spectra and get information about whether there are zone-center soft modes?

DR. DARLING: A zone-center soft mode is usually an optical -- I have not looked at zone-center acoustical soft modes which are not a result of effects at other parts of the zone. Certainly, if you have a zone-edge soft mode as in strontium titanate, we see the result here because of the pulling down of the whole dispersion curve, so we see an effect in the gradient and the dispersion at the zone center, but if such a thing exists as an acoustical soft mode only at the zone center we would see it.

DR. ANDERSON: But metals do not have optic modes and they have transitions. so --

DR. DARLING: Gold zinc is a metal and it has got optical modes. You just need to have more than one atom per primitive cell to do that.

DR. MIGLIORI: Orson, a first-phase order transition can go without a soft mode.

DR. ANDERSON: Okay, yes.

DR. DARLING: Thank you.

Contactless Mode-Selective Resonance Ultrasound Spectroscopy: Electromagnetic Acoustic Resonance

Hirotsugu Ogi[1,2] and Hassel Ledbetter[2]
[1]Osaka University
[2]National Institute Of Standards And Technology

Abstract

We describe a novel method for measuring elastic constants and internal friction in electrically conductive solids: electromagnetic acoustic resonance (EMAR). Contactless coupling based on the Lorentz-force mechanism is achieved by permanent magnets to supply the static magnetic field and a solenoidal coil surrounding a rectangular-parallelepiped specimen. Because the direction and symmetry of the Lorentz forces can be easily changed by changing the geometrical configuration of the static field and the coil, we can select a single vibration group of interest, filtering out the other vibration groups. In principle, seven vibration groups can be independently excited among eight possible vibration groups of a rectangular-parallelepiped specimen. This provides a big advantage in mode identification. The EMAR method is much less sensitive than the RUS method to the initial (guessed) C_{ij} for the inverse calculation. For a copper monocrystal, we reached the same C_{ij} with 100 %-varied guessed values. For silicon-carbide-fiber-reinforced titanium-alloy composites, we could vary the guessed values up to 20 %. We used a free-decay method to measure internal friction Q_{ij}^{-1}. The contactless EMAR method enables one to measure intrinsic internal friction, free from energy loss into transducers and grips.

Transcript

This paper describes a new RUS (Resonance Ultrasound Spectroscopy) method to selectively and independently cause one particular vibration group, using electromagnetic acoustic transducer, EMAT.

The RUS method is a powerful tool to determine all independent C_{ij} for a small specimen with a single frequency scan. One measurement provides a complete set of C_{ij}. However, successful use of the RUS method needs exact correspondence between measured and calculated

resonance frequencies, that is mode identification. For this, we need to know the elastic constants for the inverse calculation that are not far from the true values. For making exact mode identification, several methods appeared, but they are inapplicable to the material of large internal friction, because of resonance-peak overlapping. The best way to make an exact mode identification is to produce the RUS method for one particular vibration group independently.

As well as the difficulty of making mode identification, mechanical contacting causes a problem in the RUS method. Coupling force is not very large compared with the conventional contacting methods such as the pulse-echo method, but, still acoustic energy goes into the transducers that causes extra energy loss and increase the as-measured internal friction.

In this study, we develop a new contactless resonance method to selectively and independently select one vibration group among eight groups of free vibration of rectangular parallelepipeds, and apply it to determining C_{ij} and Q_{ij}^{-1}, which is internal friction tensor, of the silicon-carbide-fiber reinforced titanium alloy composite. Then, we use this method at elevated temperatures to measure the temperature dependence of C_{ij} and Q_{ij}^{-1}, which is easily realized by the EMAR feasibility at elevated temperatures.

[Transparency 1]

Figure 1 shows a typical measurement setup of EMAR, which includes a solenoid coil and permanent magnets providing the static magnetic field. The specimen is inserted in the coil. Because the coil is very loose and never tight, no external forces are applied to the specimen, except for gravity, realizing an acoustically-noncontacting situation.

We drive the solenoid coil with high-power burst signal to induce eddy currents on the specimen surface. Eddy currents interact with the magnetic field and generate the Lorentz forces that cause mechanical vibration. The same coil detects the deformation of vibration after the excitation. By sweeping the frequency of the driving bursts and getting the amplitude spectrum as a function of the frequency, we obtain the resonance spectrum.

[Transparency 2]

We can select a vibration group just by changing the geometrical configuration between the static magnetic field and the coil. Figure 2 explains the mode-selective principle with EMAR. For example, in the measurement configuration of Fig. 2 (a), the magnetic field is applied in the axial direction of the coil. In this case, we expect the Lorentz forces occurring normal to the specimen surfaces. By focusing w, which is the deformation on the x_1-x_2 plane, we easily find,

that to detect w with the same coil via the reversed Lorentz-force mechanism, w must be an even function about x_1 and x_2, and an odd function about x_3. Among eight vibration groups of rectangular parallelepipeds, only OD group (breathing vibration) satisfies this condition, meaning that only OD group is excited and detector, filtering others out, in this configuration. Similarly, in Fig. 2 (b), only the OY group and, in Fig. 2 (c), only the OX group are detected and excited. Thus, we can select the vibration group by changing the measurement configuration. In principle, with this method, we can independently cause seven vibration groups among eight groups. We found these three groups are enough to reduce all C_{ij} even for orthorhombic symmetric crystal.

[Transparencies 3 and 4]

We used copper monocrystal specimens and also silicon-carbide-fiber-reinforced titanium-alloy composite as shown in Fig. 3. Both are rectangular parallelepipeds with a few millimeter dimensions. Figure 4 shows a microstructure of the composite material, the silicon carbide fiber and the matrix. This material is a candidate for the aerospace structures and jet-engine components and it is expected to be used at elevated temperatures. Therefore, we need to know the elastic behavior at elevated temperatures.

[Transparencies 5 and 6]

First, we show a couple of the copper monocrystal results and then show the composite results. Figure 5 compares the EMAR and RUS resonance spectra. We used broken line for the RUS spectrum and solid lines for the EMAR spectra. There are many resonance peaks in the RUS spectrum, because all vibration groups are excited simultaneously. But in the EMAR case, we observe just one particular vibrational group with different measurement configuration as expected. Thus, it is much easier to make the exact mode identification. For example, OY_2 and OX_2 appeared at almost the same frequency as shown in Fig. 6. In the RUS measurement, these two modes overlap each other and it is quite difficult to identify them. However, because EMAR can excite independently these two modes, mode identification is clear, including no ambiguousness.

[Transparency 7]

Concerning internal friction, we used a free-decay method with EMAR. We drive the coil with the resonance-frequency bursts, turn off the excitation, and measure the amplitude of vibration with time. By fitting an exponential function, we obtain internal friction from the

101

decay constants. Figure 7 shows the amplitude decay with logarithmic scale, which shows a good agreement with the fitted function. We measure internal friction for all resonant peaks and determine internal friction tensor, Q_{ij}^{-1}, through the inverse calculation.

[Transparency 8]

Table I shows thus determined elastic constants and internal friction. We also used the RUS method to determine the C_{ij} and Q_{ij}^{-1}. Elastic constants between EMAR and RUS agreed well, but EMAR C_{ij} were relatively smaller than RUS C_{ij}. We attribute this to restriction of vibration by sandwiching transducers in the RUS measurement, although we tried to minimize the coupling force. This effect was found remarkably in the internal friction tensor. Internal friction for shear moduli were comparable between the two methods, but internal friction for the vibration mode accompanying volume change, EMAR internal friction was considerably smaller than RUS internal friction, especially for bulk modulus. In this frequency range, 1 MHz or less, the main contribution to the internal friction is dislocation damping. And the bulk-modulus internal friction should be very small, because, in principle, dislocation can not move with hydrostatic oscillation. EMAR measurement provided such a physically reasonable result. RUS methods provided smaller internal friction for the bulk modulus, but it is considerably larger than EMAR. Thus, we consider that this is caused by the energy loss into the transducers because of the volume-changing oscillation in the RUS method.

[Transparency 9]

Next, we will move to the composite material. Figure 8 compares the resonance spectra measured by RUS and EMAR. RUS spectrum consists of large number of peaks, especially in the higher frequency region, and some peaks overlap, making mode identification difficult. In the EMAR case, because we can detect only one vibration group, mode identification is clear.

[Transparency 10]

Table II shows the determined C_{ij} and Q_{ij}^{-1} for the composite material. We again used the RUS method to reduce C_{ij}, but in this case we employed the EMAR C_{ij} as initial values for the inverse calculation. Otherwise, inverse calculation failed to converge or converged to the false minimum. The RUS method is sensitive to the initial C_{ij}.

Note that internal friction for the wave modes propagating to the thickness direction were larger than those for other modes; internal friction for C_{33}, C_{44}, and E_{33} were larger than others. We attribute this to imperfect bonding between ply layers. This composite was fabricated by

foil-fiber-foil technique at 1173 K and imperfect bonding could occur because of the mismatch in the thermal expansion coefficient between the fiber and matrix.

[Transparency 11]

Finally, We describe the EMAR measurement at elevated temperatures. For this, we locate the solenoid coil within the stainless-steel cylinder vessel, which is surrounded by the heater. We set the permanent magnets outside the vessel (Fig. 9). This permanent magnets can rotate about the axial direction of the cylinder vessel, so that we can change the field direction and then select the vibration group. With this method we can increase the temperature as long as the specimen possesses electrical conductivity.

[Transparencies 12, 13 and 14]

Figure 10 shows the EMAR spectra of the OY group at various temperatures. Even at 1000 K, we obtained good signal-to-noise ratio of the spectrum. We determined the temperature dependence of each C_{ij} for the crossply composite as shown in Fig. 11. We found anomaly in the temperature dependence around 700K. Also we measured the temperature dependence of internal friction (Fig. 12). Internal friction considerably increased from 700 K. After heating, the internal friction failed to return to the initial value. We attribute the anomaly of the C_{ij} and increase of internal friction at 700 K to disbonding between silicon carbide fiber and the matrix. Indeed, we observed such disbonding after the heart treatment.

Here is the conclusion. We could select the vibration group by just changing the geometrical configuration between the coil and static field.

We observed some effect of the coupling force in the RUS measurement, especially, for the internal friction measurement.

EMAR showed good feasibility at elevated temperature and high-temperature measurement.

DR. SACHSE: Most of the EMATs are narrow-band devices and yet you show a pretty broad range of frequencies.

DR. OGI: No, I understand most EMATs have broadband frequency range. I just have to change the matching network.

DR. LEISURE: The EMAR technique must also be affected by energy loss outside. Do you have any idea how much that would be, what would be the limiting Q you might be able to measure?

DR. OGI: Please repeat.

DR. LEISURE: You have energy loss in the EMAR technique as well affecting Q coupling to the external source. Do you have an estimate of how much that would be?

DR. OGI: I do not know. I think it highly depends on the specimen size.

DR. ANDERSON: I noticed the elastic constants were consistently lower for your magnetic method compared to the RUS method. I do not understand why they are consistently lower.

DR. OGI: We actually observed smaller C_{ij} with the RUS method than with the EMAR method. For example, RUS provided a little bit higher resonance frequency, I do not know why exactly. There is a paper studying the coupling-force effect on the resonance frequency. In that paper, by increasing the force, the resonance frequencies shift to higher region, and then they provide a little bit higher C_{ij}.

DR. ANDERSON: Maybe the difference in Q is related, too.

DR. OGI: Yes. The difference is larger for the bulk-modulus internal friction, while almost no difference occurred for the internal friction of shear moduli. These observations suggest energy loss into the sandwiching transducers for the volume-changing vibrations.

DR. ANDERSON: Perhaps in the breathing mode you see that. _____ of the air on the specimen, so perhaps the magnetic field situation creates a different loading --

DR. OGI: I see.

DR. ANDERSON: It is very curious. But it is systematically lower and then you say it is contactless. We are interested in the loading of air on specimens, but you have to be very careful in calling it resonant frequency versus pressure.

DR. MARSTON: If you could repeat your description of how the sample was mounted, how do you support the weight of the sample?

DR. OGI: There was a plastic plate on the inside the coil and we just inserted the specimen. Just putting it on the plastic plate, only gravity is applied to the specimen because the coil is very loose and never tight. Of course, there is some coupling between the specimen and the plastic plate, but maybe the acoustic impedance between the plastic plate and metal is quite different, and little energy loss occurred.

DR. MARSTON: You might try some time just holding it like a fishing line, the corners, or some thin filaments.

DR. ISAAK: Do you ever have a problem with this method of maybe not seeing some of the modes that you expect to be there from RUS or is it usually -- if there are 12 RUS modes in this range, you ultimately will see 12 as you do all the orientations?

DR. OGI: I am sorry, I do not understand.

DR. ISAAK: When you compare the modes that you see with the EMAR and RUS, do you generally see all the modes?

DR. OGI: No. We could not observe all modes, even if the detection condition is satisfied. Around here some modes were missing. Because this method detects integrated deformation on the specimen surface, if the integrated value is very small, it fails to detect such a vibration.

Also, another disadvantage of this method is it is applicable to the material having electrical conductivity or magnetostriction.

Thank you.

ELASTIC COEFFICIENTS AND INTERNAL FRICTION
OF SILICON MONOCRYSTAL SPHERES

HASSEL LEDBETTER AND SUDOOK KIM
NATIONAL INSTITUTE OF STANDARDS AND TECHNOLOGY

ABSTRACT

Using mechanical-spectroscopy methods, we measured the elastic-stiffness coefficients of four spheres of high-quality monocrystal silicon. Within 1 part in 1000, the C_{ij} agreed with that reported by Bell Laboratories more than thirty years ago. We attribute the internal friction Q_{ij}^{-1} mainly to dislocations. Departure from the Koehler-Granato-Lucke vibrating-string model suggest dislocation-kink motion.

TRANSCRIPT

DR. LEDBETTER: Good morning.

[Transparency 1]

This morning I shall be talking about this topic and I shall focus mainly on the internal friction part, because it is no surprise that the elastic constants of silicon have been studied since the early 1960s and are quite well understood.

[Transparency 2]

The silicon that we studied is a very special silicon. It is part of an international program involving Italy, the United States, Germany, Japan, and Australia. All of these people say it is the best silicon ever made in terms of impurity content and dislocations.

The goal of that program is to propose a new mass standard, an international mass standard of silicon. It also involves some very interesting basic physics about what is the molecular weight of silicon and how the kilogram standard and Avogadro's number come into this. Actually, the existing uncertainties in Avogadro's number are a big problem for these people.

[Transparency 3]

Our specimens are shown here. We studied a total of 5 spheres. These lower spheres are 1 cm in diameter. Two of them are fine ground, one of them is polished. I mention that, because

we found no difference in their elastic constants (these were all crystals from the same boule of silicon and these happened to come from Germany).

These upper 2 spheres came from Japan and, of course, the Japanese think their silicon is best and the Germans think their silicon is best. We also complemented these measurements with some rod-resonance experiments and I am not showing it in this figure, but we have some small cylinders of silicon that we use for pulse-echo measurements, so there were 3 kinds of measurements made.

DR. SMITH: How big are those?

DR. LEDBETTER: Our cylinders were about 1.5 cm in diameter and a centimeter thick.

[Transparency 4]

This shows the fixture arrangement for measuring the spheres. It is what I call a tripod with 3 transducers. The only force is the gravitational force.

[Transparency 5]

Here is the usual, almost perfunctory, spectrum. I just want to emphasize, since we are going to talk about internal friction, that there are various ways to get it. We get it the standard way from the half-power width, $\Delta f/f$.

[Transparency 6]

Just as we try to get the complete real part of the elastic stiffness, we try to get the complete imaginary part, the internal friction. I do not want you to read these numbers (you probably cannot), but for these 5 spheres these are the measurement results.

You can go down the left-hand column and pick out your favorite elastic constant and go across and see how it changes. The numbers at the bottom are the Kröner model quasi-isotropic averages for the bulk modulus, shear modulus, and so on.

I forgot to bring a viewgraph that shows an average of these results compared with the old McSkimin (Bell Laboratories) results from the 1960s. They are the same with one part in 1000.

[Transparency 7]

If we turn to the internal friction and if we measure it versus strain, we get what was for us a rather startling curve. Right away this tells you a lot of things. One is that while silicon may be a good material for an international mass standard and probably a very good material for velocity for an elastic-stiffness standard, it is a very poor material for an internal friction standard, because, depending on your measurement conditions, you get different results.

PARTICIPANT: Is that the strain amplitude of your vibration? What is the strain?

DR. LEDBETTER: That is the strain in the crystal induced by the piezoelectric transducer.

We plotted internal friction versus the strain and it was just completely unexpected, because we have a variation of a factor of 3 or 4 between the lowest and highest values and we have, obviously, 1, 2, 3, 4 phases or processes contributing to internal friction.

We wondered how can we explain this? As Dr. Ogi mentioned, oftentimes for most materials the largest contributions to internal friction are dislocations, so we looked at that first.

[Transparency 8]

It is useful to look at a simple equation that comes out of the Koehler-Granato-Lucke vibrating string theory for vibrating dislocations. Most of these are basically material parameters. Important parameters for our purposes are gamma, the dislocation density, and L, the dislocation length. Those are things I shall be talking about, and how dislocation properties affect Q inverse.

This is a low-frequency equation where the Q inverse goes as frequency.

[Transparency 9]

If we make a schematic of the Granato-Lucke model for higher frequencies, we find that the internal friction goes through a maximum and then it has a 1/omega dependence, but the important thing is that the frequency of this maximum goes as $1/B\ell^2$. This ℓ is the same as the L

in the previous viewgraph; it is the dislocation length. B is the viscosity seen by the dislocations as they vibrate. Almost all the materials that we have measured show this kind of dependence on frequency, a linear increase.

[Transparency 10]

We measured these materials and we found the following results: Cumulative internal friction versus frequency decreased. Here is shown the Granato-Lücke slope, which approximately fits our results.

I should have said, when I showed the previous graph with the big wide resonance, that for a typical material, let's say copper, that maximum occurs at about 1 to 10 MHz and because it depends on $1/L^2$, to increase L by a factor of 10 and drops that frequency considerably.

What these results suggest is that we are on the high side of the curve and the maxima is somewhere below 400 kHz, simply because in these materials we have few dislocations, and we have few impurity atoms that serve as pinning points for dislocations.

[Transparency 11]

This is taken from the very old literature, some really almost visionary work by Thomas Read. In 1940, when most people in the world did not believe in dislocations, he was studying them. He discovered this strain effect. If we measure internal friction versus strain, we get 2 components, a strain-independent part and a strain-dependent part.

This strain-dependent part, of course, results from depinning the dislocations and increasing the loop length. This, remember, contributes to low frequencies as L^4. This is very helpful but obviously does not explain these four regions we have in our measurement results on the silicon.

[Transparency 12]

We wondered what about kinks, kinks and dislocations. This has been a big controversy since the 1950s -- I think the idea was conceived by a professor who worked on it at Northwestern but then taken up vigorously by Seeger at Stuttgart and this argument rages to this day and we have these two camps, almost with no dialogue.

For those of you who do not know what a kink is, we have a dislocation lying in a Peierls valley and if we apply a stress on it to move it, it cannot move, because the stress is less than the potential associated with the Peierls hill, but one way to make it move is to somehow get a small part of the dislocation over and then move this part, this kink, either left or right, depending on which way the force is, so it is much easier, then, and, by moving this, let's say, in this direction, then this entire dislocation moves from one valley to the next.

So then we had to wonder, well, if there are kinks, how would they affect the internal friction?

[Transparency 13]

Fortunately, actually, when I was in graduate school, I met Tetsuro Suzuki, who was a postdoc from Japan and I knew about this paper he had published with Elbaum when Suzuki was at Brown University, and they actually considered this question: If we have kinks, what is the strain dependence of the internal friction?

That is what they plotted here. They say at very low strains -- I am not sure you can read this (the lowest strains shown is 10^{-10}, and it goes 10^{-8}, 10^{-6}) -- there is a plateau. At some strain, which they calculate to be around 5×10^{-5}, Q^{-1} goes to 0. It goes to 0 because it is sort of an

exhaustion process. As these kinks move out to the ends of the dislocations -- well, they are effectively just frozen out of the deformation process.

So this was very useful, because then we could arrange them in our work, our measurements, and say the following: For low strains we have this kink plateau, we have this kink internal friction going toward 0, and about where it does we have the Granato-Lucke and the depinning process starting, and usually this curve just goes up rather indefinitely. So why does it bend over?

[Transparency 14]

It is because of this special material. There are very few pinning points. There are very long loop lengths. You really, I think, literally run out of pinning points; after a certain point there are no more dislocation pin points to break, so that is what is happening here, we are exhausting these.

We have not done any quantitative modeling of this and I think it is possible, and I also think it is possible to at least establish bounds on some of these dislocation parameters, like the dislocation density, like the dislocation length, and maybe dislocation viscosity, which still is quite uncertain despite much good research.

[Transparency 15]

Here is a viewgraph almost everyone likes to see, one with conclusions. I wrote down three. First of all, within about one part in one thousand (I did not show you all the old measurements) what I have called the new silicon elastic stiffness measurements agree with the old ones. It seems at first quite trivial but it is not trivial for two reasons.

One, there are people who really are working with these silicon devices, they really at least think they need to know the best possible numbers and, secondly, in some materials, for example, in monocrystal copper that we have measured, we can measure one purity of pure copper and one with parts per million doping and get a 2% difference in some of the elastic stiffnesses, so some materials have a very large difference.

As I said, at low strains we think the Q inverse is dominated by kink movement, which means to see this you must measure at low strains. At high strains, the effect discovered by Read and published in 1940 and then elaborated by Granato and Lucke in *The Journal of Applied Physics* in about 1955 comes in and we see that mechanism that then saturates. Thank you.

DR. SACHSE: I am not as optimistic as you that you will ever be able to do quantitative comparison. There are just too many variables. The free parameter you mentioned, that is really not well known, the loop length is not well known, the density is not well known, so that is one part of the picture; there are just so many parameters.

The second thing is, you plotted the Q - 1 versus the strain and I am not sure exactly what you mean by that. Someone else asked, "Is that the driving amplitude?"

DR. LEDBETTER: No, it was the strain in the specimen.

DR. SACHSE: Now, if this is a resonating specimen, that means the strains are not uniform in this specimen. You are going to have to worry, then, about the nonuniformity of the strain and how that affects the dislocations. It sounds like a can of worms to me to try to get a quantitative measure of what is going on there, because there will be strains on some parts of the sample that are not vibrating at large amplitudes at all, so how will you do the integration? It is interesting but I just do not know how to cope with it.

DR. LEDBETTER: I do not know how familiar you are with the literature. There has been an enormous amount of work and people over the years have generated these big broad resonance curves I showed you, you get low frequencies and high frequencies and occasionally right at the top, and some people have gone to the trouble to count and check the dislocations and this is a very difficult process.

All I can say is the model, based on the literature, has enormous acceptance and wide application, but how many variables are there? There is the density and the length. I think I did do some calculations on this and the numbers were not unreasonable, they are not imaginary, not negative, and not off by 2 orders of magnitude.

I think I share your unease but I think when we sit down and look at this, it is a little more positive.

MIGLIORI: Remind me again how you measured the strain amplitudes.

DR. LEDBETTER: You should see page 82 of Migliori and Sarrao. (Laughter)

DR. MIGLIORI: I was uneasy when I wrote that. (Laughter)

DR. LEDBETTER: You raise an interesting question and I think there really remains some question about what is the absolute number of the strain. Last year we tried to get someone going with a dynamic interferometer device to measure strains, but it did not go well, the program, and I was not sure what I would do with the results anyway, so I sort of let it go.

DR. MIGLIORI: So you use the Q and the known displacement of the transducer, roughly.

DR. LEDBETTER: And the internal friction of the specimen.

PARTICIPANT: You mentioned dislocation and length as one of the parameters. Does that imply that there is a fairly narrow distribution of planes or is that distribution also --

DR. LEDBETTER: The early model considered just one length. The later models brought variable length into a spectrum. For present purposes I assumed just this one length.

PARTICIPANT: Maybe related to it, I am not sure, it seems that this depinning occurs over a fairly narrow range of strains, that everything is over with in just a fairly narrow range. Is that significant, perhaps? I guess I wonder if you could comment on that.

DR. LEDBETTER: I had not thought about it, but it does not surprise me. After all, we are talking about trying to move dislocations or parts of dislocations through a lattice against some barrier and at a certain stress level they will not move and at higher stress they will, kind of a yield point in a sense, at a micro-level.

DR. MARSTON: To go back to the question of the strain field because you are driving a particular mode, is it understood in either the kink model or the Lücke model how the dislocations behave, how the position dependences -- in other words, suppose you are at a strain anti-node versus a node, is it understood how that dislocation varies with where the dislocations are?

DR. LEDBETTER: I am not sure.

DR. MARSTON: That would seem as if, if you had an understanding of that, that you could answer his question as opposed to some other ways these models may be tested with traveling waves where that issue would not come up.

DR. LEDBETTER: Yes, I am not sure.

DR. SACHSE: May I make a comment? You have to remember what the Granato-Lucke model is. Essentially they treat the dislocation as a string pinned at the ends and then they have that B value, which is the drag. That is the model. It is a very simple model and then they analyze this and crank out from that what is the end.

DR. LEDBETTER: It is interesting, the equation of motion for this is so widespread through solid-state physics. You can probably find 30 phenomena in some list of things that follow this same equation of motion; it is just an equation for a damped harmonic oscillator, basically.

DR. HICKEY: Since we have some extra time, Dr. Ledbetter wants to present some new results of some measurements, I believe.

DR. LEDBETTER: Yes, these really are new results.

[Transparency 16]

We got these about one week ago. We thought they were quite interesting. It is really our first start in considering piezoelectric crystals. The first author is Ming Lei, who is at DRS Company in Wyoming, the same as Dr. Willis. His contribution was that he did most of the analysis and repeated our measurements that we made in Boulder.

[Transparency 17]

Langasite may not be a material that you have heard about. It has been known for some years, especially in Russia; if you do a literature search, probably 9 out of 10 papers will be Russian. Especially they see it as a replacement material for quartz, which is really astonishing, because, according to good sources, each year there are 2 billion quartz devices made.

So what would be langasite's possible advantages? One, it does have higher piezoelectric coefficients. Secondly, it has no phase transformation. Quartz has a phase transformation at 573°C. Thirdly, there is sort of a hope, it has lower dielectric loss. As far as I know this has not been resolved yet.

[Transparency 18]

In this table I want to show you basically two things. I want to give you the chemical composition of langasite. It is $La_3Ga_5SiO_{14}$. It is interesting in terms of its crystal symmetry. It is trigonal, and has the same point group and its space group as quartz.

It is rather different from quartz, as you might expect from the chemical formulas, in that it has 23 atoms per unit cell, whereas quartz has 9.

People are now growing large numbers of single crystals.

[Transparency 19]

One of these crystals is shown in the measurement fixture. It was a cylinder about 1 cm in diameter and 2-3 cm long. As a government employee, I am not supposed to tell you what commercial apparatus we use, but anyway -- (Laughter) -- when Ming Lei measured these, he measured them three ways, edge/edge, end/end. Then, he set up a horizontal 4-point probe. All methods gave essentially the same results, he told me.

[Transparency 20]

113

Here is the spectrum for quartz. Just as before, we get the internal friction from this half-width.

DR. MIGLIORI: You did not give the elastic constants for the trigonal structure? On the previous viewgraph did you determine the elastic constants as well as the Q? You measured frequencies and Q's. Did you use the frequencies to fit elastic moduli for the trigonal single crystal?

DR. LEDBETTER: Yes, I am going to talk about the elastic and piezoelectric models.

[Transparency 21]

For the quartz case, if you look in the literature, there are lots and lots of measurements, 8 or 10 good measurements. What I am showing here is our results compared with Ohno's results using a parallelepiped -- again, the old Bell Laboratory results, and they are essentially the same.

It is especially important that they are the same for C_{14}, an elastic constant usually zero. It is nonzero in trigonal crystals and is very troublesome, both for people making measurements and for people doing any analysis or theory. Especially if you look in the literature, these numbers just vary enormously. For these three cases, at least, there seems to be some consensus about it.

[Transparency 22]

Here is the quartz compared to langasite. We see, first of all, langasite is a much more dense material. As we might expect, these longitudinal moduli, C_{11} and C_{33}, are different by approximately the density ratio, but it is interesting (I do not quite understand why yet) that the shear moduli are roughly the same.

[Transparency 23]

Here I want to distinguish between the elastic material and the piezoelectric material and there are many ways to do this. This is just the Christoffel equation, so the eigenvalues are rho v^2 and these eigenvalues depend, for the elastic model, only on the elastic-stiffness coefficients, but in the piezoelectric case they depend additionally on the piezoelectric coefficients, $epsilon_{rij}$ and the dielectric coefficients K_{mn}.

In principle, if you are making an RUS measurement, you should take these into account, but it also offers a possibility of using RUS measurements to determine these electromechanical quantities in addition to these elastic (this was one of our main initial interests).

[Transparency 24]

114

However, for the quartz case, we plot the predicted frequencies from the determined elastic stiffnesses versus the measured frequencies, and we get essentially a perfect line for the elastic model. In other words, this assumes no piezoelectricity. What it means, conversely, is, unless you have a very sophisticated measurement system (better than ours), you probably cannot get any piezoelectric coefficients from these kinds of measurements.

I think in Professor Ohno's paper on quartz he reached the same conclusion.

[Transparency 25]

The langasite results look essentially the same as the quartz. The elastic model has a perfect linear dependence; we cannot extract information about the piezoelectric coefficients.

[Transparency 26]

However, this is not true for all materials. Here are some results for lithium niobate, also a trigonal material. The open circles represent the elastic analysis, which is not on this 45° line, but when we bring in the known measured, piezoelectric coefficients and do the calculation, we get quite good agreement.

For this material, it seems, or things with similar dielectric coefficients, one could use RUS, in principle, not only to measure the elastic stiffnesses but also the piezoelectric coefficients.

[Transparency 27]

There are not many conclusions about this, since these results are about two weeks old, but here are our current plans. We are interested in focusing on the internal friction of things like quartz and perhaps langasite, especially relating it to the defect mechanism. What is the defect mechanism? I know this is an old subject with papers by Mason of 30 years ago but, nevertheless, I am not sure it is settled.

Secondly, we are quite interested in the relationship between the mechanical Q and the electrical Q. I mean, if the dipole defect is both an elastic dipole and an electric dipole, then one can probably make some simple model connecting these two terms, and we think this would be quite useful, because I think RUS measurements are much easier to make than most of the dielectric loss measurements that I see made at our laboratory.

As I just mentioned a few minutes ago, these materials that have enough coupling in the piezoelectric strain we can actually see if we can derive piezoelectric coefficients from an RUS spectrum.

DR. MIGLIORI: The distinction between the electronic and the mechanical Q, let's see, you would have to turn off the electric fields in order to measure the mechanical Q.

DR. LEDBETTER: Those would be 2 different experiments in 2 different parts of the world. I would not care.

DR. MIGLIORI: Yes, but the point being that when this stuff is vibrating mechanically it has an electric field or electric currents that are driven by the mechanical vibrations, so it is hard to see how you separate it in 2 pieces.

DR. LEDBETTER: I do not understand. I mean, we measure mechanical loss, some fellow in southern China measures electrical loss, and we make some model connecting the two.

DR. MIGLIORI: But the Q ought to be the same in either case and it is not.

DR. LEDBETTER: No, why should it be the same? It is coefficients, remember? I can guarantee you they are not the same.

DR. MIGLIORI: But the full width at half-maximum for the resonances -- you are on mechanical resonance when you are driving them electrically using it as a quartz crystal oscillator, so it is different.

DR. LEDBETTER: I do not think so. I do not think the response to an elastic dipole is the same as the response to an electric dipole. I think they are proportional in many cases, probably.

DR. MIGLIORI: But not the same?

DR. LEDBETTER: Not the same, no. [Added after workshop: Imagine an elastic dipole without charge, which gives a certain Q^{-1} (mech), but Q^{-1} (elec) = 0. Then, we add charge, Q^{-1} (mech) is unaffected, but Q^{-1} (elec) becomes nonzero.]

Thank you.

RUS Studies of Crypto-Clathrates: Perfect Crystals with the Elastic Properties of Glasses

Veerle Keppens
University of Mississippi

Abstract

The low-temperature thermal and elastic properties of glasses are known to be quite different from those of perfect crystals. For example the specific heat in amorphous solids is much larger than the Debye specific heat of crystals, and the thermal conductivity is considerably smaller. Some disordered crystals and quasicrystals were found to have properties very similar to those found in glasses, but remarkably, no amount of disorder introduced into a crystalline solid can produce a thermal conductivity which is lower than that of its amorphous counterpart. Recently, motivated by a search for improved thermoelectric materials, several compounds have been identified that combine the high electron mobilities found in crystals with the low thermal conductivities characteristic of glasses. The common structural feature of these materials is that they contain loosely bound atoms that reside in a large crystalline "cage": these materials are thus "inclusion compounds" or "crypto-clathrates". A particular class of crypto-clathrates is formed by the filled skutterudite antimonides RM_4Sb_{12}, with M a transition metal and R a rare-earth. These filled skutterudites are derived from a regular unfilled skutterudite such as $CoSb_3$, by "filling" the void in this skutterudite structure by a rare-earth. The presence of the rare-earth has a marked effect on the lattice dynamics of these materials. Resonant Ultrasound Spectroscopy measurements were performed as a function of temperature for both the filled and unfilled skutterudites to determine the elastic constants for both structures. These data reveal that an unusual elastic behavior complements the glasslike thermal properties of the La-filled skutterudite: the elastic moduli of the filled compound display a strong temperature-dependence at low temperatures, which indicates the presence of low-energy vibrational modes in addition to the normal acoustic phonons.

TRANSCRIPT

[Transparency 1]

DR. KEPPENS: I would like to talk about the elastic properties of a particular class of materials, crypto-clathrates, particular in the sense that they are perfect crystals but they tend to have very glass-like behavior.

[Transparency 2]

The measurements I am going to show you are a result of a collaboration between various institutes. The materials have been synthesized and characterized at Oak Ridge National Lab. I was very happy to have had the assistance of Albert Migliori and Tim Darling for the RUS measurements and in the past few weeks I have been working at the University of Leuven in collaboration with Professor Laermons.

[Transparency 3]

Before I start off, I would like to briefly remind you of how different glasses and crystals can behave even at very low temperatures. I have made some very schematic representations of some typical properties, like thermal conductivity, which has been plotted, in blue, for crystalline behavior, and in red, for typical glass-like behavior.

Thermal conductivity in a crystal is much higher than in a glass and has a T^3 behavior. A glass shows a linear T-dependence. The velocity change is very different, too. In a crystal there is basically no velocity change at all below a few degrees Kelvin, while in a glass the velocity will first increase according to logarithmic temperature dependence and then reach a maximum before it decreases again.

Finally, the ultrasonic absorption in a crystal is very small and independent of temperature; at low temperatures, in amorphous solids you get a much higher absorption that rises following a cubic temperature dependence and then levels off to a temperature-independent absorption at approximately a few degrees Kelvin.

[Transparency 4]

The measurements I am going to talk about today were motivated by a search for better and/or new thermoelectric materials. Recently a new class of materials has received a lot of attention in research. These materials are called filled skutterudites and they have the basic formula of RM_4X_{12}, where M is a transition metal, X is a pnicogen (phosphorus, arsenic, antimony) and R can be strontium, barium, lanthanum, or any of these listed here.

118

[Transparency 5]

These materials have a cubic structure, as can be seen in this viewgraph. The metal ions form this cubic sub-lattice. The pnicogens form these rings and the remaining 2 holes in the structure can be occupied by the rare earth. If this rare earth is not present, we have just the regular unfilled skutterudite structure.

The special thing about having these rare earth is that these atoms are sitting in an oversized atomic cage and they tend to rattle around their equilibrium position. The rattling has a remarkable effect on the thermal conductivity, specifically on the contribution of the lattice to the thermal conductivity.

[Transparency 6]

In this viewgraph, I have plotted the thermal conductivity for just a regular, unfilled, skutterudite and I have plotted it for 2 of the filled skutterudites and you see there is a dramatic increase of the thermal conductivity over the whole temperature range.

The nice thing about this decrease is that it happens without deteriorating the electronic properties too much. In other words, these materials are an excellent example of what is called an electron-crystal-phonon glass. This means that the phonon properties are very glass-like, while the electronic properties are just as expected for a perfect crystal, and this property makes these materials a very interesting class of thermoelectric materials.

[Transparency 7]

Very recently another class of materials has been discovered that behaves almost the same. These materials are the clathrates, with the formula X_8E_{46}, where E is like silicon germanium or tin, could also be aluminum or gallium, and X is sodium, potassium, rubidium, cesium, strontium, or barium.

These clathrates are built up by 20- or 24-fold polyhedra, formed by the E elements, and the X atoms are sitting, inside these cages formed by the E atoms. Just as in the skutterudites, these atoms have lots of space and rattle around their equilibrium position, with a drastic effect on the thermal conductivity, as seen in measurements taken by George Nolas and his co-workers.

[Transparency 8]

The upper panel shows the lattice contribution to the thermal conductivity as a function of temperature for 2 of those clathrates, the red curve and the green curve, and for comparison you

see the curve for amorphous germanium. The thermal conductivity has about the same order of magnitude in the crystals compared to the amorphous materials.

It is not just the order of magnitude that is glass-like; it is the whole temperature dependence. As you see in this viewgraph, the red markers represent the data for the $Sr_8Ga_{16}Ge_{30}$ clathrate. The blue markers are the data for amphorous SiO_2 and you see those two behave very alike, although one is a crystal and the other one is a glass.

[Transparency 9]

I am going to focus on the elastic properties of these materials. I was able to get RUS measurements on both filled and unfilled skutterudite samples. For the unfilled I used a $CoSb_3$ sample; I had a lanthanum-filled skutterudite to compare the specimens with each other. Both were polycrystalline, so we just had to get C_{11} and C_{44}. At Los Alamos I was able to do these measurements as a function of temperature between 5 and 300 K.

In the past few weeks I was able to do some pulse-echo measurements, not on the skutterudites but on the clathrates. I had a $Sr_8Ga_{16}Ge_{30}$ single-crystal specimen and I was able to take data at very low temperatures, between 0.4 K up to 30° K.

[Transparency 10]

Let's start off with the RUS results for the regular skutterudite $CoSb_3$. I have plotted the C_{11} and the C_{44} as a function of temperature. The red markers are the data we took and the blue solid line is a fit to what is called the Varshni function, which is a function that has been proposed by Varshni after he observed that basically all normal-behaving solids have a very typical elastic behavior that can be described by this one formula that contains two fit parameters s and t. You see this $CoSb_3$ is one of those normal-behaving solids as it can be well described with this Varshni function.

[Transparency 11]

In comparison to that, if you look at the lanthanum-filled skutterudite, I have plotted the C_{44}, here in blue for the filled sample and, just for comparison, in red, the data I got on the unfilled $CoSb_3$, you see that at low temperatures there is quite some difference in these data. The $CoSb_3$ just levels off and flattens at low temperature while there is this remarkable temperature dependence in the filled skutterudites. It is impossible to just describe this with this Varshni function, so something is happening in this filled skutterudite and, since it is not happening in

120

$CoSb_3$, we assume it has to do with the presence of this filling atom that is rattling in this skutterudite structure.

Trying to figure out what is going on here I tried to fit the data, assuming that this rattling atom causes the presence of one or maybe more harmonic oscillators in this material, but just assuming harmonic oscillators does not give this temperature dependency observed.

In a second attempt I just reduced the harmonic oscillator to a simple 2-level system.

[Transparency 12]

To get the contribution of a 2-level system to the elastic constants, all you need to do is take the second derivative of the free energy to strain, which is straight forward as long as you assume that the spacing between the 2 levels has only a linear strain dependence.

If you do that and you calculate the second derivative and plot the data, you'll find that the one 2-level system still does not do the job, but taking 2 of them, one with spacing of 50 K, one with spacing of 200 K, I got a pretty good description of the experimental data, as you can see in this viewgraph.

[Transparency 13]

If I take a background, which I estimated from the Varshni behavior of the unfilled $CoSb_3$ and I take 2 2-level systems, one with 50 K, one with 200 K spacing, it just describes these data quite nicely, not just the C_{44}, but also the longitudinal modes, C_{11}. It can be described just taking the same 2-level systems with spacing of 50 K and spacing of 200 K.

[Transparency 14]

In the meantime we have also done some specific heat measurements and neutron-scattering data and all measurements tell us the same. There are 2 2-level systems present in these lanthanum-filled skutterudites that are not present in the unfilled ones, so they have to do with these lanthanum atoms rattling around in this structure.

It would be nice to see if other materials have this same behavior and to do RUS on other filled skutterudites, or on those germanium clathrates but, unfortunately, at Leuven I do not have RUS facilities available. However, I was able to do ultrasonic absorption measurements on the germanium samples I got from Oak Ridge.

[Transparency 15]

I have brought my results, which had ultrasonic absorption data as a function of temperature down to 0.4 K. I could take data at several frequencies, so I have brought data that I took at 250 MHz (in blue) and data I got at 155 MHz (in red).

You see that at low temperatures there is basically no frequency dependence in the absorption, which rises with temperature, almost following a cubic law in temperature, leveling off to show a maximum at high temperatures.

If you remember from my first viewgraph, this is not a crystalline behavior at all, because in a crystal you would expect no temperature dependence at all in the absorption until 20 or 30° K, so this behavior, although we have a single-crystal sample, is not crystalline at all.

[Transparency 16]

On this viewgraph I have plotted ultrasonic absorption taken on germanium oxide, which is a typical example of a glass. For comparison I plotted again the data I took on this clathrate sample. As you can see, both behave very similarly, there is no frequency dependence at lowest temperatures and the absorption levels off, in the case of the germanium oxide, to a plateau-like temperature-independent absorption around a few degrees Kelvin, which is proportional to the frequency.

Both materials behave the same, although you should remember that one is a perfect crystal and the other is a glass. The only remark to make is that the clathrate does not really have a plateau around a few K, it is more like a maximum.

[Transparency 17]

I am not going to bore you too much with the model to explain glass-like behavior but I just want to mention that all glass-like properties, thermal conductivity, specific heat, absorption, velocity, they all can be explained quite well by a phenomenological model that is called the tunneling model. This model assumes that in a glass there are atoms or groups of atoms that have 2 equilibrium positions, so they usually present it as a particle that can move in a double well, 2 wells separated by distance d, having a symmetry Δ and an energy overlap Δ_0.

So transitions from one level to the other can occur at the lowest temperature through tunneling through this barrier. This model can explain glass-like behavior quite well, assuming that those parameters, Δ and Δ_0, have a very broad and uniform distribution.

The basic assumption of this model is needed to explain the temperature-independent behavior observed in all glasses around a few degrees Kelvin. The fact that we do not really

have this temperature independence in $Sr_8Ga_{16}Ge_{30}$ but some kind of a maximum may just mean that this broad distribution that is typical for glasses is not really present in our germanium clathrates, but could be limited to some particular values.

Anyhow, I think these data indicate that this germanium clathrate definitely has very glass-like behavior and has some tunneling states in it.

[Transparency 18]

This brings me to the conclusions. I tried to explain that these filled skutterudites have at least 2 local modes, and that the germanium clathrates are probably full of tunneling states. These two materials are 2 examples of perfect crystals that have very glass-like behavior as far as their elastic properties are concerned.

For future work I think it is obvious what has to be done. I would like to do some RUS measurements on this clathrate I just showed you and get some attenuation measurements on a crystalline skutterudite and compare to see if both samples behave similarly.

Thank you.

DR. MARSTON: What properties in a skutterudite material, the filled ones, extend all the way to room temperature?

DR. KEPPENS: Thermal conductivity definitely is much lower over the whole temperature range. I am not sure about the temperature dependence. For the clathrates I do not have any data up to room temperature. The data I showed you for the skutterudites were taken all the way up to room temperature and it drops just tremendously over the whole range.

DR. LEVY: I was slightly confused with one of those curves. It seems as if by adding the impurity, or whatever, the additional interstitial atom, you decreased your effective elastic constants? The background was higher.

DR. KEPPENS: Especially the effect of the 2 2-level systems brings the elastic constants down. If we had just the Varshni it would be higher than if you add those 2 oscillators which have a negative contribution.

DR. LEVY: Could you show me the original data, the ones where you were trying to explain this?

DR. KEPPENS: This one, before I did the fits.

DR. LEVY: Yes, that one. Okay, now it makes sense. Why is it softer in addition to the fact that the theory tells you it is softer? Do you have any physical idea in addition to the

theoretical explanation? I usually think if I add something it would make it stiffer and here it makes it softer.

DR. KEPPENS: Because the atom is so loosely bound, and it is bouncing around in its cage.

Thank you.

COMPARISON OF RADIATION AND SCATTERING MECHANISMS FOR OBJECTS HAVING RAYLEIGH WAVE VELOCITIES GREATER THAN OR SMALLER THAN THE SPEED OF SOUND IN THE SURROUNDING WATER

PHILIP L. MARSTON,[1] FLORIAN J. BLONIGEN,[1] BRIAN T. HEFNER,[1]
KAREN GIPSON,[2] SCOT F. MORSE[1]
[1]WASHINGTON STATE UNIVERSITY
[2]UNIVERSITY OF PUGET SOUND
[3]NAVAL RESEARCH LABORATORY

ABSTRACT

Metallic objects typically have material properties such that the characteristic Rayleigh wave velocity exceeds the speed of sound in water. As a consequence, over a wide range of frequencies, smooth objects (including empty shells) support surface guided waves having phase velocities exceeding the speed of sound in water. Such waves are effective in leaking radiation and give rise to various backscattering enhancements not necessarily associated with global resonances of the object. For example, high frequency meridional ray backscattering enhancements have been observed and modeled for tilted metallic solid cylinders [K. Gipson, Ph.D. Thesis, WSU (1998)] and shells [S. F. Morse, et al., J. Acoust. Soc. Am. **103**, 785-794 (1998)]. For "plastic" polymer objects, however, it is necessary to reexamine the significant radiation and scattering mechanisms because the intrinsic Rayleigh phase velocity is smaller than the speed of sound in water. Some novel scattering enhancement mechanisms for such objects are introduced including the caustic merging transition for waves transmitted through tilted cylinders and the tunneling to subsonic Rayleigh waves. The former has an optical analogy in the scattering of light by tilted dielectric fibers [C. M. Mount, D. B. Thiessen, and P. L. Marston, Appl. Opt. **37**, 1534-1539 (1998)] and has been observed in sound scattered by tilted truncated polystyrene cylinders [F. J. Blonigen and P. L. Marston, J. Acoust. Soc. Am. **102**, 3088 (A) (1997)]. [Work supported by the Office of Naval Research.]

DR. MARSTON: In contrast to most situations of interest in RUS, where you want to avoid fluid loading, our interest is scattering, where fluid loading plays a major role because we are interrogating objects with a sound wave.

We are going to look at some situations in both this talk and in the one this afternoon by Todd Hefner where fluid-loading effects are very important. In his talk resonances are also important. In this one, less so, but it serves to introduce the problem that he is going to address.

[Transparency 1]

We are going to start off by reviewing some situations where fluid-loading mechanisms for metallic objects that I touched upon at the last meeting are used. Then we are going to look at what happens if you consider plastic objects in water rather than metallic objects; there are some major differences if you want to consider scattering mechanisms for those. Then we will introduce some of these novel mechanisms, one of which Todd will develop this afternoon.

[Transparency 2]

This is a one-page review of what was discussed at the last meeting. If we consider a typical very stiff object in water, either metallic or, in this case, a tungsten carbide sphere, we can get large elastic contributions, because Rayleigh waves on this object have phase velocities exceeding that of the surrounding fluid.

There is a coupling condition, in this case location B, where there is a matching of the projection of the wave number of the incident wave with that of the Rayleigh wave on the object. There is radiation off, but when you get around to this point B' there is radiation in the backward direction.

You can see these with this series of echoes and you can see these echoes are decaying very rapidly. Even though this is a very dense object, the Q's are not typically very high because of the large effective radiation loading. A Q of 10 would be a large Q for this particular scattering mechanism.

In what follows we are going to express frequencies in terms of the wave number radius product, the wave number being that of the sound in water, and we call that product ka.

[Transparency 3]

The mechanism I would like to start off with at the beginning is one where these leaky waves are important and are on elastic cylinders that are bluntly truncated. There is a

mechanism for cylinders that is somewhat like the one in the diagram I just put up; that is, for a tilted cylinder you can have helical waves that run around.

It turns out at high frequencies a stronger backscattering mechanism is the meridional ray, the ray that is launched in the meridian defined by the incident wave vector and the axis of the cylinder, runs down this meridian, reflects from the edge, has a leaky wave and than radiates off, and some of that radiation goes back in the direction of the source and produces strong scattering.

This is an expanded diagram. One of the things that will come up in modeling this is the reflection coefficient of the leaky wave at the end of the cylinder. Another aspect that comes up in the modeling is the attenuation length just due to the leakage of this radiation.

For the high-frequency systems we are interested in, the attenuation length is short when compared with the length of the cylinder and, as a consequence, the resonances are actually not very important. In fact, the phenomenon is relatively frequency independent, and that is partly because the radiation damping is so large.

[Transparency 4]

One way to interrogate this and get a lot of spectral information is to use a very wide bandwidth source. We use a PVDF sheet source in water that is also sufficiently transparent that the sound that is radiated by the target reaches the hydrophone on the other side.

If you apply a voltage step to this source, it produces a pressure impulse that has broad spectral characteristics and one can then plot the spectrum of the frequencies along this axis as a function of the tilt of the cylinder, where gamma expresses the tilt, 0° is broad side, and 90° is end on.

For our purposes, we will be interested today in this meridional ridge, this ridge here that arises because of this meridional ray, and this is potentially useful because this extends all the way to the near end-on illumination. It gives you a backscattering enhancement for a wide range of angles. If one considers, say, randomly oriented cylinders that you might be looking for with a high-frequency sonar system, this is a potentially important mechanism.

The class of leaky wave of interest for shells turns out to be that which is like a_0, that is, the lowest antisymmetric Lamb wave that runs down the shell.

[Transparency 5]

To remind you of the dispersion curve for this, if you consider a plate or a cylinder by itself, in the absence of fluid loading you would get this fine dotted line here, but this line crosses the situation where the velocity matches that of water -- that is, in these units, c_t/c is equal to unity. There is a splitting of this mode and one has a supersonic part, which is the part that is relevant to the present discussion.

Notice this part exists because the Rayleigh speed for the material exceeds that of water. We know that for the a_0, the limit of the c_t is the Rayleigh phase velocity and that issue will come up when we return to plastics at the end.

[Transparency 6]

Scott Morse was able to collect data on this as a function of angle and of frequency, so this shows the tilt in our units, it is a form function. These are actually rather large form functions, because if you consider, say, just the end diffraction from a perfectly rigid cylinder, the end-diffraction contributions scale as 1/root ka and are at least an order of magnitude smaller than these peaks.

We also show on here the data are the points -- there is a ray model that is a smooth curve and then there is a somewhat structured curve that is an approximate partial wave series model that does not incorporate the proper mechanics of the radiation processes at the ends and makes a number of other assumptions, but it is a useful sanity check on what we are doing.

You will notice that we recover, really, the right behavior in the ray model but as we go up in frequency there is a discrepancy between both the predictions of the ray model and the data. We will see why this is on the next transparency.

[Transparency 7]

What we are going to look at now is walking along this ridge, that is to say, adjust the tilt angle to maximize the scattering. In this region the ray model works very well as does the approximate partial wave series. However, there is a deviation and finally there is a large difference up here.

We understand this large difference and, in fact, the dashed curve is the ray model without corrections for the reflection coefficient at the end. When the a_0 wave hits the end, we first assume that there is a unimodular reflection coefficient. What Scott Morris was able to put in the

model here is the mode threshold for generation of a propagating a_1 wave, that is, the next higher antisymmetric Lamb wave and there is mode conversion to that Lamb wave.

That clearly is evident if you just consider the simple plate problem and that is also evident in the data. We see that there is actually a precursor to that mode conversion that extends into this region. We would like to at least understand why that precursor is there and it tells us something about radiation for fluid-loaded objects.

[Transparency 8]

We can get an idea of that by considering the results of Mindlin's analysis for plate modes. On the axis are the wave numbers, the real wave number along here, frequency vertically, and the imaginary component wave number in this plane. This is for a plate in a vacuum.

The a_0 wave we have been talking about is the one that runs along this curve. The a_1 wave, if you are in the propagating region, that is to say you are above the threshold, you are in this region here. But if you go below the propagating threshold, Mindlin found that there is a purely imaginary branch -- that is this part.

Why is that relevant to radiation? When you are near the threshold, this wave number is purely imaginary but small in magnitude, which means the scale is large in magnitude and that corresponds to an exponential flopping of the end of the plate and that would give rise to a large fluid-loading effect and hence the depression of the reflectivity and hence the form function for a broad region before you get to this threshold.

[Transparency 9]

This is also evident in these very broad spectral data that Scot Morse obtained. This dip here extends a little bit below this threshold.

[Transparency 10]

I can say more about the model to you privately, later, if you interested. It is somewhat analogous to the path integral approach of quantum mechanics in that you have to take into account defective paths in addition to rays, which are the stationary phase paths.

[Transparency 11]

This same model we applied to meridional ray for Rayleigh waves on a solid cylinder. This is in the frequency range where the waves that would run down the cylinder are well approximated by, actually, Rayleigh waves for a flat half space, and the comparison between the

data and the ray theory is shown and the magnitude is also correctly recovered, and that was work of Karen Gipson.

[Transparency 12]

I would like to now transition to the problem of what happens if, instead of looking for a metallic or fairly stiff object, you want to look for a plastic object in water or perhaps in a sediment. You see that you are in trouble if you compare the properties here of water and sediment, say, with those of polymers or a rubbery object. Then you find that the Rayleigh speeds, given over here in this column, are less than that of the water.

So you do not have the same kind of leaky Rayleigh wave mechanisms and associated leaky a_0 wave mechanisms that we have for stiffer objects, so we would like to consider what some of the other mechanisms would be for giving you large backscattering.

[Transparency 13]

Reflection just is not going to do it. These are reflectivity plots with aluminum water and, say, polystyrene water, if you modeled the materials for the purpose of this plot as lossless. A typical metallic object's reflection coefficient in normal incidence exceeds 85%, but if you go down here for the plastic object we have a reflection that is quite small, about 25%, and you can understand that because the impedance is much closer to that of water.

We can learn some other things from this diagram if we consider the phase behavior. This is a 0 to 35° scale here. Here we have looked at a 0 to 90° scale for the phase behavior. There is a Rayleigh pole in the reflection coefficient that shows up beyond the shear wave critical angle -- it is about 30 degrees -- and this corresponds to this region here, where there is a 2π phase evolution of the reflection coefficient.

There is no such phase evolution in the polystyrene water case. There is about a π phase evolution but there is no corresponding Rayleigh contribution, as we have indicated, because the Rayleigh wave is subsonic.

[Transparency 14]

In addition, in working with plastics we should keep in mind that they are really very different from normal elastic solids. They have a glass transition and an associated glass transition temperature. We are interested in plastics that are relatively stiff with the temperature of our experiments typically around 20° C, well below this glass transition temperature, and there are some consequences, particularly for the plastics we have worked with, namely, that

130

over the frequency ranges of our experiments, even though the plastics are dispersive, the variation of the phase velocity for shear waves is much less than 1%.

Secondly, we have to take into account the material loss mechanisms. It has been found that you can model the loss by considering the ratio of the imaginary to the real parts of the wave number, denoted here by delta, taking that to be a constant independent of frequency. That is the work of Hartman and others.

[Transparencies 15 and 16]

What are some possible mechanisms? One of them was motivated by the following observation that I made a few years ago. In the winter I looked out my window and I saw some icicles. If you study the glints from these icicles, one realizes, in fact, they are rainbow rays within the icicles; that is, this very bright glint here comes from an exceptionally flat wave front and if one moves one's head around, one finds that these glints can disappear.

This is in contrast to there is a glint along here that is much weaker that is associated with a simple specular reflection from that.

[Transparency 17]

This raises the issue of how are rays transmitted within a tilted cylinder, and how do you describe those rays? It is easy to understand the case of normal incidence, but if you tilt the cylinder, it becomes a somewhat more complicated problem. However, you use the fact that the projection of the wave vector along the axis of the cylinder is an invariant.

From that Bravais was able to show, 150 years ago, that you can describe the refraction in such an object by looking at the projection of the rays along the orthogonal base plane and introducing an effective refractive index. It is scaled by the tilt of the object.

When you do this, you find, for example, the Descartes rays' (these are for the case of our icicle, which you model with a cylinder or for a plastic fiber that I will show you results from in a minute) angle varies with tilt and eventually gets to 0°, meaning that the Descartes rays have merged in the meridional plane that corresponds to a caustic regime transition.

[Transparency 18]

A student, Catherine Mount, did her masters thesis on this, where she took a fiber and tilted it. If you look at it at any given angle and illuminate it with light, there is a conic fan of rays that leave this and there is a resulting arc. This appears on a screen and then we videotaped the screen and then varied the tilt.

131

[Transparency 19]

What you find as you do this is there is an evolution as you vary the tilt of the Airy caustic and then at a critical tilt these merge into the meridional plane. You might say this could have nothing to do with anything you are ever going to see with sound.

[Transparency 20]

This is perhaps something I should have done before the student did the experiment I will describe in a minute but, in fact, I did this last week. I realized that I could take a code that I wrote and modify it to run the outgoing radiation as a function of azimuthal angle in the base plane as a function of the tilt of the cylinder for the infinite cylinder case, which is exactly solvable.

This is a negative of the results, so bright regions appear dark. The relevant ray diagram is shown here, where this happens to be a shear wave for a polystyrene cylinder and what we see is the rainbow caustic merging into the meridional plane at the critical tilt angle. You can verify that by superimposing the calculated caustic positions.

[Transparencies 21 and 22]

How can this have anything to do with backscattering and fluid loading? If you consider a bluntly truncated cylinder, then there is a path of rays like this in the meridional plane that go back to the source. The game is under what angles does this produce a lot of radiation coming back at you, namely, at this critical tilt angle.

[Transparency 23]

This was verified by Mr. Blonigen. Here are data he has taken with tone bursts at 300 kHz for a polystyrene cylinder where he has varied the tilt angle and there is this region near the critical tilt where there is a strong backscattering, whereas if this effect were not there, you would estimate the signal to be at least an order of magnitude smaller.

[Transparency 24]

In that case the relevant ray was the shear wave within the polystyrene. If you consider another low-velocity material, RTV rubber, which you might consider to sort of mimic an explosive -- explosives have low propagation velocities. We have, also, the enhancement in the expected region.

[Transparency 25]

132

The way you model this is by considering the shape of the outgoing wave front in the orthogonal plane and this becomes a fourth power when this Bravais index goes to 2. Because it is fourth power, the resulting diffraction integral contains a Pearcey function, which is one of the canonical forms of diffraction integrals, and one can work out a prediction for the backscattering amplitude.

[Transparency 26]

We have the slightly embarrassing result that the observed backscattering amplitude at the caustic exceeds our prediction, so we were looking for an effect and so far it has turned out to be a little bigger than what we had predicted it to be. Here is the prediction right on the caustic.

[Transparencies 27 and 28]

The student has argued that his data are right on the caustic. If I do not believe him and say, well -- I should remind you that the maximum for a scattering pattern for caustics that do not have perfect symmetry is shifted slightly from the caustic -- if I assume that, instead, he is right at the maximum of the pattern, that would give this upper line, which more or less bounds the data; that is to say, on the caustic corresponds to being here, the maximum corresponds to being here on this cut through the Pearcey function.

[Transparency 29]

On the other hand, with RTV rubber we have results that slightly are below the predictions but, again, it is a large effect compared with what you would have in the absence of this mechanism. We were only able to estimate the attenuation constants for the RTV rubber.

[Transparency 30]

Another test is considering an infinite cylinder, say, of rubber in the absence of attenuation and one can then solve this two-dimensional problem on both the computer and also with an analogous ray theory, and this shows that the two approach each other at high frequencies.

[Transparencies 31 and 32]

That is a geometrical mechanism. This afternoon Todd Hefner is going to describe a resonance-related mechanism but it is different in character from our previous resonances in that we are working with Rayleigh waves that are subsonic, so we had to worry about how to couple on to those Rayleigh waves that were subsonic.

He finds the resonances for a solid lucite sphere in water are readily observable through this kind of a ray model where there is tunneling. It happens that we had previously developed

tunneling models for shells, metallic shells, and we could really lift all the mathematics of the metallic shell over to the solid-sphere model.

[Transparency 33]

This is a summary of what was presented. Thank you for your attention.

DR. MEHL: In that a_0 region where there was a precursor, there was an earlier kink.

[return to Transparency 31]

DR. MARSTON: You mean in here? I am astonished the student was able to get data as good as these, so I am not sure I would put any significance on the kink. (Laughter)

ADDENDUM

Subsequent to this presentation the following items have been published (or accepted for publication) pertaining to the research presented.

1. K. Gipson and P.L. Marston, "Backscattering enhancements due to reflection of meridional leaky Rayleigh waves at the blunt truncation of a tilted solid cylinder in water: Observations and theory," J. Acoust. Soc. Am. **106**, 1673-1680 (1999).

2. S.F. Morse and P.L. Marston, "Meridional ray contributions to scattering by tilted cylindrical shells above the coincidence frequency: ray theory and computations," J. Acoust. Soc. Am **106**, 2595-2600 (1999).

3. F.J. Blonigen and P.L. Marston, "Backscattering enhancements for tilted solid plastic cylinders in water due to the caustic merging transition: Observations and theory," J. Acoust. Soc. Am **107**, 689-698 (2000).

4. B.T. Hefner and P.L. Marston, "Backscattering enhancements associated with subsonic Rayleigh waves in polymer spheres in water: Observation and modeling for acrylic spheres," J. Acoust. Soc. Am. **107**, 1930-1936 (2000).

Subsonic Rayleigh wave resonances on solid polymer spheres in Water and Backscattering Enhancements Associated with Tunneling: Experiments, Models, and the Relative Significance of Material and Radiation Damping

Brian T. Hefner and Philip L. Marston
Washington State University

Abstract

Rayleigh waves on typical solid "plastic" polymers have phase velocities which are less than the speed of sound in water. One consequence is that when a solid sphere or shell made of such a material is placed in water, the backscattering mechanisms can differ from the situation for ordinary solids. For example, since the Rayleigh waves on a sphere are subsonic waves instead of leaky waves, the scattering processes need to be modeled as acoustic tunneling through an evanescent region. We have experimentally confirmed the existence of the resulting resonance and backscattering enhancements. Experiments and computations also support the extension of a tunneling model previously developed for quasi-flexural waves on thin metallic shells [L. G. Zhang, N. H. Sun, and P. L. Marston, J. Acoust. Soc. Am. **91**, 1862-1874 (1992)]. For the case of PMMA spheres studied, the intrinsic material damping can significantly affect the scattering. Some models were tested for the combined effects of material and radiation damping. The material damping was sufficiently small for the quadrupole mode that the observed enhancement may be useful for sonar calibration targets as an alternative to liquid-filled shells. [Work support by the Office of Naval Research.]

Transcript

DR. HEFNER: I am following up on Dr. Marston's talk this morning. He mentioned that we are interested in looking at the scattering of sound from plastic and polymer objects in water, looking specifically at the kinds of enhancements you can get with the backscattering of sound.

[Transparencies 1 and 2]

Just to remind you, for these types of materials, the shear and Rayleigh wave velocities are much less than what is typically found for metals and, even more importantly, they are much less

135

than the speed of sound in water, which greatly changes the types of scattering mechanisms that one would expect.

Also, the specular reflection off of these kinds of plastic objects is very small and typically you would not expect much re-radiation back to the source. However, if you look at the exact form function of the backscattering amplitude for, say, a solid acrylic sphere, you find as a function of normalized frequency that you get a very large backscattering enhancement at low frequencies, much larger than you would expect for a solid steel sphere (shown at the bottom of the screen there).

It suggests that there is some type of elastic scattering mechanism present here. We believe that this type of enhancement is due to coupling between the incident sound wave and the subsonic Rayleigh wave resonances. This largest peak, for one of our spheres, which was a 2" diameter solid acrylic sphere, occurs at 15.9 kHz (I will show some data for that sphere in a second).

As I said, the incident sound is coupling into these subsonic Rayleigh waves on the sphere and, to predict the backscattering --

[Transparency 3]

-- we used a model that had been used previously for subsonic waves excited on solid metallic shells. Looking at the diagram, our incident sound wave reaches the point shown here at the top of the sphere, then couples energy into these subsonic Rayleigh waves by tunneling through the evanescent field. The Rayleigh wave then travels around the back side of the sphere, tunneling energy back through the evanescent field, and re-radiating sound as it travels around. Finally it reaches this point, labeled D2, and it re-radiates sound in the backward direction, which can be detected at the source location.

We are going to use this to approximate the Rayleigh wave contribution to the form function for the acrylic sphere. However in most polymers one has to pay attention to the material absorption, since it is much larger than what one usually finds in metals.

[Transparency 4]

To determine whether or not it would be necessary to account for this in the ray approximation, we introduced the attenuation into the longitudinal and shear wave numbers in the form function, to see how much affect the attenuation was going to have.

136

So making the shear and longitudinal wave numbers complex, we can compare the exact form function without material absorption, shown in the top graph here, with the form function were we have added the absorption, the bottom graph. You can see that for higher frequencies absorption really affects the resonances and suppresses a majority of the response, whereas the enhancements at the low frequencies are relatively unaffected, although there is still a change in the amplitudes and the Q's of those resonances. Hence it is important and we decided to add that into the theory to see if we could account for it.

[Transparencies 5 and 6]

To check it experimentally, to make sure that this really was the case, we took a 2" diameter acrylic sphere, placed it in one of the large tanks and, using a PVDF sheet source, ensonified the sphere with 10 cycles around where we expected to find the resonance -- this first resonance, which is at 15.9 kHz. These graphs show the response of the sphere measured at the hydrophone some distance away for frequencies going up to and then past the resonance.

As you can see, as we get closer and closer to the resonance, this exponential decay, the tail of the resonance that we have excited gets larger and larger until it reaches its max at the value that we expected. So this large resonance is there and we measured the Q to be about 9.31, very low compared to what everybody else has been looking at today, but that is due to this large radiation damping.

[Transparency 7]

To approximate the Rayleigh wave contribution, we look at the partial wave series solution, which I have discussed before, that form function that told us the backscattering amplitude. Using the Sommerfeld-Watson transform we can take the denominator and put it in the form of a characteristic equation, by making the index complex and, from that, we can extract the phase velocity for the various waves in the sphere, Rayleigh, whispering gallery, et cetera. Our focus here is just on the Rayleigh wave. We can also get the damping coefficient for that particular wave as well.

Once we do that, we can substitute it into a form function contribution that is a ray approximation to each circumnavigation of the Rayleigh wave. These can then be summed to find the total contribution to the backscattering form function.

To incorporate the material absorption into this equation, we can do the same thing we did before. We can make the longitudinal and shear wave numbers complex as we did before, put

them into the characteristic equation we were solving, and get out the new phase velocity and damping term which will now have both the radiation damping and the material absorption as it travels around the sphere.

Another way we can introduce material absorption into the ray approximation is to assume that the absorption is not going to affect the phase velocity very much and hence is simply additive to the radiation damping -- we tried that here below (just showing you the new terms).

To determine the material absorption we looked at the fluid-loaded acrylic half-space and used that value for the absorption -- there -- which we then added to the radiation damping.

[Transparency 8]

Going back, when we solve the characteristic equation with material absorption, we find the phase velocity for the Rayleigh wave, given in this top graph. You see that at higher frequencies it goes over to the half-space Rayleigh velocity, as one would expect. Plotted here is both with and without the material absorption results, and they are very, very close to one another. This means that the approximation I was discussing just a minute ago -- might be valid in that the Rayleigh velocity changes very little with the addition of absorption.

At the bottom here in this somewhat complicated graph we have the damping for the Rayleigh wave. The solid curve here is the calculation without the material absorption, so this is just radiation damping. You see we have a large peak right around where we found our enhancement as we might expect. This long-short dashed line here is the material absorption for the fluid-loaded half-space, which we can then add to the radiation damping to get this short dashed curve at the top.

Just below that, this long dashed curve, is the calculation where we have added material absorption and solved the characteristic equation exactly. These lines are not quite identical but they are very close, which suggests that that approximation might be useful.

[Transparency 9]

With all this information we can calculate the approximate ray synthesis to find the contribution to the form function of these subsonic Rayleigh waves, which is given at the top here. Each of these individual peaks are Rayleigh wave resonances, he first being the quadrapole mode.

If I compare that to the exact form function, given down here at the bottom, we find that these peaks overlap fairly well. The dashed line is the exact form function with material

absorption. However, this is without the specular reflection contribution subtracted. With that subtraction these 2 curves are a little bit closer but not significantly so. It seems to correspond fairly well to what we would expect. Hence we are fairly certain that we have identified these as subsonic Rayleigh wave resonances.

[Transparency 10]

We also decided to check ourselves and do a measurement of the form function experimentally with the acrylic sphere I discussed before, using a 1-3 piezocomposite transducer running in a frequency range of about 30 to 60 kHz. At the bottom here we made measurements for 2 spheres. The first has a 1" diameter and the second has a 2" diameter sphere.

The triangles correspond to the 1" diameter sphere while the diamonds correspond to the 2" diameter sphere. The reason we chose this particular frequency range, and hence have divided the graph up like this is that at these low frequencies we must be concerned about reflections from the surface and the sides of the tank.

As you can see, we find fairly good correspondence to what we measured in the form function, which is reassuring; it means that these resonances are there and we can see them.

[Transparencies 11 and 12]

A potential application of these resonances, especially this large enhancement, is that it might be possible to use it for a passive sonar target. If we consider the target strength of this type of sphere, we can choose our sphere radius so that the frequency of interest corresponds to the largest resonance of the acrylic sphere and we can get large target strengths at relatively low frequencies. This could be useful in replacing the passive sonar targets that they have used in the past, which depended on glory scattering with CFCs. With the recent ban on CFCs, there is an effort to find alternative targets and this may be a possibility.

[Transparency 13]

I am going to talk now about something a little bit different. In looking at polymers, we decided to consider scattering from an acrylic shell. There are two properties of polymers, and acrylics, specifically, that make this scattering quite different from what one expects for metals.

The first which we encountered in the solid sphere was that the Rayleigh velocity is much less than the speed of sound in water. Looking at the Lamb wave spectrum, the symmetric wave has to pass through the sonic line here and then go over to the Rayleigh wave velocity.

139

Normally for metals it is the A_0 dispersion curve that has to pass up through the speed of sound in water, so this is not what one usually encounters. Also, there is a second interesting property in that the density of the material is very close to that of water, which means that the fluid loading is not just simply a small perturbation any more; it is actually very large and has a significant effect on the waves that travel through that material.

[Transparency 14]

I will address both of those. First, just looking at the effect of the low Rayleigh velocity on the symmetric wave, we recall that for a metal plate in water, the A_0 wave divides into 2 branches; the a_0 wave and the a_0- wave (the a_0- is subsonic, the a_0 wave is supersonic).

If we look at the S_0 wave, we find the same thing happens. Once again, as the S_0 wave passes through the speed-of-sound line in water it divides into 2 branches, one subsonic and one supersonic.

This is plotted for an artificial density of water of 0.2 and we will see in a minute why I chose that value, but this just illustrates that a similar effect emerges.

[Transparency 15]

If I let the density of water go to its normal value of 1, we find some strange things happening. If I run the code to find the phase velocity, I get something that looks like this. Instead of going down to the Rayleigh velocity immediately, it actually goes up past this line here, which is the longitudinal wave velocity, and interacts with the higher order symmetric waves, until finally it drops down to the Rayleigh wave velocity.

This has been studied by Rokhlin and Freedman and essentially what is happening is that as you increase the density of water and move toward stronger and stronger fluid loading, it restricts the surface motion of the plate. Finally, if you have infinite fluid loading, the surfaces experience mixed boundary conditions and the S_0 wave goes over to a longitudinal wave running down the plate.

So the symmetric wave is beginning to move up to this line to try to run along the longitudinal phase velocity. In the process, there are relatively complicated interactions that create some very strange dispersion curves.

[Transparency 16]

If we look at a fluid-loaded shell, a 5% acrylic shell in water, we find these same things happen and they are going to greatly affect the scattering from the shell. This solid line here, and

140

the dashed lines, are for an artificial density of water, a density of 0.01. We see the same splitting of the dispersion curve and, as we let water go up to its normal value, we find that these 2 lines move apart -- this is what I call the S_0- down here -- and then the dashed line up here is the S_0 wave, which begins to turn up as we saw for the plate.

However, the program that performs this calculation does not like it because the damping becomes very large and the code dies on me. So this is as far as we can go there, but it gives me a good sense of what is happening. If we look at the damping, we find this increases very much for this top curve and as this line passes close to the speed of sound in water, large damping and then it drops off down below. These are all going to produce different kinds of enhancements.

[Transparency 17]

However, all of these enhancements are going to happen for higher frequencies than what we expected for the solid sphere and the material absorption is going to greatly suppress these features.

There are various features, such as this one here, which may still be present. We think this one is due to a backward wave or a wave that has a negative group velocity, so when the wave is incident on the shell, it turns down and, instead of going around the back side of the shell, travels along the front and then re-radiates back very quickly. It does not remain with the material for very long before it scatters sound back. Hence there is not much absorption there and we may expect to see this effect. This was observed previously by Greg Kaduchak for a stainless steel shell (I have it plotted here for a 7.5% shell, just to show you that it is present).

These are some of the things we might expect and some of the strange things that one runs into when scattering sound from acrylic objects in water.

[Transparency 18]

This is just a summary for you to look at. Thank you.

DR. MCPHERSON: Is the surface wave, as it comes around the back side, radiating all the way around?

DR. HEFNER: Yes, it is losing energy as it travels around there. Once one reaches the point where it can send energy back, then that is when one can detect it. Every time it is moving around there it is re-radiating more and more sound.

DR. HARGROVE: I think the question that was just asked is a point that is often missed when you are concentrating on what is the backscatter but, in fact, this has an enhanced radiation isotropically around, doesn't it?

DR. HEFNER: Yes.

DR. HARGROVE: You are only summing up what comes in the back, correct?

DR. HEFNER: Right, but we have to take into account what happens as it travels, the amount of loss as it travels around, to figure out those amplitudes.

Thank you.

REMOTE ULTRASONIC CLASSIFICATION OF FLUIDS USING THE ACOUSTIC RESONANCE CHARACTERISTICS OF THE CONTAINER

DIPEN N. SINHA,[1] GREGORY KADUCHAK,[1] MICHAEL J. KELEHER[2]
[1]LOS ALAMOS NATIONAL LABORATORY
[2]DEFENSE THREAT REDUCTION AGENCY

ABSTRACT

A novel technique for classifying fluids in sealed, metal containers at large stand-off distances has been developed. It utilizes a recently constructed air-coupled acoustic array to excite the resonance vibrations of fluid-filled vessels. The sound field from the array is constructed by transmitting a high frequency modulated carrier wave which is parametrically self-demodulated along its propagation path in air. The array has a narrow beam width and an operating bandwidth of greater than 25 kHz. The vibrations are detected using a laser vibrometer in a monostatic configuration with the acoustic source. Experiments demonstrate resonance classification of the fluid-filler inside steel vessels is possible with incident sound pressure levels of the demodulated wave as low as 80 dB at the container location. Preliminary experiments demonstrate stand-off distances of greater than 3 m.

TRANSCRIPT

[Transparency 1]

DR. SINHA: What I want to talk about is how one can identify chemicals or liquids in sealed containers from a distance.

[Transparency 2]

Before I do that, let me explain why we want to do such things. This is what I had talked about two years ago at this conference, how we try to identify chemical warfare agents and other toxic chemicals, inside various types of munitions.

This is a noninvasive technique, where you have the transducers outside and one does not need to drill holes into the container, but one can still derive various physical properties of the chemicals. In this figure, I have shown sound speed, sound attenuation and density, all measured noninvasively.

Based on these physical characteristics one can uniquely identify the chemicals inside a sealed container. We built a little portable instrument, battery-operated, and it does pretty much the kinds of measurements you heard about this morning. It sweeps through a frequency range that sets up an interference pattern inside the liquid. Both in-phase and quadrature measurements between 1 and 10 MHz are made that provides a spectrum from which one determines all the physical properties. That is what we had done previously.

This instrument is now delivered to the Department of Defense and is being currently used in various places.

[Transparency 3]

The next phase of the work was to do the measurements from a distance instead of getting close to the items containing hazardous chemicals. The first question is why is this capability needed? There are various situations, very hazardous conditions, where you have toxic vapors or radioactivity and you do not want to get close to the containers but you still want to identify the chemicals or figure out what is inside.

Some of the usages you can think of are such as the waste storage facilities at Rocky Flats or the WIPP (Waste Isolation Pilot Plant) facility in New Mexico. There are also law-enforcement situations where government agents run into places where they find abandoned containers, or whatever, and they want to find out what is inside before they can properly dispose of these.

The major reason we first got involved in this development project is because our application was chemical weapons compliance monitoring, where one needed to find out during challenge inspection or otherwise, what kind of chemical is inside various munitions, pipes, containers, etc.

There are also applications in the chemical and various other industries. Firefighters are very interested in this sort of thing. Before they go into a burning building they would like to know, if they see a drum or a container, whether it contains any flammable liquid.

[Transparency 4]

This picture shows Greg Kaduchak making measurements on real chemical munitions. He does not really enjoy doing this kind of work wearing masks and taking data. This is one of the reasons we decided to come up with this remote technique.

[Transparency 5]

144

Let me first mention the different principles involved in this technique. There are 3 components to this whole approach. The first thing is, we need a way to project sound and to aim the sound in a certain direction on to the target instead of exciting the whole room and becoming a nuisance.

Because of the nonlinearity of air, if you put high-intensity sound, the waves that go through, as you can see, distort, and because of this nonlinearity and distortion, you can generate harmonics, you can have self-demodulation, shock-front development, etc. These phenomena are very well understood and worked on for many, many years in underwater acoustics.

We have taken pretty much the same principles and used them in air.

[Transparency 6]

Let me show you exactly how that is done. These are the two approaches we tried. The first approach is to start with two high-frequency transducer arrays. These are at two slightly different frequencies around 200 kHz, so the beam is very well defined. The two beams mix in the air. When it mixes, you end up getting the difference frequency and the sum frequency.

The sum frequency gets absorbed as it goes through the air because air is highly absorbing at such frequencies, and so you are left with only the difference frequency. The difference frequency, then, resonantly interacts with the container and sets up guided waves. I have to thank Todd and Phil Marston, they just described the theory before me, and so I do not have to go through that again. We pick up the resonant vibration of the container surface with a laser vibrometer. The advantage of this technique is that the beam is so well collimated, if you stand anywhere close by and not directly in the path of the beam, you cannot hear a thing, it is completely inaudible, but you can still make the measurements.

[Transparency 7]

The second approach is a little more efficient than the first one, because the sound interaction volume is very small when you have two separate beams mixing at an intersection region. In this second method what we have is a parametric array of transducers that is operated at a high frequency, around 200 kHz (217 kHz, to be exact) and we amplitude-modulate it by multiplying the high frequency with a lower frequency.

As the beam propagates through the air -- here I am showing blue as the high frequency -- it self-demodulates and you end up with the low frequency, just the low frequency modulating signal, which is exactly what we need. We sweep the modulating frequency and therefore you

145

can excite a whole resonant spectrum of the container. From this spectrum, then, we can derive, just as before, the chemicals inside.

DR. SMITH: What is a parametric array?

DR. SINHA: When you generate low frequency by taking advantage of the parameters of the air, essentially the mixing, and the nonlinearity.

DR. SMITH: How remote is this?

DR. SINHA: I am coming to that.

[Transparency 8]

Let me first describe this array, how we build it. There are many ways of doing it, but we wanted the quickest and cheapest way of doing it, so we bought off-the-shelf commercial air transducers from AIRMAR. These are about $20.00 apiece.

Greg drilled regularly spaced holes in a round plastic plate and we, just like a Lego set, stuck in a whole bunch of these air transducers in there, and that is the array, essentially. The array is driven at 30 V or less. You can get pretty decent directivity.

[Transparency 9]

This is the beam spread of an array of that size at a low frequency, such as at 13 kHz, but when you use this parametric array with the mixing in air, the beam profile is much, much narrower. It is very directional.

[Transparency 10]

The distance here is about 3 meters. We have gone as far as about 5 meters. Here is the parametric array. We start with the high frequency and end up with the low frequency. Here I have two steel containers, just a cutout of a 155-mm artillery shell (the picture I showed you in the beginning). There are two liquids, isopropanol and ethylene glycol. Here is the laser vibrometer for the Doppler type of measurement. We sweep through the modulating frequency, so we can get a resonant spectrum.

[Transparency 11]

The setup is also very simple. Here's a function generator, the output from which goes through a power amplifier and boosted to about 30 V and drives the parametric array. The laser vibrometer picks up the signal and the output goes through a homodyne detector, which is very much like a tracking filter, with a 100 Hz bandwidth. A laptop computer is used to display the spectrum.

[Transparency 12]

Here is a picture of the actual setup. This is a smaller version of this array. These are the two steel containers I mentioned earlier. The yellow object in the picture is the laser vibrometer. The distance between the containers and the laser vibrometer is about 10 feet in this picture.

[Transparency 13]

The advantage of this laser vibrometer is that there are no mirrors attached to the containers, so it can be any surface that the laser beam is shining on. The red dot is the laser beam. We put antifreeze here, because it is colorful, so you can see the difference between the two liquids. The reason there is a little core, it is called a burster core, is that is where the explosive goes inside chemical ordnance.

The dimensions are all given here for these containers. We have tried various kinds of containers; these are meant for quantitative measurements.

[Transparency 14]

This is pretty much what you heard from the previous speakers. Instead of underwater, this is in air. This launched the sound wave that generates these Rayleigh modes. This is the anti-symmetric a_0 mode that Todd talked about previously. It goes around the circumference and sets up resonances each time this resonance condition is fulfilled, so you get a series of resonances, but nicely spaced according to the sound speed in the wall.

[Transparency 15]

This is pretty much the same picture that Todd had. The phase velocity is the red line here, the dotted line. These are the two phase-velocities when you have that steel container filled with isopropanol and ethylene glycol, and this is the radiation damping for the particular container that I showed. This radiation damping kind of tells you what the efficiency of coupling of sound is with the containers. It is a little difficult to see the difference between the two liquids, because these are absolute values.

[Transparency 16]

Let me show you the difference between the two and now it is much more obvious. This is the phase velocity difference between isopropanol and ethylene glycol as a function of frequency. These are derived from theory.

[Transparency 17]

I would like to show you the measured data now. This is the actual spectrum that we get from the output of the laser vibrometer. If you notice, these resonance lines are regularly spaced, with the spacing increasing continuously. This is because the sound speed is increasing with frequency.

On the top is shown the theoretical prediction for the same measurement. Agreement between experiment and the theory -- this is the a_0 mode -- looks pretty good. That means you can indeed back out the properties, the density, sound speed, et cetera, from the observed spectrum.

[Transparency 18]

This is actually a computer screen dump from the data as we take them. I have blown up the area just to show one resonance peak, how it shifts between ethylene glycol and isopropanol. Once it sweeps through, that takes only about 20 seconds, the computer program then comes up with a match.

[Transparency 19 -- unavailable at time of printing]

These data are from a contact measurement, not non-contact, just to show how, if you have different viscosities or attenuation, how the resonance Q's are damped. By measuring the resonance Q -- here, GB is Sarin and H is Mustard (the other kind, not the kind you put in your sandwich) -- it is possible to determine attenuation, too. Once you get sound speed, density, and attenuation, you can pretty much identify a lot of chemicals.

What I have just shown you is very preliminary work; it has a long way to go.

[Transparency 20]

We also tried to see if we could determine what the liquid level is inside the container. Now, instead of sweeping through the frequency we pick just one resonance frequency and move the laser beam up and down. You can see there is a dramatic change in the amplitude as you cross the liquid level. So, essentially from 10-12 feet away you can determine the liquid level, too.

[Transparency 21]

It is really possible, from a distance, to excite various guided waves on a container, look at their interaction with the fluid inside and identify chemicals. What limits our distance, how far we can go? It is the laser vibrometer. The one we currently have goes up to only about 25 kHz and about 15 feet is its limitation -- it is a pretty "el-cheapo" brand.

148

There are other laser vibrometers that have a range up to 30-35 feet. That pretty much limits how far you can go, because you can always jack up the power level in your parametric array within reason. We are nowhere near any upper limit of power that can be used. One thing I forgot to mention is the power level is about 85 dB near the low frequency that is at the target. There is a lot of absorption but, still, that was enough, 85 dB, to excite resonances and be picked up.

If you have better instrumentation, there is no reason why you cannot extend the range further.

This technique can also be used for standard nondestructive testing remotely. One can look for wall integrity, thickness, if you have rusting, corrosion. These conditions can probably be determined. There are lots of applications that one can think of but I focused on only one.

DR. SMITH: _____ levels? I may have read that graph wrong, but on your amplitude versus _____ graph, you have got a region where there is liquid and then you have an air gap and then no liquid?

DR. SINHA: No, no. This is the liquid and this is the air gap -- I mean, not the air gap.

DR. SMITH: On the graph.

DR. SINHA: On the graph? Oh, this is a very noisy signal, so it is just average; it is just a square wave. You move the laser beam up and down, the signal just bounces up and comes down; it is a dramatic change. That is all I am showing there.

DR. LEISURE: How does the technique depend on atmospheric conditions, humidity and so on?

DR. SINHA: It does not, as far as we can tell, but in Los Alamos the air is very dry. I do not think humidity has much effect. By the time you get that kind of power, the effect of humidity is very minimal. It does affect the sound speed a little bit and maybe a little bit of the attenuation, but it should not be very dramatic.

DR. MARSTON: You showed a picture of a container with an empty core in the middle. If there were another chemical in there, would you see 2 sets of resonances for each chemical?

DR. SINHA: No, because it is already so insensitive -- I mean, the sound wave goes around the outer casing, it really would not see the inside. But if I am doing contact measurements, then it has the sensitivity, and you can pick such things up but from a remote measurement it is very difficult.

149

DR. HARGROVE: It would be possible, if I were trying to get around a chemical weapons ban, to shield the resonance technique?

DR. SINHA: In principle, yes

DR. DARLING: How sensitive is this to the actual container? I got the impression that you needed to have some sort of standard measurement. It is independent?

DR. SINHA: We can put in artillery shells or anything. This was a good thing to do, the theoretical calculations, so we needed exact dimensions to really match against.

DR. DARLING: So you can tell from any container the contents?

DR. SINHA: Sure.

DR. DARLING: Just from previous measurements and physical properties?

DR. SINHA: Yes, unless it is plastic, very soft, that may be different.

DR. DARLING: It takes a surface normal to your laser beam to see --

DR. SINHA: This does not depend on the actual reflection back to the vibrometer. All it has is a kind of little telescope, it looks at that spot. It is not a direct reflection back and you do not need a mirror, either. If it is completely absorbed, sure, you are not going to see anything.

DR. MARSTON: I have 2 questions. One, the AIRMAR transducer, what was the technology?

DR. SINHA: Ordinary piezo with the little matching layer in front of it. That is about it.

There is a lot of room for improvement. We are talking to various companies that have special capacitance types of transducers, there is one company in Canada, and another just started in San Diego. These are very expensive, approximately $2000 for a single transducer. We did try these; we just did not make an array out of them.

What we have done is rather inefficient. It was just a demonstration to show that the technique does work.

DR. HARGROVE: I want to caution you against saying that you can deliver more sound at some distance by just turning up the source. I have spent too much time with people who want to do acoustic cannons and all kinds of stuff like that. There is a nonlinear saturation; there is a limit for any given medium of distance as to much you can get from here to there.

DR. SINHA: That is true, except that I am not depending on the higher frequency. After it mixes --

DR. HARGROVE: I do not care what frequency.

DR. SINHA: I am not going for unlimited. I am just talking about 30 feet versus 12 feet. There is no way you are going to go a mile or anything. No, that is not going to happen, plus the beam would spread too and you cannot focus it any more. It needs to be within reason.

DR. MARSTON: The second part of my question is what were the displacement amplitudes you typically measured with the vibrometer?

DR. SINHA: Probably anywhere from a 100th of a micron to a 10th of a micron, roughly. The vibrometer is very sensitive but, also, you saw the data that it is pretty noisy, too. The one made by Polytech has a much cleaner signal, but it is 3 times more expensive.

DR. LEVY: I am slightly confused by the data that show here is the beam. I saw a lot of other beams. Could you go back to that?

DR. SINHA: Sure.

[return to Transparency 17]

When you excite those, the a_0 waves are the ones that are really developed in the most efficient way, so those are the peaks that are much stronger, but there are smaller ones, too, there are other modes that may be generated.

DR. LEVY: You showed another graph, too.

DR. SINHA: The other graph was just an experiment straight from the computer screen, the raw data.

[return to Transparency 18]

This is the peak that shifts to this position when you have ethylene glycol versus isopropanol and I was showing how large the shift is. That is what I was showing. But if you are looking at this little one, there is some noise and there could be some other modes in there.

DR. LEVY: Those nice-looking peaks halfway between ethylene glycol and isopropanol.

DR. SINHA: You mean these? There can be a lot of other resonances (e.g., lengthwise instead of circumferential), because, it is a finite size.

DR. LEVY: How do you distinguish which one is ethylene glycol and the other one is isopropanol?

DR. SINHA: These are very large. These resonance peaks are many times larger than the smaller peaks. Also, if I turn on the filter, those little ones really go down. It is very easy to identify the ones that I am looking for. This is only one peak --

DR. LEVY: But what makes them small, the filter?

151

DR. SINHA: If you want to get rid of the noise, there is some real resonance and the other is just noise in the electronics, probably the laser vibrometer, which I do not have too much control over.

There are other modes being generated, too, sure. We just have not modeled all the other ones. We took the simplest one and it agrees with theory and that was good enough to do the job. As I mentioned, this is very preliminary work and a lot more really can be done.

PARTICIPANT: I was surprised that it does not matter what the shape or size of your container is. It is inconceivable that you do not need a base cylinder to measure before you know what is inside of it.

DR. SINHA: All the munitions that we deal with, we know their dimensions.

PARTICIPANT: So you do not need a reference shell?

DR. SINHA: No, you do not need a reference shell. All you need is the actual measurement. If I know it is made of steel, that is all I really need, or it is made of aluminum. Most of the chemical munitions are made of only a few materials, so this is not absolutely arbitrary.

Your question is if it is an absolutely arbitrary system, how does one do it? That is going to be very difficult.

Thank you.

Acoustic Gas Resonators for Measurement of Thermophysical Properties and Thermometry

James B. Mehl
University of Delaware

Abstract

Gas-filled cavity resonators can be used to measure the speed of sound c, the viscous diffusivity D_v, and the thermal diffusivity D_t. The relative sensitivity of a complex resonance frequency to these parameters depends on the shape of the resonator and choice of mode. Different choices are appropriate for different measurements. Spherical acoustic resonators are excellent for very high-precision measurements of the speed of sound in dilute gases. The experimental models of spherical resonators include the effects of the thermal and viscous boundary layers, and the elastic deformations of the solid parts of the resonator. Spherical resonators have been applied to the measurement of the gas constant R, to acoustic thermometry, and to high precision measurements of the speed of sound $c(T,p)$ as a function of temperature and pressure for very pure gases. Precisions as high as a few parts in 10 million can be achieved. The ideal-gas specific heat and information about intermolecular interactions can then be extracted from $c(T,p)$. Cylindrical acoustic resonators are easier to fabricate and are suitable for many purposes, although they cannot be modeled as completely as spherical resonators. More complex resonator shapes have been developed for determination of D_v and D_t. The Greenspan acoustic viscometer, a resonator consisting of a cylindrical duct coupled at each end to large chambers, has a low-frequency mode in which the kinetic energy is localized in the duct, and the potential energy in the chambers. Its frequency response is strongly dependent upon D_v. As an absolute instrument, it is capable of determining D_v to a precision well below 1%. A cylindrical resonator with a honeycomb structure interposed in the flow midway between the ends has been developed for measurements of the ratio of D_v to D_t. The resonator shape is similar to the Greenspan viscometer, except that the chambers are coupled by a large number of parallel ducts. The modes of interest are similar to the plane-wave modes of a cylindrical resonator without the honeycomb insert. The odd plane wave modes interact with the insert mainly through viscous

coupling, and the even numbered modes interact with the insert primarily through thermal coupling. Measurements of the complex resonance frequencies of a set of odd and even modes can be used to determine the ratio D_v/D_t A recent addition to the models of acoustic resonators is the effects of surface roughness.

TRANSCRIPT

DR. MEHL: Thank you. I think the title makes it clear I am not an RUS person. I have for some 2 decades or so worked largely in collaboration with Mike Moldover and some other colleagues at NBS, now NIST, on a variety of acoustic and electromagnetic cavity resonators used to measure different properties of gases.

[Transparency 1]

I am going to talk today about the generic experiment and how we do some of our data analyses, pick out a few things that I think might be of interest to this community and this meeting.

Here is a generic experiment. We use a frequency synthesizer, generating a sine wave at discrete frequencies, controlled by a computer, a cavity resonator customized to the particular measurement, and a 2-phase lock-in amplifier. I think for many reasons it is important to measure both phases, the in-phase and quadrature signals in experiments of this type.

What I have plotted below is the absolute value of the complex signal u + iv at a set of discrete frequencies. This is a typical set of data. Here you see the resonance properties, the center frequency, f_0, and the half-width g. A Q would be the ratio of $f_0/(2g)$, which is the width here at $1/\sqrt{2}$ of the maximum.

[Transparency 2]

If you plot the same data in the complex plane, u versus v – at the right -- you see a circular plot for this ideal resonance. As you scan across the resonance, the points go around the circle.

This is quite useful in connection with some of the ideas that have been discussed here: How do you determine the Q of a resonance, and how do you determine the resonance frequency? Let's look at the theoretical expression here for the acoustic pressure in an enclosure. If I have a source at point r', the pressure at point r is given by this expression, which you can find in Morse and Ingard. There is a resonance denominator, there is another frequency up here.

If you parameterize this, you get an expression here for the microphone output, a complex signal. There is an amplitude A_N for each mode, and a complex resonance frequency for each mode.

Normally you are looking at a single mode of interest, but you will be sitting in the tails of many other resonances. It turns out that you can work with a small number of modes using the procedure I am going to talk about. Here I have isolated a single mode and then expanded the contributions from all the rest in a Taylor series.

This (B) is a complex number, a constant. The next term is a weak frequency dependence. The background terms take the origin of this complex product here and translate it in the complex u-v plane, so that the maximum distance from a point on the resonance to the origin need not correspond to the frequency f_0.

If my origin gets moved to, say, some point over here, then the amplitude is the distance from here to whatever the maximum distance along this curve is. That will, in general, will not be at f_0. You will get some distortion in the shape as you move around. It is clearly going to depend on where your background moves the origin to -- and I have exaggerated a bit here.

I think anyone who has looked at a lot of data will see a resonance that is sitting on a lot of background and you just see a little blip. Sometimes it looks like a bimodal signal. You can see why all this happens just by looking at this picture and thinking about how the distance from the origin varies as you sweep through the resonance, considering different levels of complex background.

Computers are very good at sorting this sort of thing out. I was telling someone earlier I did it for the first time in the early 1970s on a 8-bit lab computer with 1.8 K of memory. It requires a 6-parameter nonlinear least-squares fit. Today it is trivial and I think you could probably do it fast enough for a lot of modes in, say, an RUS experiment.

What we do is fit the theoretical function to our data set using the complex parameter A_N, the complex $F_N = f_0 + ig$, plus one or two complex background parameters, as necessary.

If you are looking at some closely spaced modes, you might include several terms with different mode indices N -- I have played around with up to 5, but 3 is trivial.

[Transparency 3]

What is more, this procedure is rather robust in determining f_0 and the half-width g, as shown by the algebra on this slide. Let's suppose that your transducer is measuring an acceleration instead of a velocity, or something in-between. Does that bias the measurement?

155

Suppose I put another factor of frequency f in the numerator. I can write that as my complex resonance frequency F + Δf, and separate off the constant term here, so I get a term that looks like the resonance term, except with a different amplitude.

Then the next term has a Δf in it, but the denominator is the product of Δf= f - F_N and f+F, which is 2F+Δf, something that is slowly varying, as the numerator is, so this second term really just modifies the background term.

More generally, any frequency dependence in this coefficient, which includes your transducer, response function, your amplifier, everything down the chain, just modifies the background. If you analyze data this way, you will get the resonance frequencies in spite of minor imperfections in your transducers.

[Transparency 4]

The ultimate limit is probably your detector, how good is the lock-in. This is an old slide. It comes from a paper by Moldover, Mehl, and Greenspan from the mid-1980s. Here are the 2 functions, u and v, and these are the residuals from a fit to a total of 22 measurements, 11 taken in rising frequency and then sweeping back down, so you see some reproducibility here.

The rms difference between the data and the fit is on the order of 0.02%. That means, in practice, that you can determine g, the half-width, and f_0, the resonance frequency, to about 0.02% of g, so the dissipation is determined to 0.02%, something on that order, and the frequency itself is determined with a fractional precision that is greater than that by the Q, often better than one part in 10^7.

The extent to which you could use this information depends on how well you can build a model of the experiment, that you can build in your understanding of the frequency. My point here is that there is plenty of resonance information from which to extract that information.

[Transparency 5]

This is from the same paper. It is from a mode that is nearly degenerate, nearly threefold degenerate. The lower plots show residuals. If you try to fit a 2-mode model to the data, you get something like 2% residuals, but with 3 modes the residuals go down to 0.02%, again, and you get good resonance parameters for all modes.

In this case there were 4 parameters for each resonance, so that is 12, total, plus at least one complex background, possibly 2, it says down here, so there would be 16 parameters in this fit. You span the range of nearly degenerate modes and you will pick them up.

156

[Transparency 6]

Okay, now some applications of this: For measurements of the speed of sound a good resonator is the sphere, which has some properties that make it suitable for talking about in this context of this meeting. I will spend a little bit of time talking about that example.

We have also made resonators that are good for measuring viscosity and thermal conductivity, properties dependent upon the measurement of the resonance widths. Here we are more interested in measuring the resonance frequencies of a spherical enclosure to determine the speed of sound, here written c (on some of my slides it will be u).

In the limit of 0 pressure in an ideal gas, c^2 equals the specific heat ratio, γ, times the gas constant R times the absolute temperature divided by the molecular mass.

At NIST, this in the mid-1980s, the group led by Moldover used the spherical resonator to measure R to 1.8 ppm, using argon and helium for which γ is exactly 5/3. (The molecular masses are well known and the experiment could be done at a known temperature).

More recently, the same apparatus has been used for primary acoustic thermometry between 217 and 303 K. It is possible to determine the absolute temperature scale to 0.6 mK. Measurements of this type make an important contribution to thermometry, where there are existing discrepancies among other measurements on the order of a few mK. There are plans to extend acoustic thermometry work up to 800 K at NIST.

[Transparency 7]

Now let's take a look at the modes of the sphere. One of the disadvantages of the spherical geometry is you cannot do anything about the spectrum; it is set by mathematics. The acoustic pressure will be proportional to eigenmodes. There is a spherical Bessel function, there is an eigenvalue, $Z_{ln,}$ and this is a spherical harmonic.

If I have a rigid sphere so that the acoustic velocity normal to the boundary must vanish at the boundary, then this Bessel function must have a vanishing derivative at the outer boundary. This is the boundary condition. The sphere also has to be thermally insulating; otherwise you do not have a pure acoustic wave inside.

In that limit this is the spectrum. There is a set of modes here at the bottom. There is a 0-frequency mode with l = 0. Here is the lowest-frequency breathing mode, f and a series of similar modes with radial motion.

Then there are modes with $l = 1$, which are all threefold degenerate, which you can deal with, but you would rather not, if you can avoid it, and then there are some messy ones up above. Sometimes there is a near degeneracy. Here is a particularly bad one within 0.2% of a radial mode here, which is, therefore, essentially unusable.

This mode has index $l = 13$. It is, therefore, 27-fold degenerate in a perfect sphere. The effects of imperfect geometry lift that degeneracy and broaden out a packet of modes that is very difficult to do anything with, not surprisingly.

In practice, you can deal with about five or six modes in the low-frequency range that are very nice. The sound is incident upon the boundary normally, and everything is calculable, in principle, using exact theories; you do not have to do approximations. This is really classical physics. The major solutions go back to Kirchhoff in 1868.

[Transparency 8]

The physics of the gas is described by the longitudinal component and transverse components of the Navier-Stokes equation, Fourier's law of heat flow, conservation of mass, and conservation of energy. Kirchhoff showed that you get a fourth order partial differential equation in the temperature from this, and this, and that that has 2 modes, an acoustic mode and a temperature mode with our usual acoustic propagation parameter here, and a thermal mode that is largely confined to the region near the boundary -- this thermal penetration length here, this mode dies out to $e^{-2\pi}$ in a wavelength δ_t.

But it leads to an important correction to the frequencies, because you have a transition from an adiabatic wave within the gas to an isothermal wave at the boundary, so some fraction of the volume proportional to delta t/a has an intermediate speed of sound, and this leads to a fractional correction that is proportional to $(\gamma-1)/2$ times δ_t.

Shell motion: Some people in this room know that an isotropic solid with spherical shape is an exactly soluble problem. We have used classical elastodynamic theory to solve for the response of the shell to the internal pressure field, so that goes into the model as well.

[Transparency 9]

This slide summarizes the results of such a calculation. You have measured frequencies related to the speed of sound (u here), a mathematical eigenvalue, and the radius of the sphere.

The second term is the thermal boundary layer correction and this is the correction for shell motion. We can skip the width expressions here.

For the sphere used for measuring the gas constant, the thermal boundary layer correction is 0.17% for the lowest mode at a pressure of 1 bar and scales with the reduced pressure and frequency variables, as shown here. The shell correction is 1.7 ppm at 1 bar and it has a resonant denominator, which I will say a little bit more about.

[Transparency 10]

The other thing we have to worry about is the effect of imperfect geometry, and a sphere is nice for this. If you consider a deformed sphere, where a parameter ε sets the scale and this function, curly F is of order unity, you can show that if you pick an F that preserves the volume, then the eigenvalue spectrum for the radial modes with quantum number $l = 0$ is perturbed in order ε^2.

You can make a sphere in a good machine shop with ε on the order of a few times 10^{-4}, so you get down to corrections that are generally less than a part in 10^6 for the radial modes.

The nonradial modes, beside being degenerate, are all perturbed in order ε. This is a potential problem, because you have to measure this mean radius somehow. The only good way to do it as a function of temperature is to use the electromagnetic modes for which there is no non-degenerate s-wave-type mode. It turns out that if you consider any multiplet, do an average over the geometric perturbation, the average frequency of any multiplet is perturbed in order ε^0 -- this applies to the acoustic modes, to the electromagnetic modes of the electrical mode class, and the magnetic mode class, 3 different boundary conditions, and I would be willing to bet it also applies to solid elastic spheres.

[Transparency 11]

A little bit more about this elastic correction. I want to show you some evidence that we have for this, and then I will have to stop; I will not be able to say anything about the other experiments.

The equation at the bottom shows the effects of shell motion for different symmetries. There is a shell-admittance function, dependent on frequency and the mode index l. Fractional corrections have a coupling constant. In the numerator, ρc^2 for the gas is essentially γ times the ambient pressure, and in the denominator ρc^2 for the solid is an elastic constant. For gases this

ratio is a relatively small number and that is the source of the low magnitude -- of order 1.7 ppm, typically.

The shell admittance function is plotted at the top. For the l = 0 you see the resonance here (for the 3-1 sphere that was around 14 kHz). For l = 1 there is a 0-frequency resonance that corresponds to translational motion and another resonance over here. Here is a bending-mode resonance for l = 2 symmetry.

[Transparency 12]

These data are from an earlier, thinner, sphere. They show the shell perturbation for a series of modes. There is evidence here of the singularity at the shell breathing mode, a change in the sign of the correction as you pass through the mode.

[Transparency 13]

This shows something similar for the l = 1 triplets in that same geometry. Generally there are 3 points at each frequency, all generally falling along the same curve, and we just pick up a hint of the singularity here. But look at what happens to the lowest mode; it is going way up, up the graph and you see a separation in the 3 components of the multiplet. These modes have the gas oscillating in these directions.

The sphere is suspended, so there is a little bit of stiffness for this (vertical) motion, greater stiffness than for these 2 (horizontal) motions. The motions in the horizontal plane have about the same fractional correction and the vertical one is a little bit smaller. In fact, if you make the stiffness in the vertical direction larger and larger, you can force that correction down and even change its sign.

These experiments show us something about the coupling of the fluid inside to the mechanical motion of a shell and it makes you speculate a little bit about what can be done. Can you make the shell stiff enough so it does not matter so much?

[Transparency 14]

The answer is displayed here on this slide, where I show the resonances of a spherical shell as a function of the ratio of the outer to the inner radius. Here is the breathing mode. Its frequency decreases with increasing wall thickness. Of course, the corresponding correction gets larger at low frequencies as it gets stiffer, but you cannot make the resonance go away. You make the shell a little stiffer but you also increase the mass. The same is true for the l = 1 and l = 2 modes.

At the right some argon acoustic resonance frequencies are listed. There are generally several that fall below the extensional elastic modes here, so there is a little bit of room for doing an acoustic experiment in a gas inside of such an enclosure. If the gas is helium, there are not many modes below the shell breathing mode. If you start putting liquids in the shell, it is a real challenge. (I think some people have also found some clever solutions, too).

DR. SMITH: Have there been attempts to measure the _____ fluid by putting it inside a metal shell _____? Has that been your experience?

DR. MEHL: I have not tried to use this for liquids. We have worked with gases up to about 10 bar. The correction is 1.7 ppm. at 1 bar and only 17 ppm at 10 bar. You are up at least 2 more orders of magnitude. It should be possible if you can sort out the modes.

I would build a model that has mode coupling if I were doing such an experiment.

DR. SMITH: We did a 2-layer computation from a _____ shell. _____ they were just Rayleigh waves in the metal.

DR. MIGLIORI: Last week I talked with Mike Moldover. He had attempted to measure the elastic constants of a batch of Invar that he was using for spherical shells and he failed because the microstructure of that Invar was so bad he could not get anything close to a fit for the elastic moduli, but it appears that he needed to know the elastic moduli of the shell about 5 times better than we had any hope of ever measuring, partly because it was Invar, partly because of constraints.

Have things gotten better?

DR. MEHL: He is probably hoping that he can build an apparatus that will work up to 800 K. For the stainless steel sphere here, the breathing mode compliance was measured in situ by filling the sphere with pressurized mercury.

DR. MIGLIORI: Stainless steel is much nicer than Invar.

DR. IZAAK: You said the container needs to be thermally insulated, otherwise there would be no acoustic wave inside?

DR. MEHL: No. In a gas there is strong coupling between the pressure and temperature fields. You have an adiabatic wave. As pressure oscillates, the temperature oscillates -- in dimensionless units they oscillate about the same amount. Any solid boundary is a very good thermal conductor compared with the gas.

There will be a heat flow, an oscillating heat flow, in the boundary region, whose thickness is given by this δ_t. When I was showing you the eigenvalues in the absence of such approximation, that corresponds to the limit of an insulating shell.

DR. MARSTON: Is it common to go back and check whether the background that you introduce for any one mode, say, the local background near your mode, is consistent with the strengths you have from the adjacent modes?

DR. MEHL: I played around with that a little bit years ago. We have never pursued it very seriously, no. But it is certainly qualitatively true in that if you are working with a high mode, you are sitting on the shoulders of a lot of other resonances and you would see a high background, whereas in the lower part of the spectrum you see small background.

What we typically do is make sure that the fits are insensitive to this, that is, try adding another parameter and seeing if it makes a difference and reject data that do not fit sensible behavior patterns.

I should also mention, since I said that we use the measurements of the half-width to determine dissipative processes, that it is important to refine the models. For our acoustic viscometer we take into account the fact that the dissipation, which is viscous itself, is proportional to the square root of the frequency.

You build a resonator to measure the width, you do not want it to have such a high Q -- 100 or so is fine. When you build a model for that, it is important to put the frequency dependence of the width into the model, do not assume it is a constant. We actually do a little better than that, but that is the minimum you should do.

Thank you.

SAMPLED CW MEASUREMENTS ON SINGLE CRYSTALS OF YBA$_2$CU$_3$O$_{7-\delta}$ AND BI$_2$SR$_2$CACU$_2$O$_8$

DEBASHIS DASGUPTA

UNIVERSITY OF WISCONSIN–MILWAUKEE

ABSTRACT

Sampled Continuous Wave technique was found most suitable for investigating small single crystals of YBa$_2$Cu$_3$O$_{7-\delta}$ and Bi$_2$Sr$_2$CaCu$_2$O$_8$. A unique bonding technique has been developed where the sample is pressed on to the transducer with few threads of very thin GE varnish and the transducer is mounted between parallel gold wires and a soft spring to oscillate freely. It has been found that only an optimal coupling between sample and transducer can bring out various features in the mixed phase of the of these high T$_C$ superconducting crystals.

The results of attenuation measurements on different single crystals of YBa$_2$Cu$_3$O$_{7-\delta}$ and Bi$_2$Sr$_2$CaCu$_2$O$_8$ using such technique at frequencies of 3MHz and 5 MHz and in magnetic field up to 1.6T will be presented. Early work on untwinned YBCO revealed pronounced field dependent attenuation changes that were indicative of transitions from soft vortex system at low fields to a rigid vortex system at high fields. In addition, for untwinned YBCO, ultrasonic signatures of melting transition and possibly depinning transition of the flux line lattice were observed below the critical temperature.

For twinned YBCO crystal and BSCCO crystal, sharp field dependent attenuation drops were observed below the critical temperature and are easily identifiable with the normal-superconducting transition. In addition, in the superconducting mixed state there were field dependent transitions analogous to the melting transition of the flux lattice. This melting phenomenon was also investigated extensively for YBCO using ac-susceptometry technique.

TRANSCRIPT

DR. DASGUPTA: I am going to talk about some ultrasonic measurements on two high-temperature superconducting materials, YBCO and BSCCO.

[Transparency 1]

I learned quite a few things here and I heard the words "thermally activated" and a few other things that are there in this experiment. These are the people who are and were involved in these experiments -- I made the transparency, so I am on the top. (Laughter)

Jeff Feller is the person who I go to whenever I have an electronics problem. The name that is not here is somebody from whom I also learned a lot, and that is Mark McKenna. Carsten is the person this whole work started with and, of course, Moises and Bimal are always there. People, who funded this work, are the graduate school and physics department at UW-Milwaukee and ONR.

[Transparency 2]

The reason this project started was for developing an ultrasonic technique to investigate the properties of small high-temperature superconducting crystals. I think Jay Maynard was trying to show us some pictures about how small these HTS single crystals are and I can assure you they are small. Typically they are about 1000 by 800 microns and I work with crystals that are between 50 and 70 microns thick, so they are pretty small.

It is very hard to bond transducers on these small crystals and do conventional ultrasonics and, even if you can bond it, there are instrument limitations, pulse width, duty cycle, and all these things to worry about and do successful conventional ultrasonics.

[Transparency 3]

Moises and Carsten started this project to find out an alternate ultrasonic technique, and what came out is sampled CW. The outline of this presentation is: I will just quickly go through some essentials of type II superconductors, including flux lines and pinning, and then go through the description of the sampled CW and try to present the results on YBCO, untwinned and twinned crystal. If there is time left, probably I will present some susceptibility results as further verifications and also some ultrasonic results on BSCCO.

[Transparency 4]

This is a colorful but very complex diagram. This is a phase diagram of a type II superconductor. Many features are just a little enhanced for clarity. The most important part for this work is the mixed phase, where there is partial penetration of flux lines. What is in this phase, and how the flux lines behave, interact, and everything is what everybody is trying to study.

Most of the results that I will present here are mostly concentrated around this part. In the mixed phase the flux lines exist in two distinct phases. One is the flux liquid where they are entangled and the other one is a flux solid, where they are arranged in a hexagonal lattice form.

[Transparency 5]

The mixed phase is probed, in all experiments, through some sort of current. Whenever you try to send a small amount of current, you set up a force and these flux lines start moving. Essentially the motion of the flux lines results in dissipation in the sample.

Type II superconductors as such, pure type II superconductors, are not that useful because of free motion of flux lines resulting in dissipation. There can be different kinds of forces acting on the flux lines. One that plays the most important role is the Lorentz force, originating from a (transport-type) current and that results in a Lorentz force on these flux lines.

[Transparency 6]

To make these materials technologically useful, one can concentrate on are the defects, because the defects impede the motion of flux lines by pinning. There are different kinds of defects that are possible. Some are intrinsic, like oxygen vacancies between planes and some are introduced by external irradiation or other processes.

Most of the time externally-induced defects like columnar defects are far better in pinning than naturally occurring defects such as twin planes or so, but that is a totally different area of study. The important fact is that defects can stop the flux lines from moving and that reduces the dissipation.

[Transparency 7]

With this I will go into a brief description of what the CW technique is. Essentially you set up a resonance in the sample, a standing wave resonance, and one can lock into one of the resonances and change external parameters. Change in frequency typically results in change in velocity, and change in amplitude typically gives rise to attenuation. Monitoring the change of these quantities as a function of either temperature or magnetic field, one tries to extract information about the physical state.

[Transparency 8]

In Sampled CW, instead of sending a continuous wave into the sample, the RF signal is gated and is "ON" for a certain time and sets the transducer and the sample in oscillation. And then it goes "Off" and the transducer and the sample starts ringing down with a characteristic Q.

What we do in this experiment is look at the amplitude at two different times, where the gates are kept fixed, and see how it changes i.e. how the amplitude changes as we change the temperature or the magnetic field.

The sample is typically just placed on the transducer and then it is held onto the transducer with a few, typically four or five, GE varnish threads. When the threads dry and the sample is cooled down, the threads become stiffer and they just press the sample onto the transducer.

There is a model by Dr. Jeff Feller that discusses this aspect of coupling between the transducer and the sample. It is in the proceedings of the last resonance meeting. The argument is that the coupling between the sample and the transducer has to be optimal and this optimal coupling is not achieved by directly bonding the sample with the transducer. We tried Nonac, Epoxy, and we tried just GE varnish as direct bond materials. We tried different coupling schemes and the one that works best is the one with varnish threads pressing the crystal on the transducer.

The transducer rests on two copper wires and two RF spring contacts come from the top and slowly hold the whole thing down against the gold wires. When you apply the RF pulses, the whole transducer + sample system oscillates nearly freely.

The key is to oscillate the system at such a wavelength that, let's say, the ion on this face and the ion on this face of the YBCO crystal do not have a displacement gradient between them. They are moving in unison. The choice is to do an experiment with λ that is much, much greater than the thickness of the sample.

Typically, we do work with samples with a thickness of about 50 microns to 70 microns and I did some experiments with a 200 micron-thick sample and it did not give results as well as I thought. Actually, there is a lot of noise or something that is not right.

In what I called a micro-view here is an effort to explain what this whole technique is all about. Acoustically we induce motion in the bulk ionic lattice to which the flux lines are coupled. Thus, when I am moving the ionic lattice, it is not dragging the whole flux line lattice but it is just creating some local flux line density modulations leading to variations in interaction among flux lines and thus changes the nature of dissipation in the flux-lattice system.

[Transparency 9]

166

This is a crystal that was naturally untwinned. Naturally untwinned means the crystal has no twin boundary defects as it has grown. De-twinned is something where you physically remove the twin by applying pressure.

Anyway, so this was a naturally untwinned crystal and the only type of defect that one expects in this crystal are the oxygen vacancies. I started doing temperature sweeps instead of field sweeps because I thought field sweep is a more dynamic process. In changing the field, you are trying to push the flux lines in (or out). I wanted to keep the density of flux lines constant and, instead, vary the thermal energy and the pinning strength by changing the temperature.

What I came up with is a wonderful feature. First of all, I did get the turnaround feature of the soft-rigid transition, which was exciting. The second thing I noticed was there were some kinks in the squares.

[Transparency 10]

This is just a plot of the transitions from there and this is a plot of an empirical melting curve. The locations of the kinks are also shown here. It's apparent that the predominant transition seen here is not the melting but rather the soft rigid transition in the flux lattice system as was first seen by Hucho and Levy.

[return to Transparency 4]

The melting curve in this temperature range has a behavior like this. I said before that many features are enhanced. This gap is about 1 gauss. The gap between the H_{c1} line and the lower branch of the melting curve is about 1 gauss.

[Transparency 11]

Next, comes twinned crystal and obviously there are some features over here. A reasonable background due to the transducer and the threads has been subtracted.

There is an onset of a transition here and there is a different kind of transition here. When I plot this first onset of the transition, what I found are points like this and a fit, which coincides remarkably with dependence of H_{c2} on temperature. What is remarkable is this sample is characterized by other techniques. The T_c came out to be 93.8K. In these experiments, we sweep the temperature down or up and the thermal lag is about 0.4K.

If I add that 0.4K to this, I get the T_c back. The $H_{c2}(0)$ is 261T and essentially is the H_{c2} at zero Kelvin. That number is within ± 10Tesla of many published results. That was one of the first incidents when I thought, okay, maybe I am seeing H_{c2} in all these first set of transitions.

The slope dH/dT of this curve at T_c is a little off. Here it is -5.6 Tesla/Kelvin compared the reported number of -4.2 Tesla/Kelvin. One reason for this difference might be because I am looking at a very small field range and few data points. Nevertheless, it is interestingly close.

[Transparency 12]

The next is if I plot where this attenuation is kind of getting to a minimum point. If I plot those points, I end up with a fit that goes as $(1 - t)^2$ and this is not a mean-field type temperature dependence. It is a totally different kind of temperature dependence. This is the kind of temperature dependence that the melting curve has.

The next choice was to verify all these things, doing something else. How am I doing in time?

DR. BASS: You have a couple of minutes.

DR. DASGUPTA: May I show something without submitting the transparencies? (Laughter)

[Transparency 13]

I am going to skip all those things, partly because there are some other labs and other people involved. It is not classified but maybe there are some important things involved.

The same sample was characterized using susceptibility and that is a technique where you look at magnetization and that is very useful for an effect called peak effect. Peak effect is very closely associated with melting of flux lines.

Doing susceptibility work, what we found was that there is a re-entrant behavior of this peak effect. The only reason I asked for that permission is because this is not published and other people are involved with this work. The most important thing is that right where I am finding the melting with ultrasonic technique and that's where we also see there is melting and peak effect from susceptibility. I can also find H_{c2} from susceptibility results. The temperatures and everything else just match perfectly. I have no reason to doubt the ultrasonic results on YBCO to be melting and the other one to be to onset of superconductivity.

[Transparency 14]

I will finish by showing you -- I will take just a couple of minutes -- this is for you (Moises), for a long time you kept on telling me, why don't you just put it parallel to the c-axis and do it? I did it, not for YBCO, because the crystals are in some other lab, but for a BSCCO crystal. Once again, these broad peaks are all due to thermally activated motion of flux lines.

It is there in YBCO, also, and there are some results on that. Beyond these broad peaks BSCCO has a much larger flux-liquid region than YBCO, so I am not surprised that this peak is actually a little on lower temperature side compared to YBCO before attenuation goes down.

Once again, if I plot this transition, the first thing I do is just plot it and then try to fit it. The best fit that I get, once again, is melting transition. The good thing to come out of this is a factor called c_L, which is a Lindemann factor for melting. It comes out to be 0.18. According to melting theory, it should be between 0.1 and 0.2. I am happy with the number.

The thing that does not come out right is in this fit is the reduced temperature t (T/T_c). Here it gives me a T_c of 89, but I know that this sample has a T_c of 95. I never did experiments with H parallel to the c-axis before, so I really need to repeat these experiments again and more carefully before a conclusive argument can be made.

[Transparency 15]

To conclude, yes, sampled CW can be the ultrasonic technique for looking at small high-T_c crystals until Jay comes out with his RUS or RUS-like technique. The good thing about ultrasonics, or even this technique, is that there are minimum external perturbations; I control what the induced current is going to be and I can keep it minimum. It is also possible to look at the bulk elastic properties of the flux lines. That is something I started doing recently.

DR. BASS: We have run out of time and will have to stop. Thank you.

Resonance Acoustic Concentration of Suspended Particles for Optical Discrimination of Aerosols

Gregory Kaduchak and Dipen N. Sinha
Los Alamos National Laboratory

Copies of the transparencies used during this presentation were not available at the time of printing. Please contact the author if you would like to obtain copies of the transparencies.

Abstract

Acoustic concentration of aerosols has received much attention over the past several decades. Typical concentration devices rely on acoustic levitation techniques to localize particles near the nodal planes of an acoustic standing wave. The standing wave field is typically very dependent upon spatial alignment of the system components and often requires moderate to high input drive power levels. The present research describes an extremely simple acoustic levitation device for use in optical discrimination of aerosols in air. It is constructed from a hollow, cylindrical piezoelectric which has been slightly modified to increase the amplitude of the radial surface displacements. An acoustic standing wave is created on the interior cavity of the shell where particle concentration takes place at the nodal planes of the field. This levitation device is extremely useful since it requires no alignment, power consumption is small (< 1 Watt), and hollow PZT cylinders are commercial-off-the-shelf items.

Transcript

DR. KADUCHAK: A few weeks ago, when we got the first agendas out, I was sitting in a pretty nice position, speaking a bit earlier in the afternoon, but a little bit of shuffling went on, a little bit of jockeying, the dust cleared, and here I am. I figured I would kind of take this to my advantage. I started thinking I am at the end, it is two long days, you look out in the audience, what are you going to see? Probably glassy eyes and a lot of coffee and things like that.

I figured probably the best thing to do is actually make a talk that is simple, colorful, no equations, just something that is fun, just some fun physics and some fun things to look at it, and that is really what this is about.

[Transparency]

First we will start with the motivation. Unfortunately, if you look at the first thing on here, it is not really that fun a topic. The application for what we are doing is we are actually looking at biological and chemical aerosol detection.

In light of the recent political events and just the current activities in the world, this is actually a very serious question, and I will probably spend one or two transparencies on this, then we will just jump out of that and go to the applications, where the actual neat stuff is coming out.

The "what" is low power -- I am going to have it underlined here, because this is what we are really after, acoustic concentrator. We are going to use an acoustic resonator to give us some type of particle positioning inside a chamber.

It is going to be extremely low power, much lower power than I have actually ever seen done, and we will give reasons as to why this is necessary. The main point, as I said, is this is going to be simple, there is a very simple main point to get out of this.

We are going to get a low-cost, low-power, off-the-shelf acoustic levitator, acoustic concentrator, et cetera. We are going to give you the ability to concentrate and levitate drops, et cetera, for about a hundred bucks, no alignment, no nothing, very simple.

[Transparency]

The actual application we are looking at is a rapid early-detection system. You have some kind of biological release. Unfortunately, they do not look like this, because then we would not need a detection system, but you have something released over the horizon, it is coming, you are over here, you want something between the release and yourself. You want something to tell you, hey, something is coming, you need to go through counter measures, you need to stop this thing, you need to take cover, one of the above.

If you think of typical systems, for example, one of the typical systems today is what do you do when you sample the air. You take a large sample, take the particles out, the aerosols, et cetera, put it in solution and do a mass spec on this. It is very time-consuming, very cost-consuming.

In the battlefield it is probably a feasible thing that you could do. You could have somebody taking samples continuously, doing mass spec, et cetera, but in situations, say, like federal buildings, things along these lines, if you are looking in the future, this really is not a feasible system.

What we are working on is a trigger system. It is not going to classify what is coming at us, it is going to say, hey, it is time to start looking, it is time to open up all the bags or to start looking in other directions, or start doing these types of time-consuming events.

[Transparency]

I do not really want to dwell too long on this one. This is a project that brings several divisions of Los Alamos together. Obviously the life sciences people are going to be looking at the biological particles and how these things interact, what types of things we can see. There is us. We are going to be doing an acoustics part on here. There are people doing the laser work and the optical classification.

The actual device that we are looking at, the sizing, or the actual classification of the particles or detection is going to be done optically. Here is a cartoon of a laser cavity. For the device that we are looking at it is going to have a UV intercavity laser. We are going to be sending particles or aerosols straight down through the laser cavity.

Through there we are going to look at the light scattering. You are going to get sizing information. Typical biological particles range anywhere from 1 to 2 to 3 microns, so you start rejecting dust and things like that just from those lines.

When you start looking at scattering intensities, if you look relative to the forward direction at the intensity of 135° to the intensity of 90° coming off of these particles you can actually see that there is a separation due to the indices of refraction of these things. Here is typical dust -- this is a silica -- and these are some typical spores that you see, so we have separation there.

Another way of trying to detect these things is from fluorescence. With the UV excitation of these things, there is a group of _____ acids and proteins that fluoresce in the 200-400-nm range. Typical biotoxins are typically proteins, so we have that working for us in that direction.

Typical viable cells, or live cells, or cells that have been living at one time have things contained within the fluorescent to visible, so there is another piece of information that you can throw in and start separating things out. This is really how the optical discrimination is going to start looking at things, telling you what is about to happen or telling you that you do have an aerosol in the air.

[Transparency]

This is a cartoon of the apparatus. As I said before, you are going to have some kind of laser cavity, it is going to do some type of sorting by refractive index, sizing, fluorescence, several things like that.

What we are going to do, we are going to try to concentrate the particles before they enter the laser cavity. You might ask why, and it is this second bullet down here. Typically, in an aerosol release, you are looking at about one bioagent particle per liter of air.

You are looking at driving air through a very small cavity. The quantity of air it would take to get just one bioparticle, or the flows that you need to get good statistics on these particles you cannot blow through there.

What we are working on right is trying to acoustically concentrate these particles and actually have the air flowing into some device, concentrate the particles to one region of that chamber, run only that portion of particles through the laser cavity, and then all the extra air can go out, so now we can start getting flow rates where we can start getting sizable statistics with these bioparticles.

That is where the low power comes in. The vision for this type of device, when you start thinking about it, is a smoke detector for biological agents. You need something lightweight, you need something portable, and you need something battery-operated, hopefully, in the end, something that you can put in the air-duct systems of a federal building, for instance.

[Transparency]

Now we can put all that stuff aside and just talk about what we have done here. This is our first prototype concentrator here, or resonator. It is a simple piece of PZT. I believe it is a 5400, 3/4" diameter, 3/4" length. Notice we have gone through no pain in mounting this thing. You have typical pins here, you do not want to interrupt any moments, or anything, but we just threw in a typical ring stand and we are just holding it there.

[Transparency]

If you plot what the cavity should look like, these are plots for the n = 3 axisymmetric mode of cavity, where we have 3 nodal lines for the pressure going out from the center. Here is the center of the cavity, with the exterior cavities here. This is the absolute value of the pressure within the cavity and you can see we have 3 dark blue lines here that correspond to the pressure nodes of the resonant field within the cavity.

If you look at the force, positive numbers here correspond to forces going outward radially. Negative numbers are forces coming in. If you really look at this, you end up with 3 stable equilibrium positions within the cavity. They form 3 concentric rings that correspond to the pressure nodes of the cavity.

This is all well and good, levitation, concentration -- I dare not even guess how long that has been around. If you were to just drive it at this frequency, the odds are you are going to get nothing. I know we cannot, we cannot just drive it at some radium over the cavity and actually be able to concentrate or levitate particles.

[Transparency]

The kicker, or the simple physics, or the thing that, in hindsight, looks really simple is if you look at the electrical impedance of the cylinder that I just showed you (and this especially we picked out), the breathing-mode resonance is here, 66.7 kHz. What you have to do is match that resonance to the resonance in the cavity. Once you do that, then we can start coupling energy in the cavity in accomplishing this feat.

[Transparency]

Here it is. Here is this thing, a little 3/4", $100.00, non-alignable, perfectly aligned cavity resonator. We have 2 drops levitated.

[Transparency]

If you go back to this plot right here, gravity is playing a role in this, going in a downward direction. Here are your 3 stable equilibrium positions, here are your lowest potential energy places.

[Transparency]

This corresponds to a drop at the bottom of the center ring and here is the middle ring right here. If you look at the drop diameter, it is a little less than a meter. Gravitational force they were counteracting is about 1.59 dynes and the drive power is a minimum of 115 mW.

For typical resonators or concentrators you are talking at least watts, possibly 10 W or one or two orders of magnitude below that, and we do not even have to align the thing. The drive level on this is about 1.9 V to do this, so this is extremely efficient.

There are actually 3 drops levitating in the chamber. Due to anti-symmetries and stuff, when we get water in the machine, we can levitate as many as 6 drops from those different positions.

174

[Transparency]

Now, the thing to wake you up is the video. We have this resonator going -- I am going to explain the video before I show it and you will get a lot more out of it -- we have the cylinder, and we have modified this cylinder, we have put a crack in it. The question is, why is that?

If we put a drop of water down here, we have the pumping action of the crack, it is sucking water in and pumping it out. In the outward pump we are atomizing that into an aerosol. What you are going to see in the video is an aerosol being pumped up to the cavity and out of the cavity and that is what we are going to be trying to concentrate or show that we can get concentration going on with this.

The photography is going to be a simple Schlieren setup, so we are going to be taking something low contrast and making it high contrast. It is going to be a simple thing with mirrors, camera, light source, et cetera.

DR. SMITH: Will the fluid be flowing into the cylinder from the crack or being held in the cylinder?

DR. KADUCHAK: Both. It is going to be symmetric about the pump point.

DR. SMITH: And where is the fluid going to come from?

DR. KADUCHAK: We put a drop in the bottom of the cavity. [The video is shown]

What you can see here, here are the mounting brackets. We have the cylinder right here, it is the same one you see in the pictures. We have 3 nodal lines. You can see one out here toward the center. We have the middle one and then we have the center one. You can see these 2 here, that is where the actual aerosol is agglomerating, falling down to the lowest energy position and we are levitating drops there.

As you see, this is a drive voltage of about 2 V on here. If you look at the transient time, this is real time that you are seeing. Just as soon as the aerosol is pumping up into the cavity we are concentrating to the nodes. As you were asking, this is the pump action coming out of the bottom of the crack, and then we have the pump action going up to the top.

You will see occasionally these things will get too big, fall out, and then they will be re-emitted back into the cavity. The frequency is a little bit over 66 kHz.

[Transparency]

One question that should be really bothering you at the moment is temperature. What we have done is we have taken this crystal and we have matched its resonance to some cavity

resonance at some temperature. If we change the temperature, both frequencies are going to change, both of the cavity due to the change of the sound speed in air and the crystal itself.

So we devised a little experiment. We popped the crystal in an oven. We are going to measure the voltage and currents across the crystal. We have taken a standard sample. We are going to levitate that sample, start dropping the voltage and wait for this thing to fall out and then say that is the minimum voltage or power required to levitate that sample at a certain position and record that as a function of temperature.

[Transparency]

If you plot these things out, it is not quite as wide as we want to go, but you see pretty well over 30° C we are driving these things -- this is a 2.5 dyne sample (I do not know the exact number, it is tens of milligrams) -- under 200 mW, which is extremely efficient for a device like this.

As you can see, as we change the temperature, we actually do have to change the driving frequency for the crystal to be able to do this, as you would expect.

[Transparency]

Finally, what are we working on right now? I do not have any results from this for the moment, but I will just give you the spiel on it. Okay, everything was fine and dandy, we got 3 rings, we got low power -- that was the big thing -- so we have accomplished a lot already.

The question is, now that you have 3 rings, how do you get the stuff into a laser cavity? We want something, possibly axially. From the 3 rings right now you can envision you are going to have to come up with some type of flow tubing or something to channel things into the cavity and filter what is flowing through that tube.

One thing that we are working on to try to alleviate that is if we can get an axial node or drive things to the axis of this cylinder and match it up this way. There is only one mode for the cylindrical cavity where we do this, and that is the M = 1 mode; that would be to say that where we have 2 halves of the cylinder going out of phase.

If you look at the time-averaged force for that, you do have a restoring force to the center all 360° around the axis. This is the only mode you can do it in. Currently we are working on getting crystals to match up with this mode.

[Transparency]

176

In summary, as I said, we are going to keep it simple. You can make a low-powered, low-cost, off-the-shelf, air-coupled acoustic levitation device from a simple PZT cylindrical resonator for about a hundred bucks.

Thank you.

DR. GAITAN: What is the actual dependence of the 3 ring modes? What is the dependence of the sound field? Are these cylindrical in shape?

DR. KADUCHAK: They are cylindrical in shape, it is a Bessel function, it is symmetric.

DR. GAITAN: Bessel function radially?

DR. KADUCHAK: Radially, correct.

DR. SMITH: And they are constant?

DR. KADUCHAK: We do see effects from the end, we do have a restoring force back toward the center.

DR. SMITH: _____

DR. KADUCHAK: Right, there is a stable position. If you look halfway down the diameter of the cylinder, that is the stable position in the axial direction.

DR. LEVY: You concentrate a bubble right in the center of a cylinder. Is it different, water from air, and that is why you are having difficulty getting it --

DR. KADUCHAK: One thing is the huge impedance mismatch between water and air. It is extremely hard to couple energy into the air medium. That would probably be the most basic thing that you are looking at. The other thing is the power limitations to do that.

DR. LEVY: You need a lot more power to just get the axial mode as opposed to the 3 modes?

DR. KADUCHAK: It depends. It is almost a different problem with what you want to drive. Yes, I am not sure exactly how to go on the axial modes in water versus these 3 modes in air. The reason why we are able to do this is we take advantage of the focusing effect of the cylindrical cavity to give us those rings.

DR. LEVY: I remember _____ giving us demonstrations where he would smoke a cigar and then put some sound waves on it and the whole thing would drop down. That is not what you want to do. You can coalesce smoke from --

DR. KADUCHAK: Right, yes. The particle concentrations we are looking at are very low. As far as something like that, I do not think that is a problem.

DR. ISAAK: In your demonstration, what kind of aerosol were you using and how did you create the aerosol?

DR. KADUCHAK: It was water.

[Transparency]

As I showed, the cylinder itself, if you look at the bottom of the cylinder, we had a crack going axially down it and it served as a pump, so we put a drop of water right in the bottom of the cylinder and the pumping action sucked it in and then it atomized it and popped it out. It was the vibration of the cylinder itself that gave us the aerosol.
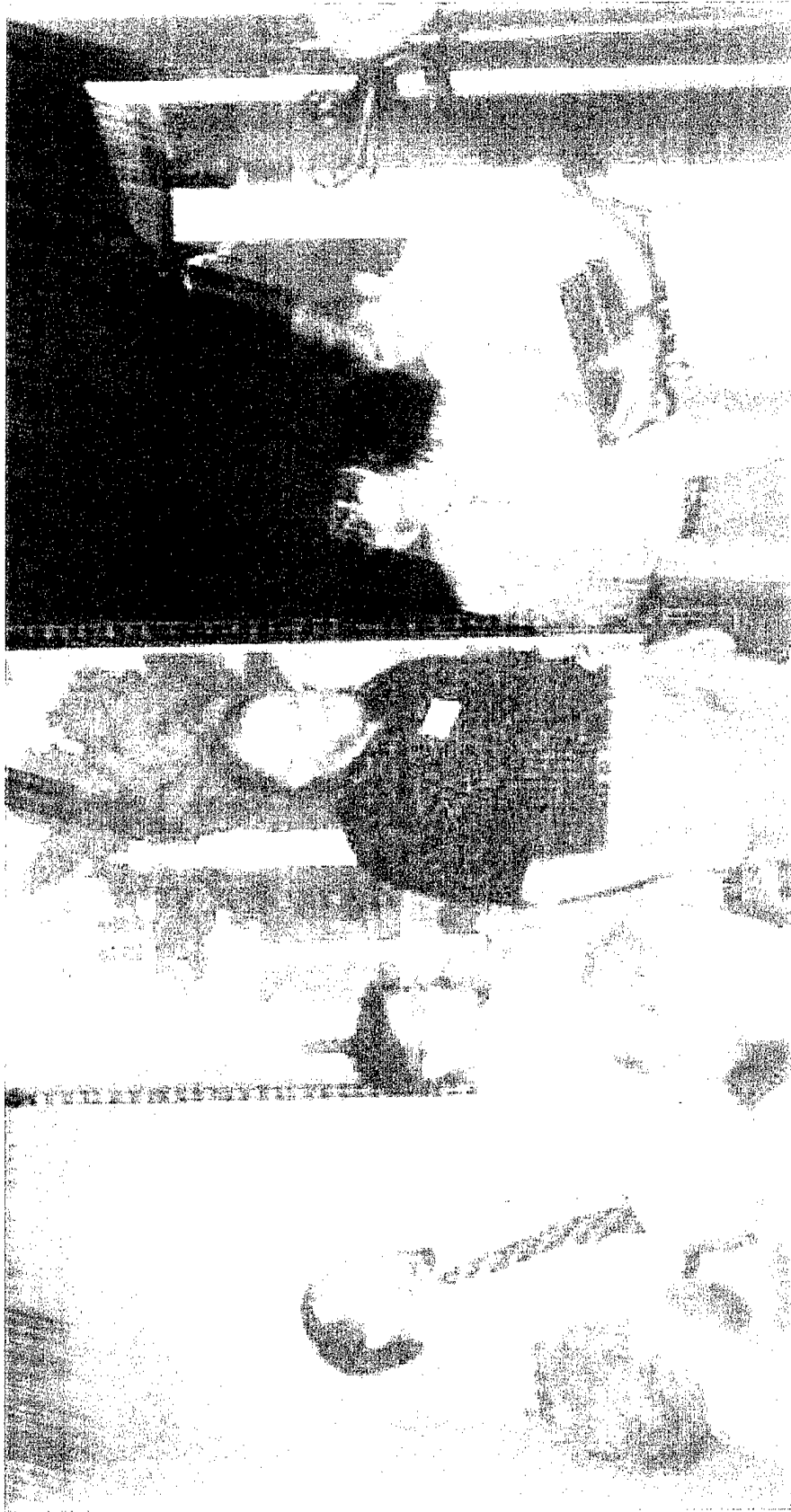
Thank you.

SPECIAL APPENDIX
BRIEF BIOS, PHOTOS AND SIGNIFICANT PAPERS

HONORING

ORSON L. ANDERSON
HAROLD H. DEMAREST JR.
ICHIRO OHNO

FOR

THEIR CONTRIBUTIONS TO THE DEVELOPMENT OF
RESONANT ULTRASOUND SPECTROSCOPY
AND RELATED RESONANCE TECHNIQUES
FOR DETERMINING THE ELASTIC
PROPERTIES OF SOLIDS

Logan Hargrove and the honorees, Ichiro Ohno, Harold Demarest, and Orson Anderson, look on as Henry Bass reads the citation presented to these three distinguished gentlemen. (picture courtesy of Wolfgang Sachse)

ORSON L. ANDERSON

Dr. Anderson received his B.S. (1948), M.S. (1949) and Ph.D. (1951) from the University of Utah. His professional experience began as an Instructor in Mechanical Engineering at the University of Utah from 1950-1951 and he was promoted to Assistant Research Professor of Physics in 1951. He joined Bell Telephone Labs as a member of the Technical Staff from 1951 to 1960. Dr. Anderson then took the position of Manager of the Materials Department, Research Division at the American Standards Research Laboratories until 1963 when he joined Columbia University's Lamont Geological Observatory as a Research Associate in Geophysics until 1964. In 1964 he was promoted to Adjunct Professor and then to Professor of Mineralogy from 1966 to 1971. In 1964, Dr. Anderson took the concurrent position of Professor of Geophysics at the Institute of Geophysics and Planetary Physics and the Department of Geophysics and Space Physics at the University of California in Los Angeles. In 1971 he left Columbia University to become a full-time Professor at UCLA until 1974 at which time he became the Director of system-wide Institute of Geophysics and Planetary Physics and held this position for 15 years. Dr. Anderson presently serves at UCLA as a Professor in the Department of Earth and Space Sciences and as a Researcher in the Center for Physics and Chemistry of the Planets.

He is a member of the American Ceramic Society, American Physical Society, and American Geophysical Union. In 1954, Dr. Anderson received the Meyer Award from the American Ceramic Society. He served as Editor-in-Chief of the Journal of Geophysical Research from 1967 to 1973. Dr. Anderson was the founding chair of the Committee on Mineral Physics of the American geophysical Union.

Dr. Anderson's research areas include mechanical properties of solids, equations of state, high pressure physics, acoustics, and physics of the earth's interior.

Under the respectful eyes of Logan Hargrove, Dr. Anderson receives his citation from Henry Bass. (picture courtesy of Wolfgang Sachse)

Rectangular parallelepiped resonance—A technique of resonance ultrasound and its applications to the determination of elasticity at high temperatures[a]

Orson L. Anderson

Center of Earth and Planetary Interiors, Institute of Geophysics and Planetary Physics, University of California at Los Angeles, Los Angeles, California 90024-1567

The experimental work on resonance ultrasound, especially using the technique called rectangular parallelepiped resonance (RPR) is reviewed and summarized. The work on high-temperature (at temperatures beyond the Debye temperature) measurements of elastic constants is emphasized. Several applications of this high temperature work are described, including thermal equations of state, the determination of thermodynamic functions, and the determination of the bulk modulus at temperatures beyond experimental capability.

PACS numbers: 43.88.Ar, 43.35.Yb

INTRODUCTION

The work of Warren Mason, magnified by his acoustical research group at the Bell Telephone Laboratories in the 1950s up to the 1970s, greatly enhanced the use of ultrasonics to investigate the properties of solids, liquids, and polymers. The necessary experimental techniques of acoustics were substantially advanced by Herbert McSkimin, and Hans Bömmel of Mason's group, and the accompanying theory was correspondingly advanced by Robert Thurston, also of Mason's group. Contributions at all levels were made by Mason himself. The history of these great advances in physical acoustics is reflected in articles in the series of books on Physical Acoustics, published by Academic Press and edited by Mason.

The writer was greatly stimulated by Mason and others during apprenticeship in Mason's group (1951–1963), and as a result has been doing experimental work in physical acoustics ever since. The applications are to geophysics, which is essentially concerned with a class of dense minerals, thought to comprise the rocks of the earth's crust and mantle.

The kinds of measurements made on these minerals—namely, the measurements of the elastic constants at high temperatures and pressures—help to refine the details of composition of the earth, and the thermal structure of the earth, from the seismic profiles of the earth using theoretical approaches that have been refined over the years in geophysics of planetary interiors.

Since the 1950s, it has been known that in order for these experimental measurements to bear on the geophysical problem of the earth's structure, the elastic constants must be measured at temperatures above the Debye temperature θ. The temperature of the earth's mantle, for example, is in the range $1.3 < T/\theta < 1.5$. The value of θ for interesting mantle mineral components is in the range of 700–1200 K, so information on elastic constants was needed well above 1000 K.

For several decades after 1950, elasticity measurements on mantle minerals were made using improved modifications of experiments essentially pioneered by McSkimin, but the upper temperature limit fell short of the geophysical requirement, so progress in geophysics of the earth's interior was limited by extrapolations of the data. Until 1980 about 800 K was the limit achievable by ultrasonic measurements of the elastic constants. One of the reasons for this limit was that the amplitude of the surface wave of the solid at the transducer is somehow not sufficient to stand out from the thermal noise at 800 K and above. Another difficulty was the adverse effect of high temperature on the glues and on the transducers, ordinarily used in ultrasonics.

A solid in a resonance mode has large surface amplitudes in oscillatory motion and for this reason resonance techniques allow the determination of elastic constants at temperatures above 800 K. For example, ceramists have made measurements on single crystals up to 900 K (Ref. 1) and on polycrystals up to 1450 K (Ref. 2) using bar resonance.

The obtaining of elastic constants by the resonance of spheres, cubes, and parallelopipeds is a relatively new field, which is called resonance ultrasound. A brief history of this field will now be given, emphasizing two techniques of resonance ultrasound.

I. RESONANCE ULTRASOUND

A. Resonant sphere technique (isotropic)

Sato and Usame[3] solved for the characteristic equations for the free oscillation of a homogeneous elastic sphere, and tabled the nondimensional frequencies of the fundamental and high modes of torsional and spheroidal oscillations. One of their results was to relate the shear sound velocity v_s to frequency f_s and diameter d by means of

$$f_s = a_s v_s / \pi d. \tag{1}$$

The parameter a_s was related to the modes, which are of two sorts: spheroidal and toroidal. The spheroidal oscillations are related to the value of Poisson's ratio, whereas the

toroidal oscillations are not; thus only one value of Poisson's ratio satisfies the sequence of measured spheroidal resonance frequencies. Knowing the diameter of the sphere and the sequence of the resonances, the shear velocity v_s can be determined from (1); and with Poisson's ratio all the elastic constants of the sphere are determinable. The experimental application of the Sato and Usame theory to small spheres was developed by Fraser and LeCraw[4] and named by them the "resonant sphere technique" (RST).

Soga and Anderson[5] used the RST to determine the thermal history of tektites, by measurements up to 850 K.

When the lunar rocks were returned to the earth for measurement in the early 1970s, it was found that the ultrasonically measured sound velocity through the rocks was unbelievably low, with v_s less than 1.7 km/s. (It was later found that meteoritic impact in a vacuum condition riddled the minerals with tiny cracks that impeded the soundwaves.) Meteoritic impact also made liquid splashes of glass, and in the lunar soil many spherules of quenched glass were subsequently found. These spherules of glass had no history of microcracks, and were of the same composition as the lunar rocks. Selecting the best spherically shaped samples of the lunar glass spherules (less than 2 mm in diameter) the fundamental resonance modes were found in the 6-MHz range using the Sato and Usame theory. For these lunar glasses the sound velocities were found to be in the normal range ($\sim$6.8 km/s).[6] Thus it was shown that the extremely low velocity of surface lunar rocks was entirely a texture effect, a consequence of considerable importance in understanding transmission of seismic signals in the lunar crust.[7]

B. Rectangular parallelepiped resonance (RPR)

In the case of a homogeneous sphere, the normal mode frequencies can be found by analytical methods.[3] But the lack of exact solutions to the problem of the free vibrations of an elastic solid of general shape and crystallographic symmetry, held up resonance measurements of elasticity for many years. It was only after the advent of high-speed computers, that the problem could be tackled. It is important to consider the resonances of a parallelepiped, because there is a great advantage in having the free surfaces parallel to principal crystallographic planes.

The first and most important step was taken by Harold Demarest, who was a graduate student in my laboratory at Columbia University during the time the lunar glass spheres were being measured by the RST. As a part of his thesis, he undertook to solve for the resonance modes of an isotropic cube and a cube with cubic symmetry, and he published his results in this Journal.[8] He used the Rayleigh–Ritz numerical technique and integral equations to define fully the free vibrations.

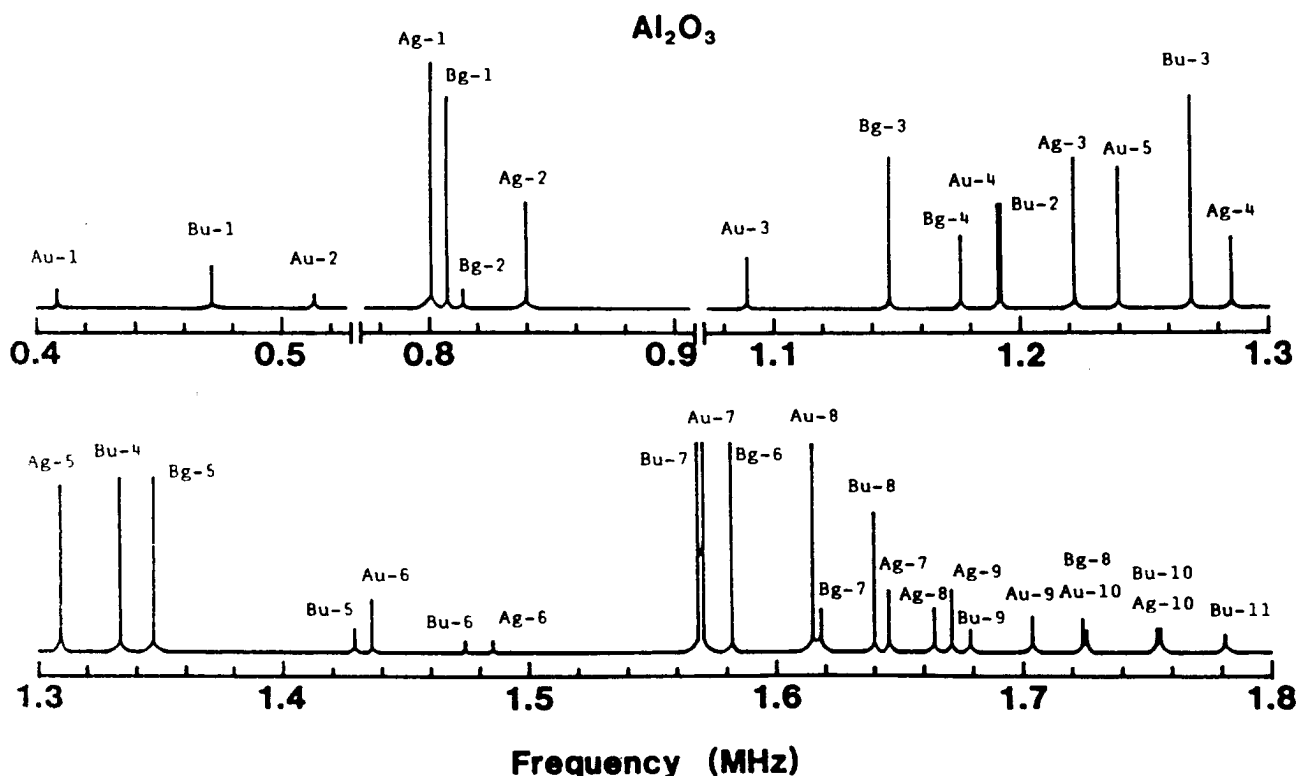Mineo Kumazawa, a visiting scholar from Nagoya University was pursuing ultrasonic measurements of minerals[9]

FIG. 1. The measured frequency spectrum of corundum at 296 K, showing mode identification. After Goto et al.[19]

184

at my Columbia laboratory during the episode on lunar glasses and rocks, and he became interested in Demarest's results. When he returned to Nagoya, he established a laboratory on resonance ultrasound, and he and his students undertook RPR measurements on minerals of low symmetry, but first the theory had to be advanced.

Most subsequent theoretical papers on resonance have adopted Demarest's approach. Ohno, in particular, further developed the theory in sufficient detail to account for orthorhombic symmetry[10] and later trigonal symmetry.[11]

The strategy of RPR technique is to first measure the normal modes of a parallelepiped of a crystal, which is a determination of the entire free oscillations spectrum of the parallelepiped. An example is the spectrum of Al_2O_3 (see Fig. 1). One initially assumes a set of elastic constants c_{ij}; and using the theory appropriate to the space group of the crystal one computes the frequencies of the crystal under study. The values of the elastic constants are perturbed until the theoretical spectrum matches the measured spectrum. Figure 2 shows what is considered as a good match of the theoretical and measured spectra. Thus the determination of elastic constants by resonance ultrasound requires that all the details of the measured spectrum be understood.

The approach is essentially that of spectroscopy, and as in that field, mode identification is often difficult. Also, as in spectrocopy, group theory is essential to understanding mode identification, and the most useful application of group theory to the RPR technique was made by Mochizuki.[12]

C. Application of RPR (high temperature and low temperature)

The RPR method is particularly suited to measurements of elasticity at high temperature, since no glues are used to connect the transducers to specimens; instead the corner of the parallelepiped lightly touches the transducer with a force of a few grams. Thus the Q of the measuring system is minimized. As a consequence, the measured spectrum closely approximates the theoretical spectrum of a specimen suspended freely in space, with no external contacts. In fact, the Q of the individual modes of vibration is typically 20 000 even at the highest temperatures (1500–1700 K), demonstrating that the effect of the external measuring system on the measured frequency spectrum is insignificant. The evidence of these high Q values is demonstrated by the sharpness of the modes in Fig. 1. No special crystal orientation with respect to the parallelepiped axes for the RPR mode measurement is necessary for frequency measurements. However, different orientations produce relatively different amplitudes.

Geophysical applications require high temperatures, and the advance to adequate higher temperatures took three distinct steps.

The Nagoya group, led by Mineo Kumazawa, after establishing the theory for computing modal frequencies for cubic and orthorombic symmetry,[10-13] began measurements between room temperature and 400 °C for MgO (Ref. 13) and the series Mn_2SiO_4, Fe_2SiO_4, and Co_2SiO_4 (all with
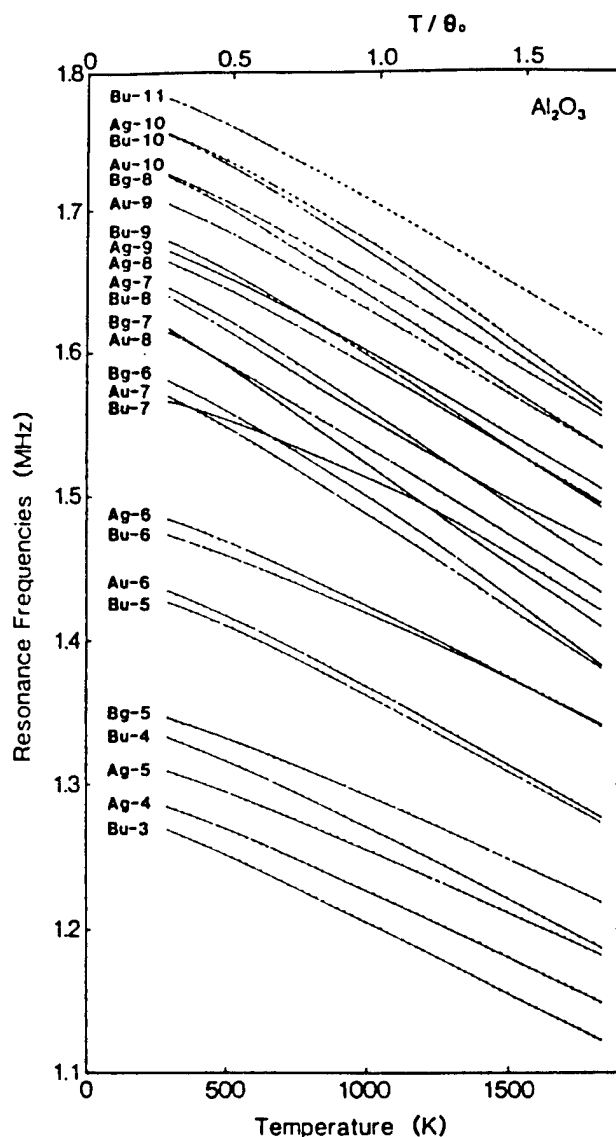

FIG. 2. The first 39 modes of corundum, showing measured and computed frequency spectra at 296, 1000, and 1825 K. The agreement between measured and calculated modes is considered sufficiently good to fix the elastic constant. After Goto et al.[19]

orthrohombic symmetry).[14] Forsterite, Mg_2SiO_4, was measured between -190 °C and 400 °C.[15] Pyrope garnet was measured between -190 °C and 80 °C.[16]

Over the next decade, students from Kumazawa's laboratory then returned one by one to my laboratory, now at UCLA, for a series of measurements on mantle minerals for the purpose of pushing the temperature measurements higher. In the 1983–1985 period, MgO_2SiO_4 (Ref. 17) and pyrope garnet[18] were measured up to the vicinity of the Debye temperature. It became apparent that the temperature dependence of physical properties changed at the Debye temperature, and it was deemed urgent to design an apparatus that allowed measurements far in excess of the Debye temperature (e.g., above 1500 K). The problem required that the transducers be separated by a thermal barrier from the specimen.

185

Kumazawa's former student, T. Goto, while working in my laboratory successfully designed an apparatus[18] in which the transducers are separated from the specimen by long, thin, alumina buffer rods, thereby allowing the transducers to remain near room temperature while the specimen is heated to temperatures limited only by creep of the buffer rods. With this instrument, a number of new measurements were made extending the temperature range up to 1800 K. They included Al_2O_3 (Ref. 19), Mg_2SiO_4 (Ref. 20), and MgO (Ref. 21).

A schematic diagram of the high-temperature RPR apparatus is given in Fig. 3. The specimen is not glued to the transducer, but only lightly touches at its diagonal corners. The transducers, to which the thin steel plates are glued, are attached at the other end of the buffer rods. The steel plates act as electrodes for the transducers.

In this experiment, $BaTiO_3$ ceramic transducers were used because the temperature of the transducers remains near room temperature.

As illustrated in Fig. 3, a cylindrical electrical furnace with one end closed was employed. This furnace is quite appropriate to provide the heating system without giving any shocks to the buffer rods that gently hold the specimen. The use of this system of buffer rods enabled us to use a one-end-closed furnace.

Pt13%Rh wire of 1-mm diameter was used as a resistance heater for heating the specimen up to ~1800 K. The temperature of the specimen was measured by the Pt–Pt13%Rh thermocouple placed near it. The temperature was manually controlled by a transformer within ± 1 K and low T and within ± 2 K and high T. The force holding the specimen upright between the transducers was exerted by a chemical balance. The mass on the scales was held to about 5 g.

Quite independently of the work on RPR done in Nagoya and UCLA, Al Migliori and his colleagues at Los Alamos National Laboratory, using what is called here RPR, discovered that resonance ultrasound was very useful for measuring the elastic constants of superconductors $(La_{1.86}Sr_{0.14}CuO_4)$ at or near the superconducting transition temperature.[22] This work is especially valuable to determine elastic mode softening. They indeed found that the elastic constant C_{66} had a substantial softening in the neighborhood of the transition temperature (about 223 K).

The resonance of superconductor specimens requires some special attention to detail because of the smallness of the specimen, and the Los Alamos group made some significant advances in experimental technique. They eliminated the Q of all parts of the measuring system, including the cable, which led to a substantial improvement of the signal-to-noise ratio. They also have automated the signal processing, enabling important interpretations of resonance, which have not been possible to see by manual controls.

The use of resonance techniques using very thin polyvinylidene fluoride (PVDF) piezoelectric films have been described in the paper by J. D. Maynard.[23]

D. The resonant sphere technique, RST (anisotropic)

Recently Mochizuki[24] developed the theory of free oscillations of homogeneous spheres with general anisotropy. Oda et al.,[25] also developed the computer algorithm and programs to evaluate the eigenfrequencies by the Rayleigh–Ritz method. Using these new results, the elastic constants of MgO have been determined,[26] which agree with previous determinations. Isoda et al.,[27] measured the vibrational spectrum of a free oscillating rutile (TiO_2) sphere, and found very good agreement between the observed and computed eigenfrequencies. It now appears that spherical resonance can be developed as a good competitor of rectangular parallelepiped resonance.

An important advantage of the RST technique is that for small specimen spheres are easier to make than a tiny parallelepiped, which must be prepared without chipped edges and corners.

II. EXPERIMENTAL RESULTS OF THE RPR EXPERIMENT

A. Inverting the spectrum for values of C_{ij}

We now discuss typical experimental findings of the RPR method and give examples of the results measured on various solids. The individual modes are measured as a function of T up to the highest temperature possible. Taking corundum, for example, the first 39 modes are each measured up to 1825 K, as illustrated in Fig. 4 (Goto et al.).[19] Note that many measurements are taken along each temperature
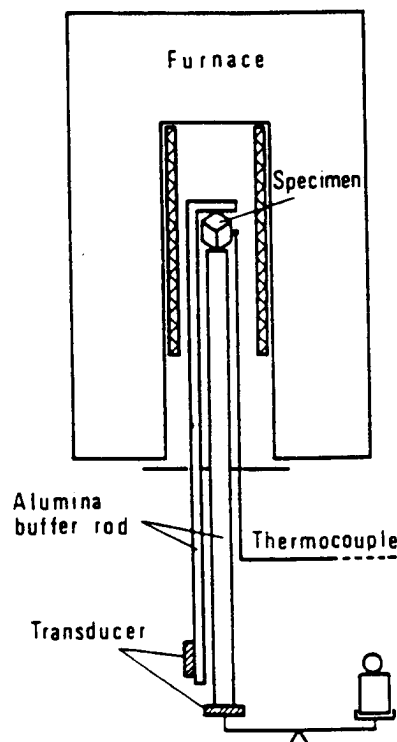

FIG. 3. A schematic diagram of the furnace and buffer rods used for determining the elastic constants above 1000 K. Note the chemical scale used to control the small forces pressing the ends of the parallelepiped into the measuring apparatus. After Gogo and Anderson.[18]
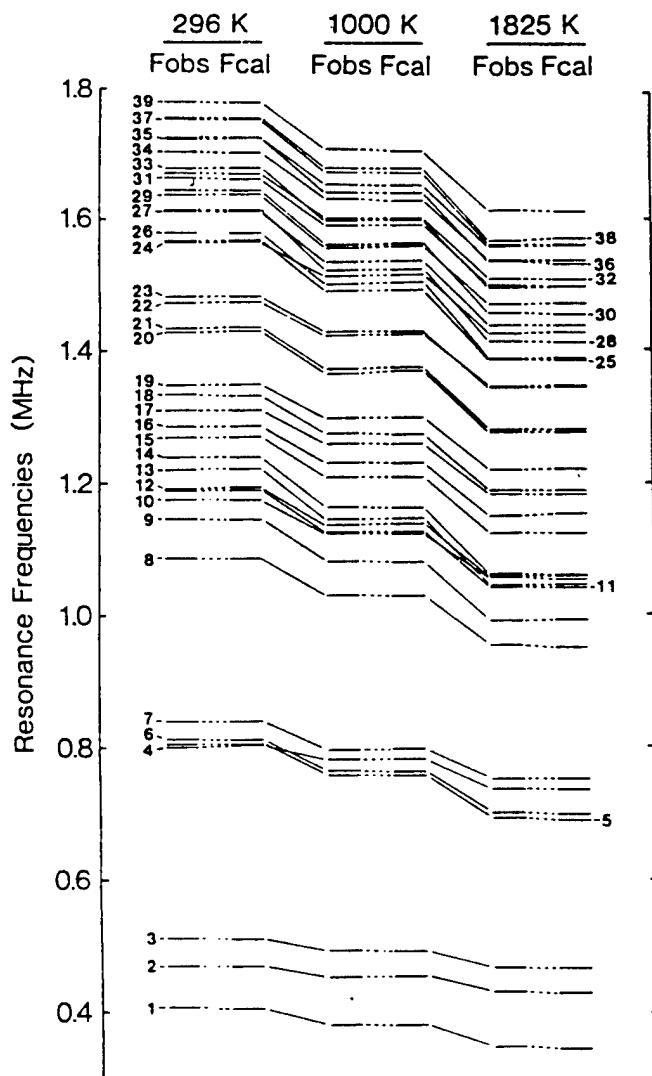
186

FIG. 4. The modal frequencies up to the 39th mode for corundum versus temperature. Each dot represents a measurement.

FIG. 5. The elastic constants of periclase MgO vs T as found by inversion of the frequencies. After Isaak et al.[21]

ue B_T. B_S is easily determined from the elastic constants by standard formulas, once they are known. B_T is found from B_S by a standard thermodynamic formula, provided we have the necessary information on α and C_p, the thermal expansivity and the specific heat. The computed values of B_S and B_T found for corundum are shown in Fig. 6 (Goto et al.).[19]

The so-called intrinsic value of the bulk modulus is $B_T(V = V_0)$ namely, the change of B_T with T at constant V. Its variation with T is important for certain thermodynamic quantities. $B_T(V = V_0)$ is found from the calculus equation

$$\left(\frac{\partial B_T}{\partial T}\right)_V = \left(\frac{\partial B_T}{\partial T}\right)_P - B_T\left(\frac{\partial B_T}{\partial P}\right)_T. \tag{2}$$

curve, so that the temperature derivatives can be carefully defined. Note also that some modes interact or couple, which requires measurements at small increments of T (in this case $T = 25$ K). The inversion of the frequency spectrum at each temperature gives the value of the elastic constants at that temperature. Taking forsterite, for example, the C_{ij} vs T are shown in Fig. 5 (Isaak et al.)[20] up to 1700 K (or $T/\Theta = 2.2$).

A significant point is that the frequency spectrum, that is, the individual values of the modal frequency, does not depend upon the orientation of the crystal undergoing measurement. Therefore the frequency spectrum is determinable from one temperature run. We find that the lines in the spectrum appear to be as sharp at the highest temperatures measured (1825 K) as at low temperatures.

B. The bulk modulus and its temperature derivatives

In many thermodynamic properties we need the bulk modulus, both its adiabatic value B_S and its isothermal value
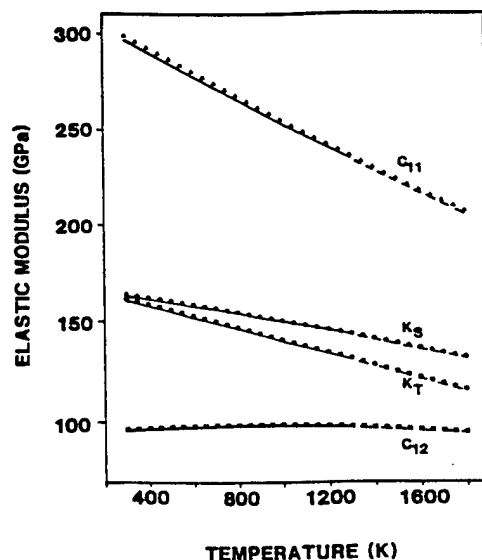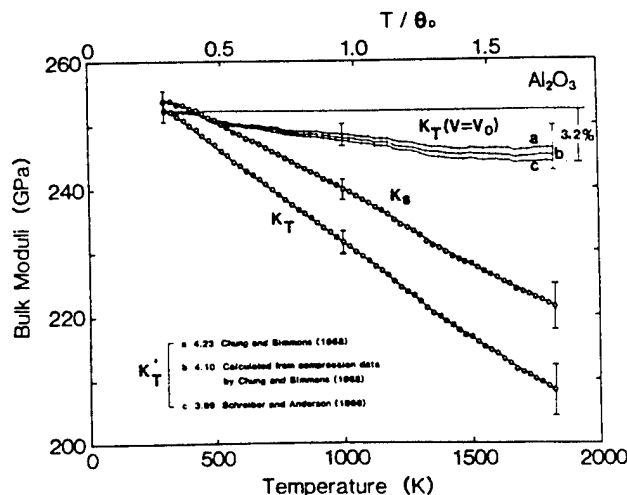
FIG. 6. The isobaric bulk modulus B_S and B_T for corundum, after Goto et al.[19] The isochoric bulk modulus $B_T(V = V_0)$ at high T indicates that $(\partial P/\partial T)_V = \alpha B_T$ is independent of volume.

Thus $B_T(V = V_0)$ can be found from RPR measurements (along with input on α and C_P) by integration of Eq. (2). The difficulty is knowing the value of $(\partial B_T/\partial P)_T$ at the highest measured T of the RPR experiment. The data plotted in Fig. 6 indicate that above the Debye temperature of corundum (1045 K) $(\partial B_T/\partial T)_V$ is very close to zero. The consequences of this will be discussed below. A solid where we know that $(\partial B_T/\partial T)_V = 0$ is NaCl (Yamamoto et al.)[28] because α and C_P are well measured. The data for NaCl are shown in Fig. 7. On the other hand, we are equally sure that $(\partial B_T/\partial T)_V$ is not close to zero for KCl (Yamamoto and Anderson).[29] Therefore, no general conclusion can be made for minerals. Measurements must be made for each mineral.

If $B_T(V = V_0)$ is zero over a wide temperature range, then we know that the interatomic potential is temperature independent.[30] What we have found is that for many solids, even when $B_T(V = V_0)$ is not zero at room temperature it can be zero at high T (above the Debye temperature).

C. Extrapolation technique for B_S

The RPR measurements have shown that a very effective tool for extrapolation of the bulk modulus is the relationship between B_S and enthalpy H. We are finding, as predicted by Anderson[31] that B_S is linear with H over a very wide temperature range. This follows from the idea that at high T, the anharmonic parameter defined by

$$\delta_S = \left(-\frac{1}{\alpha B_S}\right)\left(\frac{\partial B_S}{\partial T}\right)_S, \tag{3}$$

should be independent of temperature. An integration of B_S with T along with the additional assumption that δ_S is independent of T yields the result that B_S is linear with $\int C_p \, dT = H$, whenever αT is small compared with unity. A plot of the results of B_S measured by RPR up to 1800 K for periclase (MgO) against the measured enthalpy is shown by the circles in Fig. 8. This clearly indicates that by using the
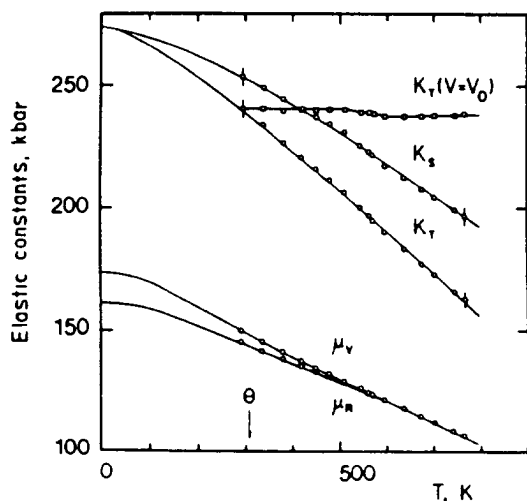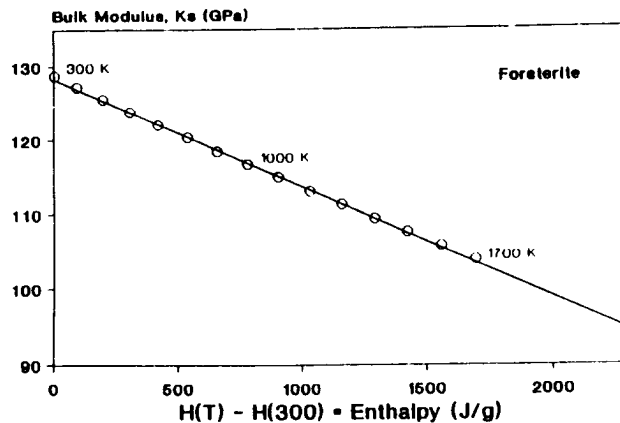
FIG. 8. The relationship between the measured bulk modulus K_r and the measured enthalpy H for Mg_2SiO_4. A good linear relationship exists up to 1800 K. The dotted line draws extrapolation. The arrow indicates the melting condition After Anderson.[31]

reported values of enthalpy (often measured up to 3000 K), the value of B_S can be extrapolated rather safely up to lower mantle temperatures. The physical principle behind this is that anharmonicity will affect both B_S and H to the same degree, so that cancellation of the anharmonicity occurs in the cross plot of B_S and H. Thus uncertainty in anharmonic effects does not hinder this extrapolation of B_S to very high temperatures, near the melting point.[31]

D. The thermal equation of state above the Debye temperature

Of considerable importance is our result that above Θ

$$\left(\frac{\partial B_T}{\partial T}\right)_V = 0, \tag{4}$$

as indicated in Fig. 7. When this is the case, $\alpha B_T = (\partial P/\partial T)_V$ is independent of V, according to the identity

$$\left(\frac{\partial(\alpha B_T)}{V}\right)_T = \frac{-1}{V}\left(\frac{\partial B_T}{\partial T}\right)_V. \tag{5}$$

Thus when Eq. (4) is satisfied

$$\frac{\partial(\alpha B_T)}{\partial V} = 0, \tag{6}$$

since

$$\alpha B_T = \left(\frac{\partial P_{TH}}{\partial T}\right)_V, \tag{7}$$

where P_{TH} is the thermal pressure. Then $(\partial P_{TH}/\partial T)_V$ is not a function of V.[32] The equation of state is thus given by

$$P(V,T) = P(V,0) + P_{TH}, \tag{8}$$

where $P_{TH} = f(T)$. This means that whenever Eq. (4) holds, no pressure correction is required for P_{TH}, which can be determined entirely from high-T measurements at 1 bar.

A great deal of our laboratory effort over a 5-year span has been devoted to showing that, to a very good approxima-

FIG. 7. The isobaric moduli B_S and B_T, along with isochoric bulk moduli $B_T(V = V_0)$ all for NaCl. After Yamamoto and Anderson.[28]

188

tion, P_{TH} is linear with temperature.[33] The latest work on corundum,[19] periclase,[21] and forsterite[20] confirms this correlation, even as high as 1800 K. Thus it is very likely that a general equation of state applicable to single-phase minerals important to Earth geophysics is

$$P(V,T) = P(V,0) + \alpha B_T T, \qquad (9)$$

where we note from Eq. (6) that αB_T is often independent of V. Note that this equation of state dispenses with the requirement that the volume and temperature dependence of the Grüneisen constant be known. It only requires that the product αB_T be known over the volume and temperature field, and as we have seen, αB_T is often independent of both V and T. Since both α and B_T are experimentally measured quantities, this is a very helpful relationship. It should be noted that the product αB_T is equal to the important thermodynamic parameter $(\partial P/\partial T)_V$. Equation (9) is not valid, even as an approximation, below the Debye temperature.

E. The Helmholtz energy computation

When the results of α, C_p, and B_T, measured at high T, are combined, the entropy S can be calculated,[34] by means of the Maxwell identity

$$\left(\frac{\partial S}{\partial V}\right)_T = \alpha B_T. \qquad (10)$$

The detailed calculations for the case of MgO have been made; taking due account of the change of αB_T with T and V,[35] over the temperature range of 300–2000 K and down to the compression $V/V_0 = 0.70$. Of critical importance is the high-temperature behavior of the product αB_T. Figure 9 shows the results of the calculations.

When the results of the calculated entropy and the calculated thermal pressure $(\alpha B_T T)$ are combined with the equation of state, $P(V,T=0)$; computed at absolute zero, the internal energy U may be computed over the correspond-
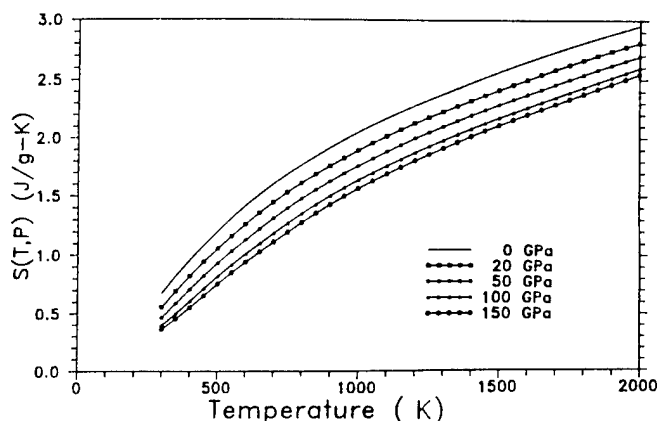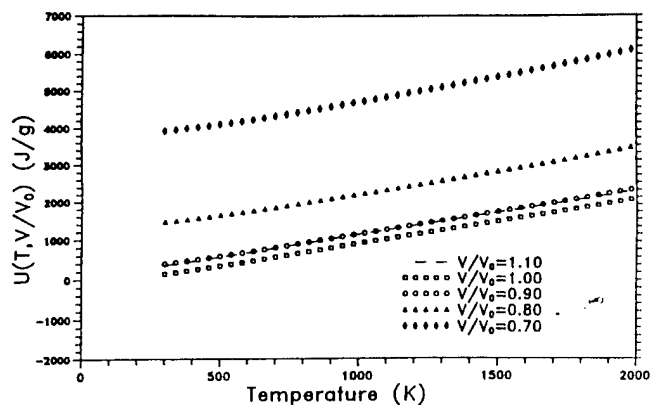

FIG. 10. The internal energy U of MgO over a wide compression and temperature range, as calculated by Anderson and Zou.[34]

ing volume and temperature range by the Maxwell relationship

$$\left(\frac{\partial U}{\partial V}\right)_T = T\left(\frac{\partial P}{\partial T}\right)_V - P, \qquad (11)$$

where, as shown above, $(\partial P/\partial T)_V = \alpha B_T$.

Details of the calculations are described at length in Anderson and Zou.[34,35] Figure 10 shows the results of the calculation for MgO.

FIG. 9. The entropy S of MgO, over a wide pressure and temperature as calculated by Anderson and Zou,[34] using the latest data of K_T measured at high temperature.[20]
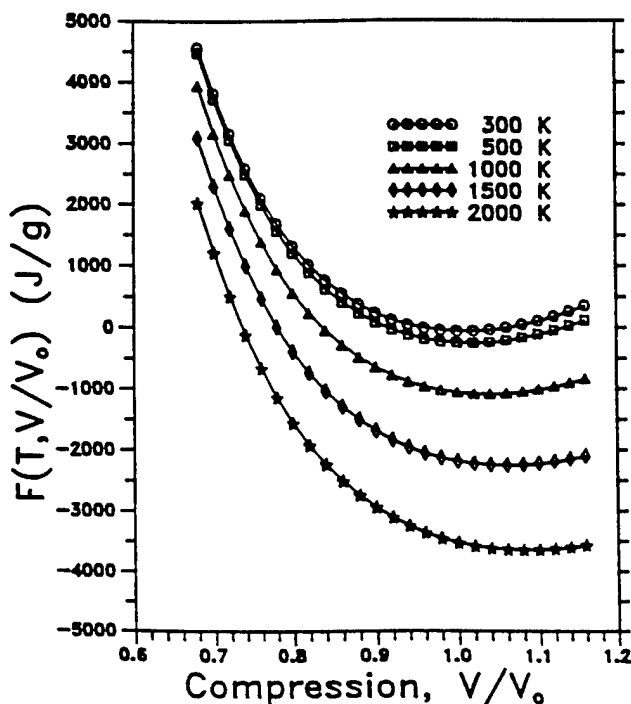

FIG. 11. The Helmholtz energy of MgO over a wide compression range for five isotherms resulting from the entropy and internal energy calculations made by Anderson and Zou.[34]

189

The Helmholtz energy is $F = U - TS$, so that once S and U are calculated, F is easily found. F for MgO is shown in Fig. 11. It is very important to try to compute from experimental data the free energy of a solid over a wide T and V/V_0 range, in order to test the *ab initio* calculations of physical properties of a solid made by theorists. A typical calculation starts with the Schrödinger equation, and by assuming the potential between adjacent atoms, taking due care of the crystallographic symmetry, arrives at the Helmholtz free energy F.[36-39] F is then used to derive mechanical properties versus V/V_0 and T.

We in resonance ultrasound are in a position to compute the Helmholtz free energy from experiments, to test the corresponding values derived by theorists. The most pressing experimental requirements are good determinations of α and B_T at high T; that is, T in ranges well above the Debye temperature.

F. Anharmonicity at high temperature

One of the fruits of the high-temperature measurement of B_S is that a check on the degree of anharmonicity in the solid can be made. By anharmonicity is meant the departure from classical theory: for example, the departure from the Dulong and Petit limit of C_V.

Table I shows the high-temperature thermodynamic data for MgO. The first five columns are the measured data. The last two columns are values of the calculated parameters C_V and γ.

The Gruneisen parameter γ is computed from

$$\gamma = (\alpha B_S)/\rho C_P; \qquad (12)$$

and the specific heat at constant V, C_V, is computed from

$$C_V = C_P/(1 + \alpha\gamma T). \qquad (13)$$

We see that above 1.1Θ, $(\partial C_V/\partial T)_P$ is negligibly small, so that there is no detectable anharmonicity insofar as specific heat is concerned.

On the other hand, we can detect a slowly descending value of γ with T. Consequently, $(\partial\gamma/\partial T)_P$ is not zero (though close to it).

TABLE I. Laboratory input data for MgO. The density ρ is calculated from the volume thermal expansivity α. It is taken from Suzuki.[40] The adiabatic bulk modulus B_S is taken from Isaak et al.[20] The source of the data on specific heat C_P is taken from Garvin et al.[41]

T (K)	ρ (g/ml)	α (10^{-6} K^{-1})	B_S (GPa)	C_P (J g^{-1} K^{-1})	C_V (J g^{-1} K^{-1})	γ
300	3.585	31.2	163.9	0.928	0.915	1.54
350	3.579	33.9	163.1	1.006	0.988	1.54
400	3.573	35.7	162.3	1.061	1.038	1.53
450	3.566	37.2	161.5	1.100	1.073	1.53
500	3.559	38.4	160.7	1.130	1.098	1.53
550	3.552	39.3	159.9	1.154	1.117	1.53
600	3.545	40.2	158.9	1.173	1.132	1.54
650	3.538	40.8	157.9	1.190	1.143	1.53
700	3.531	41.4	157.1	1.204	1.153	1.53
750	3.524	42.0	156.0	1.216	1.160	1.53
800	3.516	42.6	155.1	1.227	1.166	1.53
850	3.509	43.2	154.1	1.237	1.171	1.53
900	3.501	43.8	153.1	1.246	1.175	1.54
950	3.494	44.1	152.1	1.254	1.179	1.53
1000	3.486	44.7	151.1	1.262	1.181	1.54
1050	3.478	45.0	150.0	1.269	1.184	1.53
1100	3.470	45.6	148.9	1.276	1.185	1.53
1150	3.462	45.9	147.7	1.282	1.187	1.53
1200	3.454	46.5	146.7	1.289	1.187	1.53
1250	3.446	46.8	145.6	1.295	1.189	1.53
1300	3.438	47.1	144.4	1.301	1.190	1.52
1350	3.430	47.7	143.2	1.306	1.190	1.53
1400	3.422	48.0	142.0	1.312	1.191	1.52
1450	3.413	48.6	140.8	1.318	1.190	1.52
1500	3.405	48.9	139.7	1.323	1.191	1.52
1550	3.397	49.2	138.4	1.329	1.192	1.51
1600	3.388	49.8	137.3	1.334	1.191	1.51
1650	3.380	50.1	136.2	1.340	1.192	1.51
1700	3.371	50.4	134.9	1.346	1.193	1.50
1750	3.363	51.0	133.8	1.352	1.192	1.50
1800	3.354	51.3	132.7	1.358	1.193	1.50
1850	3.346	51.9	131.7	1.364	1.192	1.50
1900	3.337	52.2	130.7	1.370	1.194	1.49
1950	3.328	52.8	129.7	1.377	1.193	1.49
2000	3.319	53.3	128.7	1.384	1.194	1.49

[1] W. E. Tefft, J. Res. Natl. Bur. Stand. 70A, 277 (1966).
[2] N. Soga and O. Anderson, J. Am. Ceram. Soc. 49, 355 (1966).
[3] Y. Sato and T. Usame, Geophys. Mag. (Japan Meteorological Agency, Tokyo) 31, 15 (1962).
[4] D. B. Frazer and R. C. Lecraw, Rev. Sci. Instrum. 35, 1113 (1964).
[5] N. Soga and O. Anderson, J. Geophys. Res. 72, 1733 (1967).
[6] E. Schreiber, O. L. Anderson, N. Soga, N. Warren, and C. Sholtz, Science 167, 732 (1970); E. Schreiber and O. L. Anderson Science 168, 1579 (1970).
[7] N. Warren, O. L. Anderson, N. Soga, Geochem. Cosmochem. Acta Suppl. 3 3, 2877 (1972).
[8] H. H. Demarest, J. Acoust Soc. Am. 49, 768 (1969).
[9] M. Kumazawa and O. L. Anderson, J. Geophys. Res. 74, 5961 (1969); M. Kumazawa, J. Geophys. Res. 74, 5973 (1969).
[10] I. Ohno, J. Phys. Earth 24, 355 (1976).
[11] I. Ohno, S. Yamamoto, O. L. Anderson, and J. Noda, J. Phys. Chem. Solids 47, 1103 (1986).
[12] Ei Mochizuki, J. Phys. Earth 35, 159 (1987).
[13] Y. Sumino, J. Ohno, T. Goto, and M. Kumazawa, J. Phys. Earth 24, 263 (1976).
[14] Y. Sumino, J. Phys. Earth 27, 209 (1979).
[15] Y. Sumino, O. Nishizawa, T. Goto, J. Ohno, and M. Ozima, J. Phys. Earth 25, 377 (1977).
[16] Y. Sumino, and O. Nishizawa, J. Phys. Earth 26, 239 (1978).
[17] Y. Sumino, O. L. Anderson, and T. Suzuki, Phys. Chem. Min., 10, 38 (1983).
[18] T. Goto and O. L. Anderson, J. Sci. Instrum. 59, 1405 (1988).
[19] T. Goto, O. L. Anderson, I. Ohno, and S. Yamamoto, J. Geophys. Res. 94, 7588 (1989).
[20] D. Isaak, O. L. Anderson, and T. Goto, J. Geophys. Res. 94, 5895 (1989).
[21] D. Isaak, O. L. Anderson, and T. Goto, Phys. Chem. Min. 16, 704 (1989).
[22] A. Migliori, W. M. Visscher, S. Wong, S. E. Brown, J. Tanoka, H. Ko-

Harry telling tales on Orson and Ichiro. (picture courtesy of Wolfgang Sachse)

HAROLD H. DEMAREST, JR.

Dr. Demarest received his B.A. (1969) from Reed College, his M.A. (1971) from Columbia University and his Ph.D. (1974) from University of California at Los Angeles. His professional experience began as a Postdoctoral Scholar in Geophysics at UCLA from 1974 to 1975. He then joined the University of Chicago as a Research Associate in Geophysics until 1979 when he moved to Oregon State University to serve as an Assistant Professor of Geology. In 1983, Dr. Demarest left Oregon State to begin work as President of Astro Research, Incorporated.

He is a member of the American Association for the Advancement of Science, American Geophysical Union and Sigma Xi.

Dr. Demarest's research areas include physical properties of rocks and minerals, geophysics, application of statistics to geological and geophysical problems, elasticity and equations of state.

.

Cube-Resonance Method to Determine the Elastic Constants of Solids.

HAROLD H. DEMAREST, JR.

Lamont-Doherty Geological Observatory of Columbia University, Palisades, New York 10964

The Rayleigh-Ritz method of eigenvalue approximation is used to obtain a solution for the free vibrations of an elastic solid. The resonant frequencies of an isotropic cube, calculated by this method, agree with the frequencies of the Lamé modes, for which an exact solution is possible, up to eight significant digits. Experimental measurements of the 13 lowest-frequency modes of a cube of fused quartz are all within 0.5% of the results computed by using the elastic constants determined by another method. These constants differ from the elastic constants determined directly from the experimental frequencies by less than 0.2% for the shear modulus and by less than 0.003 for the value of Poisson's ratio. The cube-resonance method of elastic constant determination is also applicable to substances of more general crystallographic symmetry.

INTRODUCTION

Many methods have been devised to measure the elastic constants of solids. The utilization of resonance methods has been limited by the lack of exact solutions to the problem of the free vibrations of an elastic solid of general shape and crystallographic symmetry. Most resonance methods are either limited to special cases, such as a bar or plate in which one or two dimensions are vanishingly small in comparison to the others, or involve some rough approximation. An exception is the method of sphere resonance.[1] Since the problem of the free vibrations of an isotropic sphere can be solved exactly, the elastic constants of small isotropic specimens can be determined quite accurately from experimentally measured vibration frequencies. A method based on the resonance of a cube has been proposed.[2] The problem of determining the vibration frequencies of a free cube cannot be solved exactly,[3] however, and previous attempts at using the Rayleigh-Ritz technique to study the free vibrations of cubes and parallelepipeds have not been very accurate.[2,4] Recent work[5] has shown that this technique, when used properly, can yield accurate results. The method of elastic constant measurement described here has all the advantages of the method of sphere resonance. In addition, preparation of the specimen is easier, and there is no obstacle to using this method on nonisotropic single-crystal specimens.

I. FREQUENCY DETERMINATION

Integral equations which define fully the free vibrations of an elastic solid are developed by means of the calculus of variations. The equations are then restated in matrix form to permit an approximate determination of the displacement functions and frequencies of the normal modes.

From Hamilton's principle, it is known that the free vibrations of an elastic solid will correspond to a stationary Lagrangian. Here the Lagrangian is

$$L = \tfrac{1}{2} \int \int \int \left[\rho \dot{u}_i \dot{u}_j g_{ij} - \tfrac{1}{4} c_{ijkl} (u_{i,j} + u_{j,i})(u_{k,l} + u_{l,k}) \right] dV,$$

(1)

where ρ is the density, u_i is the vector displacement, c_{ijkl} is the elastic constant tensor, and g_{ij} is the dynamical metric tensor; $g_{ij} = 1$, where $i = j$, and 0 otherwise. The integration is over the volume of the solid, and the comma denotes partial differentiation: $u_{i,j} \equiv \partial u_i / \partial x_j$. The summation convention applies: when two subscripts are repeated in a product, summation with respect to that subscript is understood.

The fact that the Lagrangian is stationary is expressed by replacing u_i in Eq. 1 by $u_i + \epsilon \eta_i$, where ϵ is a small parameter and η_i is an arbitrary perturbation subject to

the boundary conditions that $\eta_i=0$ at $t=t_1$ or t_2. Then

$$\frac{\partial}{\partial\epsilon}\bigg|_{\epsilon=0}\int_{t_1}^{t_2}\frac{1}{2}\iiint[\rho(\dot{u}_i+\epsilon\dot{\eta}_i)(\dot{u}_j+\epsilon\dot{\eta}_j)g_{ij}$$

$$-\tfrac{1}{4}c_{ijkl}\cdot(u_{i,j}+u_{j,i}+\epsilon\eta_{i,j}+\epsilon\eta_{j,i})$$

$$\times(u_{k,l}+u_{l,k}+\epsilon\eta_{k,l}+\epsilon\eta_{l,k})]dVdt=0. \quad (2)$$

Taking into account the symmetry of g_{ij} and c_{ijkl}, we get

$$\int_{t_1}^{t_2}\iiint[\rho\dot{\eta}_j\dot{u}_jg_{ij}-\tfrac{1}{4}c_{ijkl}(\eta_{i,j}+\eta_{j,i})$$

$$\times(u_{k,l}+u_{l,k})]dVdt=0. \quad (3)$$

If we integrate by parts, Eq. 3 becomes

$$\int_{t_1}^{t_2}\iiint[\rho\eta_i\ddot{u}_jg_{ij}+\tfrac{1}{4}c_{ijkl}(\eta_{i,j}+\eta_{j,i})$$

$$\times(u_{k,l}+u_{l,k})]dVdt=0. \quad (4)$$

If $u_i=\phi(t)\mathbf{u}_i(x_j)$, and if we let $\eta_i=\Phi(t)\mathbf{u}_i(x_j)$, Eq. 4 becomes

$$\int_{t_1}^{t_2}\phi\Phi\bigg[\frac{\ddot{\phi}}{\phi}\iiint\rho\mathbf{u}_i\mathbf{u}_jg_{ij}dV+\iiint\tfrac{1}{4}c_{ijkl}$$

$$\cdot(\mathbf{u}_{i,j}+\mathbf{u}_{j,i})\cdot(\mathbf{u}_{k,l}+\mathbf{u}_{l,k})dV\bigg]dt=0. \quad (5)$$

Since Φ is arbitrary except at t_1 and t_2, the integral expression in brackets must always vanish. Since $\phi=\phi(t)$ and $\mathbf{u}_i=\mathbf{u}_i(x_j)$, the expression may be separated into two parts:

$$\ddot{\phi}/\phi=\text{const}=-\omega^2 \quad (6)$$

and

$$\frac{\iiint\tfrac{1}{4}c_{ijkl}(\mathbf{u}_{i,j}+\mathbf{u}_{j,i})(\mathbf{u}_{k,l}+\mathbf{u}_{l,k})dV}{\iiint\rho\mathbf{u}_i\mathbf{u}_jg_{ij}}=\omega^2. \quad (7)$$

The first is easily solved:

$$\phi=A\sin\omega(t+\delta), \quad (8)$$

where $\omega=2\pi f$.

Since the $u_i=\phi\mathbf{u}_i$, we may normalize the $\mathbf{u}$ in any way we wish. The most useful way is to make

$$N(\mathbf{u}_i)=\iiint\rho\mathbf{u}_i\mathbf{u}_jg_{ij}dV=1. \quad (9)$$

Then Eq. 7 becomes

$$I(\mathbf{u}_i)=\iiint\tfrac{1}{4}c_{ijkl}(\mathbf{u}_{i,j}+\mathbf{u}_{j,i})(\mathbf{u}_{k,l}+\mathbf{u}_{l,k})dV=\omega^2. \quad (10)$$

and Eq. 1 becomes

$$L=\tfrac{1}{2}\bigg[\dot{\phi}^2-\tfrac{1}{4}\phi^2\iiint c_{ijkl}(\mathbf{u}_{i,j}+\mathbf{u}_{j,i})$$

$$\times(\mathbf{u}_{k,l}+\mathbf{u}_{l,k})dV\bigg]. \quad (11)$$

From Eq. 8,

$$\dot{\phi}^2=\omega^2(A^2-\phi^2). \quad (12)$$

By substituting into Eq. 11, the Lagrangian is separated:

$$L=\tfrac{1}{2}(A^2-2\phi^2)$$

$$\cdot\frac{1}{4}\bigg[\iiint c_{ijkl}(\mathbf{u}_{i,j}+\mathbf{u}_{j,i})(\mathbf{u}_{k,l}+\mathbf{u}_{l,k})dV\bigg]. \quad (13)$$

Since the Lagrangian is stationary, the time-independent part of the Lagrangian (the integral in Eq. 10), must also be stationary when the $\mathbf{u}_i$ are the actual displacement functions normalized according to Eq. 9. Equation 10 can also be written in matrix form. A basis Ψ_i is chosen for the set of all possible displacement functions u_i in the volume V.[6] A matrix Γ_{ij} is constructed to represent the integral I in Eq. 10 so that

$$I(C_i\Psi_i)=C_iC_j\Gamma_{ij}, \quad (14)$$

$$\Gamma_{mn}=\iiint c_{ijkl}\epsilon_{ij}(\psi_m)\epsilon_{kl}(\psi_n)dV, \quad (15)$$

where the strain tensor $\epsilon_{ij}=\tfrac{1}{2}(u_{i,j}+u_{j,i})$. Another matrix is constructed to represent the integral N of Eq. 9 so that

$$N(C_i\Psi_i)=C_iC_jN_{ij} \quad (16)$$

and

$$N_{ij}=\iiint\rho\Psi_i\cdot\Psi_jdV. \quad (17)$$

Then we can express the fact that Eq. 10 is stationary and that the auxiliary condition in Eq. 9 is as follows:

$$(\partial/\partial C_k)[C_iC_j(\Gamma_{ij}-\lambda N_{ij})]=0, \quad (18)$$

where λ is an undetermined multiplier. From this, we get

$$C_i(\Gamma_{ij}-\lambda N_{ij})=0, \quad (19)$$

and multiplying by c_j, we get

$$\lambda=C_iC_j\Gamma_{ij}=\omega^2. \quad (20)$$

The eigenvectors C_i in Eq. 19 give us the coefficients for the expansion of the actual displacement functions u_i in terms of the basis Ψ_j, while the eigenvalues λ give us the actual values for ω^2. Since the infinite-dimensional eigenvalue problem cannot in general be solved, the Rayleigh Ritz method demands that only a finite-

194

Direction of Displacement	$P_i(x_1) \cdot$	$P_j(x_2) \cdot$	$P_k(x_3)$						
x_1	O	E	E		E	O	O		
x_2	E	O	E		E	E	O		
x_3	E	E	O		O	O	E		

Dilation   Torsion

O	O	O		E	E	O		E	O	E
E	E	O		O	O	O		O	E	E
E	O	E		O	E	E		O	O	O

Shear₁   Shear₂   Shear₃

E	E	E		O	O	E		O	E	O
O	O	E		E	E	E		E	O	O
O	E	O		E	O	O		E	E	E

Flexure₁   Flexure₂   Flexure₃

SCHEMATIC I. Parity of Legendre polynomials in Eq. 21 for different symmetry groups. E—even; O—odd.

dimensional set of n basis functions Ψ_j be used. Then n approximate eigenvalues and their associated eigenfunctions are obtained. The approximate eigenvalues will always be higher than the corresponding correct values. If the series of basis functions is chosen carefully, and if enough of them are used, the lower approximate eigenvalues will be quite accurate.

A. The Basis Functions

Since the integral in Eq. 10 is a function of both the displacement and its first derivative, it is important not only that a series of basis functions will converge to any reasonable displacement functions, but also that the series consisting of derivatives of the basis functions will also be convergent. This fact was not fully appreciated by Holland,[4] whose choice of basis functions required that certain derivatives be zero on the boundary. His limited accuracy can be attributed in part to this.

For a rectangular parallelepiped centered at the origin, the basis functions chosen were products of Legendre polynomials:

$$\Psi_{ijkl} = P_i\left(\frac{2x_1}{\tau_1}\right) \cdot P_j\left(\frac{2x_2}{\tau_2}\right) \cdot P_k\left(\frac{2x_3}{\tau_3}\right) \cdot \hat{x}_l, \qquad (21)$$

where $\hat{x}_l$ is the unit vector in the x_l direction, and the τ_l are the dimensions of the parallelepiped under consideration. The same results would have been obtained by use of a power series instead of Legendre polynomials. The main difference is that, for a homogeneous rectangular parallelepiped, the orthogonality of the Legendre polynomials over the interval $(-1,1)$ causes the matrix N to be diagonal, and the eigenvalue problem in Eq. 19 is much easier to solve.

When both the body and crystal lattice have symmetries in common, the displacement functions will reflect these symmetries. If the basis functions are systematically grouped in accordance with these symmetries, the cross terms between functions of different groups in the matrices Γ and N of Eq. 19

vanish. The resulting submatrices can be treated in separate eigenvalue problems and a substantial reduction in calculation time results. This situation was fully understood by Holland.[5]

When the body is a rectangular parallelepiped and the crystallographic symmetry is orthorhombic, the displacement functions will be either symmetric or antisymmetric with respect to reflection in the three mirror planes which bisect the crystal perpendicular to the axes. Eight symmetry groups will contain all possible combinations of these symmetries. Since the even Legendre polynomials are symmetric and the odd ones are antisymmetric, the determination of which functions of the type in Eq. 21 belong to which symmetry group can be done on the basis of parity. This allocation of parities is shown in Schematic I.

The eight groups of displacement functions are named in a way which somewhat describes the fundamental modes of vibration of the group: dilation, torsion, shear (three), and flexure (three). This is somewhat artificial, since the higher harmonic of a mode in one group may be in another. Nevertheless, it is helpful to be able to refer to these groups easily.

When we are dealing with a cube of cubic crystallographic symmetry, the three shear and the three flexural groups clearly yield identical results, and only one of each need be considered. The method by which the remaining four groups can be factored into ten smaller groups is shown in Schematic II.

The following notation is used to refer to particular modes of vibration. A capital letter D, T, S, or F refers to the initial of the group to which it belongs: dilation, torsion, shear, or flexure. A lower case subscript refers to the subgroup: s for symmetric, a for antisymmetric, and d for doublet. An additional integer subscript orders the modes in the subgroup by frequency. If it is necessary to refer to a particular one of the triply degenerate shear or flexure modes, an integer superscript can be used. For example, S_{s1}^1 refers to the lowest-frequency mode in the symmetric subgroup of the shear¹ group.
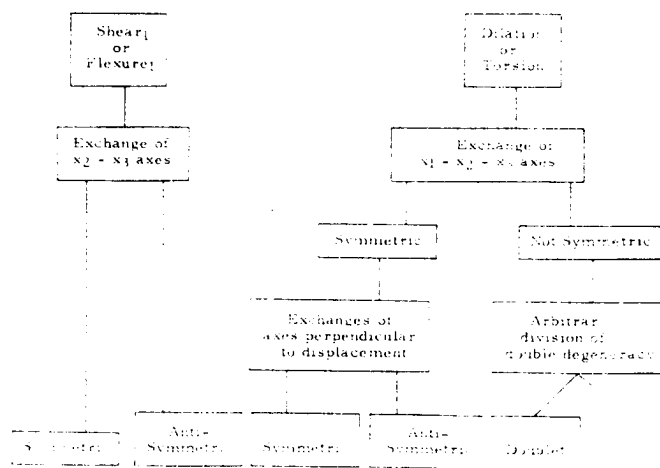
SCHEMATIC II. Grouping of functions for cubic symmetry

TABLE I. Accuracy of frequency determination for the Lamé modes.

Lamé mode	Symmetry	Error (percent)		
		Holland (99 basis functions)	Demarest (30 basis functions)	Demarest (60 basis functions)
1	D_d	0.6	0.01	$2.0 \cdot 10^{-6}$
	D_a	10.0	0.07	$2.0 \cdot 10^{-6}$
2	S_a			0.005
3	D_d	2.0	10.0	0.05
	D_a	4.0		0.002
4	S_a			0.05
5	D_d			1.5

FIG. 3. Cube vibrating in mode T_{d1}.

A computer program was used to calculate the elements of the matrix Γ, determine the eigenvalues, and print out the vibration frequencies. As many as 60 basis functions factored as shown in Schematics I and II were used. The factoring made possible the use of higher order polynomials as basis functions. In the case of the T_a and D_a groups, all combinations of Legendre polynomials up to ninth order could be used, while in some of the other groups, such as F_s, the total order of the three Legendre polynomials could not exceed 10.

B. Accuracy

The accuracy of the calculated frequencies was estimated by comparing the results of the computer
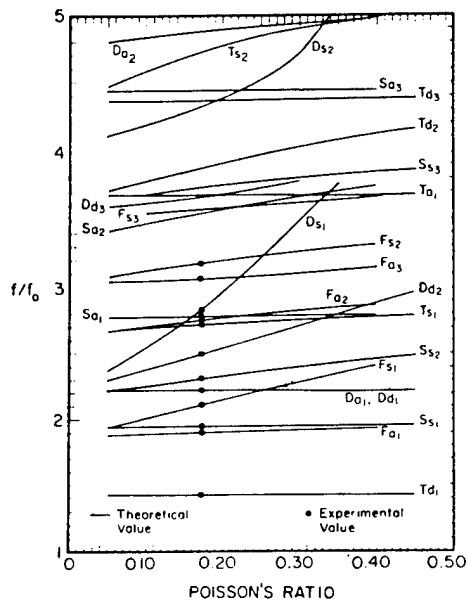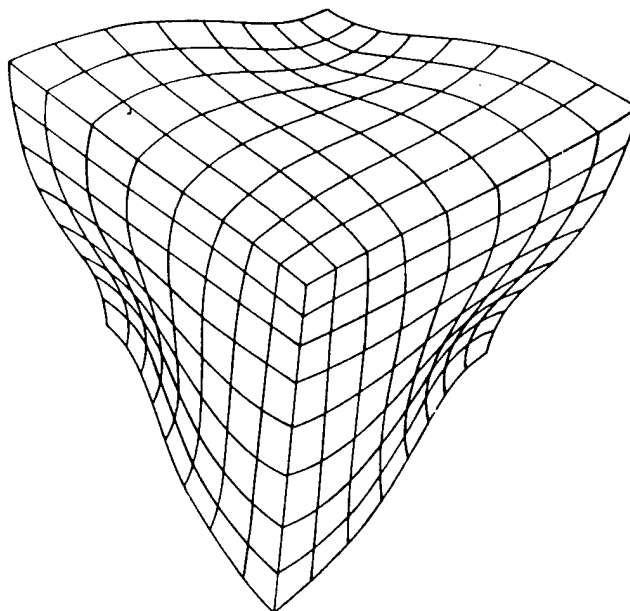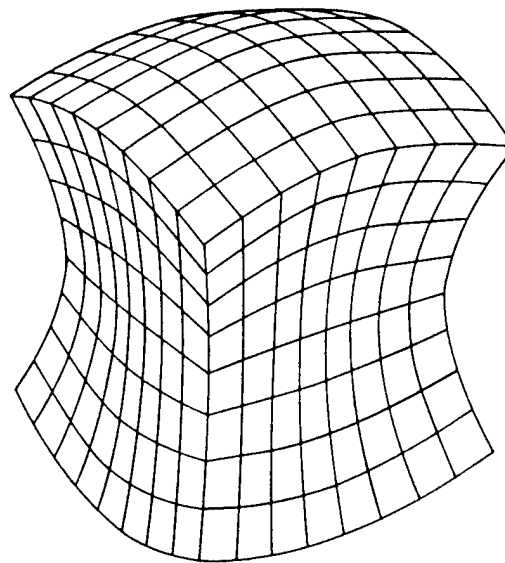

FIG. 1. Normalized frequencies of an isotropic cube as a function of Poisson's ratio.
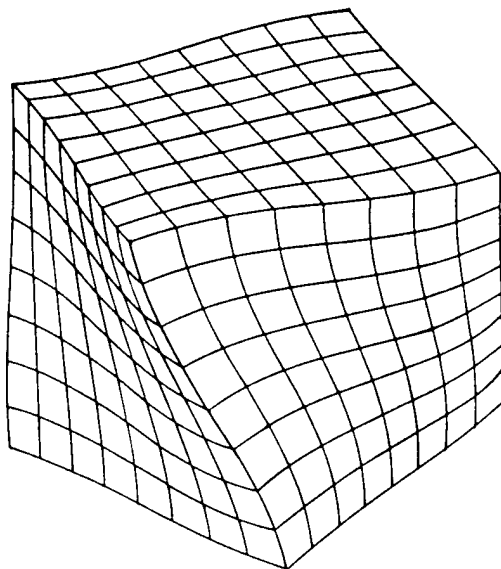
FIG. 2. Cube vibrating in mode T_{d1}.

FIG. 4. Cube vibrating in mode D_{d1}.

196

TABLE II. Physical constants of the fused quartz specimen.

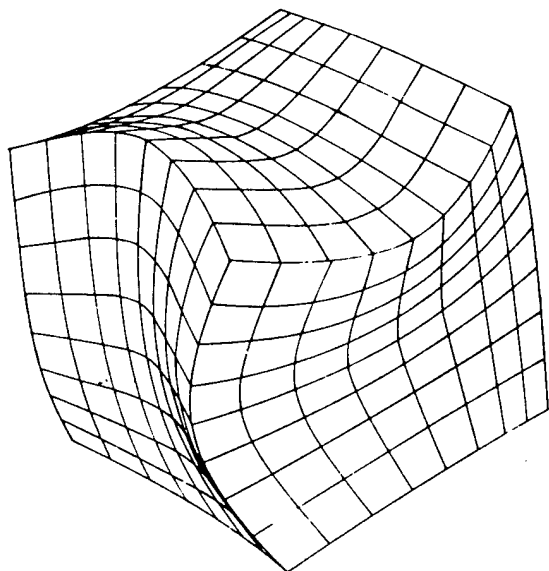| Density	Edge length L	Elastic constants
2.1896 g/cm³±0.037%	0.7828 cm 0.7842 cm 0.7852 cm	$k = 0.2077 \cdot 10^{12}$ dyn/cm²±0.05% $\mu = 0.3115 \cdot 10^{12}$ dyn/cm²±0.03%
	avg. 0.7841 cm±0.16%	$\sigma = \dfrac{3k-2\mu}{2(3k+\mu)} = 0.1697 \pm 0.12\%$

program to the results for the few modes which can be solved exactly, the so-called Lamé modes.[7,8] For comparison purposes, Table I lists the errors in calculating the Lamé modes for Holland,[4] who utilized the factoring

FIG. 5. Cube vibrating in mode D_{a1}.

FIG. 6. Cube vibrating in mode D_{a2}.

of Schematic I and 99 basis functions, and for the present results. In the first case, the factoring of Schematic I and 30 basis functions were used, and in the second case the cubic factoring of Schematic II and 60 basis functions were used. The present results are seen to be significantly more accurate than Holland's. There is no guarantee that the frequencies of the other modes are as accurate as those of the Lamé modes, but it is estimated that the accuracy is certainly no worse than 0.2% for all the low-frequency modes of interest.

Figure 1 is a graph of the normalized frequency

$$f/f_0 = f \cdot \pi \cdot \text{LENGTH} (\rho/c_{44})^{\frac{1}{2}} \qquad (22)$$

for an isotropic cube as a function of Poisson's ratio. From this chart, it is possible to determine the lower vibration frequencies of any isotropic cube. Figures 2–12 are computer-generated drawings showing several of the lower-frequency modes of deformation of an isotropic cube with $\sigma = 0.17$.
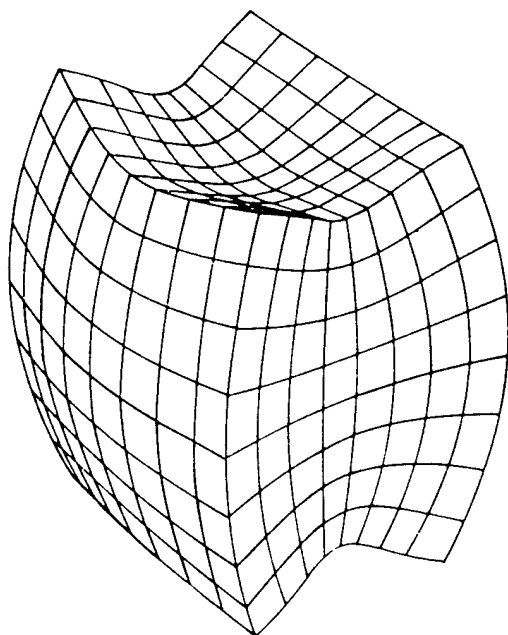
II. EXPERIMENTAL TECHNIQUE AND RESULTS

A. The Specimen

Experimental measurement of the frequency of vibration was performed on a small cube of fused quartz. The specimen had been prepared by slow cutting with a diamond saw with no further polishing. The elastic constants of this specimen had been previously measured by the pulse superposition method by Kumazawa at the Lamont–Doherty Geological Observatory. These values agree well with previously published results.[9] These and the other important physical properties are given in Table II.

B. Experimental Method

The resonant frequencies were measured by the method developed by Fraser and LeCraw[1] and modified by Soga and Anderson[10] for use with small spheres. Both P (dilatational) and S (shear) square-plate transducers were used, in contact with the faces, edges, or corners of the cube. The placement of the specimen between the two transducers was critical. An elastic force on the surface of a vibrating body must raise the frequency. The change in frequency due to the transducers was estimated to range from 0.01% to 0.3%. The

change was a minimum when the pressure of the transducer and the surface area of contact were minimal. For this reason, the transducers were placed in contact with the corners of the cube whenever possible. Figures 2–12 were useful in predicting what type of transducer placement would best detect a particular mode of vibration. For example, the first Lamé modes (Figs. 4 and 5) for which the displacement is primarily perpendicular to the surface and which have no displacement at the
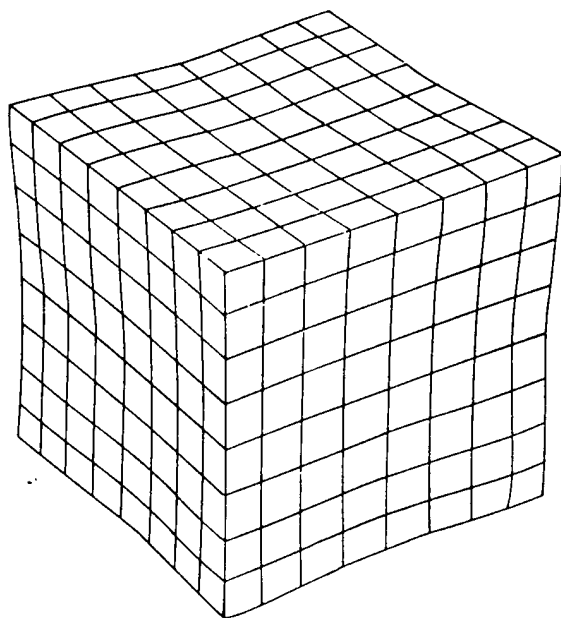
Fig. 7. Cube vibrating in mode D_{s1}.
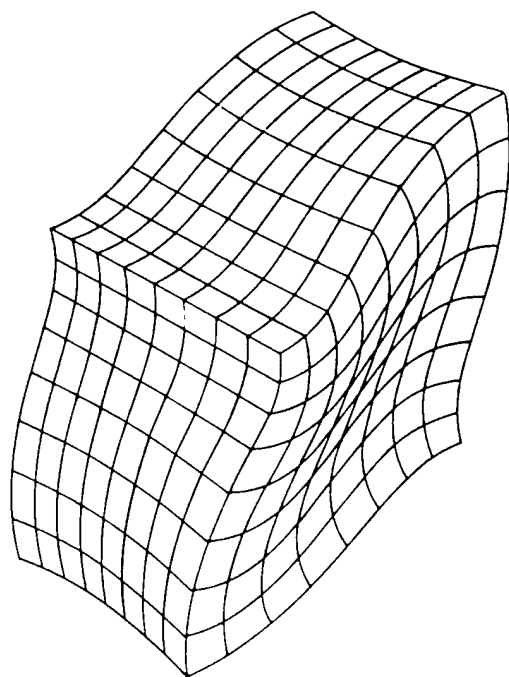
Fig. 8. Cube vibrating mode S_{s}^{1}.
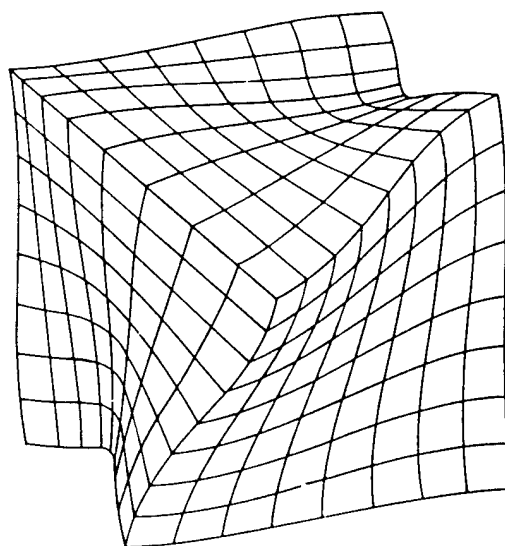
Fig. 9. Cube vibrating in mode S_{s2}^{1}.
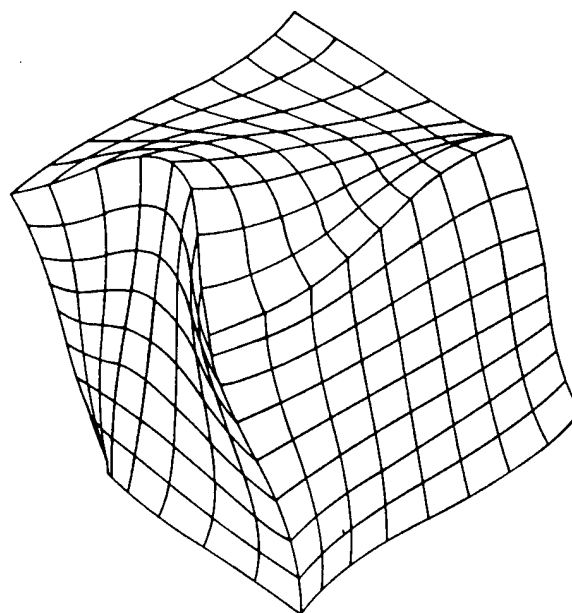
Fig. 10. Cube vibrating in mode S_{a1}^{1}.

corners could be detected only when P transducers were placed in contact with the faces or the edges. The S_{a1} mode could only be detected by a shear transducer in contact with the edge. Figure 10 shows that this mode has a large shear component of displacement along the edge. If the frequencies of an unknown substance were to be measured, mode identification could be expedited by comparing the relative amplitude of a mode under varying transducer placement with the displacement functions in Figs. 2-12.

Table III lists the experimental frequencies and the theoretical frequencies calculated by the computer. Because of the small deviation of the specimen from

Mode	F(theoretical)	F(experimental)	Error (percent)
T_{d1}	0.21886	0.21950	0.29
F_{a1}	0.29178	0.29165	−0.04
S_{e1}	0.29889	0.29874	−0.05
F_{s1}	0.32332	0.32335	0.01
D_{d1}, D_{a1}	0.34053	0.34092	0.11
S_{v}	0.35350	0.35499	0.42
D_{t2}	0.38242	0.38327	0.22
T_{s1}	0.41680	0.41700	0.05
F_{a2}	0.42173	0.42248	0.18
S_{a1}	0.42639	0.42700	0.14
D_{s1}	0.43305	0.43156	−0.35
F_{a3}	0.46969	0.46950	−0.04
F_{s2}	0.48655	0.48652	0.01
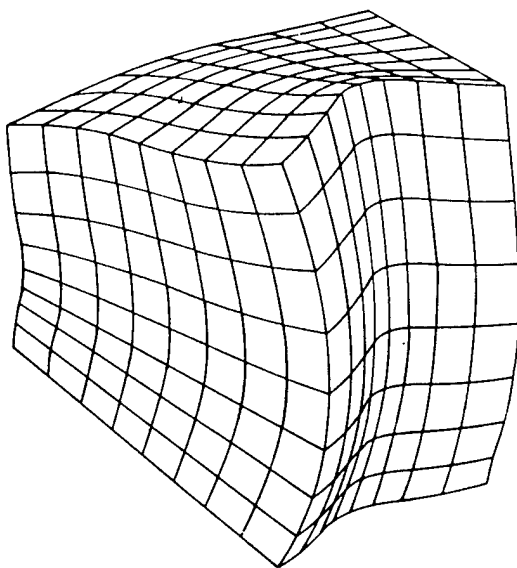
FIG. 11. Cube vibrating in mode F_{a1}.

cubic symmetry, the measured frequencies of the modes which were theoretically degenerate were split into two or three frequencies differing by from 0.1% to 0.7%. In these cases, the average of the several frequencies was taken. The experimental error, determined by comparison with the theoretical computer results, ranged from 0.01% to 0.42%.

III. ELASTIC CONSTANT DETERMINATION

In theory, the elastic constants of the isotropic specimen can be calculated from any experimentally measured frequencies whose theoretical ratio changes with σ. The simplest method is to determine μ from one of the modes which doesn't change with σ and to deter-
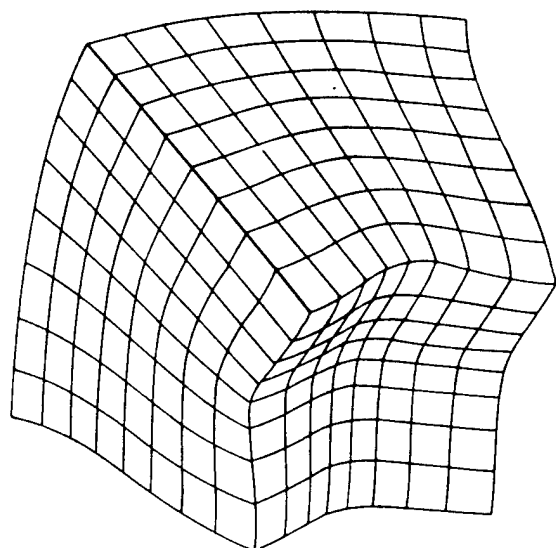

FIG. 12. Cube vibrating in mode F_{s1}.

mine σ from any other mode which does change with σ, using the graph in Fig. 1. Better accuracy can be obtained when all the experimental frequencies are used to determine good average values for μ and σ. The results were $\mu = 0.3117 \cdot 10^{12}$ dyn cm^2 ±0.2% and $\sigma = 0.169 \pm 0.003$. These values are quite close to the more accurate values determined by the pulse superposition method. The accuracy is quite good, much better than would be necessary to make this technique a useful tool for determining the elastic constants of small specimens.

A few calculations were made to discover how difficult it would be to use this method to determine the elastic constants of a substance with cubic symmetry, for which there are three independent elastic constants. It was found that the T_{d1} mode is strongly dependent upon C_{44}, while the Lamé modes are only dependent upon $C' = \frac{1}{2}(C_{11} - C_{12})$, and the breathing mode D_{s1} is primarily dependent upon the bulk modulus. Moreover, there is no further splitting of degenerate modes in the cubic case. It was therefore concluded that the determination of the elastic constants of a cubic substance would still be straightforward, although involving inherently more work than the isotropic case.

The cube resonance method has been shown to be a useful tool for calculating the elastic constants of small isotropic specimens. Since the method is not limited to the isotropic case, there should be many opportunities for its use on substances of more general symmetry.

The identification of particular modes of vibration with measured frequencies will certainly be more difficult in the case of highly anisotropic crystals of general crystallographic symmetry. Except in the isotropic and possibly the cubic case, a method of successive approximation utilizing computer calculations at each step will probably be necessary to determine the elastic constants from the measured resonance data. This procedure will not be prohibitively complicated in most cases of interest, including the orthorhombic case in which there are nine independent elastic constants.

The cube-resonance method is thus more complicated than conventional methods in which the elastic constants are determined from the velocities of plane acoustic waves traveling in various directions in a crystal. In some cases, the advantages may outweigh the disadvantages. Like the method of isotropic sphere resonance,[1,10] cube resonance is applicable when the specimen is too small for velocity measurements to be made easily. Therefore, when only a single small specimen of a crystal of orthorhombic or higher symmetry is available, the method of cube resonance may be the best method available to measure the elastic constants.

ACKNOWLEDGMENTS

[1] D. B. Fraser and R. C. LeCraw, Rev. Sci. Instr. 35, 1113 (1964).

[2] H. Ekstein and T. Schiffman, J. Appl. Phys. 27, 405 (1956).

[3] A. Sommerfeld, Mechanics of Deformable Bodies (Academic, New York, 1950), p. 315.

[4] R. Holland, J. Acoust. Soc. Amer. 43, 988 (1968).

[5] H. Demarest, Bachelor's thesis, Reed College, Portland, Oregon (1969).

[6] These basis functions need satisfy neither the stress-free boundary conditions nor the wave equation within the solid. To solve the problem under constrained boundary conditions, the basis functions must satisfy these boundary conditions.

[7] M. G. Lamé, Leçons sur la théorie mathématique de l'elasticité des corps solides (Gauthier-Villars, Paris, 1866).

[8] R. D. Mindlin, J. Appl. Phys. 27, 1462 (1956).

[9] H. J. McSkimin, J. Acoust. Soc. Amer. 31, 287 (1959).

[10] N. Soga and O. L. Anderson, J. Geophys. Res. 72, 1733 (1967).

ICHIRO OHNO

Dr. Ohno received his B.S. and Ph.D. from Nagoya University, Japan. He currently holds the position of Associate Professor in the Department of Biology and Earth Sciences at Ehime University, Japan.

Dr. Ohno's research areas include mineral physics and crustal structures by gravity measurements. He invented the rectangular parallelepiped resonance method for measurements of elastic properties of tiny crystals.

FREE VIBRATION OF A RECTANGULAR PARALLELEPIPED CRYSTAL AND ITS APPLICATION TO DETERMINATION OF ELASTIC CONSTANTS OF ORTHORHOMBIC CRYSTALS

Ichiro OHNO

Department of Earth Sciences, Nagoya University, Nagoya, Japan
(Received March 29, 1976; Revised August 2, 1976)

A theory was developed on the free vibration of a crystal of rectangular parallelepiped and of general symmetry by extending Demarest's theory of cube resonance. All vibrational modes were classified and described in detail for the case of orthorhombic symmetry. The theory is applied to determine elastic constants of crystals from the resonance frequencies of its free vibrations. The method of numerical analysis of resonance frequency data was studied to derive a practical way of elastic constant determination. As an example, the elastic constants of two specimens of single crystal olivine ($Mg_{1.8}Fe_{0.2}SiO_4$) were determined. The applicability of the resonance method is largely extended by the present theory to the precise determination of elastic constants of single crystals.

1. Introduction

The elastic property of single crystals is one of the most basic data in geological science, solid state physics, material science, etc. Many investigators, therefore, have measured elastic properties of various materials; metals, oxides, halides, semiconducting and dielectric crystals. However, more accurate data on a number of materials are still in need for a basic understanding of solids.

The most difficult problems involved in the determination of the elastic constants is the unavailability of high quality specimens of sufficient size suitable enough for applying the current technique of determining accurate elastic constants. Two possible solutions are (1) the development of crystal growing techniques which would provide larger single crystal specimens, and (2) the development of measuring techniques which would enable the determination of constants using smaller specimens. The present work is concerned with the second approach.

Recent sophisticated techniques of determining elastic constants mostly

355

employ ultrasonic interference methods; pulse superposition, phase comparison, or related techniques (MacSkimin, 1964). The minimum frequency f of acoustic waves needed to carry out measurements by an interference method is generally given by

$$f = nV_p/L$$

where n is the wave number in the round-trip path in a specimen of size L, and V_p is the largest propagation velocity of the acoustic wave. In order to have a coherent plane wave for accurate measurement, there should be at least several tens of wave lengths in the specimen. When $V_p = 8$ km/sec, $L = 1$ mm, and $n = 20$, then f amounts to 160 MHz. Thus, we are forced to use UHF above 100 MHz. At such high frequencies, ultrasonic measurement becomes difficult not only because sophisticated equipment and techniques are necessary, but also the increase in absorption and scattering of ultrasonic waves caused by microscopic defects and inhomogeneities inside and on the surface of the specimen. In addition, several pieces of a specimen have to be prepared in order to determine the acoustic wave velocities for many different orientations.

On the other hand, the resonance method seems to be promising for small specimens. The frequency of the n-th overtone of a specimen, whose representative length is L and shear wave velocity V_s, is generally given by

$$f_n = a_n V_s/L$$

where a_n is a numerical factor, whose magnitude is usually less than 10 for lower vibrational modes. When $V_s = 6$ km/sec, $L = 1$ mm, and $a_n = 3$, then f_n is only 18 MHz. This shows that the use of acoustic vibration in the range of RF is enough to determine the elastic property of specimens as small as 1 mm. Furthermore, only one piece of specimen is sufficient to determine all the elastic parameters, because all information on elasticity is included in a resonance spectrum of one specimen.

Notable progress in the resonance method has been in the development of the sphere resonance technique by Fraser and LeCraw(1964). Soga and Anderson (1967) applied the sphere resonance method to measure elastic and anelastic properties of tektites, however, the sphere resonance method cannot immediately be applied to an anisotropic body. For this purpose, there must be a theory to calculate the resonance frequencies of an anisotropic elastic body.

Demarest (1969, 1971) established such a theory giving the resonance frequencies of a vibrating specimen with cubic symmetry and a cube shape with sufficient accuracy for practical use. He further demonstrated a fine agreement between experimental and theoretical spectra on a fused quartz (isotropic) specimen. Demarest called his technique the "cube resonance"

method. In the present work cube resonance is extended to mean also "rectangular parallelepiped resonance," which is abbreviated as RPR.

The purposes of this paper are (1) to extend Demarest's theory of free vibration to the rectangular parallelepiped of a general symmetry crystal, (2) to describe all the vibrational modes in an orthorhombic crystal, (3) to establish a method of numerical analysis of spectrum data to yield elastic constants, (4) to examine this method on single crystal olivine as a test of the present theory, and (5) to present the technical details necessary for the practical utilization of the present method.

2. Theory of Free Vibration of an Anisotropic Rectangular Parallelepiped

2.1 Demarest's theory

DEMAREST (1969, 1971) applied the variational approach and the Ritz method to the problem of the free vibration of an anisotropic elastic body. We review here briefly for convenience Demarest's theory.

Through the variational approach our problem is formulated in following way; the actual motion in the form $u(x_1, x_2, x_3) \exp(i\omega t)$ is given by such a displacement function $u(x_1, x_2, x_3)$ that renders the integral

$$I = \iiint \sum_i \sum_j \sum_k \sum_l \frac{1}{4} C_{ijkl} \left(\frac{\partial u_i}{\partial x_j} + \frac{\partial u_j}{\partial x_i} \right) \left(\frac{\partial u_k}{\partial x_l} + \frac{\partial u_l}{\partial x_k} \right) dV \qquad (1)$$

an extremum under the normalization condition

$$\iiint \sum_i u_i^2 dV = 1, \qquad (2)$$

and the extremum gives $\rho \omega^2$. Here t is time, C_{ijkl}'s are the elastic stiffness constants, ρ is the density, $\omega (= 2\pi f)$ is the angular frequency, and the integral is taken over the volume of the body.

To apply the Ritz method the displacement function is expressed in a series

$$u = \sum_p a_p \phi_p \qquad (3)$$

where ϕ_p's $(p = 1, 2, \ldots)$ are normalized orthogonal basis functions, and a_p's are constants to be determined. When we construct a matrix $\Gamma = (\Gamma_{pq})$ defined by

$$\Gamma_{pq} = \Gamma_{qp} = \iiint \sum_i \sum_j \sum_k \sum_l \frac{1}{4} C_{ijkl} \left(\frac{\partial \phi_{pi}}{\partial x_j} + \frac{\partial \phi_{pj}}{\partial x_i} \right) \left(\frac{\partial \phi_{qk}}{\partial x_l} + \frac{\partial \phi_{ql}}{\partial x_k} \right) dV \qquad (4)$$

where ϕ_{pi} is the x_i component of ϕ_p, then Eqs. (1) and (2) are written

$$I = \sum_p \sum_q a_p a_q \Gamma_{pq} \qquad (5)$$

$$\sum_{p} a_p^2 = 1 \; . \tag{6}$$

The extremization of (5) under (6) is attained by a_p's which satisfy the linear equation system

$$\sum_{p} (\Gamma_{pq} - \lambda \delta_{pq}) \frac{a_p}{} = 0 \; , \qquad q = 1, 2, \dots \tag{7}$$

where δ_{pq} is Kronecker's delta and λ is an undetermined multiplier. Equation (7) is the eigenvalue problem of the matrix Γ. The n-th eigenvector of Γ gives the a_p's of the n-th eigen vibration, and the n-th eigenvalue λ_n gives the angular frequency ω_n by

$$\lambda_n = \rho \omega_n^2 \; . \tag{8}$$

Equations (1)–(8) are the most general expressions, and no crystal symmetry, no shape of the elastic body, or no particular choice of basis functions is assumed.

Demarest showed, for a vibrating cube of cubic symmetry, that when the Legendre polynomials rather than trigonometric functions are used to express u, as in Eq. (10), the eigenvalues are calculated with more accuracy with a limited number of terms in expression (3). He calculated the resonance vibration of an isotropic cube and obtained excellent agreement between the calculated and the experimentally observed frequencies of the free vibration. Demarest further suggested that the theory could be extended to the rectangular parallelepiped of orthorhombic symmetry.

2.2 Extension of Demarest's theory to the rectangular parallelepiped of a general symmetry crystal

A specimen with the shape of a rectangular parallelepiped is assumed. A rectangular coordinate system as shown in Fig. 1 is taken. Each edge of the rectangular parallelepiped with a length of $2L_i$, $i = 1, 2, 3$, is set parallel to one of the coordinate axes and perpendicular to the others, and the center
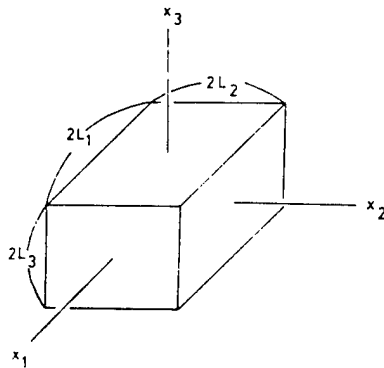

Fig. 1. Rectangular parallelepiped with a coordinate system.

of the body is put at the origin of the coordinate system. Thus the elastic body is surrounded by six planes defined by $x_i = \pm L_i$.

The elastic stiffness constants are generally expressed by

$$\begin{bmatrix} C_{11} & C_{12} & C_{13} & C_{14} & C_{15} & C_{16} \\ & C_{22} & C_{23} & C_{24} & C_{25} & C_{26} \\ & & C_{33} & C_{34} & C_{35} & C_{36} \\ & & & C_{44} & C_{45} & C_{46} \\ & & & & C_{55} & C_{56} \\ & & & & & C_{66} \end{bmatrix} \tag{9}$$

where a two-index matrix notation is used instead of a four-index tensorial notation according to conventional rules; $11 \to 1$, $23 \to 4$, etc.

The basis functions chosen are

$$\begin{aligned} \phi_p &= \frac{1}{\sqrt{L_1 L_2 L_3}} \bar{P}_\lambda\left(\frac{x_1}{L_1}\right)\bar{P}_\mu\left(\frac{x_2}{L_2}\right)\bar{P}_\nu\left(\frac{x_3}{L_3}\right)e_i \\ \phi_q &= \frac{1}{\sqrt{L_1 L_2 L_3}} \bar{P}_\xi\left(\frac{x_1}{L_1}\right)\bar{P}_\zeta\left(\frac{x_2}{L_2}\right)\bar{P}_\eta\left(\frac{x_3}{L_3}\right)e_j \end{aligned} \right\} \tag{10}$$

where e_i is the unit vector in x_i direction, and $\bar{P}_\lambda$ is the normalized Legendre polynomial of the λ-th degree. The p-th basis ϕ_p is specified by λ, μ, ν ($=0$, $1, \ldots$) and i ($=1, 2, 3$), and the q-th basis ϕ_q by ξ, ζ, η ($=0, 1, \ldots$) and j ($=1, 2, 3$).

For a specimen with a general crystal symmetry expressed by Eq. (9) and the shape of rectangular parallelepiped, and for the basis functions in Eq. (10), the Γ_{pq} in Eq. (4) is given as follows in each case of $(i, j) = (1, 1)$, $(2, 3)$, etc.

(i, j)	Γ_{pq}
$(1, 1)$	$C_{11}G_1 + C_{66}G_2 + C_{55}G_3 + C_{56}G_4 + C_{56}G_5 + C_{15}G_6 + C_{15}G_7 + C_{16}G_8 + C_{16}G_9$
$(2, 2)$	$C_{66}G_1 + C_{22}G_2 + C_{44}G_3 + C_{24}G_4 + C_{24}G_5 + C_{46}G_6 + C_{46}G_7 + C_{26}G_8 + C_{26}G_9$
$(3, 3)$	$C_{55}G_1 + C_{44}G_2 + C_{33}G_3 + C_{34}G_4 + C_{34}G_5 + C_{35}G_6 + C_{35}G_7 + C_{45}G_8 + C_{45}G_9$
$(2, 3)$	$C_{56}G_1 + C_{24}G_2 + C_{34}G_3 + C_{44}G_4 + C_{23}G_5 + C_{36}G_6 + C_{45}G_7 + C_{25}G_8 + C_{46}G_9$
$(3, 1)$	$C_{15}G_1 + C_{46}G_2 + C_{35}G_3 + C_{36}G_4 + C_{45}G_5 + C_{55}G_6 + C_{13}G_7 + C_{11}G_8 + C_{56}G_9$
$(1, 2)$	$C_{16}G_1 + C_{26}G_2 + C_{45}G_3 + C_{25}G_4 + C_{46}G_5 + C_{14}G_6 + C_{56}G_7 + C_{66}G_8 + C_{12}G_9$

$$\tag{11}$$

where

$$\begin{aligned} G_1 &= D_{\lambda\xi}\delta_{\mu\zeta}\delta_{\nu\eta}/L_1^2 \\ G_2 &= \delta_{\lambda\xi}D_{\mu\zeta}\delta_{\nu\eta}/L_2^2 \\ G_3 &= \delta_{\lambda\xi}\delta_{\mu\zeta}D_{\nu\eta}/L_3^2 \\ G_4 &= \delta_{\lambda\xi}E_{\mu\zeta}F_{\nu\eta}/L_2 L_3 \\ G_5 &= \delta_{\lambda\xi}F_{\mu\zeta}E_{\nu\eta}/L_2 L_3 \\ G_6 &= F_{\lambda\xi}\delta_{\mu\zeta}E_{\nu\eta}/L_3 L_1 \end{aligned} \right\} \tag{12}$$

206

$$G_7 = E_{\lambda\xi}\delta_{\mu\zeta}F_{\nu\tau}/L_3L_1 \quad \Big|$$
$$G_8 = E_{\lambda\xi}F_{\mu\zeta}\delta_{\nu\tau}/L_1L_2 \quad \Big|$$
$$G_9 = F_{\lambda\xi}E_{\mu\zeta}\delta_{\nu\tau}/L_1L_2 \quad \Big)$$

and

$$\delta_{\lambda\xi} = \begin{cases} 1, & \lambda = \xi \\ 0, & \lambda \neq \xi \end{cases}$$

$$E_{\lambda\xi} = \int_{-1}^{1} \bar{P}_\lambda(X)\bar{P}'_\xi(X)\mathrm{d}X = \begin{cases} \sqrt{2\lambda+1}\sqrt{2\xi+1}, & \lambda < \xi \text{ and } \lambda+\xi = \text{odd} \\ 0, & \text{otherwise} \end{cases}$$

$$F_{\lambda\xi} = \int_{-1}^{1} \bar{P}'_\lambda(X)\bar{P}_\xi(X)\mathrm{d}X = \begin{cases} \sqrt{2\lambda+1}\sqrt{2\xi+1}, & \lambda > \xi \text{ and } \lambda+\xi = \text{odd} \\ 0, & \text{otherwise} \end{cases}$$

and for $\lambda \geqq \xi$

$$D_{\lambda\xi} = D_{\xi\lambda} = \int_{-1}^{1} \bar{P}'_\lambda(X)\bar{P}'_\xi(X)\mathrm{d}X = \begin{cases} \sqrt{2\lambda+1}\sqrt{2\xi+1}\,\xi(\xi+1)/2, & \lambda+\xi = \text{even} \\ 0, & \lambda+\xi = \text{odd} \end{cases}$$

(13)

where

$$\bar{P}'_\lambda(X) = \mathrm{d}\bar{P}_\lambda(X)/\mathrm{d}X$$

and

$$X = \frac{x_1}{L_1}, \quad \frac{x_2}{L_2}, \quad \text{or} \quad \frac{x_3}{L_3}.$$

By using the mass M of the body instead of density, the eigenvalue problem (7) is written

$$\sum_p (\Gamma^*_{pq} - \lambda^*\delta_{pq})a_p = 0, \qquad q = 1, 2, \ldots$$

and

$$\lambda^* = M\omega^2$$

where

$$\Gamma^*_{pq} = 8L_1L_2L_3\Gamma_{pq}.$$

The matrix Γ^* is more convenient than Γ for practical purpose. Though the size of the specimen is changed by temperature, for example, the mass is constant and the variable properties of the specimen are all included in Γ^*.

2.3 Splitting of matrix Γ and vibrational mode types

Once we have Γ or Γ^*, we can calculate the vibrational frequencies f_n $(=\omega_n/2\pi)$ as the eigenvalues of the matrix. However, the size of the matrix is usually quite large, and thus possible splitting or factoring of the matrix would be very helpful.

Demarest has shown that the splitting of the matrix results in eight smaller ones if the symmetry of the specimen has three mirror planes intersecting one another at right angles. This splitting is based on a symmetric character of

the displacement vector u in Eq. (3), and each of the smaller matrices corresponds to a group of a particular type of the vibrational mode. Therefore, the splitting of the matrix into smaller ones is useful not only in computational problems, but also in classification of the vibrational modes. Further study on matrix splitting and classification of mode types is presented below.

2.4 Matrix splitting in a general case

In this section and in the followings we use x, y, z in stead of x_1, x_2, x_3, and u, v, w instead of u_1, u_2, u_3.

In the most general case (9), i.e., triclinic crystals, there is no way of splitting the matrix Γ.[1] This situation takes place even for a higher symmetry crystal if it is rotated to an inappropriate orientation relative to the coordinate axis. In such a case, we have to calculate the eigenvalues of Γ as it is. Every vibrational mode is coupled to another, and no systematic study of the eigen vibration is known at present.

In the case of a monoclinic crystal with a mirror plane perpendicular to x axis, the elastic constants are given by

$$\begin{bmatrix} C_{11} & C_{12} & C_{13} & C_{14} & 0 & 0 \\ & C_{22} & C_{23} & C_{24} & 0 & 0 \\ & & C_{33} & C_{34} & 0 & 0 \\ & & & C_{44} & 0 & 0 \\ & & & & C_{55} & C_{56} \\ & & & & & C_{66} \end{bmatrix}. \tag{14}$$

For the crystal symmetry (14), we arrange the basis functions in the following series expression

$$u = \frac{1}{\sqrt{L_1 L_2 L_3}} \left(\sum_{\substack{p \\ (\lambda \text{ even})}} a_p \bar{P}_\lambda \bar{P}_\mu \bar{P}_\nu e_1 + \sum_{\substack{p \\ (\lambda \text{ odd})}} a_p \bar{P}_\lambda \bar{P}_\mu \bar{P}_\nu e_2 + \sum_{\substack{p \\ (\lambda \text{ odd})}} a_p \bar{P}_\lambda \bar{P}_\mu \bar{P}_\nu e_3 \right)$$

$$+ \frac{1}{\sqrt{L_1 L_2 L_3}} \left(\sum_{\substack{p \\ (\lambda \text{ odd})}} a_p \bar{P}_\lambda \bar{P}_\mu \bar{P}_\nu e_1 + \sum_{\substack{p \\ (\lambda \text{ even})}} a_p \bar{P}_\lambda \bar{P}_\mu \bar{P}_\nu e_2 + \sum_{\substack{p \\ (\lambda \text{ even})}} a_p \bar{P}_\lambda \bar{P}_\mu \bar{P}_\nu e_3 \right). \tag{15}$$

Then zero components and non-zero components in the matrix Γ are separated as follows;

$$\begin{bmatrix} \Gamma^{XE} & 0 \\ \hline 0 & \Gamma^{XO} \end{bmatrix}. \tag{16}$$

This means that Γ is split into two small matrices Γ^{XE} and Γ^{XO},[2] and the eigenvalue problem (7) is reduced to

---

[1,2]   Demarest (personal communication, 1976) has pointed out that the matrix for triclinic and monoclinic symmetry could be further split based on whether the displacement function is symmetric or antisymmetric with respect to an inversion operation.

$$\sum_p \left(\Gamma_{pq}^{XE} - \lambda \delta_{pq}\right)a_p = 0, \qquad q = 1, 2, \ldots \Bigg\}$$

$$\sum_p \left(\Gamma_{pq}^{XO} - \lambda \delta_{pq}\right)a_p = 0, \qquad q = 1, 2, \ldots \Bigg\} . \qquad (17)$$

The matrices Γ^{XE} and Γ^{XO} correspond to two groups of vibrational modes, XE and XO, respectively. The groups are characterized by parity of displacement with respect to the mirror reflexion on the y-z plane, as known from Eq. (15) and the fact that $\bar{P}_\lambda(X)$ is an even function for an even number λ, and odd function for odd λ. The parity of displacement components u, v, w is listed in Table 1a, for each of XE and XO.

Table 1. Nomenclature and parity of displacement for each mode group in a case in which the crystal has a mirror plane perpendicular to (a) x axis, (b) y axis, (c) z axis.

(a)		x	y	z		x	y	z
	u	E	—	—	u	O	—	—
	v	O	—	—	v	E	—	—
	w	O	—	—	w	E	—	—
			XE				XO	

(b)		x	y	z		x	y	z
	u	—	O	—	u	—	E	—
	v	—	E	—	v	—	O	—
	w	—	O	—	w	—	E	—
			YE				YO	

(c)		x	y	z		x	y	z
	u	—	—	O	u	—	—	E
	v	—	—	O	v	—	—	E
	w	—	—	E	w	—	—	O
			ZE				ZO	

E denotes even, and O odd. — denotes either even or odd. This table also shows how to choose the degrees of Legendre polynomials in basis function.

In the case of a monoclinic crystal with a mirror plane perpendicular to y or z axis instead of x axis, the similar splitting of Γ to Γ^{YE} and Γ^{YO}, or to Γ^{ZE} and Γ^{ZO} is made through the choice of μ, or ν given in Table 1b, or 1c. The matrices Γ^{YE} and Γ^{YO}, or Γ^{ZE} and Γ^{ZO} correspond to mode groups YE and YO, or ZE and ZO.

For monoclinic crystals, one of the splittings (a), (b), and (c) in Table 1 is used.

In the case of trigonal crystal $(3m, 32, \bar{3}m)$ with

$$\begin{bmatrix} C_{11} & C_{12} & C_{13} & C_{14} & 0 & 0 \\ & C_{11} & C_{13} & -C_{14} & 0 & 0 \\ & & C_{33} & 0 & 0 & 0 \\ & & & C_{44} & 0 & 0 \\ & & & & C_{44} & C_{14} \\ & & & & & \frac{1}{2}(C_{11}-C_{12}) \end{bmatrix} \qquad (18)$$

the splitting of Γ to Γ^{xE} and Γ^{xo} results. In the case of trigonal $(3, \bar{3})$ represented by

$$\begin{bmatrix} C_{11} & C_{12} & C_{13} & C_{14} & C_{15} & 0 \\ & C_{11} & C_{13} & -C_{14} & -C_{15} & 0 \\ & & C_{33} & 0 & 0 & 0 \\ & & & C_{44} & 0 & -C_{15} \\ & & & & C_{44} & C_{14} \\ & & & & & \frac{1}{2}(C_{11}-C_{12}) \end{bmatrix} \qquad (19)$$

the rotation of the crystal around z axis by an angle θ given by

$$\tan 3\theta = C_{15}/C_{14}$$

makes the reduction of Eq. (19) to the same type as that in Eq. (18).

In the case of tetragonal crystal $(4, \bar{4}, 4/m)$ represented by

$$\begin{bmatrix} C_{11} & C_{12} & C_{13} & 0 & 0 & C_{16} \\ & C_{11} & C_{13} & 0 & 0 & -C_{16} \\ & & C_{33} & 0 & 0 & 0 \\ & & & C_{44} & 0 & 0 \\ & & & & C_{44} & 0 \\ & & & & & C_{66} \end{bmatrix} \qquad (20)$$

Γ is split to Γ^{zE} and Γ^{zo}. However, the appropriate rotation of a crystal around the z axis by an angle θ given by

$$C_{16}(3 \cos 4\theta - 1) = ((C_{11}-C_{12})/2 - C_{66}) \sin 4\theta$$

makes Eq. (20) the special case $(C_{13}=C_{23})$ of an orthorhombic crystal;

$$\begin{bmatrix} C_{11} & C_{12} & C_{13} & 0 & 0 & 0 \\ & C_{22} & C_{23} & 0 & 0 & 0 \\ & & C_{33} & 0 & 0 & 0 \\ & & & C_{44} & 0 & 0 \\ & & & & C_{55} & 0 \\ & & & & & C_{66} \end{bmatrix} . \qquad (21)$$

Expression (21) is a general form of elastic constants for cubic, tetragonal,

hexagonal and orthorhombic crystals set appropriately in the rectangular co-ordinate system.

The splitting of Γ for low symmetry material, such as monoclinic and trigonal crystals having one mirror plane, is made only to two smaller ones. However, this is still very helpful in reducing computation time.

There is no case in which elastic property of crystals has only two mirror planes.

2.5 Matrix splitting in orthorhombic crystals and the description of 32 mode types

When the elastic property is described by Eq. (21), there are three mirror planes perpendicular to x, y, or z axis. Therefore all of the three types of splitting of Γ given in Table 1 hold simultaneously. Therefore Γ is split into eight smaller matrices. Their parities are given in the second column in Table 2. Each of eight smaller matrices corresponds to a group of a particular type of vibrational mode.

The vibrational configuration of each of eight mode groups were then studied in detail. The vibrational configuration of each mode group is restricted by the parity of displacement shown in the second column of Table 2. Where the actual vibrational configurations are concerned, however, we can further distinguish four different types of configuration in any of eight mode groups.

Since the vibrational configuration of a three-dimensional body is too complicated to specify and visualize as it is, the way of combining the specification of three two-dimensional vibrational configurations viewed along three coordinate axes is used.

First the study of the vibrational configuration of two-dimensional case is done. When a rectangular parallelepiped of orthorhombic crystal is viewed along an axis, it looks a rectangle with two mirror planes perpendicular to each other. The vibrational mode of such a rectangle is split into four groups in the same manner as that in a rectangular parallelepiped from the view point of parity of displacement:

$$
\begin{array}{c}
\begin{array}{c|cc} & x & y \\ \hline u & O & E \\ v & E & O \end{array}
\qquad
\begin{array}{cc} E & O \\ O & E \end{array}
\qquad
\begin{array}{cc} E & E \\ O & O \end{array}
\qquad \text{and} \qquad
\begin{array}{cc} O & O \\ E & E \end{array}
\end{array}
$$

For each of these four mode groups, two cases can be distinguished

$$ uv > 0 \quad \text{and} \quad uv < 0 $$

where u, v are x, y components of displacement at a particular corner ($x > 0$, $y > 0$) of the rectangle. The eight two-dimensional mode types thus obtained

Table 2. Classification, description, and notations of vibrational modes of a rectangular parallelepiped of an orthorhombic crystal.

Group type in Table 1	Parity of displacement			The present notation of n-th mode in a mode group	Classification and description of vibrational configuration			Known modes for a thin rod or a cube	Demarest's notation and classification for a cube of cubic crystal
	x	y	z		x	y	z		
XO-YO-ZO	u O	E	E	OD-n					D (Dilation)
	v E	O	E		D	D	D	Breathing mode (DDD-1)	D_{sn} symmetric
	w E	E	O		D	E	E ⎫	Longitudinal vibration	D_{an} antisymmetric
					E	D	E ⎬	along x, y, and z axis	D_{dn} doublet (?)
					E	E	D ⎭	(Lame's mode)	
XE-YO-ZO	E	E	E	EX-n					F (Flexure)
	O	O	E		D	A	A		F_{sn} symmetric
	O	E	O		D	B	B		
					E	A	B ⎫	Symmetric flexure	F_{an} antisymmetric
					E	B	A ⎭	vibration along x axis	
XO-YE-ZO	O	O	E	EY-n					
	E	E	E		A	D	A		
	E	O	O		B	D	B		
					B	E	A ⎫	Symmetric flexure	
					A	E	B ⎭	vibration along y axis	
XO-YO-ZE	O	E	O	EZ-n					
	E	O	O		A	A	D		
	E	E	E		B	B	D		
					A	B	E ⎫	Symmetric flexure	
					B	A	E ⎭	vibration along z axis	
XO-YE-ZE	O	O	O	OX-n					S (Shear)
	E	E	O		S	A	A		S_{sn} symmetric
	E	O	E		S	B	B		
					R	A	B ⎫	Torsional vibration	S_{an} antisymmetric
					R	B	A ⎭	along x axis	
XE-YO-ZE	E	E	O	OY-n					
	O	O	O		A	S	A		
	O	E	E		B	S	B		
					R	R	A ⎫	Torsional vibration	
					A	R	B ⎭	along y axis	
XE-YE-ZO	E	O	E	OZ-n					
	O	E	E		A	A	S		
	O	O	O		B	B	S		
					A	B	R ⎫	Torsional vibration	
					B	A	R ⎭	along z axis	
XE-YE-ZE	E	O	O	EV-n					T (torsion)
	O	E	O		S	S	S		T_{sn} symmetric
	O	O	E		S	R	R		T_{an} antisymmetric
					R	S	R ⎫	Asymmetric flexure	T_{dn} doublet (?)
					R	R	S ⎭	vibration along x, y, and z axis	

are schematically shown in Fig. 2 for the lowest harmonics. Among them there are six independent types of two-dimensional configurations, D (dilation and compression), E (extension and contraction), S (shear), R (rotation), A (flexure and pinch-and-swell, type A), and B (flexure and pinch-and-swell, type B), as indicated in Fig. 2.
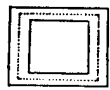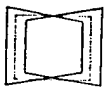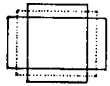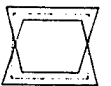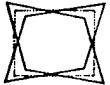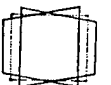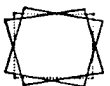
VIBRATIONAL CONFIGURATION	PARITY OF DISPLACEMENT	SIGN OF uv AT THE CORNER x>0, y>0	MODE TYPE NOTATION	VIBRATIONAL CONFIGURATION	PARITY OF DISPLACEMENT	SIGN OF uv AT THE CORNER x>0, y>0	MODE TYPE NOTATION
	u │ 0 E v │ E 0	uv>0	D (DILATION AND COMPRESSION)		u │ E E v │ 0 0	uv>0	A (FLEXURE AND PINCH-AND-SWELL, TYPE A)
	0 E E 0	uv<0	E (EXTENTION AND CONTRACTION)		0 0 E E	uv>0	
	E 0 0 E	uv>0	S (SHEAR)		E E 0 0	uv<0	B (FLEXURE AND PINCH-AND-SWELL, TYPE B)
	E 0 0 E	uv<0	R (ROTATION)		0 0 E E	uv<0	

Fig. 2.   All possible types of vibrational configuration viewed along an axis.

Second, all the possible combination of three vibrational configurations (two-dimensional) viewed along three coordinate axes are considered. We then have four different cases in each of eight mode groups as given in the fourth column in Table 2. For example, when a rectangular parallelepiped in vibration looks like an A type when viewed along x and z axes, and like a D type along y axis, then this vibrational type is denoted by ADA. Such types, as AAA or DSR, never occur in any of eight mode groups. As a result, there are 32 different mode types in total for a general orthorhombic system. All the 32 different modes are described in Table 2.

The distinction of four types in each of eight mode groups does not mean further splitting of the matrix Γ. Furthermore, for higher modes with higher harmonics, the distinction has no definite physical significance as is known from Fig. 2. For lower modes, however, it is useful in order to study their vibrational characteristics and relate them to the known vibrational modes for a thin rod or a cube, as shown in the fifth column in Table 2.

Demarest provided nomenclature for each of the eight groups as indicated in the sixth column of Table 2. However, Demarest's nomenclature does not seem to well represent the vibrational property of each group, and is confusing when we are really concerned with vibrational configuration.

Flexure vibration on one edge is accompanied by pinch-and-swell type vibration on another edge as inferred from Table 2. The R and S vibrations in Fig. 2 are graded to flexure vibration, and D and E vibrations to pinch-and-swell type when the harmonics are increased. Further, flexure with pinch-and-swell is always common to all the modes in Demarest's S (shear) as well

as F (flexure) groups, and S (shear) is not included in one-half the modes of Demarest's S group. Although D and E do not couple directly with R and S, most of them couple through both A and B types of flexure with pinch-and-swell. In other words, the vibrational configuration of a three-dimensional body is so complicated that any single term showing vibrational configuration is confusing and cannot adequately represent each mode type. Demarest's subdivision of D and T groups into symmetric, antisymmetric, and doublet types is confusing. For example, the DDD mode is actually symmetric, and the remaining three in the OD group are antisymmetric in Demarest's meaning, but they are triplet at the same time for a cube of cubic crystal because three modes DEE, EDE and EED degenerate into one.

By taking all these situations into account, the notation of each mode types based simply on the symmetry of the vibration is proposed in the third column of Table 2.

However, the mode classification based on the group theory common in lattice dynamics is expected to be better in relation to lattice vibration.[3]

When we concern ourselves with the mode types of a vibrating rectangular parallelepiped in detail, the notations in the fourth column of Table 2 become free from confusion and seem convenient. For the practical application of the RPR method for determining the elastic constants, however, the subdivision of each of the eight mode groups is usually not necessary.

3. Numerical Calculation for Determination of Elastic Constants

The determination of the elastic constants by resonance is a typical inverse problem because Demarest's and the present theories just give the resonance frequencies in terms of the elastic constants, and there is no analytical way of explicitly representing the elastic constants by resonance frequency. Therefore, the successive approximation of the assumed elastic constants is necessary to obtain the actual elastic constants until the agreement between the observed and calculated resonance spectra is reached. The procedure of successive iteration for computing the actual elastic constants follows the flow scheme shown in Fig. 3.

3.1 The first trial elastic constants and mode identification

The most important and difficult step is mode identification of the observed resonance spectrum. When we start from the trial elastic constants close enough to the actual one, there is little problem in mode identification because both calculated and observed spectra are quite similar.

---

[3]   The approach along this line is being made by Demarest (personal communication, Demarest, 1976).
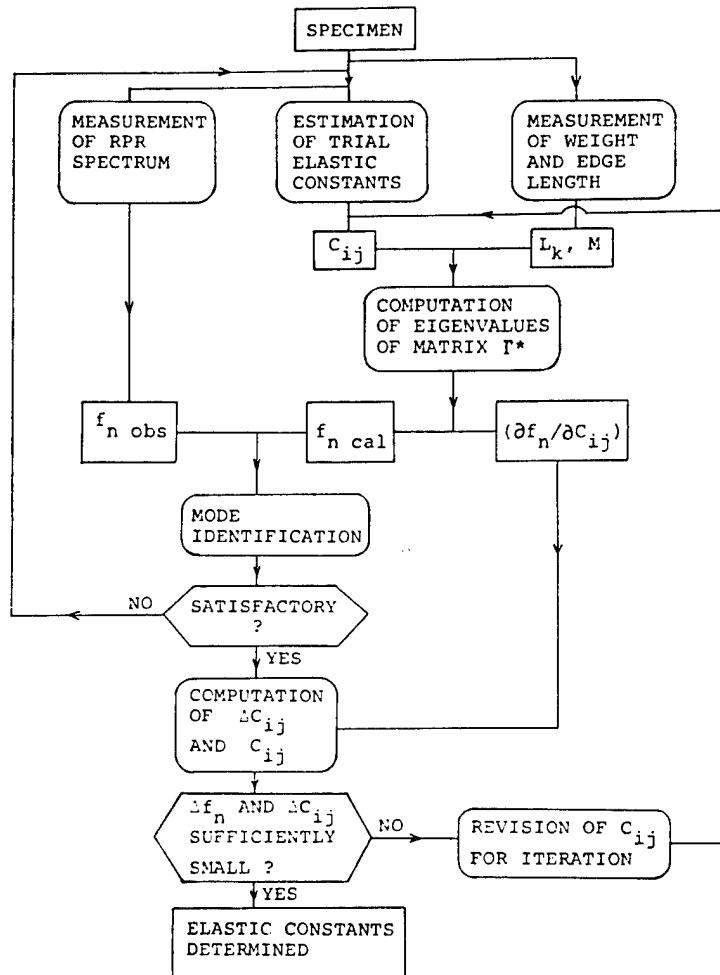
Fig. 3.   Flow diagram showing the procedure of determining elastic constants.

3.2   Numerical computation of the resonance spectrum

The necessary computation is to solve the eigenvalue problem of a symmetric matrix Γ. The size of the matrix Γ is dependent on the number of the terms in the representation of the displacement vector. It is mathematically known that in the Ritz method when the series expression such as Eq. (3), is truncated at finite terms, then the eigenvalues always become larger than the exact values. In our problem, the insufficient number of terms results in higher values of resonance frequencies and gives rise to a systematic error in the elastic constants. Therefore, a large number of terms are required so that the calculation error becomes sufficiently small enough for practical use. However, if too many terms are taken, we have to compute the eigenvalue

Table 3. Dependence of nondimensional frequencies on the number of basis vectors, calculated for EZ mode group of an olivine-1 specimen.

Number of basis vectors	EZ-1		EZ-2		EZ-3		EZ-4		EZ-5	
30	1.5579		2.0731		2.9886		3.0422		3.3182	
		−0.30%		−0.74%		−1.03%		−0.91%		−2.55%
42	1.5532		2.0579		2.9579		3.0145		3.2337	
		−0.02		−0.06		−0.17		−0.28		−1.45
54	1.5529		2.0567		2.9530		3.0061		3.1868	
		−0.01		−0.03		−0.10		−0.06		−0.18
65	1.5527		2.0560		2.9501		3.0043		3.1810	

problem of too large a matrix. Therefore it is important to determine the minimum but sufficient number of terms in series expression of the displacement vector to be able to apply the present method for the practical use.

The necessary number of terms is largely dependent on the choice of a set of arrays (λ, μ, ν) for $\bar{P}_\lambda(x_1/L_1)\bar{P}_\mu(x_2/L_2)\bar{P}_\nu(x_3/L_3)$ in Eq. (10). An efficient set that represents the actual displacement well and give accurate resonance frequencies within a limited number of terms must be selected. It is advantageous, both from experimental and computational procedures, to use the modes with lower resonance frequencies with lower harmonics. Therefore, the set of arrays (λ, μ, ν) in the order of smaller sum $\lambda+\mu+\nu$ may be chosen. Attention should also be paid to the shape of specimen on the choice of (λ, μ, ν). For example, a displacement component such as (3, 3, 4) should be included rather than those such as (1, 1, 10) for a specimen with a nearly cubic shape. On the other hand, when the specimen is a thin rod with long edges along the z axis, such terms as (1, 1, 10) may play an important role than (3, 3, 4) in the representation of the displacement vector. Therefore, some modification of the choice of the array is effective depending on the nature of the specimen, especially at the larger values of λ, μ, and ν.

Table 3 shows the dependence of the nondimensional frequency upon the number of terms, N, calculated on the EZ group of mode of the olivine-1 specimen. In the calculation of Table 3, the set of arrays (λ, μ, ν) is made up in the order of smaller sum $\lambda+\mu+\nu$ with some modification at higher values of λ, μ, and ν with reference to the shape of the olivine-1 specimen. This table suggests that fifty or sixty terms are necessary in the representation of the displacement vector to get sufficiently accurate frequencies of several lower modes for each of the eight groups.

3.3 Determination of elastic constants

Once mode identification of the observed resonance frequencies $f_{n\,obs}$ is made through the comparison with the calculated frequencies $f_{n\,cal}$, based on

the trial elastic constants C_{ij0}, these trial values are regarded as the first order approximation to the unknown actual values C_{ij}.

The Taylor expansion of the resonance frequencies with respect to $\Delta C_{ij} = C_{ij} - C_{ij0}$ is represented by

$$f_n = f_{n0} + \sum_{ij} (\partial f_n / \partial C_{ij}) \Delta C_{ij} .$$ (22)

If the number of modes used is larger than the independent number of the elastic constants, we can determine the amount of correction ΔC_{ij} to the trial values from the following simultaneous linear equation,

$$\begin{bmatrix} \partial f_1 / \partial C_{11} & \partial f_1 / \partial C_{22} & \cdots \\ \partial f_2 / \partial C_{11} & \partial f_2 / \partial C_{22} & \cdots \\ \vdots & \vdots & \end{bmatrix} \begin{bmatrix} \Delta C_{11} \\ \Delta C_{22} \\ \vdots \end{bmatrix} = \begin{bmatrix} \Delta f_1 \\ \Delta f_2 \\ \vdots \end{bmatrix}$$ (23)

or

$$T \Delta C = \Delta f$$ (24)

where $\Delta f_n = f_{n\,obs} - f_{n\,cal}$, and T is the matrix of derivatives $(\partial f_n / \partial C_{ij})$. Equation (23) and its matrix form (24) is equivalent to Eq. (22). The application of the least square determination of ΔC in Eq. (24) gives

$$\Delta C = (T^t T)^{-1} T^t \Delta f$$ (25)

where T^t is the transposed matrix of T. The elastic constants thus obtained, $C_{ij0} + \Delta C_{ij}$, are the second order approximation. The procedure is repeated until the change of the elastic constants reaches a prescribed small values in a way of iteration.

The numerical calculation of the derivatives $\partial f_n / \partial C_{ij}$ is made by a finite difference method with an interval of 0.01 to 0.05 for $\Delta C_{ij} / C_{ij}$.

4. Examples of Elastic Constant Determination

4.1 Measuring system

The electronic system for measuring the resonance of a specimen is shown in Fig. 4. A rectangular parallelepiped specimen is placed between two piezoelectric transducers. One of the transducers is excited by a monocromatic sinusoidal wave generated by a frequency synthesizer. The output signal from the other transducer is amplified, detected, and displayed on a synchroscope, and is also fed to Y axis of an X-Y recorder. Usually the amplitude of the output is very small. When the frequency of the excitation comes to coincidence with any of the resonance frequencies of the specimen, the amplitude of the output signal grows and shows a maximum. The frequency at the maximum amplitude is read by a digital frequency counter. The digital output from the frequency counter is fed to D-A converter and then to X axis
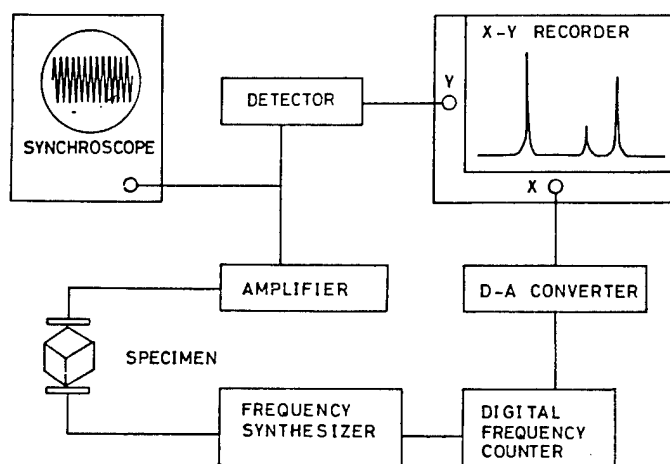
Fig. 4. Wiring diagram showing the measurement of a resonance spectrum.

of the X-Y recorder. Sweeping the frequency of the exciting sinusoidal wave continuously, we get a spectrum on the X-Y recorder showing a sequence of resonance peaks of the specimen (Fig. 5).

PZT shear mode transducers were usually used in the present work. With these transducers, all vibrational modes could be well excited and observed.

The observed resonance frequencies are somewhat affected by the way how the specimen is placed between the transducers as pointed out by DEMAREST (1969). If the specimen is in contact with transducers on its faces or edges, the resonance frequency generally shifts to higher value than when the specimen is held by its corners. However, even when the specimen is held by its corners, the frequency still shifts higher because slight force applied to the specimen gives rise to the deviation of the vibration from the ideal state of free vibration. Hence, we placed the specimen in contact with the transducers on its corners as lightly as possible without missing resonance peaks.

4.2 Specimen preparation

The crystallographic orientation of a piece of specimen of gem quality is determined within an accuracy of 0.2° by X-ray diffraction with a back reflection Laue photograph. The specimen is then cut with a diamond saw into a rectangular parallelepiped, each edge being parallel or perpendicular to the crystallographic a, b, and/or c axis. The surfaces of the cut pieces are not polished because they are smooth enough for the present method.

Tentative tests have been extensively made on numbers of small single crystal specimens of MgO and garnet, both belonging to cubic system with three independent elastic constants. In the present work, we measured the elastic constants of two pieces of single crystal olivine (orthorhombic system
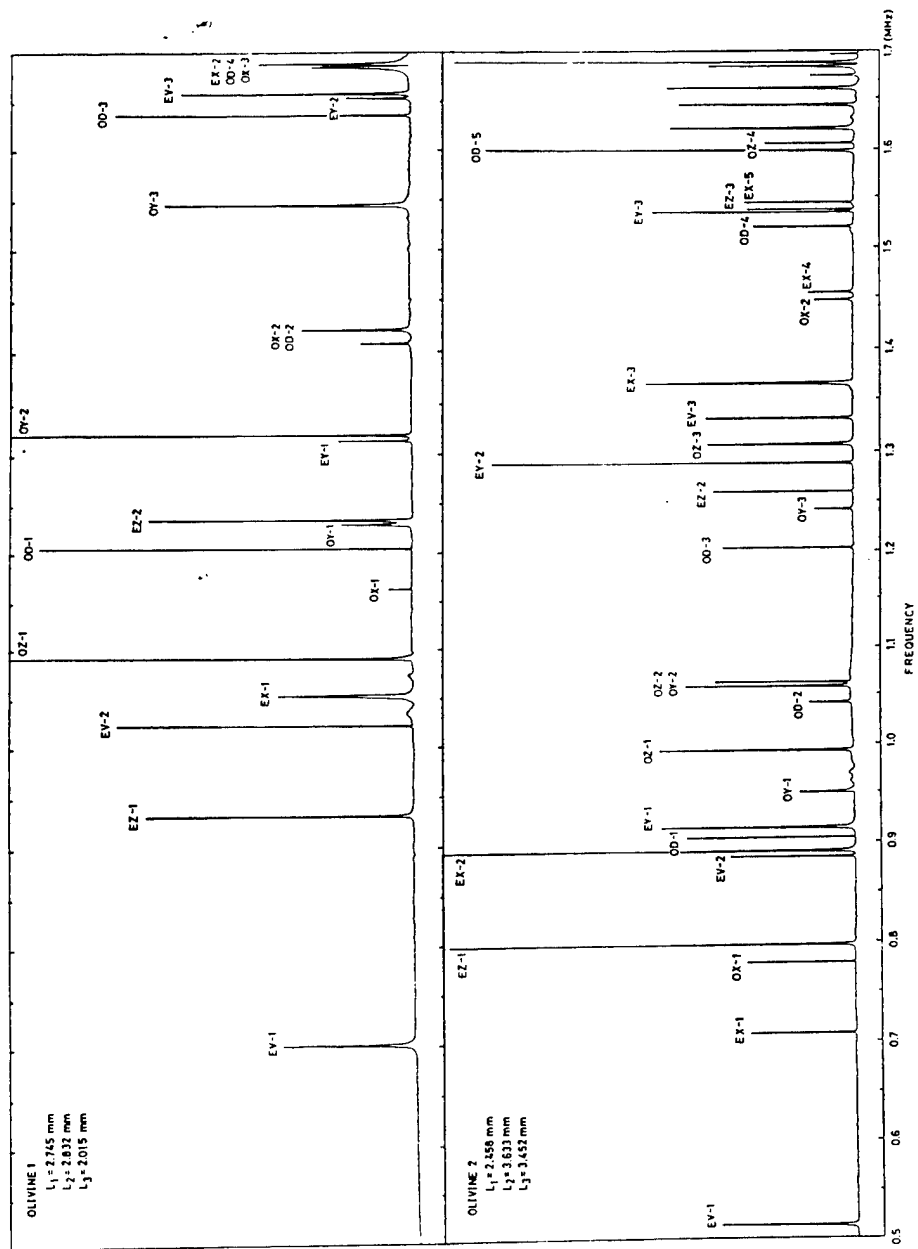
Fig. 5. Observed resonance spectra of two single crystal olivine specimens.

Table 4. Description of two olivine specimens.

	Olivine-1	Olivine-2
Edge length		
a	2.745±0.002 mm	2.458±0.001 mm
b	2.832±0.001	3.633±0.001
c	2.015±0.001	3.452±0.002
Density	3.316±0.005 g/cm³	3.299±0.004 g/cm³
Chemical composition		
Mg_2SiO_4	91.3 mole %	92.0 mole %
Fe_2SiO_4	8.1	7.5
Ca_2SiO_4	—	trace
Mn_2SiO_4	0.1	0.1
Ni_2SiO_4	0.4	0.4

with nine elastic constants) in order to determine if the present extension of the cube resonance techniques works well or not for relatively low symmetry crystal. In addition, olivine is the major constituent mineral in the earth's mantle.

The description of the specimens are listed in Table 4. Olivine-1 was collected by M. Kumazawa from Peridot ridge, Buhell Park, Arizona, and olivine-2 was collected by K. Suwa from Kondoa, Tanzania.

The size of the specimen was determined by a calibrated micrometer screw, the density was calculated from the measured weight and volume, and the chemical composition was determined by mean of EPMA by O. Nishizawa.

4.3 Results

The observed resonance spectra of olivine-1 and olivine-2 are shown in Fig. 5. Olivine belongs to orthorhombic system and it has nine independent elastic constants. Therefore, we have to obtain more than nine identified modes in order to determine all of the elastic constants.

KUMAZAWA and ANDERSON's data (1969) on olivine were used for the first trial value of elastic constants, which gave a theoretical spectrum very close to the observed one for both of two olivine specimens. Then some thirty modes with lower resonance frequencies were well identified as indicated at each spectrum peak in Fig. 5. These were sufficient to determine all of nine elastic constants. After a few steps of successive approximation, the elastic constants of two olivine specimens were well determined from these modes. The numerical data of the observed spectrum were compared with those calculated from the final elastic constants in Table 5.

The results on the elastic constants are listed in Table 6 in comparison with those reported by VERMA (1960), and KUMAZAWA and ANDERSON (1969). The error of each constant is expressed by standard deviation calculated by

Table 5. Comparison between observed and calculated spectra of olivine-1 and olivine-2.

		Olivine-1					Olivine-2		
No.	Mode	Cal. (MHz)	Obs. (MHz)	Diff. (%)	No.	Mode	Cal. (MHz)	Obs. (MHz)	Diff. (%)
1	EV-1	0.6937	0.6965	−0.40	1	EV-1	0.5104	0.5119	−0.29
2	EZ-1	0.9307	0.9303	0.04	2	EX-1	0.7091	0.7074	0.24
3	EV-2	1.0302	1.0249	0.52	3	OX-1	0.7779	0.7790	−0.14
4	EX-1	1.0401	1.0465	−0.61	4	EZ-1	0.7955	0.7961	−0.08
5	OZ-1	1.0904	1.0890	0.13	5	EV-2	0.8835	0.8850	−0.17
6	OX-1	1.1606	1.1619	−0.11	6	EX-2	0.8914	0.8904	0.11
7	OD-1	1.2100	1.2059	0.34	7	OD-1	0.9083	0.9062	0.23
8	OY-1	1.2264	1.2286	−0.18	8	EY-1	0.9127	0.9149	−0.24
9	EZ-2	1.2324	1.2338	−0.11	9	OY-1	0.9488	0.9500	−0.13
10	EY-1	1.3129	1.3129	0.00	10	OZ-1	0.9953	0.9931	0.22
11	OY-2	1.3181	1.3200	−0.14	11	OD-2	1.0385	1.0414	−0.28
12	OD-2	1.4124⎫	⎧1.4096	—	12	OZ-2	1.0608⎫	⎧1.0578	—
13	OX-2	1.4152⎭	⎩1.4201	—	13	OY-2	1.0612⎭	⎩1.0631	—
14	OY-3	1.5434	1.5450	−0.10	14	OD-3	1.2018	1.2038	−0.17
15	OD-3	1.6370	1.6358	0.07	15	OY-3	1.2419	1.2419	0.00
16	EY-2	1.6511	1.6518	−0.04	16	EZ-2	1.2633	1.2601	0.25
17	EV-3	1.6573	1.6560	0.08	17	EY-2	1.2879	1.2889	−0.08
18	OD-4	1.6844⎫	⎧1.6800	—	18	OZ-3	1.3059	1.3061	−0.02
19	OX-3	1.6849⎬	⎨1.6842	—	19	EV-3	1.3328	1.3330	−0.02
20	EX-2	1.6856⎭	⎩1.6897	—	20	EX-3	1.3628	1.3656	−0.21
21	OZ-2	1.7478	1.7463	0.09	21	OX-2	(1.45)	1.4478	
22	EZ-3	1.7720	1.7672	0.27	22	EX-4	1.4539	1.4554	−0.10
23	EX-3	1.7839	1.7885	−0.26	23	OD-4	1.5170	1.5218	−0.31
24	EZ-4	1.7977	1.8008	−0.17	24	EY-3	1.5335	1.5369	−0.22
25	EY-3	1.8270	1.8281	−0.06	25	EZ-3	1.5410	1.5398	0.08
26	EX-4	1.8509	1.8542	−0.18	26	EX-5	1.5468	1.5462	0.04
27	OD-5	1.8898	1.8908	−0.05	27	OD-5	1.6012	1.5987	0.16
28	OZ-3	1.8979	1.9004	−0.13	28	OZ-4	1.6083	1.6068	0.09
29	EZ-5	1.9093	1.9039	0.28					

Table 6. Elastic constants of two olivine specimens, in megabars, compared with the data of VERMA (1960), and KUMAZAWA and ANDERSON (1969).

	Olivine-1	Olivine-2	VERMA (1960)	KUMAZAWA and ANDERSON (1969)
C_{11}	3.24 ±0.03	3.19 ±0.08	3.24	3.237
C_{22}	1.96 ±0.03	1.92 ±0.06	1.98	1.976
C_{33}	2.32 ±0.02	2.38 ±0.06	2.49	2.351
C_{44}	0.639±0.003	0.638±0.003	0.667	0.6462
C_{55}	0.779±0.003	0.783±0.006	0.810	0.7865
C_{66}	0.788±0.004	0.797±0.004	0.793	0.7904
C_{23}	0.688±0.014	0.72 ±0.03	0.78	0.756
C_{31}	0.715±0.015	0.76 ±0.04	0.79	0.716
C_{12}	0.715±0.018	0.59 ±0.04	0.59	0.644
C_7	1.556±0.018	1.51 ±0.04	1.54	1.539
C_8	1.120±0.015	1.08 ±0.03	1.12	1.132
C_9	1.241±0.008	1.29 ±0.03	1.35	1.274
C_1	0.726±0.006	0.712±0.003	0.73	0.704
C_2	1.033±0.004	1.013±0.009	1.04	1.039
C_3	0.941±0.007	0.983±0.013	1.01	0.971

the least square fitting of the spectrum data. The previous data were obtained for two or four pieces of specimens several milimeters in size by means of the ultrasonic interference method with a carrier frequency of several tens of megahertz. The present data agree well with the previous ones. This proves the validity of the present theory of vibration and also the utility of the RPR technique as an invaluable method to determine the elastic constants of very small anisotropic solid.

5. Discussion of the RPR Technique

The utility and accuracy of the elastic constant determination by the RPR method depend on the following factors: (1) mode identification and the starting trial values of the elastic constants, (2) the sensitivity of resonance frequencies to the variation of elastic constants, and (3) the accuracy of shape and orientation of the specimen, (4) the effect of force applied to the specimen at the resonance vibration, and so on. They are discussed in the following.

5.1 Mode identification and starting trial constants

The starting trial values of the elastic constants are usually taken from theoretical and/or empirical estimation of similar or related material. Starting from the tentative identification of several spectrum peaks, the revision of the trial constants are made on a trial and error basis to identify and confirm every mode. However, when the frequencies of two or more peaks are closely spaced (e.g., EX-2, OX-3, and OD-4 of olivine-1 in Fig. 5), the mode identification is still difficult as far as we employ the numerical comparison of the observed and calculated spectra alone. In such a case, there are several ap-

Table 7. Derivatives $\partial f/\partial L_3$ calculated and observed on olivine-2 in MHz/cm.

No.	Mode	$\partial f_{cal}/\partial L_3$	$\partial f_{obs}/\partial L_3$
1	EV-1	−0.99	−0.86
2	EX-1	−0.64	−0.53
3	OX-1	−1.11	−0.91
4	EZ-1	0.56	0.65
5	EV-2	−0.20	−0.15
6	EX-2	−2.57	−2.23
7	OD-1	—*	−2.01
8	EY-1	−1.93	−1.40
9	OY-1	—	−0.90
10	OZ-1	−1.07	−0.70
11	OD-2	—	−0.97
12	OY-2	—	$\lbrace$−1.00
13	OZ-2	—	−1.24
14	OD-3	—	−2.02

* —: not calculated.

I. OHNO

proaches to achieve mode identification based on the different properties of the different modes.

1) In some particular modes, the resonance peaks are not sharp and the frequency is very sensitive to the force applied to the specimen between the two transducers while some other modes are not. In order to use this approach, some experience on the characteristics of each mode must be accumulated.

2) In some particular modes, the derivative $\partial f_n/\partial L_k$ is positive, but negative in other modes. A typical example is shown in Table 7, in which one end of the specimen A is polished to change the size, producing specimen B. By comparing the two observed spectra and two calculated spectra, the identification of modes is well established.

5.2 Sensitivity of resonance frequency to variation of elastic constants

Table 8 shows the derivatives $\partial f_n/\partial C_{ij}$ for olivine-1. The derivatives are

Table 8. Derivatives $\partial f_n/\partial C_{ij}$ calculated on olivine-1 specimen in MHz/Mb.

No.	Mode	$\partial f/\partial C_{11}$	$\partial f/\partial C_{22}$	$\partial f/\partial C_{33}$	$\partial f/\partial C_{23}$	$\partial f/\partial C_{31}$	$\partial f/\partial C_{12}$	$\partial f/\partial C_{44}$	$\partial f/\partial C_{55}$	$\partial f/\partial C_{66}$
1	EV-1	0.001	0.002	0.002	−0.003	−0.001	−0.001	0.130	0.050	0.290
2	EZ-1	0.012	0.211	0.008	−0.089	0.017	−0.104	0.165	0.012	0.011
3	EV-2	0.004	0.010	0.001	−0.005	0.000	−0.010	0.381	0.313	0.018
4	EX-1	0.007	0.257	0.030	−0.176	0.020	−0.074	0.000	0.001	0.107
5	OZ-1	0.003	0.013	0.002	−0.010	−0.004	−0.000	0.002	0.004	0.658
6	OX-1	0.001	0.029	0.002	−0.004	−0.001	−0.014	0.833	−0.001	0.000
7	OD-1	0.024	0.357	0.039	−0.234	0.050	−0.186	0.000	0.000	0.000
8	OY-1	0.010	0.177	0.013	−0.088	0.014	−0.081	0.070	0.272	0.089
9	EZ-2	0.121	0.006	0.012	−0.008	−0.069	−0.013	0.033	0.294	0.013
10	EY-1	0.134	0.021	0.032	−0.004	−0.123	−0.055	0.006	0.005	0.308
11	OY-2	0.007	0.011	0.003	−0.003	−0.005	0.005	0.020	0.773	0.013
12	OD-2	0.124	0.188	0.068	−0.126	−0.097	−0.137	0.003	0.000	0.028
13	OX-2	0.119	0.020	0.013	−0.010	−0.047	−0.085	0.219	0.204	0.065
14	OY-3	0.006	0.067	0.014	−0.050	−0.007	−0.012	0.571	0.068	0.246
15	OD-3	0.201	0.012	0.163	−0.047	−0.344	0.010	0.006	0.000	0.001
16	EY-2	0.007	0.048	0.235	−0.157	−0.043	−0.008	0.423	0.003	0.058
17	EV-3	0.009	0.031	0.005	−0.013	−0.006	0.004	0.309	0.457	0.259
18	OD-4	0.025	0.181	0.224	−0.227	0.004	−0.063	0.098	0.004	0.018
19	EX-2	0.017	0.042	0.222	−0.148	−0.061	−0.001	0.015	0.163	0.289
20	OX-3	0.052	0.033	0.014	−0.026	−0.035	−0.026	0.192	0.266	0.397
21	OZ-2	0.009	0.068	0.334	−0.297	−0.090	0.023	0.050	0.046	0.185
22	EZ-3	0.062	0.175	0.040	−0.102	−0.043	−0.078	0.484	0.093	0.009
23	EX-3	0.047	0.144	0.152	−0.066	−0.106	−0.097	0.039	0.086	0.270
24	EZ-4	0.042	0.157	0.018	−0.093	0.023	−0.083	0.653	0.103	0.014
25	EY-3	0.146	0.200	0.109	−0.174	−0.069	−0.240	0.040	0.001	0.132
26	EX-4	0.014	0.108	0.178	−0.102	−0.020	−0.048	0.016	0.123	0.333
27	OD-5	0.137	0.018	0.260	−0.014	−0.191	−0.021	0.000	0.001	0.007
28	OZ-3	0.032	0.128	0.114	−0.157	−0.054	−0.056	0.491	0.225	0.117
29	EZ-5	0.045	0.030	0.015	−0.020	−0.017	−0.025	0.410	0.323	0.303

parameters indicating the sensitivity of resonance frequencies to small variations of the elastic constants. Derivatives with respect to C_{44}, C_{55} and C_{66} for several modes are large. Therefore, shear constants, such as C_{44}, C_{55} and C_{66}, are determined with less uncertainty as shown in Table 6. With respect to the other constants, however, there are limited number of modes whose derivatives are large enough to determine the constants with very good accuracy.

In Table 8, it is shown that the two vectors $(\partial f_n/\partial C_{ij})$ and $(\partial f_m/\partial C_{ij})$ are nearly parallel in some cases of n and m. Further, in other cases the independency of the two vectors, $(\partial f_n/\partial C_{ij})$ and $(\partial f_n/\partial C_{kl})$, is not good enough. This situation lowers the determinant of matrix $(T^t T)^{-1} T^t$ in Eq. (25), and makes the determination of the elastic constants less reliable. Larger ambiguity in such constants as C_{11}, and C_{23} is partly due to this effect.

Reduction in ambiguity is made by the following two ways: (1) the use of larger number of modes, and (2) the transformation of the independent variables to constitute a derivative matrix T whose column and row vectors are more independent of one another. Both the first and the second ways are quite effective for lessening the singularity of the matrix $(T^t T)^{-1} T^t$ in Eq. (25) and then for reducing the ambiguity of elastic constants.

The second is closely related to the nature of the vibration of an elastic body. When we introduce the nine independent elastic parameters;

$$
\begin{aligned}
C_1 &= (C_{22} + C_{33} - 2C_{23})/4 \\
C_2 &= (C_{33} + C_{11} - 2C_{31})/4 \\
C_3 &= (C_{11} + C_{22} - 2C_{12})/4 \\
C_4 &= C_{44} \\
C_5 &= C_{55} \\
C_6 &= C_{66} \\
C_7 &= (C_{11} + C_{12} + C_{31})/3 \\
C_8 &= (C_{12} + C_{22} + C_{23})/3 \\
C_9 &= (C_{31} + C_{23} + C_{33})/3
\end{aligned}
\qquad (26)
$$

instead of the nine constants C_{ij} commonly used for an orthorhombic crystal, then the ambiguity of the overall determination of the elastic constants is considerably reduced. We also achieved data reduction with independent variables in Eq. (26), and the results are listed in the lower parts of Table 6. In this case, the degree of dependence of vectors in the matrix T is actually reduced. The choice of variables in Eq. (26) has indeed a physical significance; C_7, C_8, and C_9, and C_1, C_2, and C_3 being the linear bulk moduli and rigidities, respectively. For example, C_7 is the coefficient of stress σ_{zz} appearing in the isotropic dilation of the material, and C_1 is a shear constant related to the shear deformation specified by displacement along $1\bar{1}0$ on (110).

5.3   Shape and orientation of the specimen

Although no systematic studies have been made on the effects of small orientation errors and of small deviations of the specimen from an exact rectangular parallelepiped, they do not seem to be very important. If the effects had been large, the internal inconsistencies of the observed and calculated resonance frequencies would have followed. Some fraction of the final differences of the observed and the calculated resonance frequencies (diff. in Table 5) is attributed to these effects. The differences were in the order of 0.5% at most, and were usually 0.1% for the present specimens.

The surface roughness of the specimen seems also unimportant because the vibrational energy spreads over the specimen volume and the surfaces have an effect only in the stress-free conditions. Further, wavelength of the vibration is far longer than the ordinary degree of surface roughness and no interference of surface undulation is expected in the vibration of the specimen. This situation is one of the big advantages over the phase comparison or pulse superposition method in which very short waves are used.

The surface roughness of the specimen, however, produces another source of uncertainty through the accuracy of the edge lengths of the specimen, especially when the specimen is very small. Apparently the components of the matrix Γ^* and thus its eigenvalues have a dimension of (elastic constant) $\times$ (edge length). Therefore the elastic constants determined should have the same order of relative error to that of the length determination.

5.4   The effect of force applied to the specimen during vibration

In order to hold the specimen between two transducers for resonance frequency measurement, the application of static force to the specimen is inevitable. Specimen vibration is constrained to some extent, and the resonance frequencies measured are shifted higher as a result of deviation from perfectly free vibration. This effect was studied by Sumino et al. (1976), and turned out to be very small, 0.2% at most, when experiments were carefully done.

REPORT DOCUMENTATION PAGE

Public reporting burden for this collection of information is estimated to average 1 hour per response, including the time for reviewing instructions, searching existing data sources, gathering and maintaining the data needed, and completing and reviewing the collection of information. Send comments regarding this burden estimate or any other aspect of this collection of information, including suggestions for reducing this burden, to Washington Headquarters Services, Directorate for Information Operations and Reports, 1215 Jefferson Davis Highway, Suite 1204, Arlington, VA 22202-4302, and to the Office of Management and Budget, Paperwork Reduction Project (0704-0188), Washington, DC 20503.

1. AGENCY USE ONLY (Leave Blank)	2. REPORT DATE 4 Jun 01	3. REPORT DYPE AND DATES COVERED Conference Report, May 30 to Jun 30, 1999

4. TITLE AND SUBTITLE
Proceedings of the Resonance Meeting, Vol. 1. Transcripts

5. FUNDING NUMBERS
PE 61153N
N00014-98-1-0033

6. AUTHOR(S)
Elizabeth A. Furr, ed.

7. PERFORMING ORGANIZATION NAME(S) AND ADDRESS(ES)
Jamie L. Whitten National Center for Physical Acoustics
The University of Mississippi
University, MS 38677

8. PERFORMING ORGANIZATION REPORT NUMBER .

LF1000-01

9. SPONSORING / MONITORING AGENCY NAME(S) AND ADDRESS(ES)
Office of Naval Research
ONR 331
800 North Quincy Street
Arlington, VA 22217-5660

10. SPONSORING / MONITORING AGENCY REPORT NUMBER

11. SUPPLEMENTARY NOTES

12a. DISTRIBUTION / AVAILABILITY STATEMENT
Approved for public release; Distribution unlimited

12b. DISTRIBUTION CODE

13. ABSTRACT (Maximum 200 words)

The Proceedings of the Resonance Meeting held May 30 to June 1, 1999 are in two volumes. Volume I of the proceedings contains verbatim transcriptions of the presentations given . This volume also contains a special appendix honoring Orson L. Anderson, Harold H. Demarest, Jr. and Ichiro Ohno for their contributions to the development of resonance techniques for determining elastic properties of solids.. Volume II of these proceedings contains copies of the transparencies used by the presenters.

14. SUBJECT TERMS Resonance, Resonance Techniques, Acoustic Resonance, Resonant Ultrasound Spectroscopy, Elastic Properties

15. NUMBER OF PAGES
236

16. PRICE CODE

17. SECURITY CLASSIFICATION OF REPORT UNCLASSIFIED	18. SECURITY CLASSIFICATION OF THIS PAGE UNCLASSIFIED	19. SECURITY CLASSIFICATION OF ABSTRACT UNCLASSIFIED	20. LIMITATION OF ABSTRACT